

Universidad de Huelva

Departamento de Ingeniería Química, Química Física y
Ciencias de los Materiales



**Physico-chemical modification of asphalt bitumens by
reactive agents**

**Modificación físico-química de betunes asfálticos
mediante agentes reactivos**

**Memoria para optar al grado de doctor
presentada por:**

Antonio Abad Cuadri Vega

Fecha de lectura: 20 de septiembre de 2013

Bajo la dirección de los doctores:

Pedro Partal López

Francisco Javier Navarro Domínguez

Huelva, 2013



**MODIFICACIÓN FÍSICO-QUÍMICA
DE BETUNES ASFÁLTICOS
MEDIANTE AGENTES REACTIVOS**

**PHYSICO-CHEMICAL
MODIFICATION OF ASPHALT
BITUMENS BY REACTIVE AGENTS**



**Universidad
de Huelva**

**PROGRAMA OFICIAL DE DOCTORADO EN
PROCESOS Y PRODUCTOS QUÍMICOS**

Antonio Abad Cuadri Vega

Memoria de Tesis presentada por D. Antonio Abad Cuadri Vega, Ingeniero Químico, para aspirar al grado de Doctor en Ingeniería Química por la Universidad de Huelva con Mención Internacional.

Fdo.: Antonio Abad Cuadri Vega

La presente tesis ha sido realizada en el Departamento de Ingeniería Química, Química Física y Química Orgánica de la Universidad de Huelva, bajo la dirección de Dr. Pedro Partal López y Dr. Francisco Javier Navarro Domínguez, los cuales autorizan su presentación.

Fdo.: D. Pedro Partal López Fdo.: D. Francisco Javier Navarro Domínguez

Huelva, 2013



Universidad
de Huelva

AUTORIZACIÓN PARA LA DEFENSA DE LA TESIS DOCTORAL EMITIDA POR LA COMISIÓN ACADÉMICA DEL PROGRAMA DE DOCTORADO

DATOS DEL DOCTORANDO:

Apellidos y nombre: Cuadri Vega, Antonio Abad	NIF/ Pasaporte: 48935968H	Nacionalidad: Española
Dirección a efectos de notificaciones: Calle Huelva, Nº 44, Trigueros (Huelva), C.P.:21620		
Teléfono:959306187 / 627881073	EMAIL:antonio.cuadri@diq.uhu.es	

DATOS DE LA TESIS DOCTORAL:

Título: MODIFICACION FÍSICO-QUÍMICA DE BETUNES ASFÁLTICOS MEDIANTE AGENTES REACTIVOS / PHYSICO-CHEMICAL MODIFICATION OF ASPHALT BITUMENS BY REACTIVE AGENTS
Programa Oficial de Doctorado al que se adscribe y órgano responsable: Procesos y productos químicos. Departamento de Ingeniería Química, Química Física y Química Orgánica.
Línea de investigación a la que se adscribe y órgano responsable: Caracterización y procesado de productos derivados del petróleo. Departamento de Ingeniería Química, Química Física y Química Orgánica.
Directores: Dr. Pedro Partal López Dr. Francisco Javier Navarro Domínguez

A CUMPLIMENTAR POR LA COMISIÓN ACADÉMICA DEL PROGRAMA DE DOCTORADO:

Una vez valorada la Tesis Doctoral presentada por el Doctorando y haber incorporado éste las modificaciones y/o cambios que esta Comisión Académica le pudiera haber indicado, se AUTORIZA , en reunión de fecha _____, LA DEFENSA de la misma.

Huelva a _____ de _____ de _____

Firma de la Presidenta de la Comisión Académica

Fdo.: Dra. Concepción Valencia Barragán

PHYSICO-CHEMICAL MODIFICATION OF ASPHALT BITUMENS BY REACTIVE AGENTS

University of Huelva

Department of Chemical Engineering



**A thesis submitted for the degree of Doctor of Philosophy at
the University of Huelva, by Antonio Abad Cuadri Vega**

Supervisors:

Dr. Pedro Partal López, Professor in Chem. Eng.

**Dr. Francisco Javier Navarro Domínguez, Associate Professor in
Chem. Eng.**

Huelva, 2013

Acknowledgements

The results and conclusions derived from this dissertation were only possible due to the collaboration of several persons to whom I would like to express my gratitude.

First of all, I would like to thank my supervisors, Prof. Pedro Partal and Dr. Francisco Javier Navarro, for their constant interest, encouragement, suggestions, prompt response and valuable discussions that contributed immeasurably to the completion of this research.

Special thanks to Dr. Moisés García Morales who always gave me appropriate advices while conducting the project, and helped me at any time and for any reason.

I cannot forget all the members, from past and present, in the Chemical Process and Product Technology Research Center (Pro²TecS) at University of Huelva, who offered valuable suggestions during all this time, making me feel proud of working with them.

I would also like to extend my thanks to Prof. Gordon Airey and all co-workers from the Nottingham Transportation Engineering Centre (NTEC), Faculty of Engineering, University of Nottingham, who made my stay in Nottingham a good experience.

All my gratitude goes to my mother, brother and friends for their generous encouragement and, especially, to Mariche for her understanding, care and love.

Finally, this thesis is dedicated to my late father. His best memories continue helping me to never falter in my life.

Table of contents

Chapter I: INTRODUCTION.....	1
1.1. OVERVIEW.....	3
1.2. BACKGROUND.....	5
1.3. PROBLEM STATEMENT.....	8
1.4. RESEARCH OBJECTIVES.....	9
1.5. SCOPE OF THIS RESEARCH.....	10
1.6. REFERENCES.....	12
Chapter II: LITERATURE REVIEW.....	17
2.1. INTRODUCTION.....	19
2.2. BASIC CONCEPTS OF BITUMEN.....	19
2.2.1. Clarification of terminology.....	19
2.2.2. Types of bitumen.....	22
2.2.3. Bitumen applications.....	24
2.2.4. Bitumen chemical compositions.....	25
2.2.4.1. Saturates.....	27
2.2.4.2. Aromatics.....	28
2.2.4.3. Resins.....	28
2.2.4.4. Asphaltenes.....	28
2.2.5. Bitumen microstructure.....	29
2.2.5.1. Colloidal model of bitumen.....	29
2.2.5.2. The dispersed polar fluid (DPF) model.....	31
2.3. BITUMEN MODIFICATION.....	32
2.3.1. Polymer bitumen modification.....	37
2.3.1.1. Review of polymers.....	37
2.3.1.2. Modification via “passive” route.....	38
2.3.1.3. Modification via “active” route.....	40
2.3.2. Bitumen modification by reactive agents.....	44
2.4. BITUMEN RHEOLOGY.....	46
2.4.1. Classification of fluid behaviour.....	51
2.4.1.1. Newtonian fluid behaviour.....	51
2.4.1.2. Non-Newtonian fluid behaviour.....	52
2.4.2. Time-independent fluid behaviour.....	53
2.4.2.1. Shear-thinning or pseudoplastic.....	54
2.4.2.2. Viscoplastic fluid behaviour.....	54
2.4.2.3. Shear-thickening or dilatant fluid behaviour.....	55
2.4.3. Time-dependent fluid behaviour.....	56

2.4.3.1. Thixotropy.....	56
2.4.3.2. Rheopexy or negative thixotropy.....	56
2.4.4. Viscoelastic fluid behaviour.....	57
2.4.4.1. Stress Relaxation.....	59
2.4.4.2. Creep Response.....	59
2.4.4.3. Dynamic Response.....	61
2.4.4.4. Conversion among Viscoelastic Functions.....	64
2.4.5. Rheological model.....	65
2.4.5.1. The power-law or Ostwals de Waele model.....	65
2.4.5.2. The Carreau model.....	66
2.4.5.3. The Cross model.....	67
2.4.6. Time-Temperature Superposition.....	67
2.5. BITUMEN CHARACTERIZATION WITH ALTERNATIVE TECHNIQUES.....	70
2.5.1. Atomic Force Microscopy (AFM).....	71
2.5.2. Differential Scanning Calorimetry (DSC).....	73
2.5.3. Thin-layer chromatographic/flame ionization detection (TLC/FID).....	75
2.6. REFERENCES.....	76

Chapter III: MODIFIED BINDERS: PROCESSING AND TESTING.....	85
3.1. MATERIALS.....	87
3.1.1. Bitumen.....	87
3.1.2. Modifying agents.....	88
3.2. SAMPLES PREPARATION.....	92
3.2.1. Preparation of the isocyanate prepolymers.....	92
3.2.2. Preparation of the modified binders.....	93
3.3. MATERIALS TESTING.....	93
3.3.1. Technological tests.....	94
3.3.1.1. Penetration test.....	94
3.3.1.2. Ring & Ball softening point test.....	95
3.3.2. Chemical characterization.....	96
3.3.2.1. Thin-layer chromatographic/flame ionization detector analysis.....	96
3.3.2.2. Gel Permeation Chromatographic (GPC).....	97
3.3.3. Microstructural characterization.....	99
3.3.3.1. Atomic Force Microscopy (AFM).....	99
3.3.4. Rheological characterization	101
3.3.4.1. Steady state tests	101

3.3.4.2. Dynamic tests.....	102
3.3.4.3. Dynamic Mechanical Thermal Analysis.....	104
3.3.5. Thermal Analysis	104
3.3.5.1. Modulated Differential Scanning Calorimetry (MDSC).....	104
3.3.5.2. Thermogravimetric Analysis (TGA).....	106
3.4. REFERENCES.....	107

Chapter IV: BITUMEN MODIFICATION BY THIOUREA DIOXIDE.....	109
4.1. INTRODUCTION.....	111
4.2. EXPERIMENTAL.....	112
4.2.1. Materials.....	112
4.2.2. Samples preparation.....	113
4.2.3. Testing procedure.....	114
4.3. RESULTS AND DISCUSSION.....	115
4.3.1. Effect on binder formulation.....	115
4.3.1.1. Rheological behaviour at medium/high in- service temperature.....	116
4.3.1.2. Rheological behaviour at low in-service temperature.....	120
4.3.2. Effect on binder formulation.....	125
4.3.2.1. Influence on the viscous flow behaviour.....	126
4.3.2.2. Influence on linear viscoelastic behaviour.....	129
4.3.3. Bitumen modification routes and microstructure.....	132
4.4. REFERENCES.....	142

Chapter V: BITUMEN MODIFICATION BY THIOUREA.....	147
5.1. INTRODUCTION.....	149
5.2. EXPERIMENTAL.....	150
5.2.1. Materials.....	150
5.2.2. Samples preparation.....	151
5.2.3. Testing procedure.....	152
5.3. RESULTS AND DISCUSSION.....	153
5.3.1. High in-service binder performance.....	153
5.3.2. Low in-service binder performance.....	159
5.3.3. On the chemistry behind bitumen modification.....	167
5.4. REFERENCES.....	177

Chapter VI: BITUMEN MODIFICATION BY -NCO FUNCTIONALIZED CASTOR OIL PREPOLYMERS.	181
6.1. INTRODUCTION	183
6.2. TESTING PROCEDURES	185
6.3. PREPOLYMERS CHARACTERIZATION	186
6.3.1. Synthesis.....	186
6.3.2. Effects of -NCO/-OH ratio on thermo-rheological prepolymer response.....	188
6.4. BITUMEN MODIFICATION BY MDI-CO PREPOLYMERS	195
6.4.1. Materials and modified binders preparation.....	195
6.4.2. Influence of prepolymer formulation.....	196
6.4.3. Effects of processing/curing conditions.....	206
6.4.4. Enhancement of MDI-CO as modifier.....	218
6.4.4.1. Materials and modified binders preparation.....	218
6.4.4.2. Prepolymers synthesis and characteristics.....	220
6.4.4.3. Bitumen reactive modification through urethane/urea chemical bonds.....	225
6.4.4.4. Urethane-based bitumen modification.....	228
6.5. REFERENCES	234
Chapter VII: CONCLUSIONS	239
7.1. CONCLUSIONS	241
Chapter VIII: RESUMEN Y CONCLUSIONES EN ESPAÑOL	243
8.1. VISION GENERAL	245
8.2. PLANTEAMIENTO DE LA PROBLEMÁTICA	248
8.3. OBJETIVOS DE LA INVESTIGACIÓN	249
8.4. MATERIALES DE PARTIDA	250
8.5. ESTRUCTURA DE LA TESIS	252
8.6. RESULTADOS MÁS RELEVANTES	253
8.6.1. Capítulo IV: Modificación del betún mediante dióxido de tiourea.....	253
8.6.1.1. Efecto sobre la formulación de las mezclas bituminosas.....	253
8.6.1.2. Efecto de la temperatura de procesado.....	256
8.6.1.3. Rutas de modificación del betún y microestructura.....	258

8.6.2. <i>Capítulo V: Modificación del betún mediante tiourea</i>	260
8.6.2.1. <i>Respuesta a alta temperatura de servicio.....</i>	260
8.6.2.2. <i>Respuesta a baja temperatura de servicio.....</i>	261
8.6.2.3. <i>Cambios químicos del betún debido a la modificación.....</i>	263
8.6.3. <i>Modificación del betún mediante prepolímeros basados aceite de ricino funcionalizados con grupos isocianatos.....</i>	266
8.6.3.1. <i>Caracterización de los prepolímeros.....</i>	266
8.6.3.2. <i>Modificación del betún mediante prepolímeros MDI-CO.....</i>	268
8.6.3.3. <i>Mejora de los prepolímeros MDI-CO como agentes modificadores.....</i>	272
8.7. CONCLUSIONS.....	276
Chapter IX: ANNEXES.....	279
9.1. ANNEXE I: LIST OF FIGURES.....	281
9.2. ANNEXE II: LIST OF TABLES.....	288
9.3. ANNEXE III: LIST OF SYMBOLS AND ACRONOYMS	291
9.4. ANNEXE IV: PAPERS PUBLISHED AND CONFERENCE CONTRIBUTIONS.....	295
9.4.1. <i>Conference contributions.....</i>	295
9.4.2. <i>Patents.....</i>	296
9.4.3. <i>Papers published.....</i>	296

INTRODUCTION

Chapter I

*Physico-chemical modificacion of asphalt
bitumens by reactive agents*

1.1. OVERVIEW

Bitumen has long been used in numerous engineering applications that range from the construction of road pavements (Whiteoak and Read, 2003) to waterproof membranes for the roofing industry (Fawcett and Lor, 1992). On account of its properties (impermeability, adhesiveness, elasticity, ductility, etc.), bitumen is the most suitable material to be used as a binder of mineral aggregates for paving industry, and consequently, roads are mainly constructed using a composite mixture of bitumen (~ 5 wt.%) and mineral aggregates. Despite its small proportion, bitumen forms the continuous matrix and is the only deformable component in the pavements. Therefore, as bitumen is responsible for the viscoelastic behaviour characteristic of this material, it plays a relevant role in predicting roads performance (Vasiljevic et al., 2010).

It is known that, after a limited life-time, the combined action of extreme temperatures along with a continuous increase in traffic loads may lead to well-known asphalts distresses. In order to build roads that better resist climate and traffic, paving industry is continuously developing new modified binders with enhanced rheological properties. In this sense, the three following considerations must be taken account (Lesueur, 2009):

- The binder has to be fluid enough at high temperature (160 °C) to be pumpable and workable to allow for a homogeneous coating of the aggregates upon mixing.
- It has to become stiff enough at the highest in-service pavement temperature to resist rutting (around 60 °C, depending on local climate).

- It must remain soft enough at the lowest pavement temperature to resist cracking (down to around $-20\text{ }^{\circ}\text{C}$, depending on local climate).

All these properties are quite opposite, and it is therefore difficult to obtain binders that would work under all possible climates. In this sense, a considerable research effort has been expended in modifying the properties of bituminous binders to improve the performance of road pavements. One of the major types of modifiers that have found wide acceptance in the paving industry is the polymer modified bitumen (PMB). A variety of these polymer modified types have been developed to improve perceived limitations of the bitumen and mix to fatigue resistance, permanent deformation, thermal fracture and moisture sensitivity (Topal, 2010; Yildirim, 2007).

In general, polymers may be classified as: (1) dispersed or (2) reactive systems. Dispersed systems are the most common used (e.g. SBS: styrene butadiene styrene; SBR: styrene butadiene rubber; SEBS: styrene ethylene butylene styrene; EVA: ethylene vinyl acetate and PE: polyethylene) (Akmal and Usmani, 1999; Bellio and Patti, 1995; Navarro et al., 2002). Typically, these polymers create a polymer network but always remain in a separate phase from the base (unmodified) bitumen, and their binders become unstable when stored at high temperatures ($160\text{-}220\text{ }^{\circ}\text{C}$) (Pérez-Lepe et al., 2006). In contrast to dispersed system, binder modification through reactive polymers takes places by chemical reactions between the polymer and bitumen compounds.

Alternatively, the paving industry is also interested in development of modified bitumens by reactive agents such as polyphosphoric acid, sulfur, etc. These additives are capable of chemically interact with specific bitumen fractions and may help overcome that storage-related

disadvantage (Becker et al., 2003; Iqbal et al., 2006; Polacco et al., 2004a; 2004b).

In order to get novel binders with enhanced rheological properties for road paving industry, we herein propose the use of different reactive agents: two non- polymeric additives (thiourea dioxide and thiourea, abbreviated as “ThD” and “Th”, respectively) and a castor oil functionalized with isocyanate groups (isocyanate-terminated prepolymers), referred to as MDI-CO.

It is worth mentioning that the bitumen modification by these non-polymeric modifiers (well-known in many other industrial applications as a reducing agent) represent an alternative to other classic acid bitumen modification with PPA (polyphosphoric acid), with the additional benefit of anticorrosion properties of ThD and Th in opposition to storage tanks corrosion (Masson et al., 2008).

On the other hand, the use of polyurethanes as modifying agents have been extensively developed by the paving industry (Martín-Alfonso et al., 2008; Carrera et al., 2010; Izquierdo et al., 2011; Singh et al., 2003). They are produced as a result of the reaction between hydroxyl and isocyanate groups, at ambient temperatures, without the use of catalyst. In this work, a vegetable oil-based polyol (castor oil) functionalized with polymeric MDI (4,4', diphenylmethane diisocyanate) may become a promising alternative to those from petrochemical feedstock, such as PPG or PEG, in agreement with the concept of sustainable and environmental development.

1.2. BACKGROUND

The earliest record of human use of bitumen to date, is as a hafting material 180,000 years ago in the El Kowm Basin in Syria, where it was

applied to stick flint implements to the handles of various tools in a way that persisted until Neolithic time (Connan, 1999). Firstly, its adhesive and waterproofing properties were generally emphasized. Even there are various references to bitumen in the Bible.

Genesis reveals that Noah's ark was covered inside and outside by pitch, and therefore we know that it was black or dark brown in colour:

"And God said to Noah,... make rooms in the ark, and cover it inside and out with pitch. This is how you are to make it: the length of the ark three hundred cubits, its breadth fifty cubits, and its height thirty cubits." (Genesis 6:13-18 RSV).

The Tower of Babel used sticky pitch as mortar:

"Now the whole earth had one language and few words. And as men migrated from the east, they found a plain in the land of Shinar and settled there. And they said to one another, "Come, let us make bricks, and burn them thoroughly." And they had brick for stone, and bitumen for mortar." (Genesis 11:1-4 RSV).

Prior to the incineration of Sodom and Gomorrah, the area of the Dead Sea had open bitumen pits:

"Now the Valley of Siddim was full of bitumen pits; and as the kings of Sodom and Gomorrah fled, some fell into them, and the rest fled to the mountain." (Genesis 14:8-10 RSV).

The reed basket that carried the infant Moses into the Nile River was waterproofed with pitch:

"And when she could hide him no longer she took for him a basket made of bulrushes, and daubed it with bitumen and pitch; and she put the

child in it and placed it among the reeds at the river's brink. And his sister stood at a distance, to know what would be done to him." (Exodus 2:1-4 RSV).

Many thousands of years before crude oil exploration and its industrial processing began, the numerous advantages of bitumen had already been recognized. The production of this material started with the use of natural deposits of bitumen. Examples of natural deposits are the Trinidad Lake deposits on the Island of Trinidad, Bermudas Lake deposits and the tar sands throughout western Canada (Roberts et al., 1991).

The first mention of the use of bitumen in road construction dates back to Nabopolassar, King of Babylon (625-604 B.C.): a bitumen-containing mortar cemented both the foundation made of three or more courses of burnt bricks and the stone slabs put on top (Abraham, 1960). However, bitumen essentially disappeared from the pavements until the early 19th century, when the importance of natural bitumen consumption increased, for example, attempts were made to utilize rock asphalt from European deposits for road surfacing. However, at the end of the 19th century, the major use of bitumen was centered in the paving industry (Whiteoak and Read, 2003). Consequently, there was a dramatic increase in bitumen demand with the result that natural deposits could not provide enough bitumen and nowadays, the paving grade bitumen is almost exclusively obtained from vacuum residue of petroleum distillation.

Nowadays, bitumen is the residue of certain crude oils after the removal of the volatile components (Zakar, 1971) and it is a highly viscous, sticky and dark brown to black material. There are about 1500 different crude oils produced throughout the world but only a few of these are suitable for the manufacture of bitumen (Whiteoak and Read, 2003). It has a complex microstructure and contains different types of molecular species

(hydrocarbons) which, in terms of solubility in n-heptane, are classified into two major fractions: maltenes and asphaltenes. Moreover, bitumen also contains compounds of sulfur and nitrogen and small quantities of metals as iron, nickel and vanadium. Bitumen quality greatly depends on two factors: a) crude source; and b) refining process involved. Thus, crude petroleum consists mainly of aliphatic compounds, cyclic alkanes, aromatic hydrocarbons, polycyclic aromatic compounds, and metals. The proportions of these chemicals can vary greatly due to significant differences in crude petroleum from oil field to oil field, or even at different locations in the same oil field. On the other hand, the specific procedure followed in the crude oil fractionation may notoriously change the physical properties of bitumen.

1.3. PROBLEM STATEMENT

According to Eurobitume, it is estimated that the current world use of bitumen is around 102 million tonnes per year. Approximately 85 % of all the bitumen produced is used as the binder in asphalt for road applications. There exist many factors that influence the road performance: nature of aggregates, interaction between bitumen and aggregates, mixture permeability, climate, etc. With this regard, two main load-associated failures were identified as critical pavements distress in which bitumen plays an important role: a) cracking (fatigue or thermal cracking); and b) permanent deformation or “rutting” (Figure 1.1).



Figure 1.1. Some examples of the different types of distresses: a) fatigue cracking; b) rutting; c) thermal cracking.

The cracking phenomenon is associated with stress induced in the asphalt layer by wheel loads, temperature changes or a combination of both. Cracking relates to fracture of the pavement and occurs when the tensile stress and strain induced by traffic and/or temperature changes exceeds the breaking strength of the mixture (Brown and Brunton, 1986).

Permanent deformation or rutting of flexible pavements is a result of accumulated plastic deformation, which is caused by repeated application of loads (Anderson and Kennedy, 1993; Bahía and Anderson, 1995; Shashidhar et al., 1995) under moving or stationary traffic and, particularly under the high shearing stresses imposed by braking, accelerating or turning traffic (Whiteoak and Read, 2003). It occurs primarily at intermediate/high temperatures where bitumen viscoelastic behaviour is more viscous resulting in non-recoverable deformation. As a consequence, it produces the formation of longitudinal depressions (or ruts) in the vehicle wheel paths.

1.4. RESEARCH OBJECTIVES

The main goal of this work, which is a part of a research project sponsored by “Junta de Andalucía” (TEP6689) and also funded by “Ministerio de Educación” through a F.P.U. research grant (AP2008-01419), is to obtain bituminous binders with enhanced rheological properties by new reactive

bitumen modification routes. In order to successfully achieve this goal, a) thiourea dioxide, b) thiourea and c) isocyanate prepolymers (formulated with a vegetable oil-based polyol functionalized with polymeric 4,4', diphenylmethane diisocyanate) are proposed as reactive modifying agents.

The specific objectives of this work may be summarized in the following items:

- a) To find new bitumen modification routes by reactive agents for enhancing the engineering properties of bituminous binders.
- b) To understand how the bitumen modification via non-polymeric additives (thiourea dioxide and thiourea) occurs.
- c) To develop NCO-terminated prepolymers obtained from biomass-derived polyol (castor oil) as a more sustainable and environmental bitumen modification procedure.
- d) To study the effects that isocyanate-prepolymer characteristics and processing/curing conditions exert on the thermal and rheological properties of the resultant bituminous binders.

1.5. SCOPE OF THIS RESEARCH

This manuscript is organized into the following nine chapters:

CHAPTER I includes a brief introduction and a general background on the bitumen field, and presents the objectives and scope of this research.

CHAPTER II reviews general concepts on bituminous binders and provides information on those polymers commonly used for bitumen modification, with particular emphasis on “active” polymers and polyurethanes. In

addition, basic concepts of rheology, which may facilitate the understanding of further results, are included.

CHAPTER III describes the different raw materials used, processing procedures followed in the preparation of the modified binders and the testing methods for their physico-chemical, thermo-mechanical and rheological characterization.

CHAPTER IV evaluates the effect of thiourea dioxide addition on the thermo-mechanical properties, in a wide interval of in-service temperatures, of two asphaltic bitumens with different penetration grades. It also describes modification routes for each of the three selected processing temperatures.

CHAPTER V deals with the enhancement in the linear viscoelastic properties of a bituminous binder via thiourea-modification and explores the chemistry behind this bitumen modification. In addition, this chapter emphasizes the use of master curves, obtained by the application of TTSP to isothermal frequency sweeps and further frequency-temperature conversion, as a means to achieving adequate viscoelastic characterization of binders at low temperatures.

CHAPTER VI proposes NCO-terminated prepolymers obtained from biomass-derived polyols (castor oil), as an alternative to the use of other petrochemicals in the paving industry, in the manufacture of bituminous binders with enhanced rheological properties. It also studies the effects that variables such as prepolymer formulation and processing/curing conditions provoke on the bituminous rheological properties.

CHAPTER VII summarizes the most outstanding conclusions derived from this research.

CHAPTER VIII contains a summary of thesis and conclusions in Spanish.

CHAPTER IX includes a glossary with symbols and acronyms used throughout this dissertation and various relevant documents arisen as a result of this investigation.

1.6. REFERENCES

Abraham H. Asphalt and Allied Substances. 1960, 6th Edition, New York: Van Nostrand.

Akmal N, Usmani AM. Asphalt, Number One Thermoplastic Polymer, *Polym. News*, 1999, 24, 136–140.

Anderson DA, Kennedy TW. "Development of SHRP binder Specification". *J. Assoc. Asphalt Pav.*, 1993, 62, 481-507.

Bahia HU, Anderson DA. The New Proposed Rheological Properties of Asphalt Binders: Why are they Required and how do they Compare to Conventional Properties. *Am. Soc. Test. Mater.: ASTM STP 1241*, 1995, 1-27, Philadelphia.

Becker Y, Müller AJ, Rodríguez Y. Use of rheological compatibility criteria to study SBS modified asphalts. *J. Appl. Polym. Sci.*, 2003, 90, 1772–1782.

Bellio E, Patti N. Bitumens modified by polymeric compositions, *European Patent*, EP0667374 (A2), 1995.

Brown SF, Brunton JM. An Introduction to the analytical design of bituminous pavements, 3rd Edition, 1986, University of Nottingham, Nottingham.

Carrera V, Partal P, García-Morales M, Gallegos C. Effect of processing on the rheological properties of poly-urethane/urea bituminous products. *Fuel Process. Technol.*, 2010, 91(9), 1139-1145.

Connan J. Use and trade of bitumen in antiquity and prehistory: molecular archaeology reveals secrets of past civilizations. *Phil. Trans. R. Soc. Lond. B*, 1999, 354, 33-50.

Fawcett AH, Lor SK. Studies on membranes composed of polymer-bitumen blends. *Polymer*, 1992, 33(9), 2003-2006.

Iqbal MH, Hussein IA, Al-Abdul Wahhab HI, Amin HB. Rheological Investigation of the influence of acrylate polymers on the modification of asphalt. *J. Appl. Polym. Sci.*, 2006, 102, 3446-3456.

Izquierdo MA, Navarro FJ, Martínez-Boza JF, Gallegos C. Novel stable MDI isocyanate-based bituminous foams. *Fuel*, 2011, 90, 681-688.

Lesueur D. The colloidal structure of bitumen: Consequence on the rheology and on the mechanisms of bitumen modification. *Adv. Colloidal Interfac.*, 2009, 145, 42-82.

Martín-Alfonso MJ, Partal P, Navarro FJ, García-Morales M, Gallegos C. Role of water in the development of new isocyanate-based bituminous products. *Ind. Eng. Chem. Res.*, 2008, 47, 6933-6940.

Masson JF. Brief Review of the chemistry of polyphosphoric acid (PPA) and bitumen. *Energ. Fuel*, 2008, 22, 2637-2640.

Navarro FJ, Partal P, Martínez-Boza F, Valencia C, Gallegos C. Rheological characteristics of ground tire rubber-modified bitumens. *Chem. Eng. J.*, 2002, 89(1-3), 53-61.

Pérez-Lepe A, Martínez-Boza FJ, Attané P, Gallegos C. Destabilization mechanism of polyethylene-modified bitumen. *J. Appl. Polym. Sci.*, 2006, 100, 260–267.

Polacco G, Stastna J, Biondi D, Antonelli F, Vlachovicova Z, Zanzotto L. Rheology of asphalts modified with glycidylmethacrylate functionalized polymers. *J. Colloid. Interf. Sci.*, 2004a, 280(2), 366-373.

Polacco G, Stastna J, Vlachovicova Z, Biondi D, Zanzotto L. Temporary networks in polymer modified asphalts. *Polym. Eng. Sci.*, 2004b, 44(12), 2185-2193.

Read J, Whiteoak D. *The Shell Bitumen Handbook. 5th Edition London (UK)*, Thomas Telford Publishing 2003.

Roberts FL, Kandhal PS, Brown ER, Lee D, Kennedy TW. *Hot Mix Asphalt Materials, Mixture Design and Construction*: National Centre for Asphalt Technology (NCAT), 1991, NAPA Education Foundation, Lanham, MD.

Singh B, Tarannum H, Gupta M. Use of isocyanate production waste in the preparation of improved waterproofing bitumen. *J. Appl. Polym. Sci.*, 2003, 90, 1365-1377.

Shashidhar N, Needham SP, Chollar BH. Rheological properties of chemically modified asphalts. *Transp. Res. Record*, 1995, 89-95.

Topal A. Evaluation of the properties and microstructure of plastomeric polymer modified bitumens. *Fuel Procc. Technol.*, 2010, 91, 45-51.

Vasiljevic-Shikaleska A, Popovska-Pavloska F, Cimmino S, Duraccio D, Silvestre C. Viscoelastic properties and morphological characteristics of polymer modified bitumen blend. *J. Appl. Polym. Sci.*, 2010, 118, 1320–1330.

Yildirim Y. Polymer modified asphalt binders. *Constr. Build. Mater.*, 2007, 21, 66-72.

Zakar P. Asphalt. New York: Chemical Publishing Company, 1971.

LITERATURE REVIEW

Chapter II

*Physico-chemical modificacion of asphalt
bitumens by reactive agents*

2.1. INTRODUCTION

This chapter summarizes the principal findings from a review of selected literature concerning the principal aspects of bitumen as well as its modification and rheological/chemical characterization. This literature review comprises four sections:

- ✓ The first section of the literature review is concerned with general information on the bitumen field: chemical composition, types, microstructure and properties derived thereof, applications and clarification of the terminology used.
- ✓ The second one deals with bitumen modification. It aims to describe the reasons for modification, introduces different types of bituminous binders, especially those obtained by polymer (PMB) and “reactive” agents, and describes the mechanisms developed for each of them.
- ✓ In order to facilitate the understanding of further results, a comprehensive review on the basic concepts of bitumen rheology is described in the third section.
- ✓ Finally, the fourth section gathers others bitumen characterization techniques: Atomic Force Microscopy (AFM), Differential Scanning Calorimetry (DSC) and Thin-Layer Chromatography/Flame ionization detection (TLC/FID) provide interesting information.

2.2. BASIC CONCEPTS OF BITUMEN

2.2.1. Clarification of terminology

Numerous definitions have been proposed for bitumen, asphalt and related substances, some of them quite opposite and scientifically incorrect

(Abraham, 1960; Pfeiffer, 1950). They present bitumen as a pasty or semi-solid material, when the correct description would be that of a viscoelastic liquid at room temperature (as will be described in section 2.4 “Bitumen rheology”) produced by removing the lightest fractions from heavy crude oil during its refining process.

To avoid confusion and misunderstanding that may arise from the use of different terms such as bitumen, asphalt, etc., it is essential to be clear about terminology. In this sense, according to the international terminology related to these materials, an evident lack of uniformity is observed, not only in the definitions of these products but even in their nomenclature, fundamentally between the United States and the European countries.

In the European terminology, “*asphalt*” or “*native/natural asphalt*” is considered as the natural deposits consisting of natural bitumen and mineral matter. It has been used as an adhesive, sealant and waterproofing agent for over 8000 years. But it occurs only in small quantities and its properties are quite different from refined bitumen (Delano, 2007). Some of these deposits are of high historic importance. As an example, the asphalt from the Dead Sea, also called Lake Asphaltite, is the main source of asphalt described in the literature from ancient time until the modern era. It exists there in the form of an asphaltic limestone, containing typically 5 wt.% bitumen impregnating a porous limestone. The sources, from which the modern use of bitumen evolved, especially in Europe, were the deposits of Seyssel in France and Val de Travers in Switzerland. The reference material for paving applications in the U.S. at the beginning of the 20th century was the Trinidad Lake asphalt, which is one of the largest asphalt deposits in the World (Lesueur, 2009).

On the other hand, in British English, the word “*asphalt*” or “*asphalt mixture*” refers to a mixture of mineral aggregate and bitumen. It is also known as tarmac, which was once made with tar rather than bitumen. However, the differences in U.S. terminology can cause confusion:

- Bitumen is called asphalt in the U.S.
- Asphalt (or tarmac) is called pavement or asphaltic concrete in the U.S.

In addition, bitumen also may be confused with “*tar*” and “*petroleum pitch*”. Thus, although bitumen and coal tar are similarly black and sticky, they are distinctly different substances in origin, chemical composition and in their properties. Coal tar is produced by heating coal to extremely high temperatures and is a by-product of gas and coke production. Although it was widely used as the binding agent in road asphalt in the early part of the last century, it has subsequently been replaced by refined bitumen. Preferably, and in a more rigorous sense, the word tar should be restricted to the products of the destructive distillation (pyrogenation) of various organic sources (coal, wood, etc.).

In addition, bitumen is also confused with petroleum pitch which, although also derived from crude oil, is a substance produced by a different process from that used for refined bitumen. Petroleum pitches are the residues from the extreme heat treatment or “cracking” of petroleum fractions. Their properties and chemical composition are therefore quite different from those of bitumen.

In this Ph.D. research, the word bitumen is used in the European sense and the word “*asphalt mixture*” is leaved to the mixture between mineral aggregate and bitumen.

2.2.2. Types of Bitumen

According to B.P. Bitumen company bitumen is classified as follows:

Paving grade bitumen

Paving grade bitumen is the most widely used bitumen and is refined and blended to meet road engineering and industrial specifications that take into account different climatic conditions. Specifications for penetration graded bitumen normally state the penetration range for a grade, e.g. 50/70. Other tests are used to classify the bitumen for specification purposes, such as softening point, solubility, flash point, etc.

Cutback bitumen

Cutback bitumens consist of bitumen that has been diluted in solvent (cutter or flux) to make it more fluid for application. The fluidity of cutback bitumens depends on the degree of hardness of the bitumen and the proportion of diluent. Cutback is classified according to the time it takes for them to cure, or become solid due to the evaporation of the diluent. Classifications are rapid curing (RC), medium curing (MC) or slow curing (SC). A cutback varies in behaviour according to the type of cutter or flux used as the diluent with the white spirit commonly used for RC grades, kerosene for MC and diesel for SC.

Industrial bitumen

Industrial bitumens (or oxidized bitumens) are made by blowing air through hot paving grade bitumen and was the first process that led to the manufacture of bitumen from an otherwise too fluid crude source (Krchma and Gagle, 1974; Speight, 1999). It consists in air-oxidizing the oil (or soft bitumen) for a few hours at 200–275 °C, sometimes in the presence of a

catalyst, such as copper sulphate, zinc, ferric or aluminium chloride, boric acid or phosphorous pentoxide (Corbett, 1965). The properties of the resulting material depend on the crude origin (or the soft bitumen) and the operating conditions, especially blowing temperature and time. It remains the best process to make very hard bitumens, especially for waterproofing. For paving applications, however, air-blown bitumens were discarded because they were too susceptible to cracking (PIARC, 1999).

Bitumen emulsion

Bitumen emulsions are dispersions of bitumen in water. Hot bitumen, water and emulsifier are processed in a highspeed colloidal mill that disperses the bitumen in the water in the form of small droplets. Bitumen emulsions have a low viscosity compared to the bitumen from which they are produced and can be workable at ambient temperatures. Their application requires controlled breaking and setting. The emulsion must not break before it is laid on the road surface but, once in place, it should break quickly so that the road can be in service again without delay. The cationic emulsions are preferred in the most application because the positively charged globules of bitumen, better coat the majority of aggregate types and result in greater adhesion.

Modified bitumens

Modified bitumens are bituminous binders formulated with additives to improve their service performance by changing such properties as durability, resistance to ageing, adhesive or cohesion strength. These agents may be polymers (such as SBS, PBD or EVA), crumb rubber, sulphur and polyphosphoric acid, among other materials. Polymer modified binders (PMB) are one of the major advancement in bituminous binder

technology as these materials better satisfy the demands of increasing traffic volumes and loads on our road networks.

2.2.3. Bitumen Applications

Over 80 % of the 100 million tonnes of worldwide annual bitumen consumption is used for paving applications in the construction and maintenance of roads (B.P. Bitumen Company).

An understanding of how roads are built is necessary for an appreciation of the importance of the role played by bitumen. Modern road design and construction techniques are aimed at building flexible road layers or courses so that the tensile and compressive stresses imposed by passing traffic are distributed evenly through these layers, according to their relative strengths. This ensures that neither the ground supporting the road nor the individual layers are permanently deformed by these concentrated stresses.

The courses must also be made weather resistant and durable. Bitumen plays a major part in meeting this requirement because it strongly binds the aggregate particles and seals and fills the voids between them. Its effectiveness depends on the aggregate specification, the size and number of voids and the type of bitumen. By sealing the gaps, bitumen makes it difficult for water to penetrate the road courses and damage the natural foundation of the road. In addition, the viscous nature of the bitumen, which is the only deformable component of bitumen, allows the asphalt to sustain significant flexibility, creating a very durable surface energy.

The use of bitumen in others industrial applications accounts for less than 20 % of world bitumen consumption. It is nevertheless important to those manufacturers and engineers who rely on its particular properties as an

economical binder and protector. In many parts of the world it is used extensively to waterproof the roofs of houses, often in the form of shingles, which are strips of felt first impregnated with bitumen and then covered on both sides with harder bitumen and a coating of mineral granules. A similar construction technique involves sheets of bitumen saturated felt laid onto a flat roof with layers of bitumen below, between and above them. By contrast, bitumen is also used in damp-proofing and floor tiles.

Other materials, particularly felts and papers, are impregnated with bitumen to improve their performance as insulators. Packaging papers, printing inks, linoleum, sound deadening felts hidden inside car bodies and undersealing compounds beneath them, electrical insulating compounds and battery boxes are some of the hundreds of industrial and domestic products likely to contain industrial grade bitumen.

2.2.4. Bitumen Chemical Composition

The chemical constitution of bitumen has a strong influence on its rheological behavior, solubility, volatility and attachment to other materials. Bitumen is a complex mixture of molecules of a predominantly hydrocarbon nature with a minor amount of structurally analogous heterocyclic species and functional groups containing sulphur, nitrogen and oxygen atoms (Traxler, 1936; Romberg et al., 1959; Traxler and Coombs, 1936). Bitumen also contains traces of metals such as vanadium (the most numerous, up to 2000 ppm), nickel (up to 200 ppm), iron, magnesium and calcium which occur in the form of inorganic salts and oxides or in porphyrin structures (Speight, 1999).

Table 2.1. Chemical composition of bitumen. Data from Lesueur (2009).

Element	Concentration (wt.%)
Carbon	80 – 88
Hydrogen	8 – 12
Sulphur	0 – 9
Oxygen	0 - 2
Nitrogen	0 - 2

The number-average molecular weight of bitumen is typically in the range 600-1500 g/mol (Branthaver et al.,1936). Still, the distribution extends to molecular weights up to 15000 g/mol and the values found in the literature can vary somewhat depending on the experimental set-up (Domin et al., 1999).

The bitumen chemistry on a global basis is not sufficient to understand the properties of bitumen. Therefore, researchers generally gain an insight into bitumen chemical structures by examining the behaviour of some “typical” functional groups. The separation of bitumen into different chemical groups has generally been made by many different techniques (Nelson, 1948; Thomas, 1973). These techniques divide bitumen based on molecular size, chemical reactivity and/or polarity. The fractions so obtained are made up of two broad families of compounds, maltenes and asphaltenes. The maltenic fraction can still be divided into three generic groups of different molecular weight and aromaticity (in decreasing order of these features): resins, aromatics and saturates (Claudy et al., 1990; Claudy et al., 1991).

The most common method available for separating bitumen into fractions is by means of various chromatographic techniques. There are, however, many modifications and variations of this essential technique, but the basis

is to precipitate the asphaltenes using n-alkane (usually n-pentane or n-heptane) (ASTM D3279), followed by chromatographic separation of the remaining maltene material. Therefore, its composition is usually given in terms of the relative quantities of the SARAs fractions (Saturates, Aromatics, Resins and Asphaltenes).

2.2.4.1. Saturates

Saturates comprise straight and branched-chain aliphatic hydrocarbons together with alkyl-naphthenes and some alkyl-aromatics. They are non-polar viscous oils, straw or white in colour, with a similar molecular weight range to aromatics (Figure 2.1). Their solubility parameter lies between 15 and 17 MPa^{0.5} (Speight, 1999) and their density, at 20 °C, around 0.9 g/cm³ (Corbett, 1965).

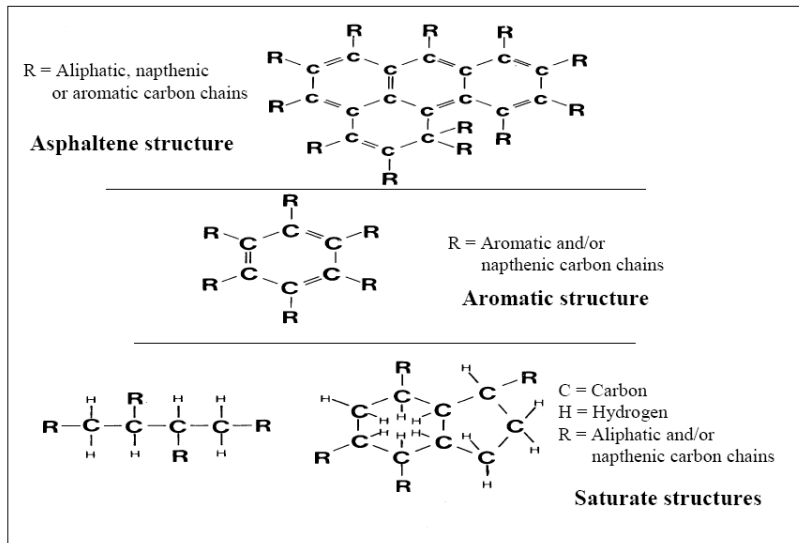


Figure 2.1. Schematic representation of the molecular structures of different components of bitumen. Data from Shell bitumen Handbook (2003).

2.2.4.2. Aromatics

The aromatic portion is mostly naphtheno-aromatic hydrocarbons with three or four naphthenic rings per molecule. They are the most abundant constituents of bitumen together with resins. They are dark brown viscous liquids with the average molecular weight ranging from 300 to 2000 (Whiteoak and Read, 2003). Aromatics (and saturates) have a key feature of dispersing polar agglomerations of asphaltenes and resins. Thus, this component is very important and it is responsible for viscosity and fluidity of the asphalt (Figure 2.2). Their solubility parameter lies between 17 and 18.5 MPa^{0.5} (Speight, 1999) and their density, at 20 °C, around 1 g/cm³ (Corbett, 1965).

2.2.4.3. Resins

Resins are semi-solid and sometimes solid materials of dark red colour at room temperature. They are chemically very similar to the asphaltenes. They also contain carbon, hydrogen, oxygen, sulfur, nitrogen and many other elements including metals. Resins are not as polar as asphaltenes and their molecular weight ranges from 500 to 50000. Resins provide adhesion, ductility, malleability and plasticity, and are dispersing agents or peptisers for the asphaltenes. The proportion of resins to asphaltenes governs the solution (SOL) or gelatinous (GEL) character of the bitumen. (Whiteoak and Read, 2003). Their solubility parameter lies between 18.5 and 20 MPa^{0.5} (Speight, 1999) and their density, at 20 °C, around 1.07 g/cm³ (Corbett, 1965).

2.2.4.4. Asphaltenes

They are the most complex molecules present in bitumen. They are black or brown coloured, hard, non-plastic, non-malleable, high molecular

weight compounds ranging between 600 and $2 \cdot 10^5$. They contain predominantly carbon and hydrogen with sulfur, oxygen, nitrogen and other heteroatoms (Figure 2.1). Asphaltenes are agglomerations of the most highly polar molecules and they are responsible for the presence of structure in bitumen. They are insoluble in low molecular weight normal paraffins and are classified by the precipitating solvent; different solvents precipitate different amount of asphaltenes. They impart strength, stiffness and colloidal structure in bitumen (Thomas, 1973, Oyenkunle, 2006). Their solubility parameter lies between 17.6 and 21.7 MPa^{0.5} (Speight, 1999) and their density, at 20 °C, around 1.15 g/cm³ (Corbett, 1965). It was, however, shown by Rogel (1995) that the solubility parameter can vary with the aggregation state and, therefore, these values must be used with care.

2.2.5. Bitumen Microstructure

2.2.5.1. Colloidal model of bitumen

The theory of the colloidal structure of bitumens, although not universally accepted, is one of the most known. This colloidal model was first proposed by Nellensteyn in the 1920's (Nellensteyn, 1923; 1924) and, later, the model was developed by Pfeiffer and co-workers to explain the difference in rheological properties between what they called SOL and GEL bitumen (Pfeiffer and Saal 1940; Saal and Labout 1940).

The basic premise of this model is that colloidal micelles, consisting of moderately polar molecules surrounding highly polar asphaltenes, are dispersed throughout a continuous, non-polar phase (Anderson and Christenson, 1991). Thus, the asphaltenes, which are the highest molecular weight components, are dispersed in the lower molecular weight maltenes (i.e. aromatics, saturates, resins) (Figure 2.2). According to this model, the rheology of bitumen can be greatly affected by the degree of effectiveness

to which the resins can keep the asphaltene fraction dispersed in the maltene oil fraction. Bitumens containing highly peptized asphaltenes generally exhibit Newtonian behaviour, while non-Newtonian flow is usually the characteristic of bitumens with lower amounts of dispersed asphaltenes (Roberts et al., 1991).

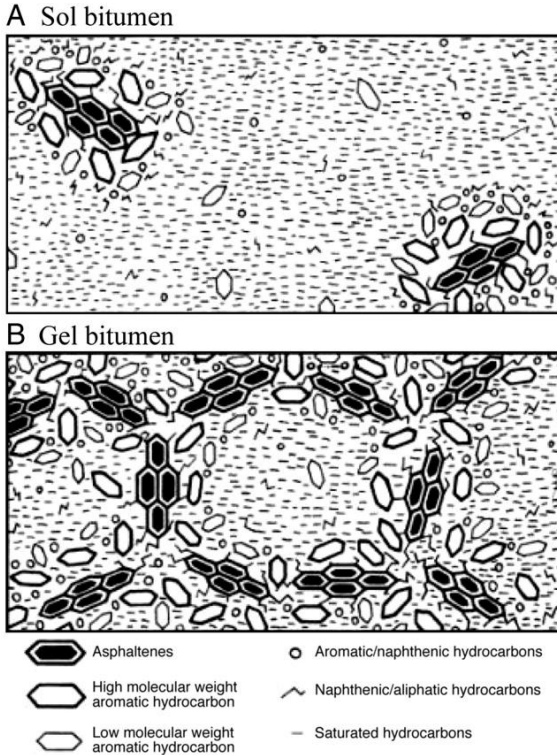


Figure 2.2. Schematic representation of bitumen. Data from Shell bitumen Handbook (2003).

Furthermore, the physico-chemical properties of bitumen are a function of the relative proportion of these fractions. In general, the colloidal construction of bitumen depends on the following factors (Zakar, 1971):

- Chemical nature and percentages quantity of the asphaltenes.

- Chemical character and percentages quantity of the maltenes.
- Temperature of the system.

As mentioned previously, bitumen can be classified as SOL bitumens (fluid type) and GEL bitumens (structured type) on the basis of the extent of micelle dissolution. Figure 2.2 shows the schematic of these two colloidal types. If the maltenes contain a sufficient amount of aromatics/resins relative to the quantity and quality of the asphaltenes, a SOL structure will be formed, whereas with a low aromatic/resin content a GEL structure will result. Thus, the colloidal constitution of bitumen does not only depend on the quantity of the asphaltenes.

Temperature affects the degree to which the asphaltenes are dissolved in the oily maltene medium. Increasing the temperature results in a greater dissolution with the GEL structure being changed into a SOL structure, whereas decreasing the temperature results in the opposite rheological properties becoming dominant. Therefore, it can be concluded that the colloidal constitution determines the thermo-rheological properties of the bitumen to a great extent. The colloidal constitution also causes bitumens, which are solid at room temperature to become liquid at high temperatures.

2.2.5.2. The dispersed polar fluid (DPF) model

A number of researchers have discarded the colloidal hypothesis and concluded that bitumen is instead a simple homogeneous fluid (Petersen et al., 1994); some have labeled this model a dispersed polar fluid (DPF).

The model described is based on findings on the microstructure of bitumen using nuclear magnetic resonance (NMR) and chromatography techniques. These findings describe bitumen microstructure as a dispersed polar fluid

(DPF) in which a continuous three-dimensional association of polar molecules (generally referred to as "asphaltenes") are dispersed in a fluid of non-polar or relatively low-polarity molecules (generally referred to as "maltenes"). All these molecules are capable of forming dipolar intermolecular bonds of varying strength. Since these intermolecular bonds are weaker than the bonds that hold the basic organic hydrocarbon constituents of asphalt together, they will break first and control bitumen behaviour. Therefore, bitumen physical characteristics are a direct result of the forming, breaking and reforming of these intermolecular bonds or other properties associated with molecular superstructures (Anderson and Christenson, 1991). More recently, Redelius claimed that asphaltenes in bitumen form a molecular solution defined by the asphaltene solubility parameter (Redelius, 2006).

The result of the above chemistry is a material that behaves elastically through the effects of the polar molecule networks, and viscously because the various parts of the polar molecule network can move relative to one another due to their dispersion in the fluid non-polar molecules.

Moreover, the proponents of the homogeneous model of bitumen cannot explain why direct investigation of bitumen structure using X-ray or neutron scattering confirm its heterogeneous nature. For all these reasons, the colloidal model is the only one at the moment that can reasonably explain the peculiar features of bitumen properties (Lesueur, 2009). This is why it is used throughout this research.

2.3. BITUMEN MODIFICATION

On the majority of roads, conventional asphalts perform well. However, demand made upon roads increase year by year. Ever increasing numbers

of commercial vehicles with super single tyres and increased axle loads take their toll and it is clear that this trend will continue in the future.

There is no doubt that bitumen is one of the main factors influencing pavement behaviour. In this sense, it plays a large part in determining many aspect of road performance, particularly resistance to permanent deformation and cracking (Whiteoak and Read, 2003). For this reason, the selection of a suitable bitumen for specific conditions such as climate, traffic and pavement structure is one of the aims of a pavement engineer. However, when bitumen does not meet the requirements, modification of the bitumen with an additive can be an effective engineering solution. For many years, the scientific community has experimented with modified bitumen, mainly for industrial uses, adding asbestos, special filler, mineral fibres and rubbers. In the last thirty years many researchers have looked at a wide spectrum of modifying materials for bitumens used in road.

The selection of additive to meet the requirements is not an easy task. For the modifier to be effective and for its use to both practicable and economic, it must (Whiteoak and Read, 2003):

- Be readily available
- Resist degradation at asphalt mixing temperatures
- Blend with bitumen
- Improve resistance to flow at high road temperatures without making the bitumen too viscous at mixing and laying temperatures or too stiff or brittle at low road temperatures
- Be cost effective

For many years, conventional testing methods have been used to help with the selection of modifiers of bitumen. For example, bitumen contribution to the permanent deformation process (rutting) has traditionally been

handled by looking at bitumen consistency based on penetration and softening point tests (EN-1426 and EN-1427, respectively). However, these results are difficult to interpret and the need for rational specifications led to fundamental studies on the rheological behaviour of bitumen. Thus, in 1987, the Strategic Highway Research Program (referred to as SHRP) began developing new tests for measuring physical properties of bitumen that can be directly related to field performance. The Superpave performance graded binder specifications (AASHTO MP1), arisen from this study, are performance-related specifications based on the rheological properties of the binder, and the climate and loading conditions of the pavement where it is to be placed (Bahía et al., 1993). Among many others, the document gave special relevance to the oscillatory shear test in the linear viscoelastic region. Thus, the importance of the knowledge of the rheological behaviour of bitumen is apparent. Bitumen is a Newtonian fluid when handled and mixed with mineral aggregates at high temperatures. The linear viscoelastic region describes the resistance of bitumen to traffic loading (rutting and cracking due to fatigue). Finally, at or below the glass transition temperature, thermal cracking is likely to occur under certain loading conditions. As a result, understanding bitumen rheology is of major concern, as the mechanical properties of this binder are linked to the in-service performance of the actual asphalt pavements.

Therefore, improving one or more of the basic properties of bitumen related to one or more pavement distress modes (rutting, fatigue cracking and thermal cracking) is generally the aim of using modified bitumens. Also, different modifiers that affect different properties can be combined to improve several properties (Richard, 2009). The desirable basic properties of bituminous binders, which are obtained by bitumen modification, can be classified into four main groups: rigidity, elasticity, brittleness and durability.

- **Rigidity:** modification can reduce the rigidity of bitumen at intermediate and low temperatures or at intermediate and short loading times. This results in increased resistance of the pavement to fatigue and thermal cracking. Modification can also increase resistance of the pavement to rutting by increasing the rigidity of bitumen at high temperatures or long loading times.
- **Elasticity:** the ability of the binder to store deformational energy at high in-service temperatures and to dissipate it through flow at low temperatures is called elasticity and flexibility, respectively (Lu and Isacsson, 1997). Modification can decrease the elasticity of bitumen at low temperatures in order to increase material flexibility and, therefore, its resistance to low temperature cracking. It can also increase elasticity at intermediate and high temperatures and so improves the resistance of the bitumen to rutting and fatigue cracking.
- **Brittleness:** modification can increase the ductility of the bitumen to improve resistance to fatigue and thermal cracking. Modification can decrease failure at low strain by increasing strain tolerance.
- **Durability:** modification can improve the durability of bitumen in terms of resistance to ageing and oxidation.

Bitumen modifiers can be classified on the basis of the mechanism by which the modifier alters the bitumen properties, the composition and physical nature of the modifier, and the target bitumen property that must be modified (Bahia et al., 1998). A large number of bitumen modifiers, shown in Table 2.2 have been used. However, bitumen modification for paving application is mostly carried out by means of polymers.

Table 2.2. Bitumens modifiers. Extracted from Bahía et al., 1998.

Type of modifiers	Class
Fillers	Carbon black Mineral: Hydrated lime Fly ash Portland cement Baghouse fines
Extenders	Sulphur Wood lignin
Polymers-Plastomers	Ethylene vinyl acetate (EVA) Ethylene propylene diene monomers (EPDM) Polyisobutylene Polyethylene Polypropylene
Crumb rubber	Different sizes, treatments and processes
Oxidants	Manganese compounds
Hydrocarbons	Aromatics Naphthenics Paraffinics / wax Vacuum gas oil Asphaltenes: ROSE process resins SDA asphaltenes Tall oil Natural bitumens: Trinidad Gilsonite
Antistrips	Amines: Amidoamines Polyamines Hydrated lime Organo-metallics
Fibres	Polypropylene Polyester Reinforcement Natural: Cellulose Mineral
Antioxydants	Carbamates: Lead Zinc Carbon black Hydrated lime Phenols Amines

2.3.1. Polymer bitumen modification

2.3.1.1. Review of polymers

Polymers are large chain-like molecules formed by the conjunction of small chemical units. Many polymers are synthesized from their constituent monomers via a polymerization process.

They are often commonly referred to as "*plastics*". However, this is somewhat of a misnomer. The term "plastic" refers to one class of polymers known as "*thermoplastic*". There are several ways to classify polymeric materials:

- Classification based on the overall composition of the polymers, i.e., if the polymer contains only one type of unit or monomer then it is known as a homopolymer, whereas if more than one unit is present then it is known as a copolymer.
- Classification based on structural considerations, i.e., from knowledge of how the individual components of the polymers fit together. They have three main structures: linear, branched and cross-linked polymers.
- Polymers can also be classified depending upon its final usage as elastomers, plastomers, fibres or liquid resins. When a polymer is formed into hard and tough articles by application of heat and pressure then it is used as a plastomer. When a polymer is vulcanized into rubbery materials, which show good strength and elongations, then it is used as an elastomer. When it is drawn into long filament-like materials, whose length is at least 100 times its diameter, then it is used as a fibre. When the polymer is used in the liquid form, such as in sealants, adhesives, etc., they are said to be used as liquid resins (Varadan et al., 2003).

- Furthermore, polymers can be classified based upon their physical properties related to heating: thermoplastics and thermosets. *Thermoplastic* polymers are normally produced in one step and then made into products in a subsequent process. They become soft and formable when heated. The polymer melt can be formed or shaped when in this softened state. When cooled significantly below their softening point they again become rigid and usable as a formed article. This type of polymer can be readily recycled because each time it is reheated it can again be reshaped or formed into a new article. On the other hand, *thermosetting* polymers are normally produced and formed in the same step. Upon heating, thermosetting polymers will become soft, but cannot be shaped or formed to any great extent, and will definitely not flow.

The use of polymers in binders can be traced back to the early 1950's in Europe. Addition of polymers to bitumen is well-known to enhance the mechanical properties of the resulting binder at both low and high in-service temperatures, which in turn results in widening the temperature interval over which the pavement can offer a satisfactory performance. In that sense, Gregg and Alcock (1954) published the earliest research available on polymer modified asphalt. They studied bitumen modified with a copolymer of styrene-butadiene, and found that the addition of polymers to bitumen improved or reduced temperature susceptibility. Also, the polymer modified bitumen improves resistance to permanent deformation, thermal and fatigue cracking (Brown et al., 1990). Since then, much work has been developed on this field.

2.3.1.2. Modification via “passive” route

The polymer modifiers can be divided in two general categories depending on the polymer-bitumen interaction observed. On the one hand, “passive”

polymers are those conventionally used, such as SBR (styrene butadiene rubber), SBS (styrene butadiene styrene), LDPE (low density polyethylene) and EVA (ethylene vinyl acetate). In this case, the polymer is added to bitumen and physically mixed. Among them, the styrene butadiene styrene block copolymer (SBS) has proved to present the greatest potential when blended with bitumen (Whiteoak and Read, 2003).

SBS copolymers derive their strength and elasticity from physical cross-linking of the molecules into a three-dimensional network. The polystyrene end-blocks impart the strength to the polymer while the polybutadiene, rubbery matrix mid-blocks give the material its exceptional elasticity. The effectiveness of these physical cross-links diminishes rapidly above the glass transition temperature of polystyrene (approximately 100 °C), although the polystyrene domains will reform on cooling restoring the strength and elasticity of the copolymer (Isacsson and Lu, 1995; Whiteoak and Read, 2003).

When SBS is blended with bitumen, the elastomeric phase of the SBS copolymer absorbs the maltenes (oil fractions) from the bitumen and swells up to nine times its initial volume (Isacsson and Lu, 1995; Cavaliere et al., 1993). At suitable SBS concentrations (commonly 5–7 wt.%), a continuous polymer network (phase) is formed throughout the PMB, significantly modifying the bitumen properties.

As thermoplastic rubbers have molecular weights similar to or higher than that of the asphaltenes, they compete for the solvency power of the maltene phase and phase separation can occur if insufficient maltenes are available. This phase separation is an indication of the incompatibility of the base bitumen and polymer and care should be taken when blending thermoplastic rubber PMBs. The compatibility of the SBS-bitumen blend can be improved through the addition of aromatic oils. However, too high

an aromatic content in the blend will dissolve the polystyrene blocks and destroy the benefits of the SBS copolymer.

Although considerable research has been undertaken in this area, SBS PMBs have still to be comprehensively characterized, due to the complex nature and interaction of the bitumen and polymer system (Brule et al., 1988; Isacsson and Lu, 1999)

2.3.1.3. Modification via “active” route

On the other hand, “active” polymers are designed to chemically react with bitumen. Examples of these polymers used for bituminous applications are terpolymers of ethylene and glycidyl methacrylate, and MDI-derived prepolymers (Polacco et al., 2004a; Polacco et al., 2004b).

Among all the “active” polymers currently commercially available, polyurethanes are the most versatile. The wide range of starting compounds that can be used to produce these materials, together with their flexible and diverse chemistry, has enabled products to be produced that exhibit physical properties that range from hard plastics to soft elastomers. This diversity is also manifest in the number of types of products that are available: foams, coatings, adhesives, sealants and elastomers (Segura et al., 2005).

Polyurethanes include polymers containing a significant number of urethane groups, which gives this class of polymers their name. It is produced as a result of the reaction between a hydroxyl group and an isocyanate at ambient temperatures without the use of catalyst.



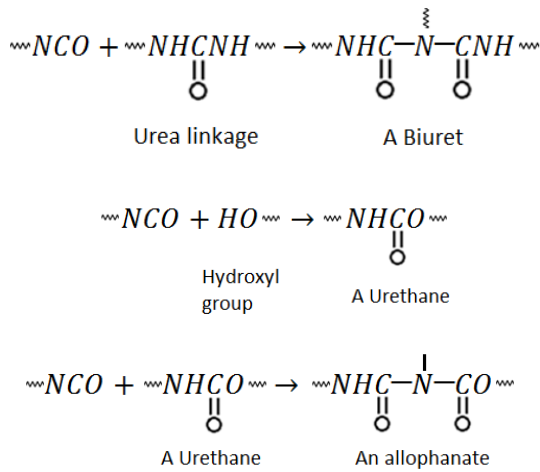


Figure 2.3. Reactions of the isocyanate group.

As shown in Figure 2.3, the isocyanates react with water to form carbamic acid, which is an unstable intermediate, and decomposes readily to evolve carbon dioxide and amine. This amine, in turn, reacts with additional isocyanate to form substituted urea linkages. In addition, a number of cross-linking reactions may take place, depending on the reaction conditions such as temperature, the presence of catalysts, and the structure of the isocyanate, alcohols and amines involved (Szycher, 1999).

In the manufacturing process of a number of polyurethane products a material known as a prepolymer is employed. A prepolymer is produced by reacting an isocyanate with a polyol (either a polyester or a polyether type) to give a product that is a relatively high molecular weight viscous liquid or waxy solid. The ratios of the isocyanate and polyol are carefully controlled to ensure that the prepolymer has reactive isocyanate end groups. These end groups are then used to “chain extend” the prepolymer to create a high molecular weight crosslinked product.

the resultant polyol will have a functionality of two; conversely, if the initiator is a triol, the resultant polyol will have a functionality of three. Polyether-based polyols produce very high quality polyurethane foams and elastomers.

Polyester polyols. These are polyalkylene glycol esters such as polybutylene terephthalate or adipate, or caprolactone polyesters. Polyalkylene adipates are prepared by condensation polymerization of the alkylene glycol and the corresponding diester or diacid. They are used to provide high strength to polyurethane elastomers. Polyester-based urethanes thermal behaviour is dependent upon the concentration of ester groups on the polyester. An increase in ester group concentration leads to reduce flexibility at low temperatures and conversely, reducing the ester group concentration improves the low temperature flexibility.

Polyols with three hydroxyl groups, such as glycerine, are known as trihydroxyl polyols or triols. When triols are reacted with isocyanate, the resulting polyurethane is cross-linked. The amount of crosslinking affects the stiffness of the polymer. If a rigid foam is required, the polymer structure must be highly cross-linked; for flexible foams, less cross-linking is needed.

2.3.2. Bitumen modification by reactive agents

The modification of bitumen by chemical reaction using “reactive agents” (non-polymeric products) is not a new subject. As described in section 2.2.2 “Types of bitumen”, air-blowing of soft bitumen is an industrial application of the chemical reactivity of bitumen, in use more than a century. However, the process was quite complicated and could only be done in specific production units available to refiners (Lesueur, 2009).

Still, it was early observed that bitumen could be reacted with other compounds such as sulphur, chlorine or various acids (sulphuric, nitric, acid sludge, fatty acids, etc.) in normal storage tank. For example, the reaction of Venezuelan bitumen with chlorine at 200 °C gave a final bituminous binder with properties comparable to those obtained by air-blowing process.

However, these processes did not get industrial success because of the corrosion problem involved with manipulating such products and their reaction by-products, together with the low economical interest given that the same effect on properties could be obtained by the cheaper air-blowing process (Siegmann, 1950). In parallel, air-blowing was progressively abandoned for paving bitumen because of the increased fragility of the binders and higher ageing susceptibility.

Recently, bitumen acid modification was rediscovered because it turned out to start to make economical sense and seemed to lack the fragility problem of air-blown bitumens (Edwards et al., 2006; Herrington et al., 1999). In particular, polyphosphoric acid (PPA) modification is currently gaining industrial importance since it permits to significantly harden bitumen in an easily controllable way. As a result, the reaction of 1 wt.% of PPA to bitumen typically allows for a change of one class of paving grade (Orange et al., 2004).

Some works proposed that PPA acts through the neutralisation of polar interactions between the stacked asphaltene molecules, either by protonation of basic sites or by esterification. The overall effect is to increase the solvation of the asphaltene, increasing in turn the solid fraction and hence, the viscosity (Orange et al., 2004). However, other researchers (Baumgardner et al., 2005) proposed various bitumen-dependent mechanism of PPA modification which also affect the lower

weight components of the bitumen: co-polymerisation of the saturates, alkyl aromatisation of the saturates, cross-linking of neighboring bitumen segments, the formation of ionic clusters and the cyclisation of alkylaromatics.

Therefore, although the oxidative effect of acids was long recognized as well as its similarities with air-blowing (Siegmann, 1950), the reactivity of bitumen towards acids is still not completely understood. It is known that not all bitumens show the same reactivity, depending primarily on their crude source (Orange et al., 2004; Bonemazzi and Giavarini, 1999; Baumgardner et al., 2005).

2.4. BITUMEN RHEOLOGY

Rheology is the study of the deformation and flow of matter under the influence of an applied stress. This definition was accepted when the American Society of Rheology was founded in 1929. However, the term was coined in 1920 by Eugene C. Bingham, a professor at Lehigh University, from a suggestion by his colleague Markus Reiner. The word rheology is derived from the Greek words “ρεω”, which translates literally as “to flow” and “λογος” meaning “science”. Therefore, it literally means “the study of the flow” (Macosko, 1994). All the materials have rheological properties which are relevant in many fields of study: geology and mining, concrete technology, soil mechanics, plastics processing, polymer and composites, tribology, paint flow and pigment dispersion, blood, bioengineering, interfacial rheology, structural materials, electrorheology, cosmetics and toiletries, pressure sensitive adhesion, etc. (Steffe, 1996).

The place of rheology among other natural sciences and applied problems is shown in Figure 2.5. One can see that rheology is a multidisciplinary science having many points of relationship with fundamental physics and

chemistry, as well as having applications to real technological and engineering materials in life.

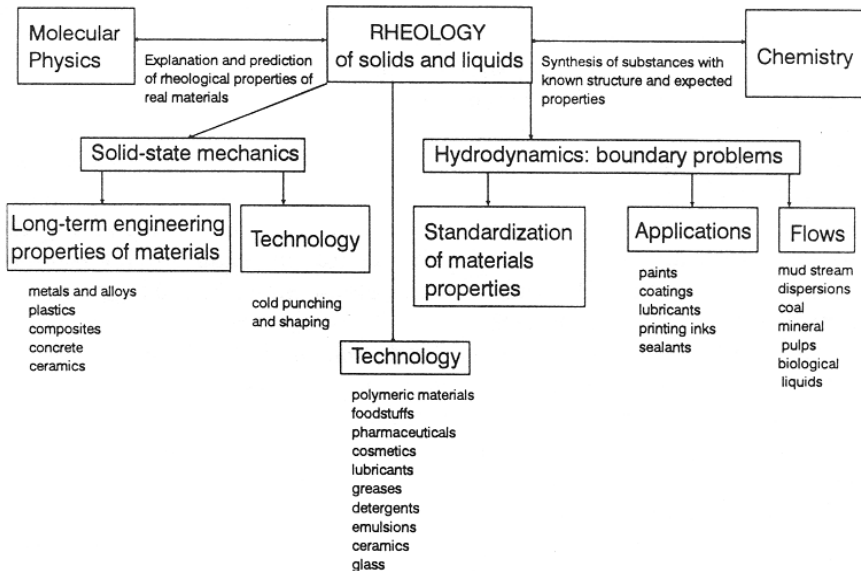


Figure 2.5. Rheology - its place among other sciences considering applied problems.

This science is dominated by inquiry into the flow behaviour of complex fluids such as polymers, foods, biological systems, slurries, suspensions, emulsions, pastes, and other compounds. The relationship between stress and deformation for these types of materials differ from the classical theory of elasticity to the classical theory of hydrodynamics.

The classical theory of elasticity (from 1678) deals with mechanical properties of elastic solids, for which, in accordance with Hooke's law, stress (τ) is always directly proportional to strain (γ) in small deformations but independent of the rate of strain ($\dot{\gamma}$). The proportionality constant (G) is called the elastic modulus:

$$\tau = G \cdot \gamma \quad (2.3)$$

The classical theory of hydrodynamics (from 1687) deals with properties of viscous liquids, for which, in accordance with Newton's law, the stress is always directly proportional to the rate of strain but independent of the strain itself. The proportionality constant (η) is called viscosity:

$$\tau = \eta \cdot \dot{\gamma} \quad (2.4)$$

These two categories are idealizations. However, the vast majority of materials show a rheological behaviour that classifies them to a region somewhere between the liquids and the solids.

The rheological properties of materials are established analyzing the relation between stress or strain applied to a material and the flow or/and the resultant deformation (Whorlow, 1992). However, before making a classification of fluid behaviour, it would be appropriate to understand some important concepts.

Rheological properties define the relationship between stress and strain/strain rate in different types of shear and extensional flows. As shown in Figure 2.6, in shear flows liquid elements flow over or past each other; in extensional flow, instead, adjacent elements flow towards or away from each other (Barnes et al., 2000).

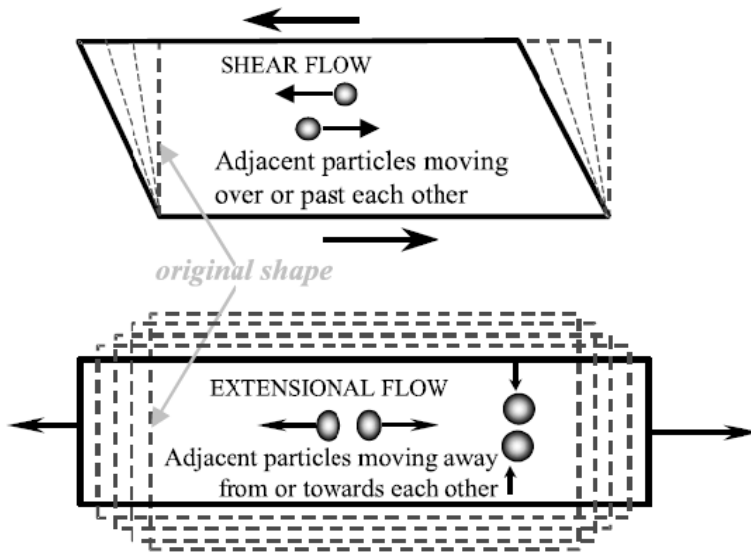


Figure 2.6. Particle motion in shear and extensional flows.

The *stress* is defined as the force F acting on a unit area A . Since both force and area have directional as well as magnitude characteristics, stress is a second order tensor and typically has nine components. *Strain* is a measure of deformation or relative displacement and is determined by the displacement gradient. Since displacement and its relative change both have directional properties, strain is also a second order tensor with nine components.

When a force F is applied to a piece of material (Figure 2.7), the total stress acting on any infinitesimal element is composed of two fundamental classes of stress components (Darby, 1976):

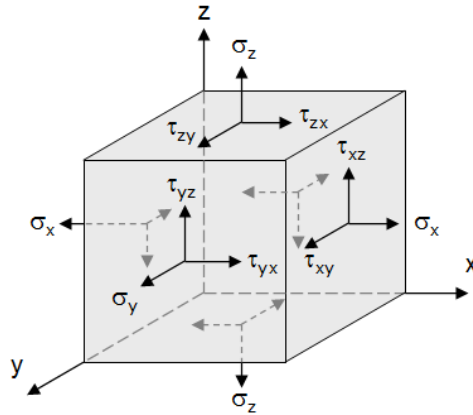


Figure 2.7. Stress components on a cubical material element.

Normal stress component, applied perpendicularly to the plane (σ_x , σ_y , σ_z).
 Shear stress components, applied tangentially to the plane (τ_{xy} , τ_{xz} , τ_{yx} , τ_{yz} , τ_{zx} , τ_{zy}).

There are a total of nine stress components acting on an infinitesimal element (i.e., two shear components and one normal stress component acting on each of the three planes). Individual stress components are referred to as τ_{ij} , where i refers to the plane the stress acts on, and j indicates the direction of stress component (Bird et al., 1987). The stress tensor can be written as a matrix of nine components as follows:

$$\tau = \begin{Bmatrix} \sigma_x & \tau_{xy} & \tau_{xz} \\ \tau_{yz} & \sigma_y & \tau_{yx} \\ \tau_{zx} & \tau_{zy} & \sigma_z \end{Bmatrix} \quad (2.5)$$

One of the most useful types of deformation for rheological measurements is simple shear. In this type, a material element is placed between two parallel plates (Figure 2.8) where the bottom plate is stationary and the upper plate is displaced in x -direction by applying a force F tangentially to

the surface A. The velocity profile in simple shear is given by the following velocity components:

$$v_x = \dot{\gamma} \cdot y ; v_y = v_z = 0 \quad (2.6)$$

The corresponding shear stress is given as:

$$\tau = \frac{F}{A} \quad (2.7)$$

In this simple case, the shear rate may be expressed as the velocity gradient in the direction perpendicular to that of the shear force, i.e.,

$$\dot{\gamma} = \frac{dV_x}{dy} = \frac{\tau}{\eta} \quad (2.8)$$

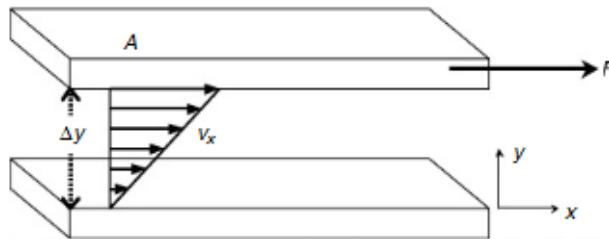


Figure 2.8. Simple shear between two parallel plates.

2.4.1. Classification of fluid behaviour

2.4.1.1. Newtonian fluid behaviour

A Newtonian fluid is characterized by a linear relationship between the applied shear stress and the rate of shear:

$$\tau_{yx} = \frac{F}{A} = \eta \cdot \dot{\gamma}_{yx} \quad (2.9)$$

According to the above-described Newton's law, the proportionality constant (η) is called shear viscosity. This parameter is a property of the material and depends on its physical constitution, pressure and temperature. A Newtonian fluid is, of course, an idealization, but in many cases it is a very good representation of a large number of liquids under normal "everyday" conditions.

2.4.1.2. Non-Newtonian fluid

A non-Newtonian fluid is one whose flow curve (shear stress versus shear rate) is nonlinear or does not pass through the origin. So, its apparent viscosity, shear stress divided by shear rate, is not constant at a given temperature and pressure, but it depends on flow conditions (such as flow geometry, shear rate, etc.) and sometimes even on the kinematic history of the fluid element under consideration. Such materials may be conveniently grouped into three general classes, although most of real materials often exhibit a combination of two types of non-Newtonian features:

(1) Fluids for which the rate of shear at any point is determined only by the value of the shear stress at that point at that instant; these fluids are variously known as "time independent", "purely viscous", "inelastic" or "generalized Newtonian fluids" (GNF).

(2) More complex fluids for which the relation between shear stress and shear rate depends, in addition, upon the duration of shearing and their kinematic history. They are called "time-dependent fluids".

(3) Substances exhibiting characteristics of both ideal fluids and elastic solids and showing partial elastic recovery, after deformation; these are categorized as “visco-elastic fluids”.

Each type of non-Newtonian fluid behavior will now be dealt with in some detail.

2.4.2. Time-independent fluid behaviour

In simple shear, the flow behavior of this class of materials may be described by a constitutive relation of the form,

$$\dot{\gamma}_{yx} = f(\tau_{yx}) \quad (2.10)$$

This equation implies that the value of $\dot{\gamma}_{yx}$ at any point within the sheared fluid is determined only by the current value of shear stress at that point or vice versa. Depending upon the form of the function in equation (2.10), these fluids may be further subdivided into three types (Figure 2.9):

- (a) Shear-thinning or pseudoplastic.
- (b) Viscoplastic.
- (c) Shear-thickening or dilatant.

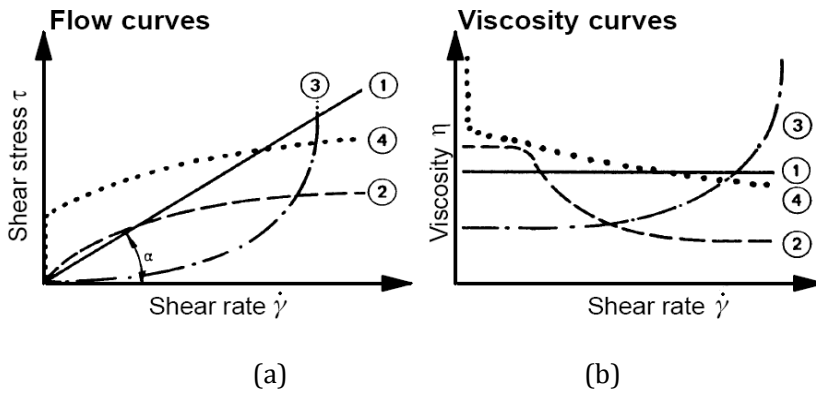


Figure 2.9. Flow curves (a) and viscosity curves (b) for fluids: [1] Newtonian, [2] shear-thinning, [3] shear-thickening and [4] viscoplastic.

2.4.2.1. Shear-thinning or pseudoplastic

It is the most common type of time-independent non-Newtonian fluid behavior, characterized by an apparent viscosity which decreases with increasing shear rate. Many substances such as emulsions, suspensions, or dispersions of high technical and commercial importance belong to this group (Gebhard Schramm, 1998).

For most fluids, the shear-thinning effect is reversible, often with some time lag. It should be mentioned that the shear-thinning or pseudoplastic behavior is not uniform over the range of very low to very high shear rates.

2.4.2.2. Viscoplastic fluid behaviour

This type of fluid behavior is characterized by the existence of a yield stress (τ_y) which must be exceeded before the fluid will deform or flow. Conversely, such a material will deform elastically (or flow *en masse* like a rigid body) when the externally applied stress is smaller than the yield stress. Once the magnitude of the external stress has exceeded the value of the yield stress, the flow curve may be linear or non-linear but will not pass

through origin. A fluid with a linear flow curve for $|\tau_{yx}| > |\tau_y|$ is called a Bingham plastic fluid.

It is interesting to note that a viscoplastic material also displays an apparent viscosity which decreases with increasing shear rate. At very low shear rates, the apparent viscosity is effectively infinite at the instant immediately before the substance yields and begins to flow. It is thus possible to regard these materials as possessing a particular class of shear-thinning behavior.

Strictly speaking, it is virtually impossible to ascertain whether any real material has a true yield stress or not, but nevertheless the concept of a yield stress has proved to be convenient in practice because some materials closely approximate to this type of flow behavior (Barnes and Walters, 1985; Schurz, 1990; Evans, 1992).

2.4.2.3. Shear-thickening or dilatant fluid behaviour

Shear-thickening fluids are similar to shear-thinning systems in that they show no yield stress, but their apparent viscosity increases with increasing shear rate. This type of fluid behavior was originally observed in concentrated suspensions.

Of the time-independent fluids, this sub-class has received very little attention. Consequently very few reliable data are available. Until recently, shear-thickening fluid behavior was considered to be much less widespread in the chemical and processing industries. However, with the growing interest in the handling and processing of systems with high solids loadings, it is no longer so, as is evidenced by the number of recent review articles on this subject (Barnes, 1989; Boersma et al., 1990; Goddard and Bashir, 1990).

2.4.3. Time-dependent fluid behavior

Apparent viscosities may depend not only on the rate of shear but also on the time for which the fluid has been subjected to shearing.

Time-dependent fluid behavior may be further sub-divided into two categories: thixotropy and rheopexy or negative thixotropy.

2.4.3.1. Thixotropy

A material is said to exhibit thixotropy if, when it is sheared at a constant rate, its apparent viscosity (or the corresponding shear stress) decreases with the time of shearing. If the flow curve is measured in a single experiment in which the shear rate is steadily increased at a constant rate from zero to some maximum value and then decreased at the same rate to zero again, a hysteresis loop of the form shown in Figure 2.10 is obtained; the height, shape and enclosed area of the hysteresis loop depend on the duration of shearing, the rate of increase/decrease of shear rate and the past kinematic history of the sample. Broadly speaking, the larger the enclosed area, stronger is the time-dependent behaviour of the materials.

2.4.3.2. Rheopexy or negative thixotropy

The relatively few fluids for which the apparent viscosity (or the corresponding shear stress) increases with time of shearing are said to display rheopexy or negative thixotropy. Again, hysteresis effects are observed in the flow curve, but in this case it is inverted, as compared with a thixotropic material.

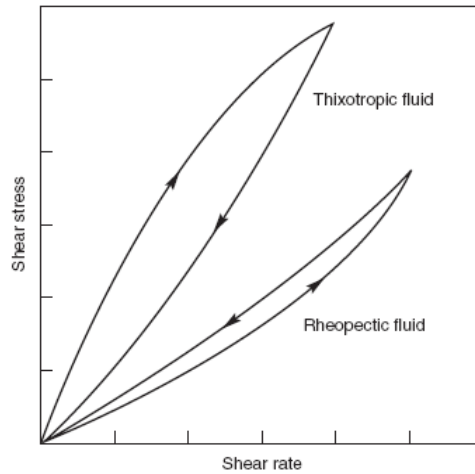


Figure 2.10. Schematic shear stress-shear rate behaviour for time-dependent fluid behaviour.

2.4.4. Viscoelastic fluid behaviour

The behaviour of linear viscoelastic materials combines both linear elastic and linear viscous behavior. If a constant strain is applied to this material, the stress, which is required to maintain this deformation, decreases gradually or relaxes. Also, when a constant stress is applied, deformation increases slowly with time or creeps. Under oscillatory testing, the stress in a viscoelastic material is not exactly in phase with strain (pure elastic solid), and also not 90° out of phase with strain (pure viscous fluid) but is between these two extremes (Figure 2.11). The difference between linear viscoelastic and non-linear viscoelastic materials is that in linear viscoelastic materials the ratio of stress and strain is a function of time (or frequency) and temperature but not of stress magnitude (Darby, 1976).

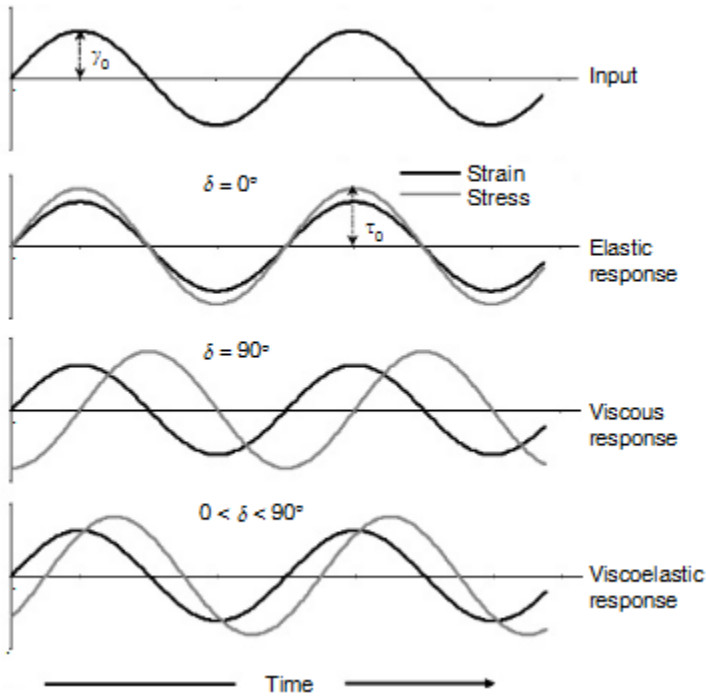


Figure 2.11. Input and response functions differing in phase by the angle δ .

Viscoelastic properties can be measured by experiments which examine the relationship between stress and strain, and strain rate in time dependent experiments. These experiments consist of stress relaxation, creep, and small amplitude oscillatory measurements. Stress relaxation (or creep) consists in instantaneously applying a constant strain (or stress) to the test sample and measuring change in stress (or strain) as a function of time (transient response). Dynamic testing consists in applying an oscillatory stress (or strain) to the test sample and determining its strain (or stress) response as a function of frequency. All linear viscoelastic rheological measurements are related, and it is possible to calculate one from the other (Ferry, 1980; Macosko, 1994).

2.4.4.1. Stress Relaxation

In a stress relaxation test, a constant strain (γ_0) is applied to the material over a very short period of the time, and the change in the stress $\tau(t)$ is measured (Darby, 1976; Macosko, 1994). Ideal viscous, ideal elastic, and typical viscoelastic materials show different responses to the applied step strain as shown in Figure 2.12. Shear strain and stress reach a maximum value after the loading time, but while the strain remains constant, shear stress begins to decrease.

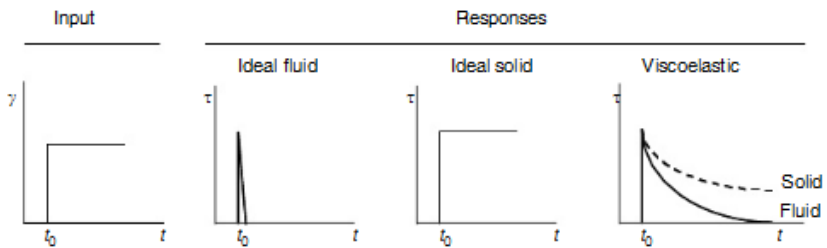


Figure 2.12. Response from stress relaxation test.

A relaxation modulus, which relates the measured shear stress and the applied shear strain, can be calculated from the following equation:

$$G(t) = \frac{\tau(t)}{\gamma_0} \quad (2.11)$$

The relaxation modulus is a time-dependent parameter in the linear region but it is a function of both time and strain in the non-linear range of response. The relaxation modulus has unit of stress (Pascal in S.I.).

2.4.4.2. Creep Response

In a creep test, a constant stress (τ_0) is applied at time t_0 and removed at time t_1 , and the corresponding strain $\gamma(t)$ is measured as a function of time.

As in the case with stress relaxation, various materials respond in different ways as shown by typical creep data given in Figure 2.13. In a stress relaxation test, stress decreases for constant strain, whereas in creep, strain increases at constant stress.

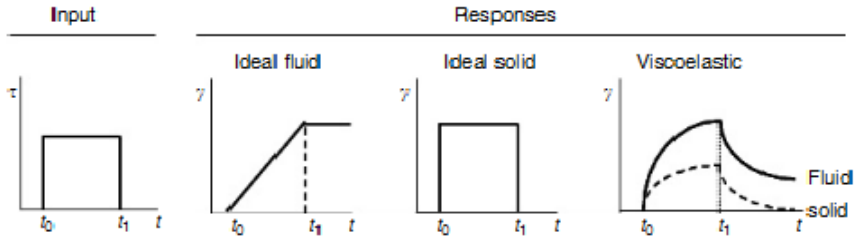


Figure 2.13. Response from creep test.

Data are usually expressed in terms of the compliance as follows:

$$J(t) = \frac{\gamma(t)}{\tau_0} \quad (2.13)$$

The compliance has the units of reciprocal modulus but in general it does not equal $1/G$. However, because in the linear viscoelastic regime strain is linear with stress, strain versus time data at different τ_0 collapse into one $J(t)$ plot. This is analogous to the reduction of stress relaxation curves to one $G(t)$.

A steady state creep compliance, J_e^0 , is defined by extrapolation of the limiting slope to $t=0$. The slope is the inverse of the viscosity at low shear rate, η_0 . Thus, in the steady creeping regime, we have:

$$J(t) = \frac{\gamma_0}{\tau_0} + \frac{t \cdot \dot{\gamma}_\infty}{\tau_0} \quad (2.14)$$

or

$$J(t) = J_e^0 + \frac{t}{\eta_0} \quad (2.15)$$

2.4.4.3. Dynamic Response

Dynamic mechanical analysis is the most widely used method for characterizing viscoelastic behavior. Dynamic (oscillatory) tests may be performed in stress controlled or strain controlled modes. In stress controlled testing, a sinusoidal stress is applied to the sample and the resultant strain is monitored with time, whereas in strain controlled testing a sinusoidal strain is applied to the sample and the resultant stress is monitored with time. When considering tests in the controlled strain mode, the applied strain is expressed according to the following equation:

$$\gamma(t) = \gamma_{max} \cdot \sin(\omega \cdot t) \quad (2.16)$$

where: $\omega = 2 \cdot \pi \cdot f$

f = frequency of the sinusoidal strain (Hz), and

γ_{max} = the amplitude of strain.

Differentiating equation 2.16 results in the strain rate:

$$\dot{\gamma}(t) = \omega \cdot \gamma_{max} \cdot \cos(\omega \cdot t) \quad (2.17)$$

On the other hand, the corresponding stress can be represented as

$$\tau(t) = \tau_0 \cdot \sin(\omega \cdot t + \delta) \quad (2.18)$$

where τ_0 is the amplitude of stress and δ is shift angle (Figure 2.13).

By employing complex notation, the complex modulus, $G^*(\omega)$, is defined as

$$G^*(\omega) = \frac{\tau(t)}{\gamma(t)} = G'(\omega) + iG''(\omega) \quad (2.19)$$

$$|G^*(\omega)| = \frac{\tau^*}{\gamma^*} = \sqrt{(G'(\omega))^2 + (G''(\omega))^2} \quad (2.20)$$

where: $\tau(t)$ =dynamic oscillatory shear stress

$\gamma(t)$ =dynamic oscillatory shear strain

As previously mentioned, the behaviour of viscoelastic materials, such as bitumen, falls between ideal elastic solid behaviour and ideal viscous fluid response. A solid-like viscoelastic material exhibits a phase angle smaller than 45° , while a liquid-like viscoelastic material exhibits a phase angle greater than 45° . Thus, from dynamic tests, the following two rheological properties can be defined:

$$G'(\omega) = \frac{\tau_0}{\gamma_0} \cdot \cos \delta \quad (2.21)$$

$$G''(\omega) = \frac{\tau_0}{\gamma_0} \cdot \sin \delta \quad (2.22)$$

$G'(\omega)$ and $G''(\omega)$ are two frequency dependent functions, termed the shear storage and loss moduli, respectively. The storage modulus, G' , is related to the elastic character of the fluid (energy storage during deformation), whilst the loss modulus, G'' , is related to the viscous character of the material (energy dissipation during the experiment). Therefore, for a perfectly elastic solid, all the energy is stored, that is, G'' is zero and the stress and the strain will be in phase. However, for a perfect viscous material all the energy will be dissipated, that is, G' is zero and the strain will be out of phase by 90° .

Another commonly used dynamic viscoelastic property, the loss tangent, $\tan \delta(\omega)$, denotes ratio of viscous and elastic components in a viscoelastic behaviour:

$$\tan \delta = \frac{G'(\omega)}{G''(\omega)} \quad (2.23)$$

If the equations (2.21) and (2.22) are expressed for complex compliance, the following equations are derived (Ferry, 1980):

$$J^*(\omega) = \frac{\gamma(t)}{\tau(t)} = J'(\omega) + iJ''(\omega) \quad (2.24)$$

$$|J^*(\omega)| = \frac{\gamma^*}{\tau^*} = \sqrt{(J'(\omega))^2 + (J''(\omega))^2} \quad (2.25)$$

where: J^* = the complex compliance,

J' = the storage compliance, and

J'' = the loss compliance.

The relationship between these parameters is shown in Figure 2.15.

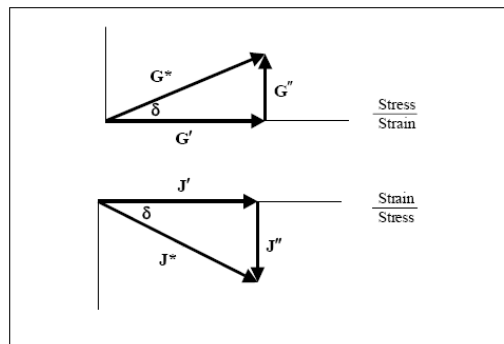


Figure 2.14. Components of complex modulus and compliance in sinusoidal shear deformation.

2.4.4.4. Conversion among Viscoelastic Functions

The ability to convert a viscoelastic function from one form to another is extremely useful. The following approximate equation is one of the simplest equations, which can be used to convert shear modulus to an uniaxial modulus for bitumen. This equation is based on the assumption that the Poisson's ratio is 0.5 (Anderson and Christenson, 1991).

$$E^*(\omega) = 3 \cdot G^*(\omega) \quad (2.26)$$

Where: $E^*(\omega)$ = the uniaxial complex modulus, and

$G^*(\omega)$ = the shear complex modulus.

The same equation can be used for calculating the uniaxial creep compliance, $D(t)$, from the shear creep compliance, $J(t)$ (Anderson and Christenson, 1991).

$$D(t) = \frac{J(t)}{3} \quad (2.27)$$

Other important conversions are the equations used for converting creep stiffness parameters to dynamic complex modulus parameters. Van der Poel (1954) defined the following equation for direct conversion between creep compliance and dynamic complex modulus:

$$G^*(\omega) \approx \frac{1}{J(t)} \quad (2.28)$$

$t \rightarrow 1/\omega$

This means that the dynamic complex modulus at a frequency of $\frac{1}{t}$ equals the inverse of the creep compliance at time t .

The following equations can be used for direct conversion between the storage/loss compliance and the storage/loss modulus (Ferry, 1980):

$$J' = \frac{G'}{(G'^2 + G''^2)} = \frac{1/G'}{1 + \tan^2 \delta} \quad (2.29)$$

$$J'' = \frac{G''}{(G'^2 + G''^2)} = \frac{1/G''}{1 + (\tan^2 \delta)^{-1}} \quad (2.30)$$

$$G' = \frac{J'}{(J'^2 + J''^2)} = \frac{1/J'}{1 + \tan^2 \delta} \quad (2.31)$$

$$G'' = \frac{J''}{(J'^2 + J''^2)} = \frac{1/J''}{1 + (\tan^2 \delta)^{-1}} \quad (2.32)$$

where $\tan \delta = G''/G' = J''/J' = E''/E'$. These methods of converting are approximate; however, in most cases, they are accurate enough for engineering calculations.

2.4.5. Rheological models

Many mathematical expressions of varying complexity and form have been proposed in the literature to model non-Newtonian fluids.

2.4.5.1. The power-law or Ostwald de Waele model

The relationship between shear stress and shear rate for a shear-thinning fluid can often be approximated by a straight line over a limited range of shear rate (or stress). For this part of the flow curve, an expression of the following form is applicable:

$$\tau = k' \cdot \dot{\gamma}^n \quad (2.33)$$

For $n < 1$, the fluid exhibits shear-thinning properties

$n = 1$, the fluid shows Newtonian behaviour

$n > 1$, the fluid shows shear-thickening behaviour

In these equations, k' and n are two empirical curve-fitting parameters known as the fluid consistency coefficient and the flow behaviour index, respectively.

2.4.5.2. The Carreau model

When there are significant deviations from the power-law model at very high and very low shear rates, it is necessary to use a model which takes into account the limiting values of viscosities, η_0 and η_∞ .

Based on the molecular network considerations, Carreau (1972) put forward the following viscosity model which incorporates both limiting viscosities, η_0 and η_∞ :

$$\frac{\eta - \eta_\infty}{\eta_0 - \eta_\infty} = \frac{1}{1 + (\dot{\gamma}/\dot{\gamma}_c)^2} \quad (2.34)$$

Where: η = shear rate viscosity.

η_0 = zero shear rate viscosity.

η_∞ = upper limiting Newtonian viscosity.

$\dot{\gamma}_c$ = the critical shear rate for the onset of the shear-thinning region.

s = parameter related to the slope in that region

2.4.5.3. The Cross model

Another four parameter model which has gained wide acceptance is due to Cross (1965) which, in simple shear, is written as:

$$\eta = \eta_{\infty} + \frac{\eta_0 - \eta_{\infty}}{1 + (\lambda \cdot \dot{\gamma})^p} \quad (2.35)$$

In equation (2.35), p (<1) and λ are two fitting parameters whereas η_0 and η_{∞} are the limiting values of the apparent viscosity at low and high shear rates, respectively.

This model reduces to the Newtonian fluid behaviour as $\lambda \rightarrow 0$. Similarly, when $\eta_{\infty} \ll \eta \ll \eta_0$, it reduces to the familiar power-law model.

Although Cross (1965) initially suggested a constant value of $p = 2/3$ for approximating the viscosity data of many systems, it is now thought that treating the index ' p ' as an adjustable parameter offers considerable improvement over the use of the constant value of p (Barnes *et al.*, 1989).

2.4.6. Time-Temperature Superposition

Viscoelastic material responses are both time and temperature dependent. This means that the moduli values found through dynamic mechanical analysis are simultaneously functions of frequency and temperature. As performing tests over large frequency ranges is impractical, it is necessary to use methods that extend the frequency scale of measurements taken over a limited frequency range. Tobolsky and Eyring (1943) observed the similarities in response curves obtained at different temperatures. Differences between these curves were seen to be their location along the time (or frequency) axis. Consequently, time and frequency dependencies are separable, leading to the time temperature superposition principle (Schwartzel and Sraerman, 1952; Tobolsky, 1956). This principle states

that viscoelastic data taken at any temperature may be translated to other temperatures by multiplicative translation along the time scale. This asserts that a change in temperature is equivalent to a shift in the logarithmic time scale. The principle of time-temperature superposition is also known as the method of reduced variables (Ferry, 1980).

The mathematical description of time-temperature superposition is as follows:

$$f(T_1, \omega) = f(T_2, \omega \cdot a_T) \quad (2.36)$$

where

$f(T_1, \omega)$ = value of viscoelastic function at temperature T_1 and frequency ω ;

$f(T_2, \omega \cdot a_T)$ = value of viscoelastic function at temperature T_2 and frequency $\omega \cdot a_T$; and a_T = horizontal shift factor, a function of T_1 and T_2 .

Dynamic mechanical tests are performed at several selected temperatures over a limited range of frequency (or time). The test results for one viscoelastic function are plotted versus frequency (or time). A curve corresponding to one temperature is selected as the reference curve. All other curves are shifted along the frequency axis to partially overlap the reference curve and form a continuous smooth curve, extending across a wide range of frequency, referred to as the master curve. The shift factor, a_T , is the amount of shift required for each individual curve to fit the master curve and is a measure of the temperature dependency of the response. A graphical explanation is presented in Figure 2.15.

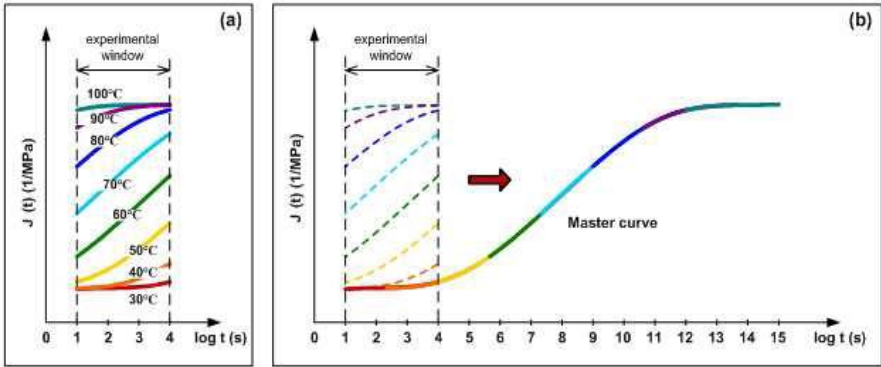


Figure 2.15. Time-temperature superposition scheme. (a) Segments obtained at each temperature in the time experimental window; (b) Master curve developed.

According to Ferry (1980), the use of time-temperature superposition requires three conditions to be met:

- Shapes of adjacent response curves should exactly match;
- The shift factor for each function must be unique; and
- The variations in the shift factor with temperature should follow a rational pattern, compatible with experience.

Shift factors can be determined by trial and error or by sophisticated computer softwares. They are generally described using either a Williams-Landel-Ferry (WLF) equation (Ferry, 1980) or Arrhenius function:

WLF equation:

$$\log a_T = \frac{-C_1 \cdot (T - T_{ref})}{(C_2 + T - T_{ref})} \quad (2.37)$$

where:

a_T = shift factor

T = temperature (K)

T_{ref} = reference temperature (K)

C_1 and C_2 (K) = constants

Arrhenius function:

$$\log a_T = \frac{\Delta H_a}{R} \cdot \left(\frac{1}{T} - \frac{1}{T_{ref}} \right) \quad (2.38)$$

where:

a_T = shift factor

ΔH_a = activation energy.

R = universal gas constant = 8.314 J/K·mol

T = temperature (K)

T_{ref} = reference temperature (K)

2.5. BITUMEN CHARACTERIZATION WITH ALTERNATIVE TECHNIQUES

Bitumen chemistry directly affects binder final properties. However, the way in which bitumen components organize themselves and give rise to a certain microstructure is still an open question. On these grounds, the aim of this section is to provide the reader with a theoretical background on those techniques typically used to characterize bitumen microstructure. It will be assumed that the previously detailed colloidal model may reasonably explain the peculiar features of bitumen properties.

2.5.1. Atomic Force Microscopy (AFM)

The understanding of bitumen morphology was significantly improved by probing the samples locally with the aid of microscopic techniques. The use of Atomic Force Microscopy (AFM) techniques can be very useful to gain an insight into colloidal model of bitumen. During AFM measurements, the specimen is scanned by a silica cantilever with a small tip placed near its free end. The deflection of the cantilever, ω_s , describing the interaction between the AFM tip and the sample surface, is monitored by an optical lever method. Based on the deflection ω_s and the stiffness k of the cantilever, the force acting at the tip is obtained as $F = k \cdot \omega_s$. Moreover, phase mode imaging, an extension of tapping mode in AFM, provides nanometre-scale information about surface structure and properties often not revealed by other scanning probe microscopy techniques. Phase imaging, which is simultaneously monitored with topography data, measures the phase shift between the oscillation driving the tip and the oscillation produced by the tip as it interacts with features on the sample surface. The phase lag is very sensitive to many material properties such as variations in composition, adhesion, friction and viscoelasticity, and may show patterns of stiffness on the sample surface. However, the interpretation of phase images is still at an early stage, so that there is currently no simple correlation between phase contrast and a single material property. The phase image shows a surface with two different intensity levels (light and dark) irrespective of the changes in local topography. Light areas should correspond to the asphaltene-rich regions, with a higher stiffness. The light regions are surrounded by dark (softer) regions, which would correspond to some of the molten maltenic compounds (Figure 2.16).

Several authors (Pfeiffer and Saal, 1940; Loeber et al., 1996; Lesueur, 2009) presented the idea of bitumen being composed of 'primary aggregates' of asphaltenes, undergoing flocculation, forming colloidal and micellar aggregates in an ordered structure: Asphaltene colloids at the core of the micelles, surrounded by a shell of surfactant like resins, and shielded by the aromatics and saturates (paraffins).

According to Shell-Bitumen-U.K. (1990), asphaltenes and resins behave as solid-like material, resulting in an increased stiffness. Hence, these larger-size molecules seem to form the stiffer parts observed during AFM testing. In earlier atomic force microscopy (AFM) work on bitumen, a bee-like structure, called catana phase, was attributed to asphaltene (Loeber et al., 1996; Masson et al., 2006). This model was supported by Pauli et al. (2011) who after doping a bitumen sample with asphaltenes observed an increase in the density of the catana phase in the doped material. The bee structure does not have a defined pattern but can usually be visualized by AFM as composed of a series of aligned protrusions and depressions.

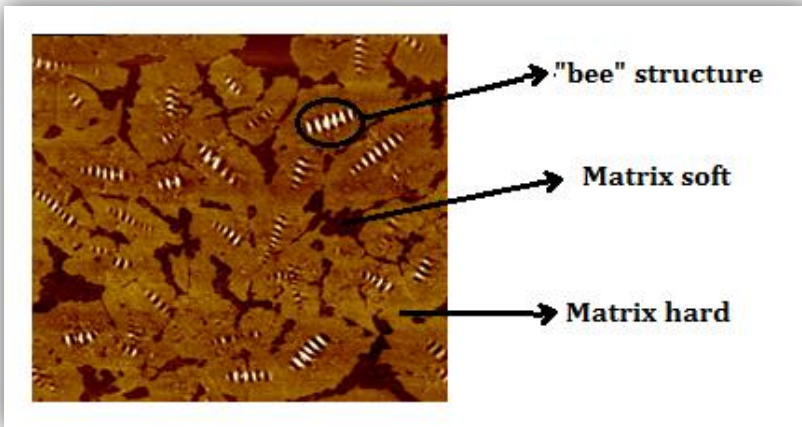


Figure 2.16. Topographic AFM image of bitumen.

The fact of alternating topography within the “bees” is still unanswered. A possible explanation is given by the arrangement of micelles, whereby the size of the “bees” is significantly larger than typical dimensions of micelles given in the literature. On the other hand, the soft matrix would be composed of the smaller-size saturates and aromatics.

In addition to this “bee-like” arrangement, other bitumen microstructures will be described in the next chapters.

2.5.2. Differential Scanning Calorimetry (DSC)

As defined by Höhne et al. (2003) in their own book, Differential Scanning Calorimetry (DSC) means the measurement of the change of the difference in the heat flow rate to the sample and to a reference sample while they are subjected to a controlled temperature program. In other words, this widely used thermoanalytical technique determines the quantity of heat that is either absorbed or released by a substance undergoing a physical or chemical change, being monitored against time or temperature.

Such changes alter the internal energy of the substance. At constant pressure, this internal energy is known as enthalpy. Processes that increase enthalpy are said to be endothermic (glass transition, melting, evaporation) while those that lower it are called exothermic (crystallization, decomposition). Both sample and reference pans are heated by a single furnace (Figure 2.17). At every phase transition, there is a large change in the heat capacity of sample, which leads to a difference in temperatures between the sample and the reference pan. Mathematical equations convert the signal into heat flow information.

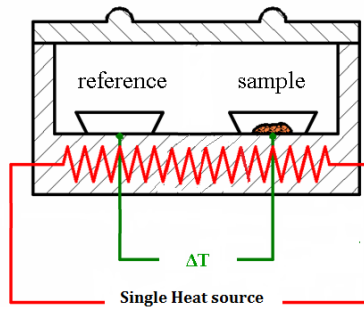


Figure 2.17. Principal scheme of the heat flux DSC.

One of the most important parameters determined with DSC is the heat capacity (C_p), which is calculated from the relation between heat flow (\dot{Q}), heating rate (ν_T), and sample mass (m) as described in the following equation:

$$C_p = \frac{\dot{Q}}{m \cdot \nu_T} \quad (2.39)$$

This ratio clearly shows the most important factors that have significant influence on the experiment results – the heating (or cooling) rate, ν_T , and the sample mass, m .

With regards to the most common thermal events, the glass transition temperature can be determined by observing the change in slope when plotting the heat flow against time or temperature (see region A in Figure 2.18). By heating partially crystallized materials, crystals begin to fall apart and chains come out of their ordered arrangement in what we call melting. This endothermic transition is represented by a negative peak in the heat flux, where the minimum of the peak is considered the melting temperature and from whose area above the latent heat can be estimated (see region B in Figure 2.18). A similar approach is also valid for the

crystallization, in this case considered an exothermic transition (see region C in Figure 2.18).

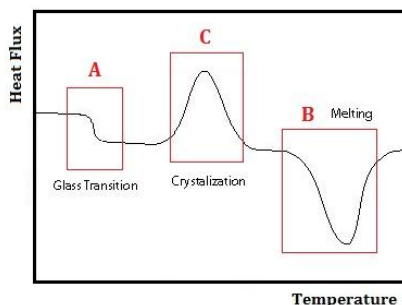


Figure 2.18. Schematics of DSC curve as a function of temperature.

2.5.3. Thin-layer chromatography/flame ionization detection (TLC/FID)

As seen in previous section 2.2.4 “Bitumen Chemical Composition”, bitumen is composed of two fractions: maltenes (which is separated into three different types of compounds: saturates, aromatics and resins) and asphaltenes. Thin-layer chromatography/flame ionization detection (TLC/FID) allows for the fractionation of bitumen into these four compounds, named SARAs. The technique is rapid and economical, but it may have low reproducibility. This fact is attributed to the separation rods condition and the time elapsed between bitumen dissolution and its analysis (Masson and Polomark, 2001).

The Chromarod Iatroscan system consists of a combination of two independent units: TLC unit and FID scanner.

The Iatroscan FID scanner basically consists of a hydrogen flame jet and ion collector. The sample is burnt, the ions are collected by the collector electrode and the signal is amplified in a similar way as in the gas chromatography.

The colloidal structure of bitumen can change. A sol type structure occurs when the asphaltenes micelles are fully dispersed and do not interact. However, a non-Newtonian behaviour arises from fully interconnecting asphaltenes micelles. In the middle, the sol-gel structure results from the coexistence of sol-type micelles and a gel structure. These changes in the binder colloidal nature have been assessed through the definition of a colloidal index calculated from of the binder SARAs fractions, introduced by Gaestel and co-workers (Gaestel et al., 1971):

$$I_c = \frac{\text{saturates+asphaltenes}}{\text{aromatics+resins}} \quad (2.40)$$

According to equation (2.40), a higher modified colloidal index would mean larger asphaltene clusters, leading to materials with more significant gel-like behaviour.

2.6. REFERENCES

Abraham H. Asphalt and Allied Substances. 6th Ed. New York: Van Nostrand, 1960.

Anderson DA, Christenson DW, Bahia HU. Physical properties of asphalt cement and the development of performance-related specifications. *J. Assoc. Asphalt Pav.*, 1991, 60, 437-475.

Bahia HU, Anderson DA. The new proposed rheological properties of asphalt binders: why are they required and how do they compare to conventional properties. *ASTM Conference: Physical Properties of Asphalt Cement Binders*, 1993, Texas, 1-27.

Bahia HU, Hislop WP, Zhai H, Rangel A. Classification of asphalt binders in to simple and complex binders. *J. Assoc. Asphalt Pav.*, 1998, 67, 1-41.

- Barnes HA, Walters K. The yield stress myth?. *Rheol. Acta*, 1985, 24, 323-326.
- Barnes HA. Review of shear-thickening of suspensions, *J. Rheol.*, 1989, 33, 329-366.
- Barnes HA, Hutton JF, Walters K. An introduction to rheology. Elsevier, 2000, Amsterdam.
- Baumgardner GL, Masson JF, Hardee JR, Menapace AM, Williams AG. Polyphosphoric acid modified asphalt: proposed mechanisms. *J. Assoc. Asphalt Pav.*, 2005, 74, 283-305.
- Bird RB, Stewart WE, Nightfoot EN. Transport phenomena. Second edition, Wiley-Interscience, 1987, New York,
- Bonemazzi F, Giavarini C. Shifting the bitumen structure from sol to gel. *J. Pet. Sci. Eng.*, 1999, 22, 17-24.
- Boersma WH, Levan J, Stein HN. *AIChE Journal*, 1990, 36, 321 .
- Branthaver JF, Petersen JC, Robertson RE, Duvall JJ, Kim SS, Hansberger PM, Mill T, Ensley EK, Barbour FA, Schabron JF. Binder characterization and evaluation, SHRP-A-368, *Strategic Highways Research Program*, National Research Council, 1994, 1, Washington, D.C.
- Brown SF, Rowlett RD, Boucher JL. Asphalt Modification. Proceedings of the conference on Us. *SHRP Highway Research Program: Sharing the Benefits, Ice*, 1990, 181-203.
- Brule B, Brion Y, Tanguy A. Paving asphalt polymer blends: relationship between composition, structure and properties. *Proc. Assoc. Asphalt Paving Technologists*, 1988, 57:41-64.

Carreau PJ. Rheological equation from molecular network theories. *Trans. Soc. Rheol.*, 1972, 16, 99.

Claudy P, Letoffe JM, King GN, Brule B, Planche JP. Characterization of road bitumens by differential calorimetric analysis. *Bull Liaison Lab. Ponts Chaussees*, 1990, 165, 185-192.

Claudy P, Letoffe JM, King GN, Brule B, Planche JP. Characterization of paving asphalts by differential scanning calorimetry. *Fuel Sci. Technol. Int.*, 1991, 9, 71-92.

Cavaliere MG, Diani E, Vitalini Sacconi L. Polymer modified bitumens for improved road application. Proc. Fifth Eurobitume Congr, Stockholm 1993;1A(1.23):138-42.

Corbett LW. Manufacture of petroleum asphalt. In: Hoiberg AJ. Bituminous Materials: Asphalts, Tars and Pitches. New York: Interscience Publishers; 1965, 2 (1), 81-122.

Cross MM. Rheology of non-Newtonian fluids, a new flow equation for pseudoplastic systems. *J. Colloid Interf. Sci.*, 1965, 20, 417.

Darby R. Viscoelastic fluids: An introduction to their properties and behavior. Deckker Inc., 1976, New York.

Delano WH. Twenty years' practical experience of natural asphalt and mineral bitumen. Whitefish, MT: Kessinger Publishing, 2007.

Domin M, Herod A, Kandiyoti R, Larsen JW, Lazaro MJ, Li S, et al. A comparative study of bitumen molecular weight distributions. *Energ. Fuel.*, 1999, 13, 552-557.

Edwards Y, Tasdemir Y, Isacson U. Influence of commercial waxes and polyphosphoric acid on bitumen and asphalt concrete performance at low and medium temperatures. *Mat. Struct.*, 2006, 39, 725–737.

EN 1426:2007: Bitumen and bituminous binders. Determination of needle penetration.

EN 1427:2007: Bitumen and bituminous binders. Determination of the softening point. Ring and Ball method.

Evans ID. On the nature of the yield stress. *J. Rheol.*, 1992, 36, 1313-1316.

Ferry JD. Viscoelastic properties of polymers. 3rd edition. Wiley & Sons, 1980, New York.

Forrest MJ. Chemical characterization of polyurethanes. Ed.:Rapra technology limited, 2001.

Gaestel C, Smadja R, Lamminan KA. Contribution à la connaissance des propriétés des bitumes routiers. *Revue Générale des Routes et Aérodrômes*, 1971, 466, 85–97.

Goddard JD, Bashir Y. Recent developments in structured continua II (Chapter 2), *Longman, London*, 1990.

Gregg, L.E.; Alcock, W.F., Investigations of rubber additives in asphalt paving mixtures. *J. Assoc. Asphalt Pav.*, 1954, 23-28.

Göhne GWH, Hemminger WF, Flammershein HJ. Differential scanning calorimetry. Springer-Verlag, 2003, Germany.

Herrington PR, Wu Y, Forbes MC. Rheological modification of bitumen with maleic anhydride and dicarboxylic acids. *Fuel*, 1999, 78, 101–110.

Isacsson U and Lu X. Testing and appraisal of polymer modified road bitumens: state of the art. *Mater Struct* 1995;28:139–59.

Krchma LC, Gagle DW. A U.S.A. history of asphalt refined from crude oil and its distribution. *Proc. Assoc. Asphalt Paving Techn.*, 1974, 43A, 25–88.

Lesueur D. The colloidal structure of bitumen: Consequence on the rheology and on the mechanisms of bitumen modification. *Adv. Colloidal Interfac.*, 2009, 145, 42-82.

Loeber L, Sutton O, Morel J, Valleton JM, Muller G. New direct observations of asphalts and asphalt binders by scanning electron microscopy and atomic force microscopy. *J. Microsc-Oxford*, 1996, 182, 32-39.

Lu X, Isacsson U. Rheological characterization of styrene-butadiene-styrene copolymer modified bitumens. *Constr. Build. Mater.*, 1997, 11, 23–32.

Isacsson U, Lu X. Laboratory investigation of polymer modified bitumens. *J Assoc Asphalt Paving Technologists* 1999, 68, 35–63.

Macosko CW. Rheology: principles, measurements and applications. Wiley-VCH, 1994, Canada

Masson JF, Leblond V, Margeson J. Bitumen morphologies by phase-detection atomic force microscopy. *J. Microsc-Oxford*, 2006, 221, 17-29.

Masson FJ, Polomark GM. Bitumen microstructure by modulated differential scanning calorimetry. *Thermochim. Acta*, 2001, 374, 105–114.

Nellensteyn FJ. Bereiding en Constitutie van Asphalt, Ph.D. Thesis: Delft University Netherland, 1923.

Nellensteyn FJ. The constitution of asphalt. *J. Inst. Pet. Technol.*, 1924, 10, 311–325.

Nelson WL. Evaluation of Oil Stocks. *Petroleum Refinery Engineering*, 4th Edition Mc Graw-Hill, New York , 1958.

Orange G, Dupuis D, Martin JV, Farcas F, Such C, Marcant B. Chemical modification of bitumen through polyphosphoric acid: properties–microstructure relationship. Proc. 3rd Eurasphalt & Eurobitume Congress, Vienna, 2004, 1, 733–745.

Oyenkunle OL. Certain relationships between Chemical Composition and Properties of Petroleum Asphalts from Different Origin. *Oil Gas Sci. Technol.*, 2006, 61, 3, 433-441.

Pauli AT, Grimes RW, Beemer AG, Turner TF, Branthaver JF. Morphology of asphalts, asphalt fractions and model wax-doped asphalts studied by atomic force microscopy. *Int. J. Pavement Eng.*, 2011, 12 (4), 291-309.

Petersen JC, Robertson RE, Branthaver JF, Hansberger PM, Duvall JJ, Kim SS et al. Binder characterization and evaluation, SHRP report A-367, 1994, 1, Washington, DC: National Research Council.

Pfeiffer JP, Saal RNJ. Asphaltic bitumen as colloid systems. *J. Phys. Chem.*, 1940, 44, 139–149.

Pfeiffer JP. Introduction. Definitions, nomenclature and conceptsin. In: Pfeiffer JP. *The Properties of Asphaltic Bitumen*. Amsterdam, Elsevier, 1950, 1–12.

PIARC (World Road Association). Use of modified bituminous binders, special bitumens and bitumens with additives in road pavements, routes/roads 303 also available from LCPC. Eds, Paris (France), 1999.

Polacco G, Stastna J, Biondi D, Antonelli F, Vlachovicova Z, Zanzotto L. Rheology of asphalts modified with glycidylmethacrylate functionalized polymers. *J. Colloid Interf. Sci.*, 2004a, 280(2), 366-373.

Polacco G, Stastna J, Vlachovicova Z, Biondi D, Zanzotto L. Temporary networks in polymer modified asphalts. *Polym. Eng. Sci.*, 2004b, 44(12), 2185-2193.

Read J, Whiteoak D. The Shell Bitumen Handbook. *5th Edition London (UK)*, Thomas Telford Publishing 2003.

Redelius P. The structure of asphaltenes in bitumen. *Road Mater. Pavement Des.*, 2006, 143-162.

Richard Kim Y. Modelling of asphalt concrete. Eddition Mcgraw Hill Construction, 2009.

Roberts FL, Kandhal PS, Brown ER, Lee D, Kennedy TW. Hot mix asphalt materials, mixture design and construction: National Centre for Asphalt Technology (NCAT), NAPA Education Foundation, Lanham, MD, 1991.

Rogel E. Studies on asphaltene aggregation via computational chemistry. *Colloids Surf.*, 1995, 104, 85-93.

Romberg JW, Nesmith SD, Traxler RN. Some chemical aspects of the components of asphalt. *J. Chem. Eng.*, 1959, 4(2), 159-161.

Saal RNJ, Labout JWA. Rheological properties of asphaltic bitumens. *J. Phys. Chem.*, 1940, 44, 149-165.

Schramm G. A practical approach to rheology and rheometry. Haake rheometers, 1998, Germany Schurz J. The yield stress-an empirical reality. *Rheol. Acta*, 1990, 29, 170-171.

Schwartzel F, Sraverman AJ, Time-Temperature dependence of linear viscoelastic behavior. *J. Appl. Phy.*, 1952, 23, 8, 838-843.

Segura DM, Nurse AD, McCourt A, Phelps R, Segura A. Chemistry of polyurethane adhesives and sealants. *Handbook of Adhs. and Seal.* **2005**.

Speight JG. The Chemistry and Technology of Petroleum, 3rd Edition Marcel Dekker, New York, 1999.

Siegmann MC. Manufacture of asphaltic bitumen. In: Pfeiffer JP. The properties of asphaltic bitumen. Amsterdam: Elsevier, 1950, 121-54.

Steffe JF. Rheological methods in Food Process Engineering. 2nd Edition, Freeman Press, East Lansing, MI, 1996.

Szycher M. Szycher's Handbook of Polyurethanes. Second edition, 1999, Taylor & Francis Group.

Thomas WH. Quality Assessment, in Modern Petroleum Technology, 4th Edition, Applied Science Publishers Ltd, Barking, Essex, England, 1973, 855-872.

Tobolosky AV. Stress relaxation studies of the viscoelastic properties of polymers. *J. Appl. Phys.*, 1956, 27, 7, 673-685.

Tobolosky AV, Eyring A. Mechanical properties of polymeric materials. *J. Appl. Phys.*, 1943, 11, 3, 125-134.

Traxler RN. The physical chemistry of asphaltic bitumen. *Chemical Review*, 1936, 19, 2.

Traxler RN, Coombs CE. The colloidal nature of asphalt as shown by its Flow Properties. *The Barber Asphalt Company*, Maurer New Jersey, June 11, 1936.

Van Der Poel C. A general system describing the visco-elastic properties of bitumens and its relation to routine Test Data. *J. Appl. Chem.*,1954, 4, 221-236.

Varadan VK, Vinoy KJ, Jose KA. RF MEMS and their applications. Pennsylvania State university, USA , 2003.

Whorlow RW. Rheological Techniques, *Ellis Horwood*, Chichester, 1992, 460.

Zakar P. Asphalt. New York: Chemical Publishing Company, 1971.

MODIFIED BINDERS: PROCESSING AND TESTING

Chapter III

*Physico-chemical modificacion of asphalt
bitumens by reactive agents*

3.1. MATERIALS

3.1.1. Bitumen

Three different neat bitumen samples, with different hardness and chemical composition, were used as base materials for bitumen modification. These bitumen samples, kindly provided by different oil companies, will be further referred to as:

- Bitumen 40/50
- Bitumen 100/150
- Bitumen 150/200

They have been produced from feedstock with different origin. Hence, their chemical composition (Table 3.1), which largely depends on the crude oil type, and mechanical properties and compatibility with reactive agents, varies from one to another.

Additionally, the results of penetration grade trials and ring-and-ball (R&B) softening temperature tests, determined by following the standards EN 1426:2007 and EN 1427:2007, respectively, are also included in Table 3.1.

Table 3.1. Penetration values, ring & ball softening temperatures, SARA's fraction and colloidal index values for the neat bitumens studied.

	Bitumen 40/50	Bitumen 100/150	Bitumen 150/200
Penetration (dmm)	49	114	168
R&B softening point (°C)	53.5	40.0	41.0
Saturates (wt.%)	6.2	6.9	7.4
Aromatics (wt.%)	50.3	60.6	57.6
Resins (wt.%)	24.5	19.8	15.1
Asphaltenes (wt.%)	19.0	12.7	19.9
Colloidal Index (C.I.) ^a	0.34	0.24	0.38

^aColloidal Index = (asphaltenes + saturates) / (resins + aromatics)

3.1.2. Modifying agents

Different types of bitumen modifying agents, which lie within the categories of “active” and “physical” modifiers, were studied in the present work. Regarding the first category, two non-polymeric additives (dioxide thiourea and thiourea) and an isocyanate-based prepolymer, have been employed:

A) On the one hand, thiourea dioxide and thiourea (abbreviated as “ThD” and “Th”, respectively, and illustrated in Figure 3.2), supplied by Sigma Aldrich, are well-known additives in many other industrial applications such as: reducing agent used for vat dye, reduction of ketones to alcohols and hydrocarbons, reduction of conjugated unsaturated acids to the corresponding saturated acids, etc.

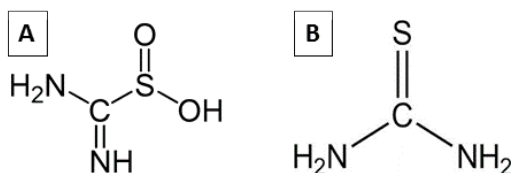


Figure 3.1. Structure of thiourea dioxide (A) and thiourea (B). Their melting point and molecular weight are gathered in Table 3.2.

Table 3.2. Melting point and molecular weight of thiourea dioxide and thiourea.

Additive	Melting point (°C)	Molecular weight (g/mol)
Thiourea Dioxide (ThD)	124-127	108.12
Thiourea (Th)	175-179	76.12

B) On the other hand, isocyanate-based prepolymers turn out from the reaction of a compound containing isocyanate groups with different types of polyols. This polymer is expected to bring about “chemical” modification of bitumen, via $-\text{NCO}$ groups reactions with specific bitumen fractions.

NCO groups-containing compound

Polymeric 4,4'-diphenylmethane diisocyanate (Pol-MDI) was used in this study as the NCO groups-containing compound in the synthesis of the prepolymers. This substance is actually a mixture that contains 25–80 wt.% monomeric 4,4'-MDI, as well as oligomers containing between 3 and 6 rings and other minor isomers, such as the 2,2'-isomer. The exact composition of Pol-MDI varies with the manufacturer and use. The polymeric MDI used in this study was provided by T.H. TECNIC, S.L. (Sevilla, Spain).

Pol-MDI is a dark reddish brown liquid with a glass transition temperature around $-50\text{ }^\circ\text{C}$. Its structure is shown in Figure 3.2.

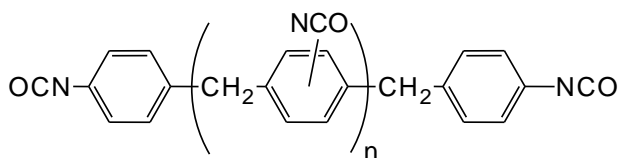


Figure 3.2. Structure of Pol-MDI.

Instead, monomeric 4,4'-MDI is a white to pale yellow solid at room temperature, with a molecular weight of 250 g/mol. At atmospheric pressure, it melts between 39–43 °C and has a boiling point higher than 300 °C. It presents a vapor pressure lower than 1 mPa at 20 °C and a low solubility in water. However, it is soluble in octane, benzene and kerosene.

Polyols

The term “polyol” describes long chain compounds with hydroxyl groups, which can react with isocyanates to produce polyurethane polymers. Typically, polyols have average molecular weight between 200 and 8000, and can be either polyether or polyester type (see Chapter II). NCO-terminated prepolymers obtained from biomass-derived polyols (castor oil, abbreviated as “CO”) have been considered in this research.

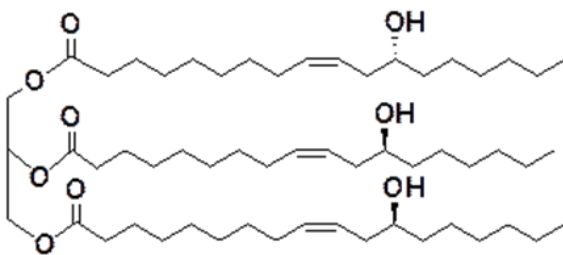


Figure 3.3. Structure of castor oil.

In order to increase its hydroxyl index, castor oil was modified by the addition of pentaerythritol (see Figure 3.4) with lead oxide (PbO) as catalyst. Pentaerythritol, a white and crystalline polyol with a molecular weight of 136.15 g/mol, is a versatile building block for the preparation of many polyfunctionalized compounds. The transesterification procedure of castor oil is described in the Chapter VI.

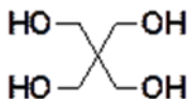


Figure 3.4. Structure of pentaerythritol.

In addition, a polyethylene glycol (PEG) was also used as petroleum-based polyols in the formulation of NCO-prepolymers. It will allow us to establish a comparative analysis on the thermal stability between MDI-PEG and MDI-CO prepolymers.

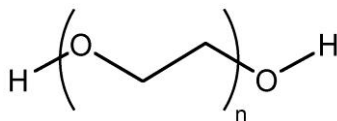


Figure 3.5. Structure of polyethylene glycol.

Finally, regarding the second category of modifier agents, a commercial SBS rubber (Tri-block copolymer styrene-butadiene-styrene), which produces a “physical” modification by its solely dispersion within the bitumen bulk, was considered in this research.

This thermoplastic elastomer (SBS), typically used in the paving industry, was employed as a modifying agent in the preparation of the reference sample. SBS is known to significantly increase the binder strength at high temperatures, as well as its flexibility at low temperatures. As shown in Figure 3.6, it is made up of a butadiene block in the middle of two styrene

blocks. Hence, styrene blocks form rigid domains which act as junction points of a three-dimensional network, with flexible butadiene chains. However, interactions among styrene blocks are reduced with increasing temperature, leading to a notable decrease in the copolymer strength.

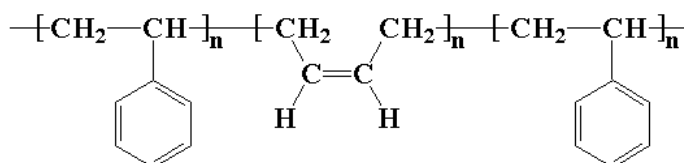


Figure 3.6. Structure of tri-block SBS.

SBS Kraton D-1101, supplied by Shell Chemical Co. (U.K.), was employed in the present work. Some physical and mechanical properties of this rubber are presented in Table 3.3.

Table 3.3. SBS Kraton D-1101 properties.

SBS Kraton D-1101	
Styrene content (wt.%)	31
Density ISO 2701 (kg/m ³)	940
Tensile strength (MPa)	33
Ultimate elongation (%)	880

3.2. SAMPLES PREPARATION

3.2.1. Preparation of the isocyanate prepolymers

The isocyanate-based prepolymers were synthesized by reaction of the different polyols (castor oil and PEG) and the polymeric MDI by following the steps below:

1. The adequate quantity of polyol, depending on its hydroxyl index, was added to a 50 mL flask equipped with a mechanical stirrer and purged with a flow of dry nitrogen, and located on an electric heater where temperature was maintained at 60 °C.
2. The Pol-MDI, with a -NCO content of 31.1 wt.% (ASTM D2572), was added to the above flask in such a quantity that a selected -NCO/-OH molar ratio was attained. The molar ratios will be detailed in chapter VI.
3. The mixture was kept under vigorous stirring for 24 h at the above conditions.

3.2.2. Preparation of the modified binders

The neat bitumen was received in 4-5 kg containers, which were placed in an oven at 140 °C until it became sufficiently fluid to be poured. Subsequently, the content was distributed in cylindrical glass vessels (approximately 200 g bitumen each).

The general modification procedure used in this work consisted in mixing every bitumen type with the modifier agent at different processing conditions. With this procedure, the influence that processing and formulations variables (i.e. concentration of reactive agent and processing temperature) exert on the final thermo-rheological properties of the binders was evaluated. In this sense, detailed information on the specific method followed will be further provided in the “Experimental Section” of the corresponding chapter.

3.3. MATERIALS TESTING

This section details the different tests performed in order to characterize the materials studied in this research.

3.3.1. Technological tests

A number of traditional tests are usually used to characterize bitumen physical properties.

3.3.1.1. Penetration test

This test quantifies bitumen consistency at medium in-service temperature (25 °C).

The standardized procedure for this test can be found in UNE-EN 1426:2007. A standard needle under a total load of 100 g is applied to the surface of a bitumen sample at 25 °C for 5 sec. The amount of penetration of the needle is measured in units of 0.1 mm (or penetration unit). “Soft” bitumens will have high penetrations while “hard” bitumens will have low penetrations.

Measurements were carried out with the universal penetrometer (Figure 3.7).



Figure 3.7. Penetration test device.

3.3.1.2. Ring & Ball softening point test

The R&B softening point test is a method to determine bitumen consistency at high in-service temperatures. It measures the temperature at which the consistency of the bitumen is between solid and liquid state. Therefore, regardless of the bitumen grade, the consistency will be the same for different bitumens at their respective R&B softening temperatures.

The standardized procedure for this test can be found in UNE-EN 1427:2007. Two steel balls are placed on top of two bitumen disks set in test rings, dipped in a bath whose temperature is gradually increased at 5 °C/min. The two specimens start softening, and the result is the average value of the two temperatures at which each of the balls touch a steel shelf 25.4 mm below the rings.

Measurements were carried out with the Ring and Ball test unit SETA 21000 (Figure 3.8).

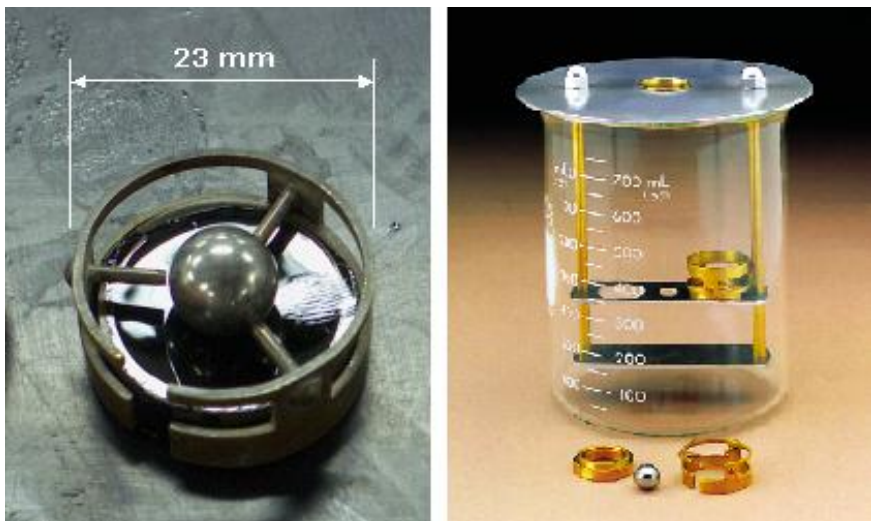


Figure 3.8. Softening point test apparatus.

3.3.2. Chemical characterization

3.3.2.1. Thin Layer Chromatography-Flame Ionization Detector analysis

Bitumen chemical composition is very complex. The most extended method of analysis quantifies bitumen composition in terms of the so-called SARAs fractions, which divides bitumen components according to their polarity (solubility in different solvents). A widely used experimental set-up consists of coupling between thin layer liquid chromatography on silica gel rods and flame ionization detection.

Measurements were carried out using the Iatroscan MK-6 analyzer (Iatron Corporation Inc., Japan) in Figure 3.9A.

The separation takes place in quartz rods coated with silica (chromarods) by consecutive elution in several solvents. The sample is dissolved in toluene and, once set in the chromarod by means of a micro-syringe, successively eluted with hexane, toluene and a 95/5 dichloromethane/methanol mixture (Ecker, 2001). The elution sequence is as follows:

- Saturated hydrocarbons
- Aromatic hydrocarbons
- Resins
- Asphaltenes

After the four fractions are isolated, the chromarod is placed on a moving device that passes it through the FID flame at an appropriate rate to ensure optimal response and resolution of the components studied. This procedure provides a chromatogram where the four fractions are well-resolved (Figure 3.9B).

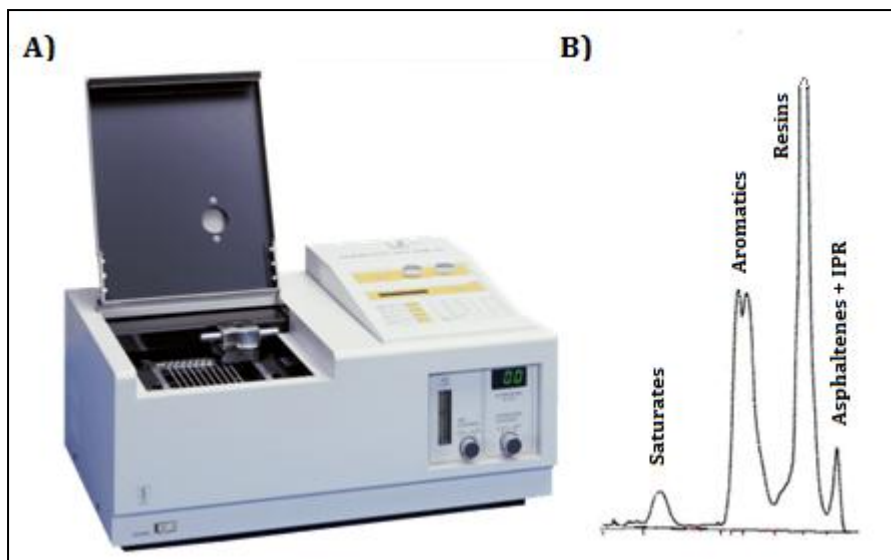


Figure 3.9. A) TLC-FID analyzer Iatrosan MK-6. B) Chromatogram obtained.

3.3.2.2. Gel Permeation Chromatography (GPC)

Gel Permeation Chromatography (GPC) is a type of Size Exclusion Chromatography (SEC) that separates molecules on the basis of size. This technique is typically utilized for polymer characterization for examining the molecular weight (Mw), molecular weight distribution and polydispersity index (Mw/Mn) of polymers.

The principle of GPC is the separation of molecules based on their hydrodynamic radius (R_h) or volume (V_h), not molecular weight. The separation process takes place in a column which is packed with porous, microparticulate material of typically 5 to 20 μm such as silica gel.

Because of their size, the larger molecules are excluded from some of the pores in the packing material and therefore elute faster through the column than the smaller ones.

The equipment used is the Waters model 500 GPC (U.S.A.) device shown in Figure 3.10, equipped with a refractive index detector 2414. The eluent is tetrahydrofuran (THF) flowing at a rate of 1.0 mL/min through a Styragel HR 4E column, designed specifically for polymer characterization from low-to-mid molecular weight samples at 35 °C.



Figure 3.10. Waters model 500 GPC.

In order to assign a molecular weight to the different polymers studied, a calibration curve has to be obtained. The most suitable way is to use a calibration based on a set of standards of low polydispersity, with similar chemical nature to the polymers to be characterized. Thus, calibration was performed with 5 different polypropylene-glycol standards, supplied by Sigma-Aldrich, and pure MDI. These cover a molecular weight range

between 455 and 3080. GPC measurements were carried out on solutions containing approximately 0.1 wt.% of the standards in THF.

A calibration curve was obtained by plotting the molecular weights provided by the supplier versus the retention times determined (Figure 3.11). Once the calibration curve is obtained, the molecular weight of any polymer studied can be determined by interpolation of its retention time.

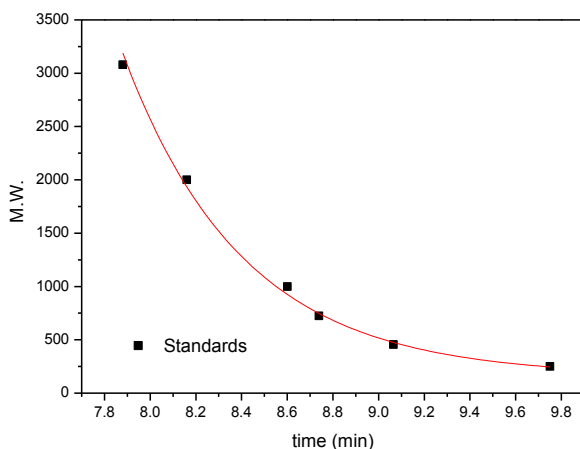


Figure 3.11. Calibration curve performed with the different polypropylene-glycol standards.

3.3.3. Microstructural characterization

3.3.3.1. Atomic Force Microscopy (AFM)

The AFM, introduced by Binnig et al. (1986), provides insight into the surface topography (down to nano-scale level) and mechanical properties of bitumen. The Atomic Force Microscope used in this thesis was the MultiMode™ AFM connected to a Nanoscope IV scanning probe microscope controller (Digital Instruments, Veeco Metrology Group Inc., Santa Barbara, U.S.A.), shown in Figure 3.12. All the images were acquired

in tapping mode at 30 °C, which simultaneously monitors topography and phase data.

Phase imaging is a powerful extension of tapping mode AFM that measures the phase shift between the oscillation driving the tip and the oscillation produced by the tip as it interacts with features on the sample surface. The phase lag is very sensitive to many material properties, such as variations in composition, adhesion, friction and viscoelasticity.

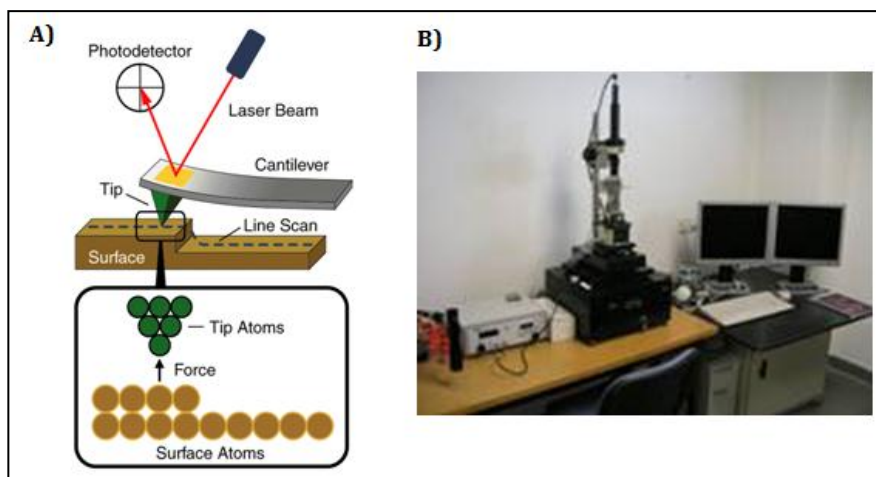


Figure 3.12. A) Principle of AFM. B) MultiMode™ AFM (Digital Instruments, Veeco Metrology Group Inc., Santa Barbara, U.S.A.).

Preparation of films

Bitumen films were prepared by following the procedure found in Masson et al. (2006). Hence, a drop of bitumen is applied onto a 12 mm steel disk and kept for 1-2 min at about 90°C (bitumen softens, but oxidation is negligible). Once bitumen was in a “quasi-liquid” state, it was spread out with a blade to form a round film of about 5 mm in diameter. This hot film was left on the hot plate undisturbed for 1 min to allow the surface to flow to a smooth and glossy finish. For AFM, the film was then cooled down to

room temperature, covered to prevent dust pick-up and annealed for 24 h before imaging.

3.3.4. Rheological characterization

The viscous flow behaviour (which accounts for the material's resistance to flow) and linear viscoelastic properties (related to the material's microstructure when still in unperturbed state) of bitumen were studied through different types of rheometers (both controlled-stress, CS, and controlled-strain, CR).

Prior to any of the proposed tests, the sample was always allowed to rest and reach equilibrium for at least 20 min at the testing temperature. All the tests were carried out at least twice in order to assure repeatability of the results.

3.3.4.1. Steady state tests

Viscosity curves

Basic rheometry tests showing the viscosity dependence with shear rate at a certain temperature. Viscosity is the measure of the resistance to flow of a liquid and is defined as the ratio between the applied shear stress and the rate of shear strain.

Viscosity curves were measured, at 60 °C, using both controlled-strain ARES rheometer (Rheometric Scientific, USA) and controlled-stress rheometer PHYSICA MCR-301 (Anton Paar, Austria) shown in Figure 3.13 and 3.14, respectively. In that sense, 60 °C is assumed to be the maximum expectable temperature which may be reached by a bituminous surface exposed to ambient in most of warm countries. Depending on the sample

different plate-and-plate geometries (serrated and smooth; 20 and 50 mm diameter; 1 mm gap) were used.



Figure 3.13. CR Rheometer ARES (USA).



Figure 3.14. CS Rheometer PHYSICA MCR-301 (Anton Paar, Austria).

3.3.4.2. Dynamic tests

All these dynamic tests were performed with a controlled-stress rheometer PHYSICA MCR-301 (Anton Paar, Austria) (see Figure 3.16), using different plate-and-plate geometries.

Stress Sweep tests (Oscillatory Shear)

They were performed at two different temperatures (30 and 60 °C) at a constant frequency of 1 Hz. They allow the linear viscoelastic region (LVR), within which the viscoelastic functions are independent of the applied stress or strain, to be determined. Instead, once in the non-linear region of response the moduli will be dependent on stress or strain.

Frequency Sweep tests (Oscillatory Shear)

Frequency sweep tests were performed (between 10^{-2} and 10^2 rad/s) within the LVR (value of stress previously determined by stress sweep tests) at two temperatures (30 and 60 °C).

Frequency sweeps resulted in the measurement of the dynamic shear storage and loss moduli, G' and G'' , respectively, over the entire range of frequencies tested. Additionally, the rheometer calculated the complex dynamic shear modulus and phase angle over the range of frequencies.

Oscillatory Shear Temperature Sweep tests

These tests are used to analyze the linear viscoelastic properties of unmodified and modified bitumen as a function of temperature at fixed values of frequency and strain, while applying an increasing linear temperature ramp.

Temperature sweep tests in oscillatory shear were performed, from -20 to 200 °C (for MDI-CO prepolymers) and from 30 to 100 °C (for modified binders), at a heating rate of 1 °C/min, a frequency of 10 rad/s and deformation of 1% (within LVR interval).

Results derived from this test can be conveniently plotted as $|G^*|/\sin \delta$ (referred to as rutting parameter, established by Superpave protocol in

1994) versus temperature. It allows to determine temperature the at which the binder presents a value of $|G^*|/\sin \delta$ at 1.66 Hz (10 rad/s) equal to 1kPa, maximum value of temperature at which the binder is expected to show suitable performance (indicator of the binder rutting resistance).

3.3.4.3. Dynamic Mechanical Thermal Analysis

Dynamic Mechanical Thermal Analysis (DMTA) tests were performed on rectangular samples of 50 mm length, 10 mm width and 3 mm thick, with a Seiko DMS 6100 (Seiko Instruments Inc., Japan) in double cantilever (bending) mode. Frequency sweep tests from 10^{-2} to 100 Hz were carried out, in the linear viscoelasticity (LVR) region, at four selected temperatures from -30 to 15 °C, in 15 °C-increments. Liquid nitrogen was employed as cooling system.

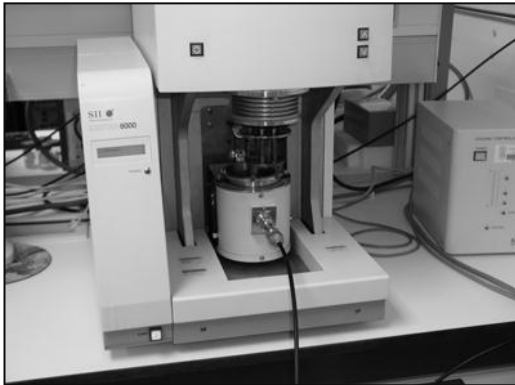


Figure 3.15. Seiko DMS 6100, Seiko Instruments Inc..

3.3.5. Thermal analysis

3.3.5.1. Modulated Differential Scanning Calorimetry (MDSC)

Differential Scanning Calorimetry (DSC) is a thermal analysis technique used to measure changes in heat flows associated with material transitions. DSC measurements provide both qualitative and quantitative data on

endothermic (heat absorbing) and exothermic (heat evolving) processes during physical transitions that are caused by phase changes, melting, oxidation, and other heat-related changes.

An advanced version of DSC, known as modulated DSC (MDSC), has been used in this thesis. This technique allows for the deconvolution of overlapping reversing and non-reversing thermal events, and so, the observation of transitions not visible on the thermal curve obtained by standard DSC (Masson and Polomark, 2001). Reversing events include those that can be brought to equilibrium during the period of a modulated temperature signal. Effects that cannot be modulated and brought to equilibrium are excluded from the reversing curve and show as non-reversing, e.g., oxidation, evaporation, decomposition, relaxation, reaction (Reading, 1993; Gill et al., 1993).

MDSC tests were performed with a TA Q-100 (T.A. Instruments, U.S.A.) (Figure 3.16). Samples of 5-10 mg were always subjected to the following testing procedure: temperature range between -70 and 150 °C; heating rate of 5 °C/min; amplitude of modulation of ± 0.5 °C; a period of 60 s; and nitrogen as purge gas, with a flow rate of 50 mL/min. In order to provide the same recent history, all the samples were paced into hermetic aluminium pans and stored at room temperature for 24 h before measurements.



Figure 3.16. DSC Q100 TA instruments.

3.3.5.2. Thermogravimetric Analysis (TGA)

The TGA technique provides information about the chemical and thermal stability of materials and is commonly used to investigate decomposition, dehydration, oxidation reactions, reaction pathways, kinetics of reaction and quantity of specific component. The TG device, also called a thermobalance, records changes in mass of a specimen as a function of temperature or time. The sample is placed in the thermobalance and is subjected to programmed heating and cooling cycles by a furnace in which the purge gas can be varied. The mass change is accompanied by various physical and chemical processes which are detected (Keattch and Dollimore, 1975; Sorai, 2004).

TGA tests were conducted in a Seiko TG/DTA 6200 (Seiko Instruments Inc., Japan), which simultaneously performs derivative thermogravimetric analysis (DTG) and differential thermal analysis (DTA) (Figure 3.17). Between 5-10 mg samples were placed into aluminium pans and then subjected to a testing protocol with the following parameters: temperature ramps were set at $10\text{ }^{\circ}\text{C}\cdot\text{min}^{-1}$, between 40 and 600 $^{\circ}\text{C}$.



Figure 3.17. TG/DTA6200, Seiko Instruments Inc..

3.4. REFERENCES

ASTM D2572 - 97(2010) Standard Test Method for Isocyanate Groups in Urethane Materials or Prepolymers

Binnig G, Quate CF, Gerber Ch. Atomic force microscope. *Phys. Rev. Lett.* 1986, 56 (9), 930.

Ecker A. The application of Iatroscan-technique for analysis of bitumen. *Petrol. Coal*, 2001, 43, 51-53.

EN 1426:2007: Bitumen and bituminous binders. Determination of needle penetration.

EN 1427:2007: Bitumen and bituminous binders. Determination of the softening point. Ring and Ball method.

Gill PS, Sauerbrunn SR, Reading M. Modulated differential scanning calorimetry. *J. Therm. Anal.*, 1993, 40 (3), 931-939.

Keattch CJ, Dollimore D. An introduction to thermogravimetry. 2nd Edition
London: Heyden, 1975, London.

Masson JF, Polomark GM. Bitumen microstructure by modulated
differential scanning calorimetry. *Thermochim. Acta*, 2001, 374 (2), 105-
114.

Masson JF, Leblond V, Margeson J. Bitumen morphologies by phase-
detection atomic force microscopy. *J. Microsc.-Oxford*, 2006, 221, 17-29.

Reading M. Modulated differential scanning calorimetry - A new way
forward in materials characterization. *Trends Polym. Sci.*, 1993, 1, 248-253.

Sorai M. Comprehensive handbook of Calorimetry & Thermal Analysis, J.
Wiley & Sons Ltd., The Atrium, 2004, Southern Gate, Chichester, West
Sussex, England.

BITUMEN MODIFICATION BY THIOUREA DIOXIDE

Chapter IV

*Physico-chemical modificacion of asphalt
bitumens by reactive agents*

4.1. INTRODUCTION

Unfortunately, even the best designed and constructed road pavements deteriorate overtime under the combined effects of traffic loading and weathering, with the most common distresses being rutting (or permanent deformation of the pavement at high temperatures) and thermal cracking (or thermal fracture due to its lack of flexibility at low temperatures) (Kandhal et al., 2003; Lu et al., 2003).

In addition, bitumen may undergo ageing processes, which also affect its performance as asphaltic binder. First, there is a rapid chemical ageing upon mixing hot bitumen with hot aggregates. Second, there occurs an in-situ ageing during the service life of the pavement. Bitumen molecules may irreversibly evolve through chemical ageing, which is mainly related to oxidation reactions and polymerisation between asphaltene molecules and, to a lesser extent, some evaporation of the lightest bitumen compounds. As a result, chemical ageing leads to a global hardening of the material, which increases the cracking probability (Lesueur, 2009).

For all these reasons, bitumen performance has been traditionally improved through the addition of virgin polymers (SBS, SBR, EVA, etc.) and waste polymers (plastics from agriculture, crumb tire rubber, etc.) (García-Morales et al., 2006; García-Morales et al., 2004). A promising alternative to the above-commented modifiers is the use of non-polymeric reactive agents able to form chemical bonds with bitumen compounds such as sulphur, polyphosphoric acid (PPA) (Masson, 2008), a mineral acid (Giavarini et al., 2000) or organic molecules (Martínez et al., 2008).

On these grounds, this chapter deals with the use of thiourea dioxide (ThD) as a potential reactive agent for paving industry. Bitumen modification by ThD is expected to occur on a reducing/decomposition action that may

lead to different pathways depending on the selected processing conditions. In this sense, the rheological response, thermal behaviour, chemical composition and microstructure of two different bitumen types, and their corresponding thiourea dioxide-modified binders, were analysed.

4.2. EXPERIMENTAL

4.2.1. Materials

Two different types of bitumen, with penetrations within the intervals 40/50 and 150/200, respectively, were used as base material for the modification. The results of two selected technological tests (penetration grade and softening temperature, according to EN 1426:2007 and EN 1427:2007, respectively) and the chemical composition, in terms of SARAs fractions, corresponding to each of them are shown in Table 4.1.

Table 4.1. Penetration values, ring & ball softening temperatures, SARAs fraction and colloidal index values for the two neat bitumens studied.

	Bitumen 150/200	Bitumen 40/50
Penetration (dmm)	168	49
R&B softening point (°C)	41.0	53.5
Saturates (wt.%)	7.4	6.2
Aromatics (wt.%)	57.6	50.3
Resins (wt.%)	15.1	24.5
Asphaltenes (wt.%)	19.9	19.0
Colloidal Index (C.I.) ^a	0.38	0.34

^aColloidal Index = (asphaltenes + saturates) / (resins + aromatics)

Two different modifying agents, a non-polymeric additive and a thermoplastic elastomer, have been employed:

a) Thiourea dioxide (ThD), supplied by Sigma Aldrich, has been the selected reactive agent used for bitumen modification. It melts at around 124-127 °C, and has a molecular weight of 108.12 g/mol.

b) On the other hand, commercial Styrene-Butadiene-Styrene, SBS, triblock copolymer “Kraton D-1101”, provided by Shell Chemical Company U.K., was selected for “physical modification”, through mere physical dispersion in bitumen. It has a molecular weight of $1.5 \cdot 10^5$ g/mol and a styrene content of 31 wt.%.

4.2.2. Samples preparation

Blends of bitumen with 3 and 9 wt.% ThD were prepared for 1 h, in a cylindrical vessel (60 mm diameter, 140 mm height) and at three different temperatures (90, 130 and 180 °C). A low-shear mixer IKA RW20 (Germany), equipped with a four-blade impeller, was used at a rotating speed of 1200 rpm. Just after processing, a part of this binder was poured onto aluminium foil, forming a thin layer which was exposed to ambient (curing period) for up to 12 months.

The specific effects of temperature and agitation on neat bitumen were assessed by subjecting neat bitumen, without ThD addition, to the same processing conditions as described above (referred to as the “blank” sample). Finally, because sulphur is formed during the ThD decomposition reaction, a 2 wt.% sulphur modified bitumen was also processed under the same conditions (2 wt.% sulphur is the equivalent quantity produced after reaction R1; see below). This study will allow us to establish its effect on the rheological response of the modified binder.

In addition, a reference bituminous binder containing 3 wt.% commercial SBS was prepared for 1.5 h, at 180 °C under high shear conditions.

4.2.3. Testing procedures

Viscous flow measurements, at 60 °C, were carried out in a controlled-strain ARES rheometer (Rheometric Scientific, USA). Linear viscoelastic frequency sweep tests, between 10^{-2} and 10^2 rad/s (at 30 and 60 °C), and temperature sweep tests in oscillatory shear at constant frequency and strain (10 rad/s and 1 %, respectively) and a heating rate of 1 °C/min from 30 to 100 °C, were conducted in a controlled-stress rheometer PHYSICA MCR-301 (Anton Paar, Austria). A serrated plate-and-plate geometry (25 mm diameter and 1 mm gap) was used for all rheological shear measurements.

Dynamic Mechanical Thermal Analysis (DMTA) tests were performed on neat and modified bitumens with a Seiko DMS 6100 (Seiko Instruments Inc., Japan) in double cantilever bending mode, using 50 x 10 x 3 mm specimens, and liquid nitrogen as cooling system. Frequency sweep tests from 10^{-2} to 10^2 Hz were carried out, in the linear viscoelasticity (LVR) region, at four selected temperatures from -30 to 15 °C, in 15 °C-increments. Furthermore, temperature sweep tests, ranging from -35 to 35 °C, were conducted at a fixed frequency of 1 Hz and strains within the LVR region, by selecting a temperature ramp of 2 °C·min⁻¹.

Modulated Differential Scanning Calorimetry (MDSC) was performed with a TA Q-100 (TA Instruments, USA). Samples (5-10 mg) were subjected to the same testing procedure: a temperature interval between -80 and 100 °C; a heating rate of 5 °C/min; an amplitude of modulation of ± 0.5 °C, a period of 60 s; and nitrogen as purge gas, with a flow rate of 50 mL/min. To

provide the same recent thermal history, all the samples were placed into hermetic aluminium pans for 24 h before measurement.

Simultaneous thermo gravimetric/differential thermal analyses (TG/DTA) were conducted using a Seiko TG/DTA 6200 (Japan). Temperature ramps at 10 °C/min, from 40 to 600 °C, under N₂ atmosphere were carried out on 5-10 mg of sample.

The bitumen SARAs fractions were determined by thin layer chromatography coupled with a flame ionization detector (TLC/FID), using an Iatroscan MK-6 analyzer (Iatron Corporation Inc., Japan). The elutions were performed in hexane, toluene and dichloromethane/methanol (95/5), following the procedure outlined elsewhere (Ecker, 2001).

4.3. RESULTS AND DISCUSSION

4.3.1. Effect on binder formulation

The main objective of this section was to study binder modification degrees achieved by adding thiourea dioxide (ThD), at a processing temperature of 130 °C, to two different types of bitumen, with penetrations within the intervals 40/50 and 150/200, as well as to explore the effect that ThD concentration provokes on the rheological behaviour at medium/high in-service temperatures. In addition, a selected ThD modified binder (bitumen 40/50 containing 9 wt.% ThD, after 60 days of ambient curing) was used to assess the linear viscoelastic response at low in-service temperatures.

4.3.1.1. Rheological behaviour at medium/high in-service temperatures

Figure 4.1 shows the viscous flow curves, at 60 °C, of selected ThD-modified binders prepared from two different bitumens, as a function of curing time. As can be seen, neat and 3 wt.% ThD-modified binder from bitumen 150/200 display Newtonian behaviour in the whole shear rate range studied, even when ThD content is increased up to 9 wt.% (results not shown here). On the contrary, neat and 9 wt.% ThD-modified binder from bitumen 40/50 show a Newtonian behaviour in the low-intermediate shear rate range studied, followed by a shear-thinning region when shear rate is increased further. It can also be observed that ThD addition to neat bitumen leads to a first slight increase in viscosity after one hour of processing, which continues during storage at ambient conditions (curing time). However, such a time-dependent evolution of viscosity is strongly influenced by the neat bitumen used. Thus, bitumen 150/200 undergoes a very significant increase between 20 and 60 days of curing, much more apparent than that observed for bitumen 40/50 (Figure 4.1).

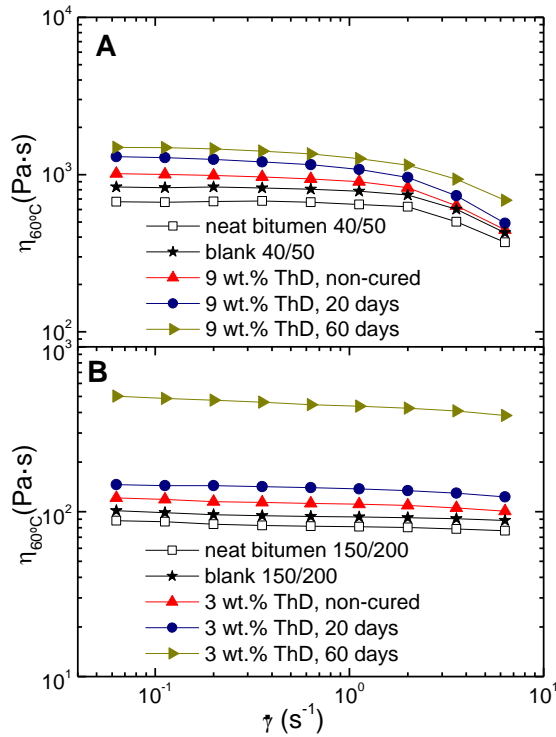


Figure 4.1. Viscous flow curves, at 60 °C, for (A) 9 wt.% ThD modified bitumen 40/50 and (B) 3 wt.% ThD-modified bitumen 150/200, as a function of curing time.

The estimation of a modification index (M.I.^{60°C}) from the values of the zero-shear-rate limiting viscosities of the binders may be considered as a useful parameter to quantify bitumen modification at high in-service temperatures. This modification index has been defined as follows:

$$\text{M.I.}^{60^\circ\text{C}} = \frac{\eta_{0,\text{mod}} - \eta_{0,\text{proc}}}{\eta_{0,\text{proc}}} \quad (4.1)$$

where $\eta_{0,\text{mod}}$ is the zero-shear-rate-limiting viscosity of the ThD-modified bitumen, and $\eta_{0,\text{proc}}$ is the zero-shear-rate-limiting viscosity of the “blank” sample, both of them at 60 °C.

Hence, this parameter quantifies viscosity changes due to the addition of the modifying agent (ThD), regardless of the expected bitumen oxidation produced during binder processing. Figure 4.2 displays the evolution of the modification index (M.I.^{60°C}) with curing time for three selected samples. As commented above, the addition of ThD leads to a first increase in the M.I.^{60°C} values just after processing (“non-cured” samples) that, for bitumen 150/200 samples, becomes much more important as modifying agent concentration is raised from 3 to 9 wt.%.

This fact suggests the existence of chemical reactions between bitumen and modifier during blending. Moreover, such a viscosity enhancement continues after 20 and, even, 60 days of curing, mainly for bitumen 150/200. These results lead to establish two different bitumen modification pathways: a) a “short-term” modification, during blending of bitumen and ThD, at 130 °C; b) a “long-term” modification, as a consequence of curing, at room temperature. As a result, bitumen viscosity may increase up to more than 5 times its original value after 60 days of curing (see bitumen 150/200, in Figure 4.2).

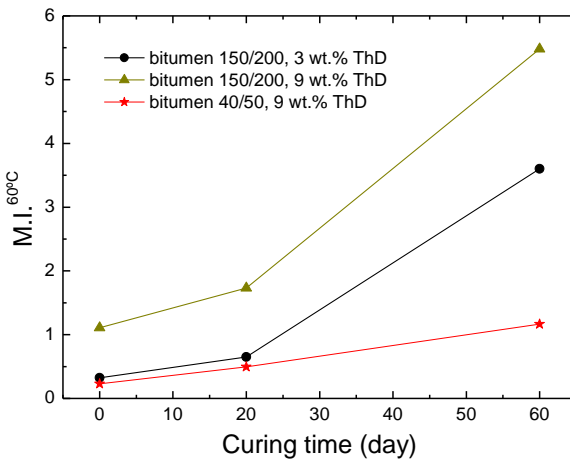


Figure 4.2. Evolution of the modification index with curing time, for three selected ThD-modified bitumen samples.

Temperature sweep tests in oscillatory shear (10 rad/s and 1°C/min heating rate), from 30 to 75 °C, were carried out on neat bitumen 150/200 and their corresponding modified bitumen samples (3 and 9 wt.% ThD). Figure 4.3 shows the evolution with temperature of the loss tangent (ratio of viscous, G'' , and elastic, G' , moduli), as a function of curing time. A predominantly viscous character ($\tan \delta > 1$), which is more apparent as temperature rises, is noticed for all samples. Still, ThD addition produces a decrease in $\tan \delta$ values (enhancing binder elastic properties), mainly for those systems with the highest concentration of modifier, and which is favoured by long curing times.

On the other hand, the average slope of the curve of the loss tangent vs. temperature, within the interval 40-60 °C, can be related to binder thermal susceptibility at high in-service temperatures. Thus, this average slope decreases from 0.024 for neat bitumen 150/200 down to 0.013 for its corresponding 9 wt.% ThD-modified binder, after 60 days of curing at room temperature. This result would suggest a lower thermal susceptibility, in the temperature range considered, and, consequently, an improved thermal resistance would be expected for these modified binders (Chebil and Chaala, 2000).

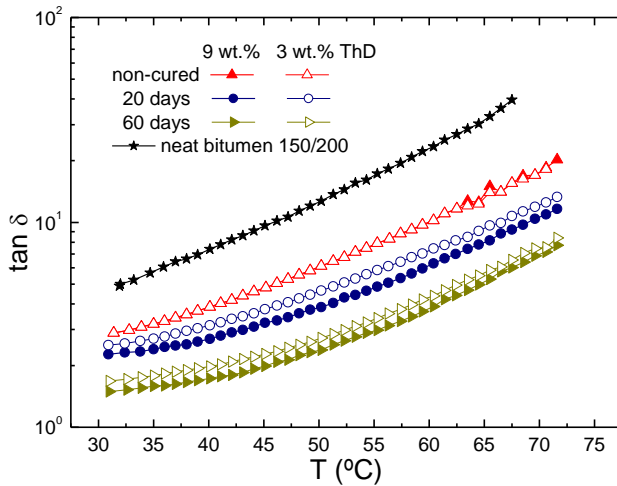


Figure 4.3. Evolution of the loss tangent with temperature, for modified bitumen 150/200 samples, as a function of curing time.

In summary, the modification of bitumen with ThD seems to yield an improvement in bitumen behaviour at medium/high in-service temperatures, since it increases binder viscosity (at 60 °C) and enhances both its elastic properties and thermal susceptibility. However, the kinetics of this modification appears to be quite slow, as may be deduced from the evolution of the rheological properties with curing time. Thus, it takes up to 60 days to obtain a modified binder with significantly improved properties.

4.3.1.2. Rheological behaviour at low in-service temperatures

Frequency sweep tests, performed in bending mode, have been used to assess the linear viscoelastic response, between -30 and 15 °C, of a selected modified binder (bitumen 40/50 containing 9 wt.% ThD, after 60 days of curing) and neat bitumen 40/50.

The experimental results obtained at the different temperature studied demonstrate that the mechanical spectra of both samples show predominantly elastic characteristics ($E' > E''$) at low temperatures (i.e. up to around 0 °C). The experimental frequency sweep curves have been superposed onto a master curve by using a shift-factor, a_T (see Figure 4.4). The reference temperature, T_{ref} , was arbitrarily chosen to be 0 °C. In addition, neat bitumen behaviour is presented for the sake of comparison. Within the temperature range studied, the temperature dependence of the shift factor may be described by the Williams-Landel-Ferry (WLF) equation fairly well:

$$\log a_T = \frac{-C_1 \cdot (T - T_{ref})}{C_2 + (T - T_{ref})} \quad (4.2)$$

The parameters C_1 and C_2 are presented in Table 4.2, showing similar values of C_1 for both neat and modified bitumen, but slightly higher values of C_2 for the modified binder. The fitting of this equation is shown in the inset of Fig. 4.4B for both types of binders.

Table 4.2. Parameters C_1 and C_2 of WLF equation for the neat bitumen and 9 wt.% ThD-binder after 60 days of curing.

Binder	C_1	C_2 (°C)
Neat bitumen	51.6	142.5
9 wt. % ThD, 60 days curing	51.2	144.9

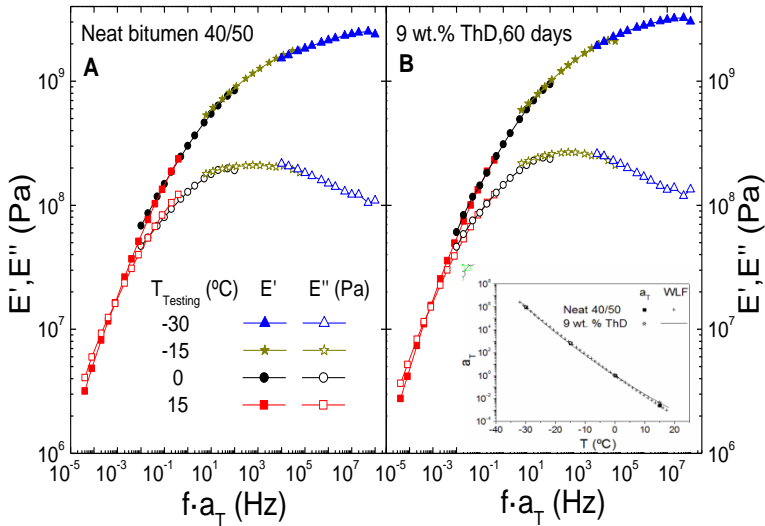


Figure 4.4. Master curves of the linear viscoelastic moduli in dynamic bending, E' and E'' , for (A) neat bitumen 40/50 and (B) 9 wt.% ThD-binder, after 60 days of curing time. (Inset: Temperature dependence of the shift factor, and WLF fitting, for both binders.)

In addition, frequency sweep tests results in dynamic bending, at the different temperatures studied, have been combined in the form of “Black” diagrams. Thus, phase angle (δ) vs. complex flexural modulus ($|E^*|$) curves for neat bitumen 40/50 and its corresponding 9 wt.% ThD-modified bitumen (after 60 days of curing) are shown in Figure 4.5. In order to shed some light on binder rheological behaviour in a wider temperature range, complex shear modulus ($|G^*|$) values, from oscillatory shear tests performed at 30 and 60 °C, have been also included. Phase angle is a relative measure of binder viscoelasticity, i.e. Newtonian liquids and Hookean solids are characterized by phase angles of 90 and 0°, respectively. The ability of the samples to store deformational energy at high in-service temperatures and to dissipate it through flow at low

temperatures is called elasticity and flexibility, respectively (Lu and Isacsson, 1997). As can be seen, at a fixed value of the complex modulus of 10^9 Pa (within the low temperature region), the modified bitumen presents a slightly higher phase angle value than the neat bitumen, suggesting that the addition of ThD may slow down the approach to an ideal elastic solid (i.e. to a more brittle material). On the other hand, for relatively low complex modulus values (down to 10^2 Pa), that is, in a temperature range comprised between 30 and 60 °C, the trend seems to be reversed. Lower values of phase angle are found for the ThD-modified bitumen, with the consequent increase in its elastic features. As a result, an enhanced material performance is expected because the addition of ThD leads to improved elasticity and flexibility, at high and low in-service temperatures, respectively.

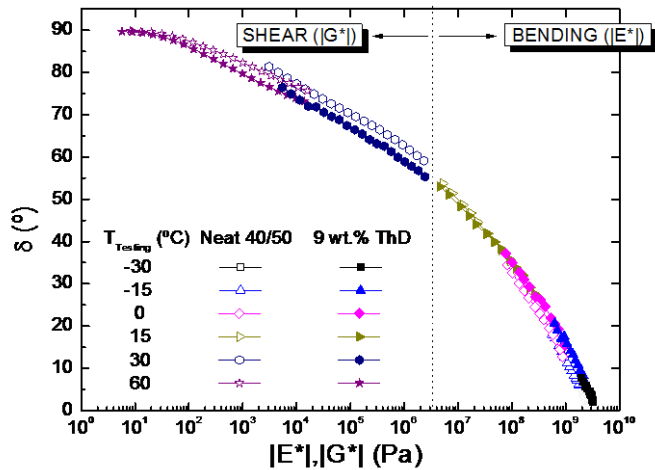


Figure 4.5. “Black” diagram for neat bitumen 40/50 and its corresponding 9 wt.% ThD-binder, after 60 days of curing.

In the same way, Figure 4.6 shows the temperature sweep curves, at 1 Hz and from -30 to 35 °C, for the 40/50 neat bitumen, and its corresponding “blank” sample and 9 wt.% ThD-modified binder after 60 days of room

curing. These thermo-rheological tests have widely been used to assess the end-performance of polymer modified bitumens at low temperatures (Fawcett et al., 1999; Navarro et al., 2010).

It can be observed a clear transition from the glassy to the Newtonian region (with a crossover point between E' and E'') with increasing temperature (Partal et al., 1999). No plateau is found between both regions, a fact that indicates the non-existence of entanglements (Ferry, 1980). As temperature decreases, it can be observed a maximum in the loss modulus, which characterizes the onset of the glassy region. The glassy state leads to brittle materials, which are more likely to undergo thermal cracking under loading. For this reason, modification should focus on shifting the above-mentioned onset temperature to lower ones. Thus, a characteristic temperature $T_{g(1Hz)}$ has been calculated (see values in Figure 4.6) from the maximum value in the loss modulus curves. Despite $T_{g(1Hz)}$ depends on frequency, and should be considered as a “*mechanical*” *glass transition temperature*, it is a suitable parameter to establish a comparative analysis of the low temperature behaviour of neat and modified binders. As can be seen, the value of this mechanical glass transition temperature is reduced around 8 °C (relative to the “blank” binder) after ThD addition, which suggests enhanced mechanical properties at low in-service temperatures.

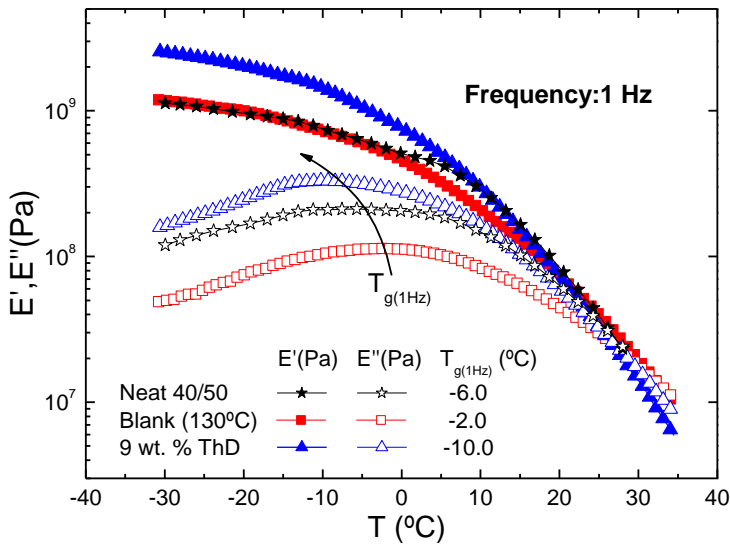


Figure 4.6. Evolution of E' and E'' with temperature (temperature sweep tests) for 9 wt.% ThD-modified bitumen 40/50, after 60 days of curing, and its corresponding “blank” sample.

4.3.2. Effect of processing temperature

The previous section showed that bitumen modification by ThD, at 130 °C, produces modified binders with enhanced thermo-mechanical properties in a wide interval of in-service temperatures, more significant as ambient curing time increases. Looking further into this modifying agent, interest is now focused on the effect that processing temperature may exert on the modification mechanism observed, as well as properties enhancement thereof derived. With this aim, neat bitumen 40/50 was modified, at three different processing temperatures (90, 130 and 180 °C), by adding 9 wt.% ThD.

4.3.2.1. Influence on the viscous flow behaviour

Viscous flow curves, at 60 °C, for 9 wt.% ThD-modified bitumen binders, prepared at two different temperatures ($T_{\text{proc}}=90$ and 180 °C), are presented in Figure 4.7, as a function of curing time. Neat bitumen and their corresponding “blanks”, at both temperatures, have been included as references. These samples always present a Newtonian region with a constant viscosity at low shear rates, η_0 , followed by shear-thinning region above a “critical” shear rate value, $\dot{\gamma}_c$. Table 4.3 reveals a decrease in the values of this parameter with curing time and so, the development of a more complex microstructure, which is more susceptible to shear forces (Martín-Alfonso et al., 2008).

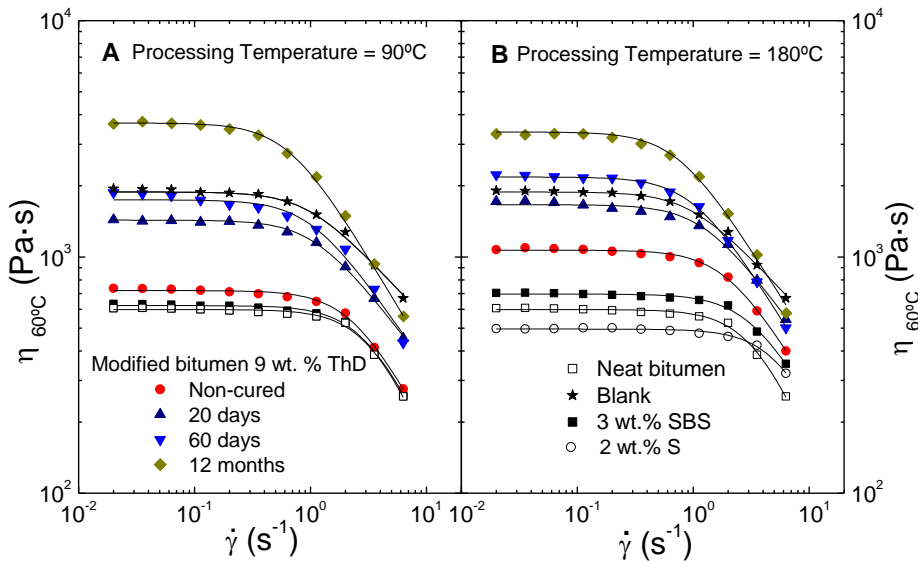


Figure 4.7. Viscous flow curves, at 60 °C, for 9 wt.% ThD-modified binders, processed at 90 °C (A) and 180 °C (B), as a function of curing time.

Table 4.3. Evolution with curing time of zero-shear limiting viscosity, η_0 , and critical shear rate, $\dot{\gamma}_c$, for 9 wt.% ThD-modified binders prepared.

	Binders	η_0 (Pa·s)	$\dot{\gamma}_c$ (s^{-1})
		Neat	598.8
$T_{\text{processing}} (^{\circ}\text{C})=90$ °C	Blank	622.3	3.1
	Non-cured	720.6	2.4
	20 days	1431.1	1.1
	60 days	1744.1	1.0
	12 months	3686.5	0.7
$T_{\text{processing}} (^{\circ}\text{C})=130$ °C	Blank	665.0	3.2
	Non-cured	907.6	2.5
	20 days	1270.9	1.6
	60 days	1467.2	1.3
	12 months	2314.8	0.8
$T_{\text{processing}} (^{\circ}\text{C})=180$ °C	Blank	696.0	3.2
	Non-cured	1068.2	2.0
	20 days	1663.1	1.3
	60 days	2178.5	1.0
	12 months	3378.5	0.8

Table 4.3 and Figure 4.7 show that, for any of the processing temperatures presented, ThD addition always leads to a viscosity increase, which is further enhanced when samples are stored at ambient conditions for a period of up to 12 months. Thus, after 60 days of curing, the sample processed at 90 °C presents viscosities very similar to those of the reference sample, containing 3 wt.% SBS (commonly used in paving applications), and at 180 °C, its viscosity is even higher. After 12 months, any of the two processing temperatures studied give rise to ThD-modified binders with higher viscosity than that measured for the SBS reference binder.

As can be observed for the “blank” sample processed at 180 °C, binder manufacture itself causes an increase in viscosity, due to oxidation of the

maltene fraction (Navarro et al., 2009), showing very similar viscosities to those observed for the “non-cured” 9 wt.% ThD-modified bitumen prepared at 90 °C, for which oxidation is negligible. In that sense, the evolution of η_0 , at 60 °C, with curing time, shown in Table 4.3, describes the absolute degree of bitumen modification at high in-service temperature. Once again, in order to take account viscosity changes only to ThD addition, the previous modification index ($M.I.^{60^\circ C}$) can be used to study the enhancements attained with the curing time (equation 4.1).

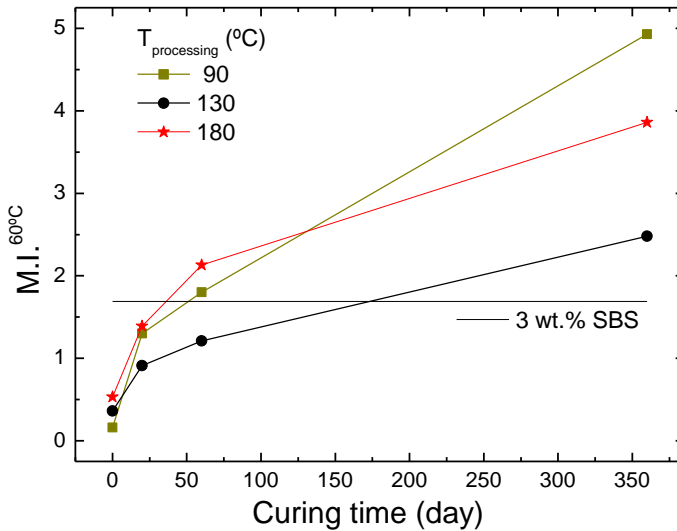


Figure 4.8. Evolution of the modification index with curing time for 9 wt.% ThD-bitenders at the three selected processing temperatures.

As observed in Figure 4.8, which presents the evolution of $M.I.^{60^\circ C}$ with curing time for bitumen modification carried out at 90, 130 and 180 °C, a remarkable increase in viscosity, larger than that merely induced by bitumen oxidation, results from ThD addition. It can also be noticed that, for “non-cured” samples, the $M.I.^{60^\circ C}$ increase undergone by the samples become more significant as temperature increases. However, Figure 4.8 demonstrates that long-term bitumen modification is quite a more complex

issue, as deduced from the results obtained for the sample processed at 90 °C, which exceeds the M.I.^{60°C} value of the sample processed at 130 °C; after 60 days it displays a higher modification degree than that found for the sample containing 3 wt.% SBS; and after 12 months, it shows even a higher modification index than that measured for the system processed at 180 °C. Consequently, this suggests, for every processing temperature studied, the formation of different reaction products which would evolve with time in a different way.

4.3.2.2. Influence on the linear viscoelastic behaviour

The influence of processing temperature on the linear viscoelastic behaviour of the ThD-modified binders was studied by means of temperature sweeps test in oscillatory shear (medium/high temperatures) and bending (low temperatures).

Figure 4.9A shows the evolution of G' and G'' (oscillatory shear mode) with processing temperature (90, 130 and 180 °C) for “non-cured” samples. It can be seen that G' and G'' values monotonously decrease with increasing testing temperature from 35 up to 90 °C. Moreover, the viscous modulus clearly prevails over the elastic one in the entire temperature interval tested, which points out a predominantly viscous behaviour. In addition, an increase in the viscoelastic moduli of the “non-cured” samples is also observed as processing temperature increases from 90 up to 180 °C (results similar to those found for the viscosity, shown in Figure 4.7).

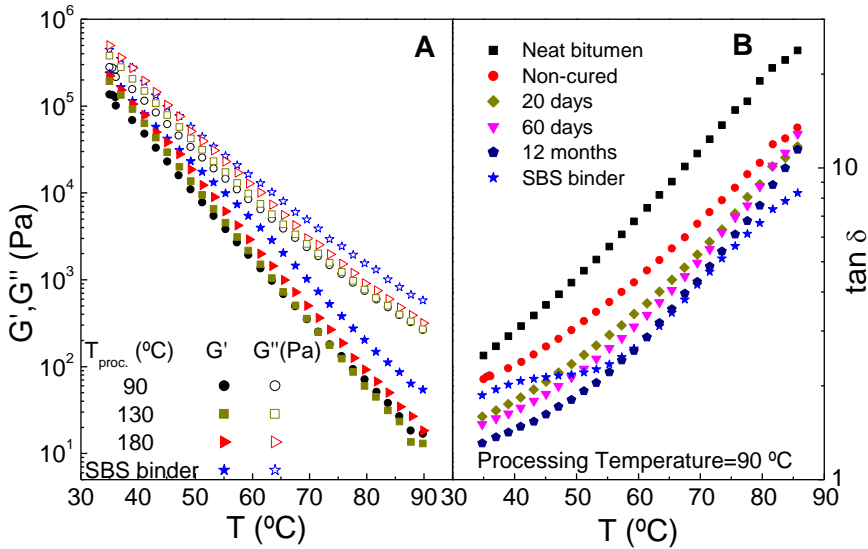


Figure 4.9. Evolution with temperature of the (A) linear viscoelastic moduli, in oscillatory shear (G' and G''), for “non-cured” 9 wt.% ThD-binders processed at different temperatures and (B) loss tangent for 9 wt.% ThD-binders, processed at 90 $^{\circ}\text{C}$, as a function of curing time.

The evolution of G' and G'' was also studied as a function of curing time for ThD-modified binders processed at 90 $^{\circ}\text{C}$. Figure 4.9B makes clear the prevailing viscous behaviour of the samples, with loss tangent values always higher than 1. However, an enhancement in the elastic features is observed with increasing curing time, as deduced from the lower values of $\tan \delta$ after 2 and 12 months of curing.

On the other hand, the ThD-modified binders, after 60 days of curing, have proved to present satisfactory results in the low temperature region, as can be deduced from Figure 4.10, which shows the temperature dependence, between -35 and 35 $^{\circ}\text{C}$, of the flexural moduli (E' and E''), within the LVR strain limits, at 1 Hz.

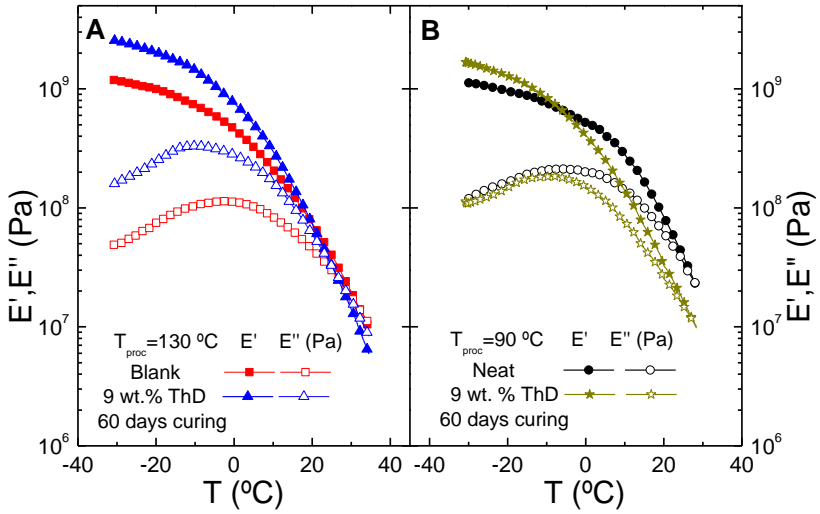


Figure 4.10. Evolution with temperature of the linear viscoelastic moduli, in dynamic bending (E' and E''), for 9 wt.% ThD-bitumens cured for 60 days and processed at 130 °C (A) and 90 °C (B). Neat bitumen and “blank”, processed at 130 °C, are included as reference.

As can be observed, below the crossover point between E' and E'' , the evolution from the transition to the glassy region (this latter characterized by high material brittleness and, therefore, high probability of thermal cracking under loading) with increasing temperature is apparent for every sample tested (Partal et al., 1999).

Once again, a “mechanical” (and so, frequency-dependent) *glass transition temperature*, taken as the value at the maximum peak in the E'' curve, may be used to establish a comparative analysis between the low temperature performance of the modified bituminous binders (after 60 days of curing) and their corresponding “blank” samples. Thus, values of the glass transition temperature measured from isochronal E'' curves, at 1 Hz, are shown in Table 4.4. A significant decrease in $T_{g(1\text{Hz})}$ values (8 °C), from -2 °C for the “blank” sample at 130 °C, down to -10 °C for its corresponding modified sample, demonstrates that ThD addition and ambient curing

process enhance binder resistance to thermal fracture at low in-service temperatures and, consequently, it is expected to have similar benefits on the asphalt mixtures thereof obtained. For samples processed at 90 °C, at which “primary ageing” during mixing is negligible, $T_{g(1Hz)}$ corresponding to the neat sample can be taken as the reference value for comparison. In that sense, just a decrease in $T_{g(1Hz)}$ of 3 °C is noticed.

Finally, it is worth mentioning that the “blank” sample at 180 °C was not possible to measure in DMTA rheometer, because this sample presented very low flexibility at low temperatures. However, its corresponding ThD modified samples, after 60 days of curing time, shows similar rheological response than those binders processed at the other temperatures (see $T_{g(1Hz)}$ in Table 1.4).

Table 4.4. DMTA glass transition temperatures ($T_{g(1Hz)}$) for 9 wt.% ThD-binder processed at different temperatures, after 60 days of curing.

Binder	$T_{g(1Hz)}$ (°C)
Neat bitumen	-6.0
Blank ($T_{proc}=130$ °C)	-2.0
Modified ($T_{proc}=90$ °C)	-9.0
Modified ($T_{proc}=130$ °C)	-10.0
Modified ($T_{proc}=180$ °C)	-9.0

4.3.3. Bitumen modification routes and microstructure

The above mentioned enhancements in viscous and viscoelastic behaviours, at both medium/high and low in-service temperatures, hint significant changes in binder microstructure, as a consequence of chemical reactions involving ThD, which seems to follow different pathways depending on the processing temperature. Hence, thermal analysis

(TG/DTA and MDSC tests) and thin layer chromatography (TLC-FID) may shed some light on this issue.

TG and DTA tests, which allow enthalpy and sample mass loss to be determined simultaneously in an open system (Yang et al., 1999), may provide valuable information about possible modification pathways and their resulting reaction products.

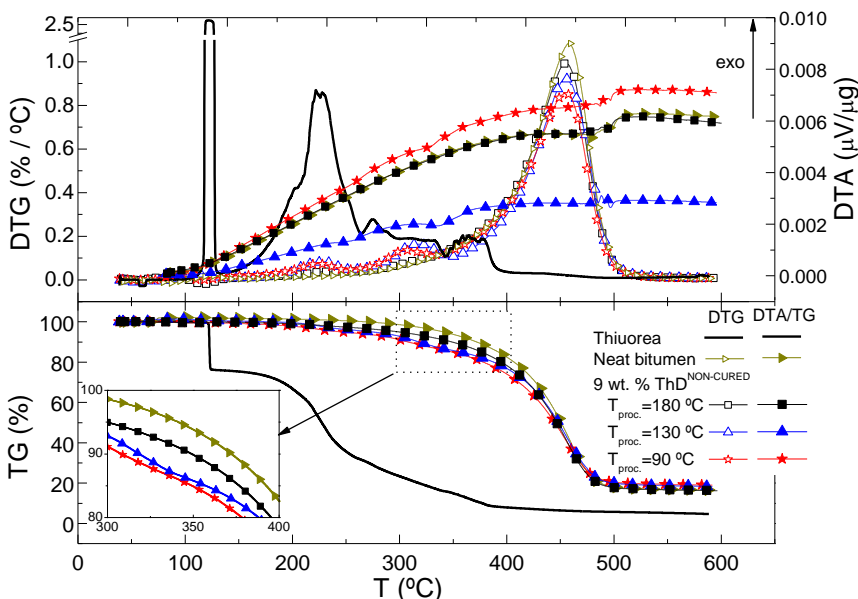
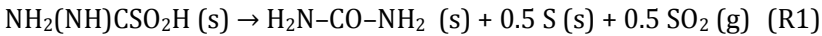


Figure 4.11. TG/DTG and DTA curves between 40 and 600 $^{\circ}\text{C}$ and under N_2 atmosphere for thiourea dioxide, neat bitumen, and “non-cured” 9 wt.% ThD binders processed at the three selected processing temperatures.

Figure 4.11 reveals that an increase in processing temperature leads to significant differences in the TG/DTA curves obtained. Thus, neat bitumen presents a large mass loss process, extending over a wide temperature interval (from 300 to 500 $^{\circ}\text{C}$, with a DTG peak at 455 $^{\circ}\text{C}$), which involves decomposition/volatilization of chemical compounds with very different molecular weights. However, “non-cured” ThD modified bitumens shown

in Figure 4.11 also present some other peaks. Firstly, it can be observed that the height of the peak at 455 °C decreases as processing temperature does, as a consequence of the existence of two new significant peaks: the first one arisen at 220 °C, and the second one at 300 or 310 °C, for processing temperatures of 90 or 130 °C, respectively. Interestingly, those peaks almost vanish at the highest processing temperature (180 °C).

Aiming to understand the origin of the news peaks, the thermal decomposition of thiourea dioxide was studied, and the result included in Figure 4.11. According to Wang et al. (2005), thiourea dioxide thermal decomposition occurs in two stages. The first one, located between 121 and 144 °C (with a marked DTG peak at 135 °C), is related to the release of SO₂ and involves a significant mass loss of about 17 wt.%:



The second stage in thiourea dioxide decomposition (shown by a shorter but broader DTG peak at around 220 °C) is governed by continuous melting, vaporization and decomposition of urea produced by the first reaction. Although it is a complex process, the overall chemical reaction can be written as:



Accordingly, the peak appearing at 220 °C in the modified binders should be attributed to urea decomposition. However, the second peaks, at 300 or 310 °C, which cannot be related to any identified process, might correspond to new products formed through bitumen modification by ThD (or even upon heating over 120 °C in TG/DTA tests). Figure 4.11 also reveals that they do not appear when bitumen modification has been carried out at 180 °C.

On the other hand, it is well known that bitumen is a colloidal system composed of two fractions: maltenes (which can be separated into three different types of compounds: saturates, aromatics and resins) and asphaltenes. In general, road paving distresses caused by bitumen ageing are related to changes in its colloidal structure. In chemical terms, it is accepted that oxidative ageing leads to a transformation among bitumen components as follows: aromatics → resins → asphaltenes. Saturates, instead, remain essentially unchanged, pointing out their low chemical reactivity. These changes result in a slightly higher glass transition temperature (Lesueur, 2009). However, the opposite trend has been observed for the ThD-modified binders studied (see, for instance, Table 4.4), a fact that hints a different type of chemical modification.

Moreover, the evolution with curing time of the SARAs fractions for the ThD modified bitumens processed at 90 and 130 °C (see Figure 4.12) may be of some help to understand these results. Changes in the different bitumen fractions evidence chemical interactions. Also, a very significant decrease in the asphaltenic fraction concentration with increasing curing time is observed for the binder processed at 130 °C. Much less important is the decrease noticed for the binder processed at 90 °C.

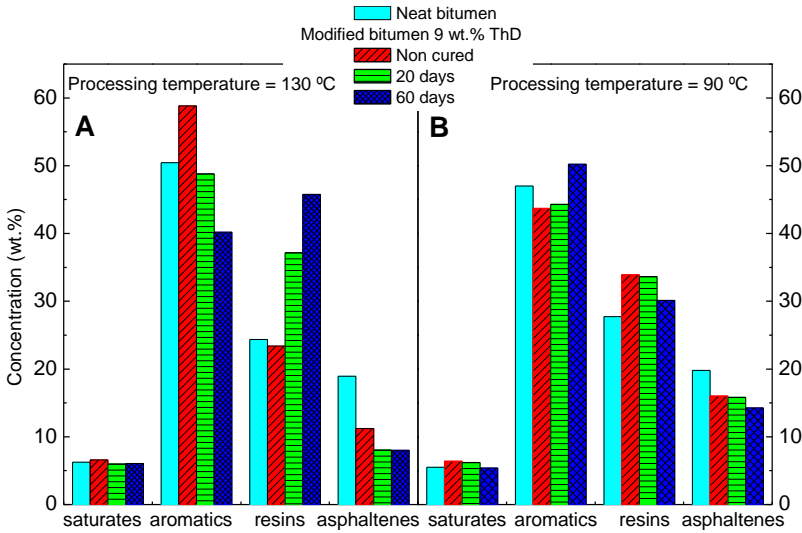


Figure 4.12. Evolution of SARAs fractions with curing time for 9 wt.% ThD binders processed at 90 (A) and 130 °C (B).

In any case, the contribution of each single SARAs fraction to the overall colloidal structure of the resulting modified bitumen can be quantified by means of a colloidal index (Lesueur, 2009), which can be written as follows:

$$C.I. = \frac{\text{saturates} + \text{asphaltenes}}{\text{aromatics} + \text{resins}} \quad (4.3)$$

Table 4.5 presents the evolution of this parameter for ThD-bitumen binders, processed at 90 and 130 °C. In general, a higher C.I. means larger asphaltene clusters, leading enhanced rheological properties. By contrast, a decrease in C.I. with increasing curing time is observed, which does not support the increase in viscosity and elastic features, at medium/high in-service temperatures, previously found (see Figures 4.7 to 4.9). However, equation (4.3) defines C.I. in terms of the SARAs fractions, determined through a chromatographic method whose starting point consist of

dissolving 5 mg of sample in 10 mL of toluene. Hence, C.I. only considers those compounds which dissolve in toluene. So, we may assume that an important part of those new products responsible for the mechanical properties enhancement are basically insoluble in toluene.

Table 4.5. Evolution with curing time of the colloidal index (C.I.) for 9 wt.% ThD binders processed at the three selected processing temperatures.

Binder	Curing time		
	Non-cured	20 days	60 days
Modified ($T_{\text{proc}}=90\text{ }^{\circ}\text{C}$)	0.29	0.28	0.24
Modified ($T_{\text{proc}}=130\text{ }^{\circ}\text{C}$)	0.21	0.16	0.15
Modified ($T_{\text{proc}}=180\text{ }^{\circ}\text{C}$)	0.27	0.22	0.20

Filtration tests and thermogravimetric analysis in Figure 4.13 confirm this assumption. In this sense, photographs of residues collected after filtration of modified bitumens (after 60 days of curing) dissolved in toluene are shown as an inset. Interestingly, the dark-coloured residue of the sample prepared at 130 °C may indicate the presence of asphaltene-derived compounds, confirmed in Figure 4.12 by a significant reduction in the asphaltenic fraction of the sample processed at this temperature. On the contrary, a light-coloured residue is observed when bitumen modification is carried out at 90 °C, and therefore, it demonstrates the existence of a different modification mechanism.

Moreover, those residues were analysed by means of TG/DTA tests. For the sample processed at 130 °C, the DTG curve points out that the dark-coloured residue is mainly composed of urea (peak at 220 °C) and new reaction compounds (peak at 310 °C). In this case, only a small quantity of residual non-reacted ThD is noticed. Thus, the evolution with curing time of viscosity and elasticity, at high in-service temperatures, may be mainly attributed to the formation of products between polar bitumen compounds

(above all, asphaltenes) and urea formed through reaction R1. Just to ensure that sulphur formed after ThD decomposition is not contributing to the overall rheological response, it was added to neat bitumen in equivalent quantity to that produced in reaction R1 (about 2 wt.% over the total binder weight). The decrease in viscosity shown in Figure 4.7 demonstrates that, far from being a viscosity enhancing agent, such a small percentage of sulphur can only produce a plasticizing effect (Gawel, 2000).

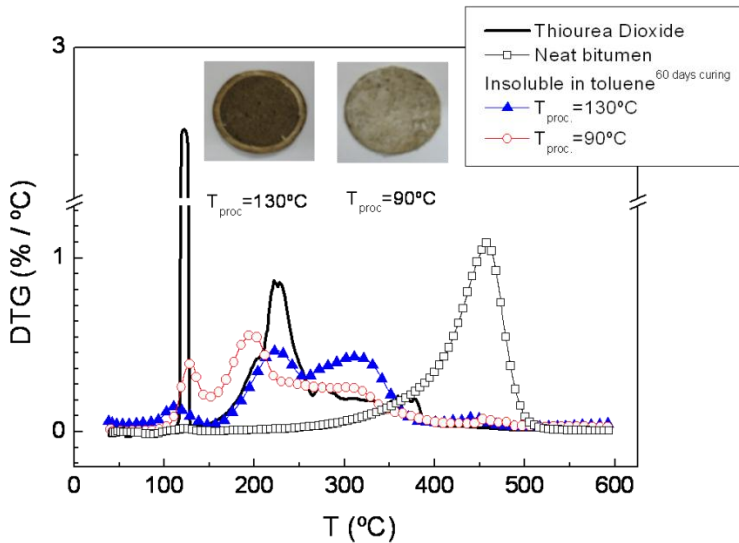
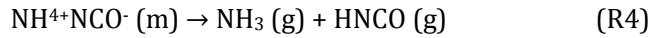
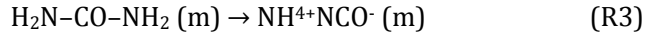


Figure 4.13. DTG curve between 40 and 600 °C and under N₂ atmosphere for thiourea dioxide, neat bitumen, and filtration residues of 9 wt. ThD-bitumens cured for 60 days and processed at 90 and 130 °C. Inset: photographs of residues described in the text.

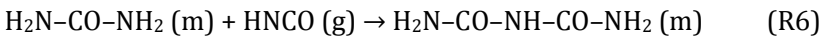
By contrast, for the sample processed at 90 °C, a much higher quantity of residual non-reacted ThD appears (peak at 135 °C), as reaction R1 does not happen during modification at that temperature. Also, a peak, at 200 °C, appears as a consequence of the urea formed upon heating over 120 °C in the TG/DTA test, although no major peak, due to formation of new products, is observed at 300 °C, as the residue does not contain a

significant quantity of asphaltenes. Thus, at 90 °C, neat ThD and urea are thought to be the main responsible for the modification observed. The presence of urea in the sample processed at 90 °C (below the ThD melting/decomposition temperature) would arise from a slow decomposition of ThD, typically found in acidic to weakly alkaline aqueous media, toward urea and sulfoxylic acid. In that sense, a slow diffusion into bitumen of water from the surrounding environment (i.e. due to air moisture) could explain the long-term curing process observed for at least 12 months (Martín-Alfonso et al., 2008; Fujiyasu et al., 1986). Small molecules such as urea and thiourea derivatives have demonstrated strong hydrogen bonding activity and have emerged as potential organocatalysts. Similarly, polyphosphoric acid (PPA) has been proposed as both a reaction catalyst and a reactant able to change the hydrogen bond network of bitumen (Masson et al., 2008).

Regarding the binder manufactured at 180 °C, no residue after filtration was observed, while none of the characteristic peaks appear in the DTG curve, other than that corresponding to the bitumen decomposition, which can be seen in Figure 4.11. In fact, the DTG results in this figure reveal that 150 °C is the onset for urea decomposition; so, both reactions R1 and R2 may be occurring during processing at 180 °C. Hence, urea finally decomposes into two gaseous components. However, although NH_3 and HNCO represent the final products of reactions, urea thermal decomposition is known to be a complex process involving further decomposition of primary products through secondary series of reactions (Schaber et al., 2004). Thus, at 152 °C decomposition begins, accompanied by vigorous gas evolution from the melt. In this case, the overall reaction R2 is split into the two following partial reactions:



On the basis of these facts, a modification mechanism via reaction between cyanic acid and polar bitumen compounds with the formation of urethane linkages (reaction R5) is herein proposed. In addition, a product of urea decomposition, HNCO, may also react with non-reacted urea to produce biuret-derived compounds (reaction R6), at approximately 160 °C:



Finally, the above-commented chemically-induced changes in bitumen composition yield an important modification of the bitumen microstructure, which can be studied by means of the non-reversing component of the heat flow curve, obtained by modulated DSC. According to Masson and Polomark (Masson and Polomark, 2001), saturates are semicrystalline, aromatics are amorphous, and resins and asphaltenes are mesophasic. They order in four stages upon cooling from the melt, yielding four specific thermal events in the non-reversing heat flow curve.

Figure 4.14 shows the non-reversing thermograms for neat bitumen, as well as its corresponding “blank” sample and ThD-binders processed at 90 and 130 °C, after 60 days of curing. If attention is first focused on neat bitumen, a broad endothermic background extending, approximately, from -40 to 80 °C (first event) can be observed. Also, two exotherms, located at about -9 °C and 40 °C (second and third events, respectively), are noticed. Finally, an endothermic peak appears at around 50 °C (fourth event). Second and third thermal events are caused by a time-dependent cold-

crystallization of low and high molecular weight saturated segments upon cooling, respectively. Hence, above the frozen state ($T > T_g$), chain mobility is increased and those segments can crystallize (Navarro et al., 2009; Masson and Polomark, 2001; Masson et al., 2002).

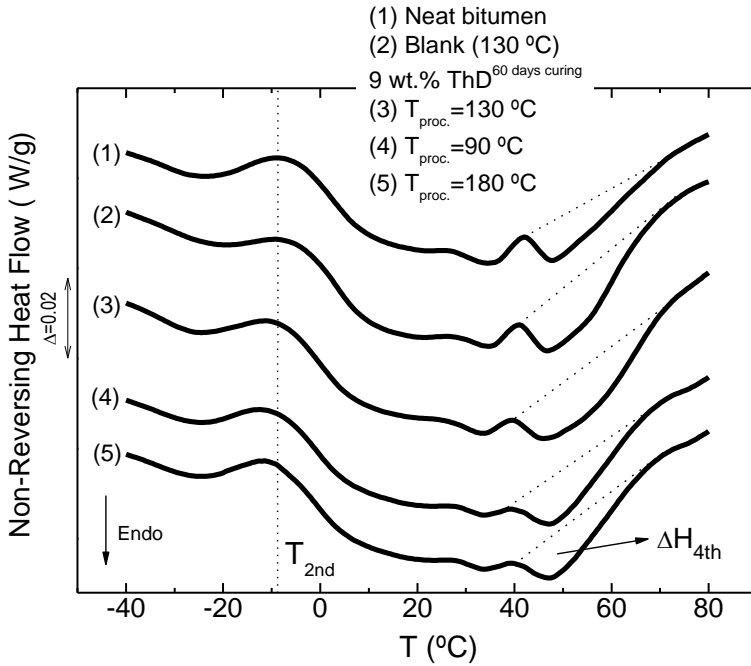


Figure 4.14. Non-reversing heat flow thermograms for 9 wt.% ThD binders cured for 60 days and processed at 90 °C and 130 °C. Neat bitumen and “blank” samples included as references.

Table 4.6, which gathers temperatures at which the second event (T_{2nd}) appears, shows a similar value, of about -9 °C, for neat bitumen and its corresponding “blank” sample at 130°C. By contrast, T_{2nd} decreases down to -11.3 and -12.6 °C after addition of 9 wt. % ThD and 60 days of curing, at processing temperatures of 130 °C and 90 °C, respectively. These results are supported by the lower T_g values after ThD addition observed in DMTA tests, which would increase the chain mobility, which consequently would reduce temperature at which cold crystallization begins.

Table 4.6 Second event temperatures (T_{2nd}) and fourth event enthalpies (ΔH_{4th}) for 9 wt.% ThD binder processed at different temperatures, after 60 days of curing.

Binder	T_{2nd} (°C)	ΔH_{4th} (J/g)
Neat bitumen	-9.0	2.14
Blank ($T_{proc}=130$ °C)	-9.3	2.97
Modified ($T_{proc}=90$ °C)	-12.6	2.38
Modified ($T_{proc}=130$ °C)	-11.3	3.57
Modified ($T_{proc}=180$ °C)	-11.8	2.44

On the other hand, the endotherm at 50 °C (fourth event) is related to the diffusion of relatively large and high molecular weight structures, as those found in resins and asphaltenes, to form independent domains. In that sense, the area taken up by this event is clearly seen to increase with ThD addition at 130 °C, suggesting the formation of larger structures. Thus, results in Table 4.6 indicate that ΔH_{4th} (calculated from areas in Figure 4.14) increases from 2.14 up to 3.57 J/g for this binder, whilst no significant changes are observed for the ThD binders processed at 90 °C and 180 °C.

4.4. REFERENCES

Chebil S, Chaala A, Roy C. Use of softwood bark charcoal as a modifier for road bitumen. *Fuel*, 2000, 79, 671-683.

Ecker A. The application of Iatroscan-technique for analysis of bitumen. *Petrol. Coal*, 2001, 43, 51-53.

EN 1426:2007: Bitumen and bituminous binders. Determination of needle penetration.

EN 1427:2007: Bitumen and bituminous binders. Determination of the softening point. Ring and ball method.

- Fawcett AH, McNally T, McNally GM, Andrews F, Clarke J. Blends of bitumen with polyethylenes. *Polymer*, 1999, 40, 6337-6349.
- Ferry JD. Viscoelastic properties of polymers. 3rd edition. Wiley & Sons, 1980, New York.
- Fujiyasu K, Shigeki Y, Ito H. Method of activating thiourea dioxide. U.S. Patent 4,610,802, 1986.
- García-Morales M, Partal P, Navarro FJ, Gallegos C. Effect of waste polymer addition on the rheology of modified bitumen. *Fuel*, 2006, 85, 936-943.
- García-Morales M, Partal P, Navarro FJ, Martínez-Boza F, Gallegos C, González N et al. Viscous properties and microstructure of recycled EVA modified bitumen. *Fuel*, 2004, 83, 31-38.
- Gawel I. Sulphur-Modified Asphalts. *Dev. Petr. Sci.*, 2000, 40, (B), 515-535.
- Giavarini C, Mastrofini D, Scarsella M, Barré L, Espinat D. Macrostructure and rheological properties of chemically modified residues and bitumens. *Energ. Fuel*, 2000, 14, 495-502.
- Kandhal PS, Cooley LA. Transport Res. Board, National Cooperative Highway Research, Program Report, 2003, 508.
- Lesueur D. The colloidal structure of bitumen: Consequence on the rheology and on the mechanisms of bitumen modification. *Adv. Colloidal Interfac.*, 2009, 145, 42-82.
- Lu X, Isacson J, Ekblad J. Influence of polymer modification on low temperature behaviour of bituminous binders and mixtures. *Mater. Struct.*, 2003, 36, 652-656.

Lu X, Isacsson U. Rheological characterization of styrene-butadiene-styrene copolymer modified bitumens. *Constr. Build. Mater.*, 1997, 11, 23-32.

Martínez A, Paez A, Martin N. Rheological modification of bitumens with new poly-functionalized furfural analogs. *Fuel*, 2008, 87, 1148–1154.

Masson JF. Brief Review of the chemistry of polyphosphoric acid (PPA) and bitumen. *Energ. Fuel*, 2008, 22, 2637–2640.

Masson FJ, Polomark GM. Bitumen microstructure by modulated differential scanning calorimetry. *Thermochim. Acta*, 2001, 374, 105-114.

Masson JF, Polomark GM, Collins P. Time-dependent microstructure of bitumen and its fractions by modulated Differential Scanning Calorimetry. *Energ. Fuel*, 2002, 16, 470-476.

Martín-Alfonso MJ, Partal P, Navarro FJ, García-Morales M, Gallegos C. Use of a MDI-functionalized reactive polymer for the manufacture of modified bitumen with enhanced properties for roofing applications. *Eur. Polym. J.*, 2008, 44, 1451-1461.

Martín-Alfonso MJ, Partal P, Navarro FJ, García-Morales M, Gallegos C. Role of water in the development of new isocyanate-based bituminous products. *Ind. Eng. Chem. Res.*, 2008, 47, 6933-6940.

Navarro FJ, Partal P, Martinez-Boza FJ, Gallegos C. Novel recycled polyethylene / ground tire rubber / bitumen blends for use in roofing applications: Thermo-mechanical properties. *Polym. Test.*, 2010, 29, 588-595.

Navarro FJ, Partal P, García-Morales M, Martín-Alfonso MJ, Martinez-Boza F, Gallegos C et al. Bitumen modification with reactive and non-reactive

(virgin and recycled) polymers: A comparative analysis. *J. Ind. Eng. Chem.*, 2009, 15, 458-464.

Partal P, Martinez-Boza F, Conde B, Gallegos C. Rheological characterization of synthetic binders and unmodified bitumens. *Fuel*, 1999, 78, 1-10.

Schaber PM, Colson J, Higgins S, Thielen D, Anspach B, Brauer J. Thermal decomposition (pyrolysis) of urea in an open reaction vessel. *Thermochim. Acta*, 2004, 424, 131-142.

Wang S, Gao Q, Wang J. Thermodynamic analysis of decomposition of thiourea and thiourea oxides. *J. Phys. Chem.*, 2005, 109, 17281-17289.

Yang J, Roy C. Using DTA to quantitatively determine enthalpy change over a wide temperature range by the "mass-difference baseline method". *Thermochim. Acta*, 1999, 333, 133-140.

BITUMEN MODIFICATION BY THIOUREA

Chapter V

*Physico-chemical modificacion of asphalt
bitumens by reactive agents*

5.1. INTRODUCTION

Previous results demonstrated that the chemically-induced changes, after thiourea dioxide addition, significantly enhance bitumen thermo-mechanical properties in a wide interval of in-service temperatures. So, rheological measurements revealed an increase in the binder resistance to thermal cracking and permanent deformation under loading at low and medium/high in-service temperatures, respectively. In addition, a different bitumen modification routes for each of the three selected processing temperatures were also identified, by means of TLC/FID, filtration tests and thermal analysis.

Looking further into this bitumen modification based on reactive agents, interest is now focused on another novel additive, thiourea. For this, the present chapter assesses the viscous flow and viscoelastic properties of bituminous binders derived from bitumen modification by thiourea, and highlights the importance of rheology in determining quantitatively the induced enhancement.

In addition, we emphasize the use of master curves, obtained by application of the Time-Temperature-Superposition Principle (TTSP) to isothermal frequency sweep tests at different temperatures (and frequency/temperature-dependence conversion) as a means of achieving glass transition temperature values which, in contrast to isochronal temperature sweep tests, do not depend on the selected heating rate.

With this aim, the rheological response, thermal behaviour, chemical composition and microstructure of different thiourea-modified binders were studied.

5.2. EXPERIMENTAL

5.2.1. Materials

Bitumen with a penetration grade of 40/50 has been used as base material for the modification. Details on its technological properties (penetration grade and R&B softening temperature, according to EN 1426:2007 and EN 1427:2007, respectively) and chemical composition, in terms of SARAs fractions, are shown in Table 5.1.

Table 5.1. Penetration value, ring & ball softening temperatures, SARAs fraction and colloidal index values for the neat bitumen studied.

	Bitumen 40/50
Penetration (dmm)	47
R&B softening point (°C)	52.5
Saturates (wt.%)	5.1
Aromatics (wt.%)	52.6
Resins (wt.%)	23.9
Asphaltenes (wt.%)	18.4
Colloidal Index (C.I.) ^a	0.31

$$^a\text{Colloidal Index} = (\text{asphaltenes} + \text{saturates}) / (\text{resins} + \text{aromatics})$$

Two different modifying agents, a non-polymeric substance and a thermoplastic elastomer, have been employed:

a) On the one hand, thiourea (Th), supplied by Sigma Aldrich, is an additive which leads to chemical reactions with bitumen molecules. It has a molecular weight of 76.12 g·mol⁻¹, and its melting point lies within the interval 175-179 °C.

b) On the other hand, commercial Styrene-Butadiene-Styrene, SBS, triblock copolymer “Kraton D-1101”, provided by Shell Chemical Company U.K., was selected for “physical modification”, through mere physical dispersion in bitumen. It has a molecular weight of $1.5 \cdot 10^5 \text{ g} \cdot \text{mol}^{-1}$, and a styrene content of 31 wt.%.

5.2.2. Samples preparation

In relation to “chemical” modification, two blends of bitumen with 3 and 9 wt.% Th, respectively, were prepared in a cylindrical glass vessel (60 mm diameter, 140 mm height), for 1 h, at 180 °C and mixing speed of 1200 rpm. Agitation was carried out by means of an IKA RW-20 stirring device (Germany) equipped with a four-bladed turbine. After being processed, both modified binders were poured onto aluminium foil (forming a thin layer), and cured for up to 24 months, exposed to the ambient. The specific effects of temperature and agitation were assessed by subjecting the neat bitumen, without addition of Th, to the conditions described above (sample referred to as “blank”, hereinafter).

In addition, Th-modified binders were also processed at 120 °C, temperature lower than thiourea’s melting point. However, these binders do not present a good dispersion this bitumen additive, and the rheological response under shear turned out to be unreliable. For this reason, binders prepared at 180 °C are only taken into consideration.

For the sake of comparison, “physical” modification was carried out by adding 3 wt.% SBS to the base bitumen (formulation commonly used in the paving industry). This blend was processed for 2 h, at 180 °C, in a high shear mixing device.

5.2.3. Testing procedures

Viscous flow measurements, at 60 °C, were carried out in a controlled-strain ARES rheometer (Rheometric Scientific, USA). Linear viscoelastic frequency sweep tests, between 0.01 and 100 rad/s (at 30 and 60 °C), and temperature sweep tests in oscillatory shear at constant frequency and strain (10 rad/s and 1 %, respectively) and a heating rate of 1 °C/min from 30 to 100 °C, were conducted in a controlled-stress rheometer PHYSICA MCR-301 (Anton Paar, Austria). A serrated plate-and-plate geometry (25 mm diameter and 1 mm gap) was used for all rheological shear measurements. At least two replicates of each test were done in order to assure the repeatability of the results.

Dynamic Mechanical Thermal Analysis (DMTA) tests were performed on neat and modified bitumens with a Seiko DMS 6100 (Seiko Instruments Inc., Japan) in double cantilever bending mode, using 50 x 10 x 3 mm specimens, and liquid nitrogen as cooling system. Frequency sweep tests from 0.01 to 100 Hz were carried out, in the linear viscoelasticity (LVR) region, at four selected temperatures from -30 to 15 °C, in 15 °C-increments. Furthermore, temperature sweep tests, ranging from -35 to 35 °C, were conducted at a fixed frequency of 1 Hz and strains within the LVR region, by selecting different temperature ramps (4, 2, 0.2 °C·min⁻¹).

Modulated Differential Scanning Calorimetry (MDSC) was performed with a TA Q-100 (TA Instruments, USA). Samples (5-10 mg) were subjected to the same testing procedure: a temperature interval between -80 and 100 °C; a heating rate of 5 °C/min; an amplitude of modulation of ± 0.5 °C, a period of 60 s; and nitrogen as purge gas, with a flow rate of 50 ml/min. To provide the same recent thermal history, all the samples were placed into hermetic aluminium pans for 24 h before measurement.

Simultaneous thermo gravimetric/differential thermal analyses (TG/DTA) were conducted using a Seiko TG/DTA 6200 (Japan). Temperature ramps at 10 °C/min, from 40 to 600 °C, under N₂ atmosphere were carried out on 5-10 mg of sample.

The bitumen SARAs fractions were determined by thin layer chromatography coupled with a flame ionization detector (TLC/FID), using an Iatroscan MK-6 analyzer (Iatron Corporation Inc., Japan). The elutions were performed in hexane, toluene and dichloromethane/methanol (95/5), following the procedure outlined elsewhere (Ecker, 2001).

5.3. RESULTS AND DISCUSSION

5.3.1. High in-service binder performance

Figure 5.1 shows the viscous flow behaviour, at 60 °C, of 3 and 9 wt.% Th-modified binders, as a function of curing time. For the sake of comparison, results corresponding to neat bitumen, “blank” sample and 3 wt.% SBS modified binder have been included.

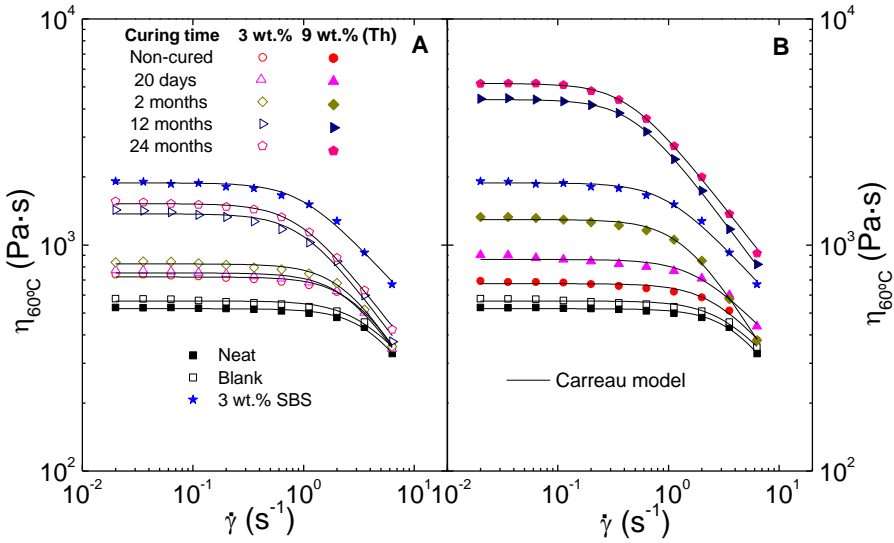


Figure 5.1. Viscous flow curves, at 60 °C, for a 3 wt.% Th binders (A) and a 9 wt.% Th binders (B), as a function of curing time.

It can be observed that thiourea addition induces significant increases in bitumen viscosity, mainly for the highest concentration and after a prolonged period of storage at room conditions (i.e. curing period). Furthermore, all the samples present a Newtonian region, at low shear rates, followed by a shear-thinning drop beyond a threshold (or “critical”) value of shear rate. This behaviour can be described by the Carreau’s model fairly well:

$$\frac{\eta}{\eta_0} = \frac{1}{[1+(\lambda \cdot \dot{\gamma})^2]^s} \quad (5.1)$$

where η_0 is the zero-shear-viscosity, λ is a time constant whose inverse approximately matches the threshold shear rate above, and “s” is a parameter related to the slope in the shear-thinning region. Table 5.2 includes those fitting parameters for all the samples studied.

Table 5.2. Evolution with curing time of Carreau’s model parameters and SHRP maximum temperatures for neat bitumen, “blank” sample, reference SBS binder and Th-modified binders.

		Carreau’s model parameters			
	Binders	η_0 (Pa·s)	λ (s)	s	$T_{ G^* /\sin \delta=1 \text{ kPa}}$ (°C)
	Neat	553	0.23	0.39	74.0
	Blank	567	0.32	0.28	74.2
3 wt.% Th	Non-cured	723	0.34	0.40	75.8
	20 days	753	0.41	0.38	76.6
	60 days	825	0.47	0.41	77.1
	12 months	1374	1.00	0.34	75.6
	24 months	1520	0.75	0.29	---
9 wt.% Th	Non-cured	675	0.39	0.29	74.9
	20 days	864	0.56	0.25	76.8
	60 days	1296	0.73	0.39	80.2
	12 months	4402	2.07	0.33	80.8
	24 months	5180	2.33	0.31	---
	3 wt.% SBS	1883	1.04	0.27	82.4

In order to more conveniently visualise the degree of modification achieved at high in-service temperatures, a modification index (M.I.^{60°C}), in terms of the Newtonian viscosities at 60 °C included in Table 5.2, has been defined as follows:

$$\text{M.I.}^{60^\circ\text{C}} = \frac{\eta_{0,\text{mod}} - \eta_{0,\text{proc}}}{\eta_{0,\text{proc}}} \quad (5.2)$$

where $\eta_{0,\text{mod}}$ is the zero-shear-rate-limiting viscosity of the Th-modified bitumen, and $\eta_{0,\text{proc}}$ is the zero-shear-rate-limiting viscosity of the “blank” sample, both of them at 60 °C.

This index expresses the relative viscosity increase due to thiourea addition with reference to the blank sample. It is worth mentioning neat bitumen may increase its viscosity during high temperature mixing due to oxidation processes, the so-called “primary ageing”, giving rise to the blank sample (Navarro et al., 2009). Hence, $M.I.^{60^{\circ}C}$ only quantifies changes due to the modifying agent, regardless of bitumen “primary ageing” that occurs during the binder processing.

Figure 5.2 displays the evolution of the modification index ($M.I.^{60^{\circ}C}$) with curing time. Two different bitumen modification pathways, referred to as “short-term” and “long-term” modification and further tackled in subsection 5.3.3, have been identified. Thus, the effects of “short-term” modification are noticed in the freshly prepared (“non-cured”) binders and results more significant for the lowest thiourea concentration. This observation might be attributed to a larger quantity of non-reacted thiourea which, as such, would act as a “viscosity-reducing” substance.

On the other hand, the “long-term” modification, caused by curing at room temperature, yields much more significant increases in viscosity, if compared to the former pathway. Thus, for instance, bitumen viscosity increase may be of up to eight times its original value after modification with 9 wt.% Th and curing for 24 months. This represents a viscosity even larger than that corresponding to the SBS reference binder. Furthermore, the degrees of modification attained for the two binders studied tend to level off after a prolonged time of 2 years.

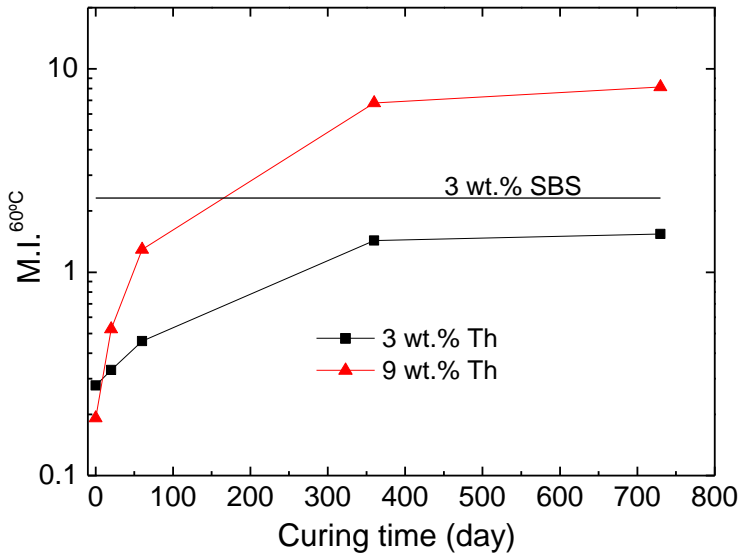


Figure 5.2. Evolution of the modification index with curing time for all Th-modified binders studied.

In addition, the fitting parameters obtained from the Carreau's model provide information about changes in the material microstructure as a consequence of the modification. Thus, the values of " λ " increase with curing time, mainly for the highest thiourea concentration (see Table 5.2). Consequently, the "critical" shear rates which mark the onset of the shear-thinning region decrease, a fact that reveals a more complex microstructure as binder curing proceeds (Martín-Alfonso et al., 2008).

On the other hand, dynamic shear temperature sweep tests, from 30 to 100 °C, were carried out on the neat bitumen and its corresponding Th-modified binders. Figure 5.3A shows the evolution with temperature of the loss tangent, as a function of curing time, for the 9 wt.% Th-modified binders. It can always be observed a prevailing viscous behaviour, with $\tan\delta > 1$ over the entire temperature interval tested, which becomes much more significant at the highest temperatures. However, $\tan\delta$ values are seen to notably decrease after addition of 9 wt.% thiourea, mainly for the

two longest curing times. In consequence, this increase in elasticity is expected to reduce the progressive accumulation of permanent deformation (the so-called “rutting”) produced by traffic at high in-service temperatures (Carrera et al., 2010).

On the other hand, they show a notable decrease in the average slope of their $\tan\delta$ vs. temperature curves (related to thermal susceptibility at high in-service temperatures), a fact which demonstrates an enhanced resistance to temperature changes. In that sense, the Strategic Highway Research Program (SHRP) proposed the parameter $|G^*|/\sin\delta$ as a manner to efficiently determine the maximum temperature below which bitumen will show a satisfactory performance. According to the criterion outlined in AASHTO MP1 (1993), that temperature is assigned to the value at which $|G^*|/\sin\delta$ equals 1 kPa. This has been a controversial matter of debate, as some authors (Morea et al., 2010; Biro et al., 2009) have claimed others parameters (like zero-shear-viscosity, ZSV) to be more adequate in predicting the resistance of bitumen to permanent deformation at high in-service temperatures.

Anyway, if compared to the time-consuming method of the ZSV determination at several temperatures, the testing procedure presented in Figure 5.3B for 9 wt.% Th-modified binders stands for an easier way to establish a comparative analysis of the degree of improvement attained. As shown in Table 5.2, SHRP maximum temperature and so, rutting resistance, is notably increased after modification and curing. If compared with the neat bitumen, an increase of nearly 7 °C is observed after addition of 9 wt.% Th and curing for 12 months, which almost equals the value reached after SBS modification.

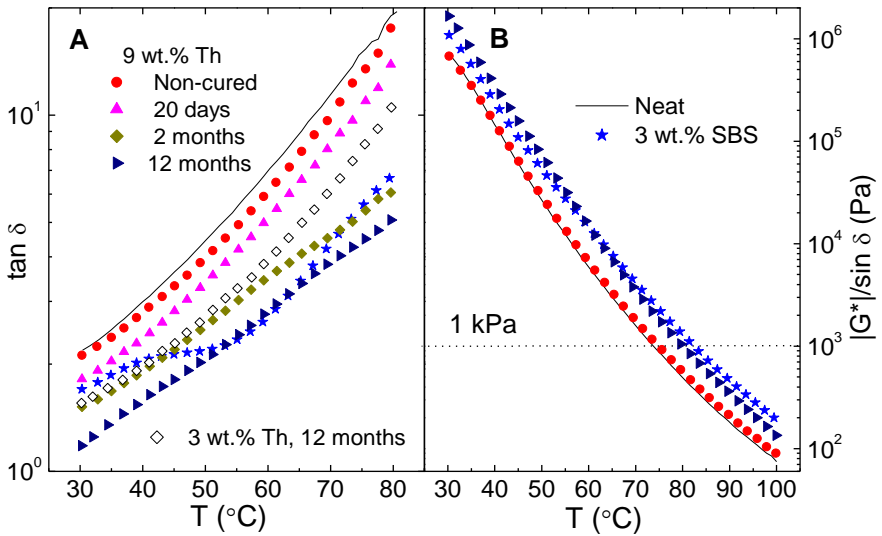


Figure 5.3. Evolution with temperature of loss tangent (A) and "rutting parameter", $|G^*|/\sin \delta$ (B), for selected Th-binders, as a function of curing time.

5.3.2. Low in-service binder performance

The rheological response at low in-service temperatures of the neat bitumen, reference sample (3 wt.% SBS) and a selected modified binder (60 days-cured 9 wt.% Th) have been evaluated. As an example, Figure 5.4 shows the results of double-cantilever frequency sweep tests, at four different temperatures between -30 to 15 °C, for the neat bitumen. The experimental results show the existence of a maximum in the viscous modulus, whilst the storage modulus tends to a constant value of about 2 GPa. Additionally, a prevailing elastic behaviour deduced from values of E' higher than E'' , at all temperatures tested, is also noted.

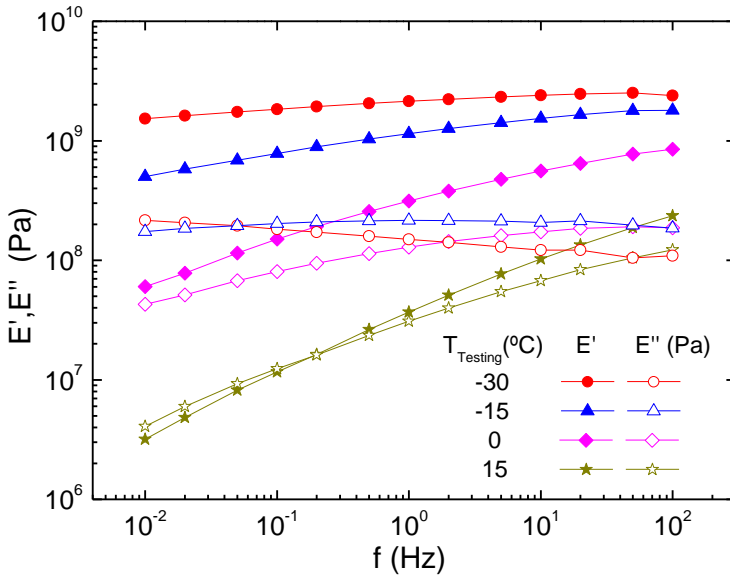


Figure 5.4. Evolution with frequency of the elastic (E') and viscous (E'') moduli in dynamic bending, as a function of temperature, for neat bitumen.

On the other hand, bitumen thermo-rheological simplicity, reported by different authors, has become quite controversial. Several authors have claimed that the Time-Temperature Superposition Principle (TTSP) fails at high temperature, especially for high asphaltene and/or high crystalline content materials (Lesueur et al., 1996) and is, therefore, very unlikely to apply to most polymer modified bitumens (Lesueur et al., 1998). In contrast, some others sustain that the mechanical spectrum of many modified bituminous products can be represented, reasonably well, by master curves of their linear viscoelastic material functions (Stastna and Zanzotto, 1999). Anyway, the TTSP has been widely applied to both neat and polymer-modified bitumens (Becker et al., 2003; Newman, 1998; Polacco et al., 2004; Carreau et al., 2000).

Hence, the experimental values of the linear viscoelastic functions, E' and E'' , were “empirically” superposed onto a master curve by using a shift-

factor, a_T , with 273 K as the reference temperature (see Figure 5.5A). Within the temperature range studied in this work, the temperature-dependence of the shift factor is described by an Arrhenius-type equation (Ferry 1980) reasonably well:

$$a_T = \exp \left[\frac{E_a}{R} \left(\frac{1}{T} - \frac{1}{T_{\text{ref}}} \right) \right] \quad (5.3)$$

where T_{ref} is the reference temperature (arbitrarily chosen to be 273 K), E_a is the activation energy and “R” is the universal gas constant. Thus, the significant decrease in E_a observed for the 60 days-cured 9 wt.% Th-modified binder (see Table 5.3) points out a reduction in the material thermal susceptibility (García-Morales et al. 2004) in the range of low temperatures selected.

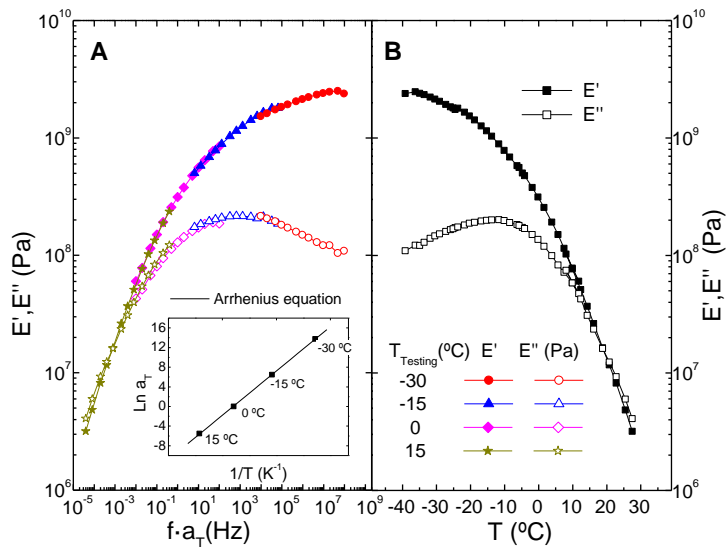


Figure 5.5. (A) Empirical master curves of storage (E') and loss (E'') moduli vs. reduced frequency, $f \cdot a_T$, for neat bitumen (Inset: Temperature dependence of the shift factor and Arrhenius fitting). (B) Evolution of the linear viscoelastic functions vs. temperature obtained by frequency/temperature-conversion.

Table 5.3. Activation energy values (E_a) and DMTA glass transition temperatures ($T_{g,DMTA}$) for neat bitumen, reference SBS binder and 9 wt.% Th binder after 60 days of curing time.

Binder	E_a (kJ/mol)	$T_{g,DMTA}$ (°C)
Neat bitumen	250.4	-13.0
3 wt.% SBS	244.6	-15.0
9 wt.% Th 60 days of curing	230.2	-18.0

However, the most important aspect of the rheological properties of bituminous binders is their dependence on temperature. In this sense, temperature-dependence of the linear E' and E'' moduli, at a fixed frequency value of 1 Hz, was obtained from isothermal frequency sweep tests by following the procedure described by Martinez-Boza et al. (2000). The values of the frequency sweep master curves have been converted using the Arrhenius-like relationship between the shift factor and temperature as follows:

$$T = \frac{E_a \cdot T_{ref}}{R \cdot T_{ref} \cdot \ln\left(\frac{\omega_{exp}}{\omega_R}\right) + E_a} \quad (5.4)$$

where E_a is the activation energy obtained from frequency sweep tests, ω_{exp} is the reduced frequency calculated from the superposition of experimental frequency sweep curves at different temperatures, and ω_R is the frequency at which the temperature sweep tests are carried out (chosen to be 1 Hz). As a result of this frequency/temperature-dependence conversion, isochronal E' - E'' curves over a wide temperature interval are obtained.

Results for the neat bitumen are shown in Figure 5.5B. A clear transition from the glassy to the Newtonian region can be observed, with a crossover point between E' and E'' , with increasing temperature (Partal et al., 1999). Moreover, no plateau at intermediate temperatures (like that which characterises polymer melts and solutions) was detected, which demonstrates the non-existence of entanglements (Ferry, 1980). In addition, a maximum in E'' , which characterises the onset of the glassy region is observed.

Thus, in order to establish a comparative analysis on the effect of modification on the low-temperature performance, Figure 5.6 shows the frequency-temperature converted master curves for the neat bitumen, the SBS reference sample and the 60 days-cured 9 wt.% Th-modified binder. For each of these three selected binders, a “mechanical” glass transition temperature ($T_{g,DMTA}$), taken as the value of temperature at the maximum in E'' curve (Partal et al., 1999), has been obtained (see Table 5.3). This parameter, which accounts for the onset of the glassy region (at which the binder is expected to be affected by thermal cracking under loading), has widely been used to evaluate the end-performance of polymer modified bitumens at low temperatures (Fawcett et al., 1999; Navarro et al., 2010). In consequence, a decrease in the T_g is a highly desirable result of modification.

In this sense, it has been widely reported in the literature (Yildirim et al., 2007; Airey, 2004; Lu and Isacson, 1997) that SBS remarkably enhances the binder performance at low temperatures. Surprisingly, enhancement in resistance to thermal cracking after chemical modification with 9 wt.% thiourea and curing for 2 months is even higher than that for SBS. Thus, a decrease of nearly 3 °C in $T_{g,DMTA}$, from about -15 °C for the 3 wt.% SBS sample down to -18 °C for Th-modified binder (after 2 months of curing),

was observed. If compared to the neat bitumen, which presents a value close to $-13\text{ }^{\circ}\text{C}$, an outstanding reduction of $5\text{ }^{\circ}\text{C}$ was obtained.

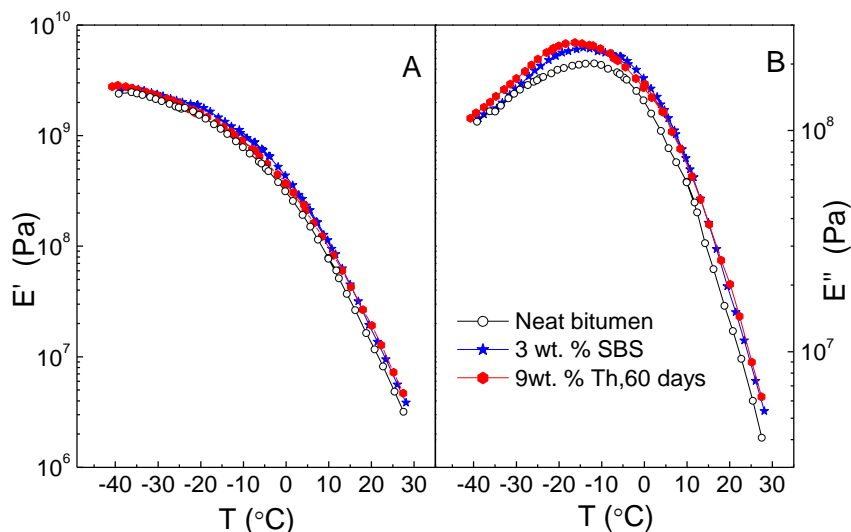


Figure 5.6. (A) Evolution of the linear viscoelastic functions (E' , E'') with temperature, obtained from frequency/temperature-conversions, for neat bitumen, reference SBS binder and 9 wt.% Th-binder after 60 days of curing time.

Interestingly, the application of TTSP allowed values of T_g not affected by the selected heating rate to be obtained. Thus, in contrast to those derived from isochronal temperature sweep tests carried out by applying a certain temperature-ramp, the values of T_g in Table 5.3 were obtained by conversion of frequency sweep tests on specimens which were allowed to achieve thermal equilibrium at every selected temperature.

In order to validate above results, dynamic temperature sweeps within the LVR region, at a fix frequency of 1 Hz, were conducted on the 60 days-cured 9 wt.% Th-modified binder, at three different decreasing heating rates (4 , 2 and $0.2\text{ }^{\circ}\text{C}\cdot\text{min}^{-1}$) from -35 to $30\text{ }^{\circ}\text{C}$. Figure 5.7, which shows the evolution with temperature of the elastic and viscous flexural moduli,

evidences the strong dependency of the viscoelastic functions with the temperature ramp selected.

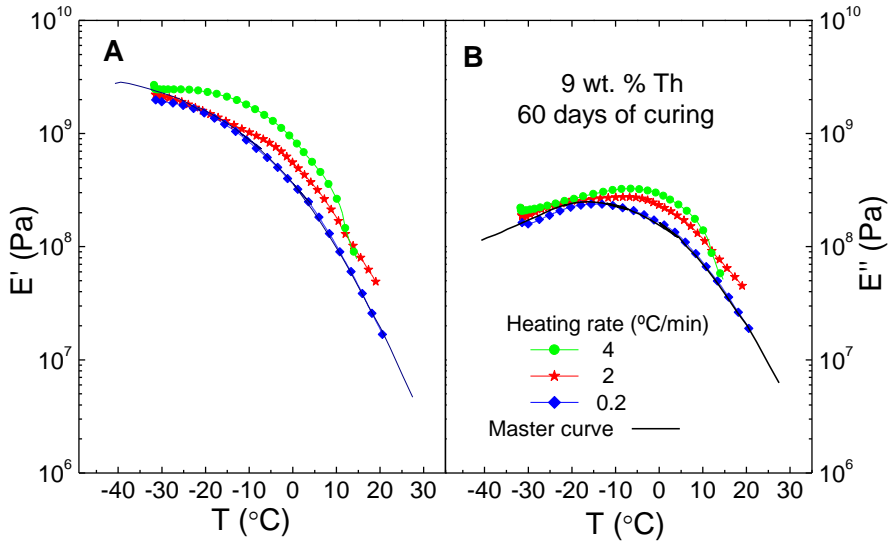


Figure 5.7. Effect of heating rate on temperature sweep tests performed at 1 Hz for a 9 wt.% Th-binder after 60 days of curing. Results compared with viscoelastic functions (E' , E'') obtained from the frequency/temperature conversion (master curve).

In fact, temperature sweeps curves only match their corresponding converted master curves at very low values of the heating rate (ideally, as heating ramp approaches to zero). As expected from the low thermal conductivity of bitumen (Read and Whiteoak, 2003), a fast heating rate provokes big differences between the temperature programme (set temperature) and the actual value the sample presents at every measured point. Consequently, only temperature sweeps tests performed at very low rates (below $0.2 \text{ } ^\circ\text{C}\cdot\text{min}^{-1}$) would lead to a “strictly” adequate viscoelastic characterisation of bituminous binders at low temperatures. Hence, under that condition, every measured point might be considered to be in a thermal “pseudo-equilibrium” state.

Finally, the linear viscoelastic behaviour of non-modified and modified bituminous binders in a wide temperature range can also be studied by means of “Black” diagrams, which represent phase angle (δ) vs. either complex shear (medium/high temperature) or complex flexural (low temperature) moduli. “Black” diagrams for the 9 wt.% Th-modified binder (60-days-cured) and neat bitumen are shown in Figure 5.8. On the one hand, it can be observed that, for the highest values of $|E^*|$, which correspond to the lowest temperatures, the selected Th binder presents slightly higher δ -values (so, enhanced viscous behaviour) than the neat bitumen. On the other hand, for relatively low $|G^*|$ values, that is, over a temperature range comprised between 30 and 60 °C, lower δ -values for the Th-modified binder are found (with the consequent increase in its elastic features). Therefore, an enhanced material performance is expected because Th-modification leads to improve elasticity and flexibility, at medium/high and low in-service temperatures, respectively (Lu et al., 1997).

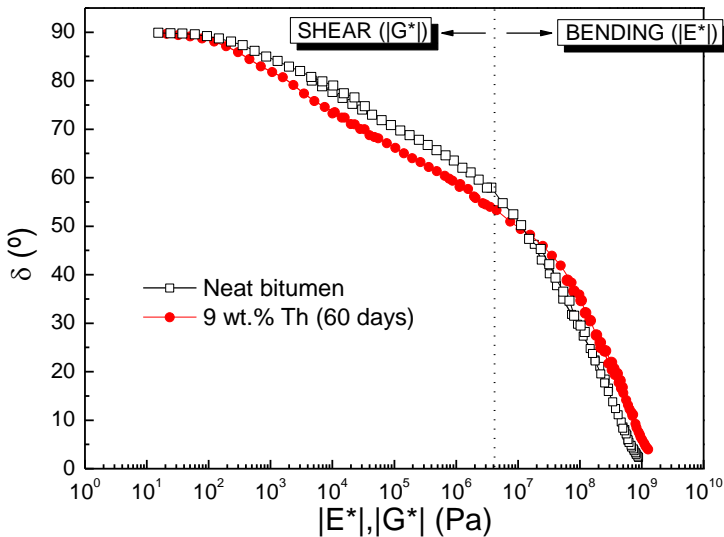


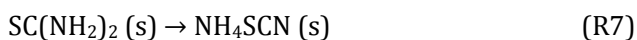
Figure 5.8. “Black” diagram for neat bitumen and 9 wt.% Th binder (60 days-cured).

5.3.3. On the chemistry behind bitumen modification

The above enhancement in the viscoelastic behaviour of the Th-modified binder suggests changes in its microstructure, as a consequence of the interaction between thiourea and some bitumen fractions. Thermal and chemical analysis (TG/DTA, MDSC and TLC/FID) may shed some light on this issue.

The thermal decomposition of the pure components (neat bitumen and thiourea) was studied by simultaneous measurements of DTA (Figure 5.9A) and DTG (Figure 5.9B). DTG curve for neat bitumen presents a broad peak located at 455 °C, which involves mass loss due to volatilization/decomposition of chemical compounds with very different molecular weights from 300 up to 500 °C (Figure 5.9B). Likewise, DTG profile for Th shows a major peak located at 210 °C, which ranges from 170 to 300 °C.

In addition, the DTA curve for thiourea displays two overlapped endothermic processes. The first one, between 170 and 190 °C (with DTA minimum peak located at 175 °C), is dominated by the melting of thiourea, hardly involving mass loss. The isomeric reaction R7, with the production of NH₄SCN (ammonium thiocyanate), is suggested to take place during this first endothermic process (Wang et al., 2005):



In contrast to that, the second stage involves NH₄SCN (derived from R7) thermal decomposition, into CS₂, HNCS and NH₃ (between 190 and 270 °C, with DTA minimum peak at 228 °C) and leads to the significant mass loss associated to the DTG peak found at 210 °C. Hence, such a NH₄SCN

decomposition is not expected to occur at the temperature at which mixing of bitumen and thiourea was carried out (180 °C).

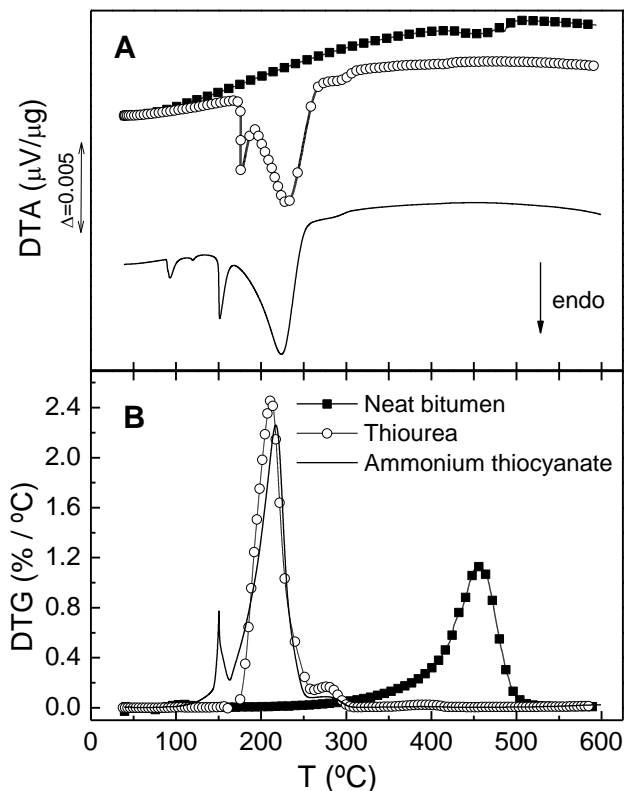


Figure 5.9. (A) DTA and (B) DTG curves for neat bitumen, pure thiourea and pure ammonium thiocyanate, NH_4SCN .

Aiming to confirm NH_4SCN formation from thiourea, the thermal decomposition of this substance has been also included in Figure 5.9. As expected, DTA curve presents an endothermic peak at around 149 °C, which corresponds to the ammonium thiocyanate melting point (lower than thiourea's, at 175-179 °C), and another peak at 228 °C, which stands for its decomposition. The small endothermic peak observed at 90 °C is due to a reversible phase transition from monoclinic to orthorhombic structure (Mayer et al., 1997).

Consequently, we will assume that bitumen modification and the resulting improvement in the binder mechanical behaviour over a broad in-service temperature interval is attributed to NH_4SCN arisen from R7, and new compounds derived from its interaction with bitumen. In this regard, chemical analysis further confirmed such an assumption and may provide valuable information on the colloidal nature of binders studied. Figure 5.10 shows chromatograms, obtained by TLC/FID, for neat bitumen, pure thiourea and the 9 wt.% Th-modified binder after 60 days of curing.

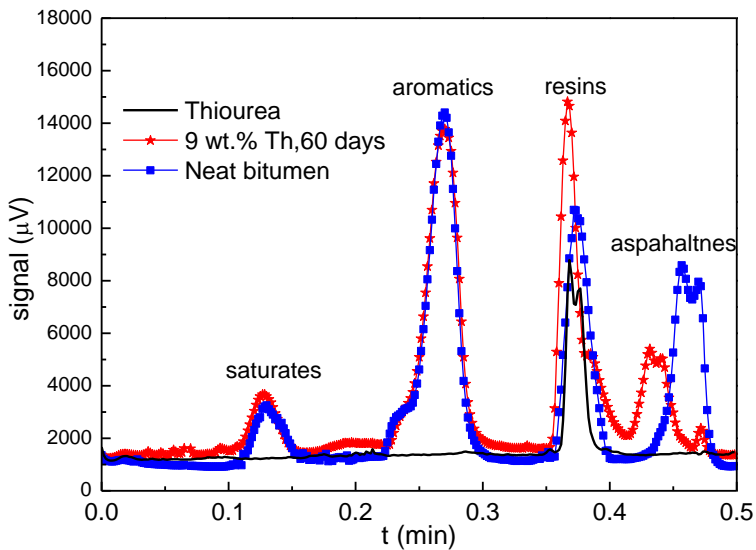


Figure 5.10. TLC/FID chromatograms for neat bitumen, pure thiourea and 9 wt.% Th-modified binder (60 days-cured).

On the one hand, four peaks (which stand for the so-called SARAs fractions) corresponding to saturates, aromatics, resins and asphaltenes, respectively, are shown by neat bitumen. On the other hand, thiourea presents a single signal, located at the bitumen resins peak position, and no peak was found for NH_4SCN due to its insolubility in the selected chromatographic solvents. In contrast to the neat bitumen, asphaltenes in the modified binder split into two new peaks, which will be referred to as

low and high polarity asphaltenes, LPAs and HPAs, respectively. Thus, the largest of them (LPAs), which was partially eluted by dichloromethane/methanol solvent and would be associated to bitumen compounds less polar than “standard” asphaltenes, is thought to be the result of the interaction between ammonium thiocyanate (from R7) and bitumen, and is assumed to be the responsible for the enhancement in the linear viscoelastic properties of the resulting binder after modification. In addition, saturates and aromatics remain essentially unchanged (pointing out a lower chemical reactivity), whilst resins increase.

In order to confirm this, two different solutions of neat bitumen in toluene were prepared. Then, thiourea or ammonium thiocyanate was added to each solution, respectively, and kept at 25 °C for 5 hours under agitation. TLC/FID analysis conducted on them demonstrated that separation of asphaltenes into two new peaks only occur when ammonium thiocyanate is added, revealing this specie (derived from R7 during processing of the binder at 180 °C), instead of thiourea itself, is the actual substance producing the new LPAs fraction.

Graphic integration of the chromatogram peaks allowed for the quantification of the different SARAs fractions. In this way, Figure 5.11 shows the weight percentage of every fraction for the neat bitumen, its corresponding blank, and modified binders, with 3 and 9 wt.% thiourea, as a function of curing time.

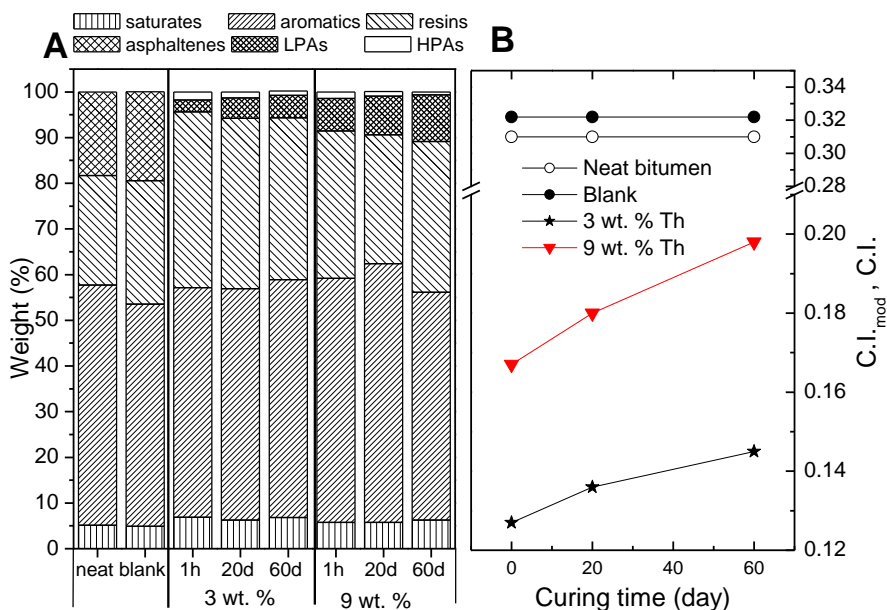


Figure 5.11. (A) SARAs fractions contents and (B) “modified” colloidal index values for neat bitumen, “blank” sample and 3 and 9 wt.% Th-modified binders at different curing times.

First of all, it can be observed that bitumen oxidation occurred during mixing causes an increase in the asphaltenes and resins fractions, whilst aromatics decrease. This transformation of aromatics into resins and these into asphaltenes is known as “bitumen primary ageing” (Navarro et al., 2009). Interestingly, both Th-modified binders show an increase in the resins concentration, which might be attributed to “standard” asphaltenes which are transformed into less polar compounds after thiourea addition and, in a much lesser extent, to non-reacted thiourea. Thus, as shown in Figure 5.12, LPAs can also be eluted by the solvent used to separate the resins fraction (95/5 dichloromethane/methanol), although at lower rate than that, with the consequent formation on the silica rod of a new fraction in between resins and HPAs (5 rods on the left hand side). In contrast, LPAs

fraction does not appear if the elution sequence is performed on the non-modified bitumen (5 rods on the right hand side).

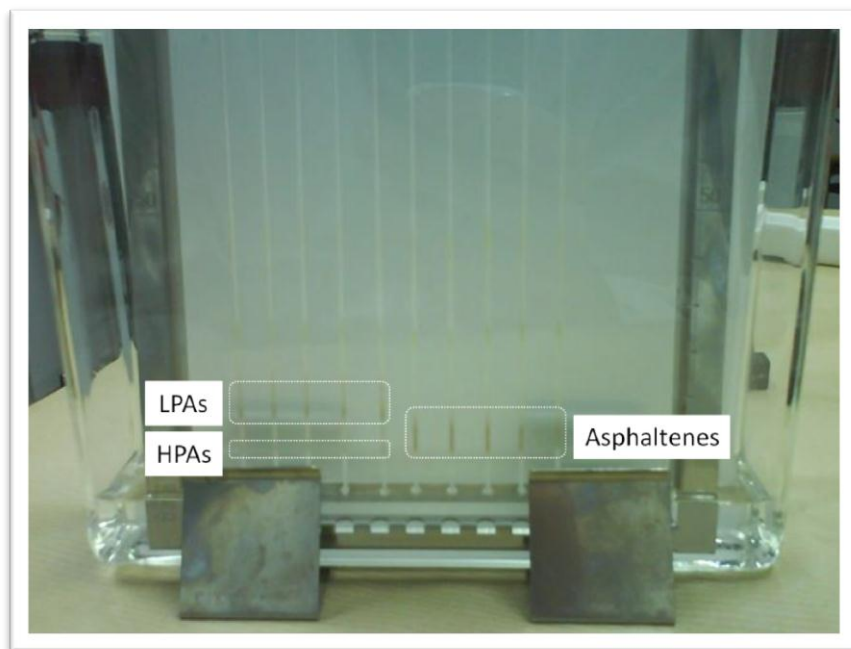


Figure 5.12. Picture taken during the elution of the resins fraction with a blend of dichloromethane/methanol (95/5).

On the other hand, high polarity asphaltenes are negligible if compared to low polarity asphaltenes, whose concentration seems to increase as curing time does (mainly for the highest thiourea content). However, the total content in asphaltenes (LPAs + HPAs) decreases in relation to neat bitumen or blank sample. Finally, it is noticeable, once again, that saturates and aromatics remain essentially unchanged (see Figure 5.11).

On these grounds, changes in the modified binder colloidal nature may be quantified through a new index, defined in terms of the five fractions derived from the chromatographic method, which accounts for changes

originated from bitumen reactive modification by thiourea. This “modified” colloidal index, which derived from that used elsewhere (Lesueur et al., 2009) and expressed in terms of the “standard” SARAs fractions, is defined as follows:

$$C.I._{\text{mod}} = \frac{\text{saturates} + \text{LPAs} + \text{HPAs}}{\text{aromatics} + \text{resins}} \quad (5.4)$$

where LPAs and HPAs refer to low and high polarity asphaltenes, respectively. Figure 5.11B displays the evolution with curing time of the “modified” colloidal index, for 3 and 9 wt.% modified binders, and “classic” colloidal index (in which LPAs + HPAs should be replaced by asphaltenes) for neat and blank bitumen. It can be noted a remarkable decrease in the colloidal index values after modification via thiourea, as saturates and aromatics nearly remain constant, resins increase, and the “asphaltene equivalent fraction” (that is, LPAs and HPAs) decreases. This would provide an explanation to the lowest values of the mechanical glass transition temperature measured (see Figure 5.6 and Table 5.3).

In this way, modulated DSC performed on the samples also discloses changes induced in the bitumen microstructure by the addition of thiourea. Figures 5.13A and 5.13B show the non-reversing thermograms and derivate heat capacity (dCp/dT), respectively, for neat bitumen and its corresponding 9 wt.% Th binders at different curing times. According to Masson and co-workers (Masson and Polomark, 2001; Masson et al., 2002), non-reversing heat flow curves for a neat bitumen presents four clearly marked thermal events: i) a broad endothermic background which approximately extends from -40 up to 80 °C; ii) and iii) two exotherms located at about -9 and 40 °C; iv) an endothermic peak, at around 50 °C, being related to the diffusion of relatively large structures, as those

typically found in asphaltenic micelles. Enthalpy associated to this fourth event can be ascertained by mere integration of the corresponding peaks (see Figure 5.13A).

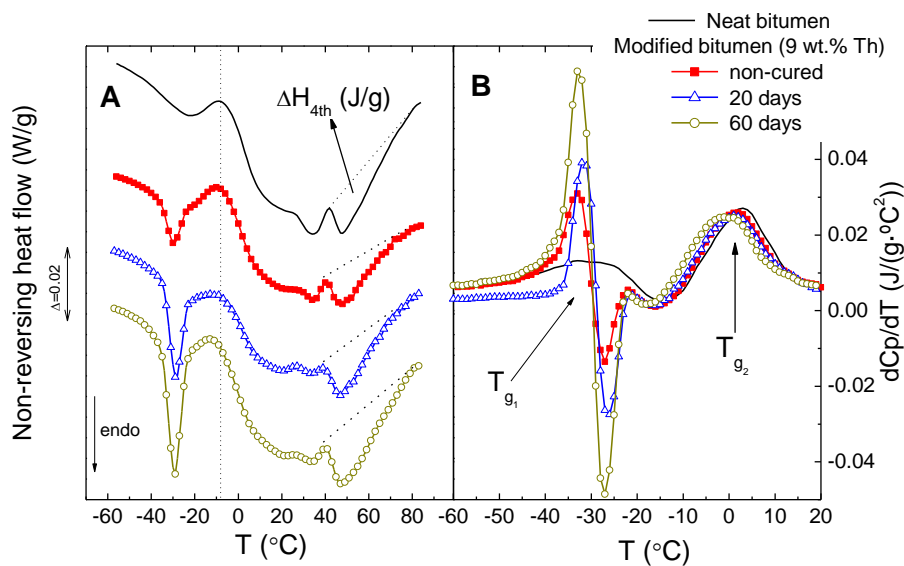


Figure 5.13. (A) Non-reversing heat flow and (B) C_p -derivate curves obtained by MDSC for neat bitumen and 9 wt.% Th binders at different curing times.

Table 5.4 demonstrates that enthalpy values increase with increasing curing time, what suggests the development, after thiourea addition and further curing, of new structures which would require a larger quantity of energy to melt. This would relate to an enhanced resistance to permanent deformation at high temperatures (see Figures 5.1-5.3). In this regard, small molecules containing N-H links coming from urea/thiourea derivatives, have demonstrated strong hydrogen bonding activity, which would contribute to a slow change (or enhancement) in the hydrogen-bond network of bitumen during its curing at room temperature (as previously seen in Chapter IV).

Furthermore, derivative heat capacity for neat bitumen in Figure 5.13B presents two well-defined peaks (with peak maximum, T_{g1} and T_{g2} , located at -30.5 and 3.0 °C, respectively) which, according to Masson et al. (Masson and Polomark, 2001; Masson et al., 2002), derive from two overlapped glass transitions corresponding to saturates and aromatics. T_{g2} values were also determined for the modified binders studied, and compare with neat bitumen's. Interestingly, that temperature is seen to shift to lower temperature (from 3 °C down to 0 °C) after modification with 9 wt.% thiourea and 60 days of curing time, observation which matches with the results obtained from DMTA measurements (see Table 5.2) and would support the enhancement in the binders low temperature properties. Note that overlapping with a new endothermic thermal event arising at -30 °C in Th-modified binders (see Figure 5.13A) does not allow T_{g1} values to be obtained.

Table 5.4. Glass transition temperatures obtained by MDSC (T_{g1} and T_{g2}); second event temperatures (T_{2nd}); and energy associated with the endothermic fourth even (ΔH_{4th}), for selected binders studied.

Binder		T_{g1} (°C)	T_{g2} (°C)	T_{2nd} (°C)	ΔH_{4th} (J/g)
Neat bitumen		-30.5	3.0	-9.0	2.21
9 wt. Th	Non-cured	---	1.6	-9.8	2.66
	20 days	---	0.7	-12.1	2.81
	60 days	---	0.0	-12.8	3.35

Moreover, the second and third (exothermic) thermal events derive from a time-dependent cold-crystallization of a certain quantity of saturates which, upon cooling from the melt, were unable to adequately crystallize. Hence, above the frozen state defined by $T > T_g$, molecular mobility increases and those saturates segments order into crystalline domains (Masson et al., 2001; Masson et al., 2002). Table 5.4, which displays second

event temperatures (T_{2nd}), confirms a decrease after addition of 9 wt.% Th and 60 days of curing, as the frozen state threshold was shifted to lower temperatures.

Yet, the controversy on the origin of that new endothermic thermal event at -30 °C remains. With the purpose of shedding light on this issue a MDSC test was carried out on a sample of ammonium thiocyanate. Results in Figure 5.14 allow us to conclude that the new event can be attributed to ammonium thiocyanate derived from R7, and most probably arises as a consequence of a low-temperature “non-identified” reversible phase transition, similar to that observed at 90 °C.

On the other hand, three successive cycles were conducted on the 9 wt.% Th binder (60 days-cured): i) quenching from room temperature down to -60 °C and subsequent heating at 5 °C/min up to 100 °C; ii) quenching from 100 down to -60 °C; iii) second heating at 5 °C/min up to 110 °C. In contrast to the first heating cycle, prior to which the sample was annealed at room temperature, the endothermic events at -30 and 50 °C become strongly reduced in the second heating cycle, as quenching from the melt did not provide sufficient time for the structures to adequately reorganise. This outcome points out the time-dependent ordering process of bitumen mesophases and the existence of physical interactions among bitumen molecules and Th derivatives (e.g. hydrogen bonds), instead of chemical bonds (Navarro et al., 2009).

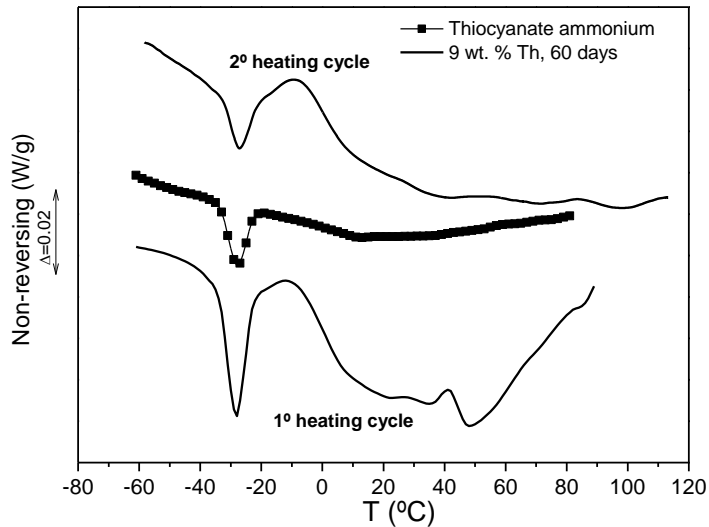


Figure 5.14. Non-reserving heat flow for curves for pure ammonium thiocyanate and 9 wt.% Th-modified binder (60 days-cured).

5.4. REFERENCES

Airey GD. Styrene butadiene styrene polymer modification of road bitumens. *J. Mater. Sci.*, 2004, 39, 951-959.

American Association of State Highway and Transportation Officials (1993) Standard specification for performance graded binder. AASHTO Designation MP1, Gaithersburg

Becker Y, Müller AJ, Rodriguez Y. Use of rheological compatibility criteria to study SBS modified asphalts. *J. Appl. Polym. Sci.*, 2003, 90, 1772-1782.

Biro S, Gandhi T, Amirkhanian S. Determination of zero shear viscosity of warm asphalt binders. *Constr. Build. Mater.*, 2009, 23, 2080-2086.

Carrera V, Partal P, Garcia-Morales M, Gallegos C, Perez-Lepe, A. Effect of processing on the rheological properties of poly-urethane/urea bituminous products. *Fuel Process. Technol.*, 2010, 91, 1139-1145.

Carreau PJ, Bousmina M, Bonniot F. The viscoelastic properties of polymer modified asphalts. *Can. J. Chem. Eng.*, 2000, 78, 495-502.

EN 1426:2007: Bitumen and bituminous binders. Determination of needle penetration.

EN 1427:2007: Bitumen and bituminous binders. Determination of the softening point. Ring and ball method.

Ecker A. The application of Iatroskan-technique for analysis of bitumen. *Petrol. Coal*, 2001, 43, 51-53.9

Fawcett AH, McNally T, McNally GM, Andrews F, Clarke J. Blends of bitumen with polyethylenes. *Polymer*, 1999, 40, 6337-6349.

Ferry JD. Viscoelastic properties of polymers. 3rd edition. Wiley & Sons, 1980, New York.

García-Morales M, Partal P, Navarro FJ, Martínez-Boza F, Gallegos C, González N et al. Viscous properties and microstructure of recycled EVA modified bitumen. *Fuel*, 2004, 83, 31-38.

Lesueur, D. The colloidal structure of bitumen: Consequences on the rheology and the mechanisms of bitumen modification. *Adv. Colloid. Interfc.*, 2009, 145, 42-82.

Lesueur D, Gérard JF, Claudy P, Letoffe JF, Planche JP, Martin D. A structure-related model to describe asphalt linear viscoelasticity. *J. Rheol.*, 1996, 40, 813-836.

Lesueur D, Gérard JF, Claudy P, Letoffe JM, Martin D, Planche JP. Polymer modified asphalts as viscoelastic emulsions. *J. Rheol.*, 1998, 42, 1059-1074.

Lu X, Isacsson U. Rheological characterization of styrene-butadiene-styrene copolymer modified bitumens. *Constr. Build. Mater.*, 1997, 11, 23-32.

Martínez-Boza F, Partal P, Conde B, Gallegos, C. Influence of temperature and composition in the linear viscoelastic properties of synthetic binders. *Energ. Fuel*, 2000, 14, 131-137.

Martín-Alfonso MJ, Partal P, Navarro FJ, García-Morales M, Gallegos. Use of a MDI-functionalized reactive polymer for the manufacture of modified bitumen with enhanced properties for roofing applications. *Eur. Polym. J.*, 2008, 44, 1451-1461.

Masson FJ, Polomark GM. Bitumen microstructure by modulated differential scanning calorimetry. *Thermochim. Acta*, 2001, 374, 105-114.

Masson JF, Polomark G.M, Collins P. Time-dependent microstructure of bitumen and its fractions by modulated Differential Scanning Calorimetry. *Energ. Fuel*, 2002, 16, 470-476.

Mayer T, Mayer J, Wasiutynski T. A DSC study of $K_{1-x}SCN$ mixed crystals. *Thermochim. Acta*, 1997, 299, 109-111.

Morea F, Agmusdei JO, Zerbino R. Comparison of methods for measuring zero shear viscosity in asphalts. *Mater. Struct.*, 2010, 43, 499-507

Navarro FJ, Partal P, Martínez-Boza FJ, Gallegos C. Novel recycled polyethylene / ground tire rubber / bitumen blends for use in roofing applications: Thermo-mechanical properties. *Polym. Test.*, 2010, 29, 588-595.

Navarro FJ, Partal P, García-Morales M, Martín-Alfonso MJ, Martínez-Boza F, Gallegos C, Bordado JCM, Diogo AC. Bitumen modification with reactive

and non-reactive (virgin and recycled) polymers: A comparative analysis. *J. Ind. Eng. Chem.*, 2009, 15, 458-464.

Newman, JK. Dynamic shear rheological properties of polymer modified asphalts binder. *J. Elastom. Plast.*, 1998, 30, 245-263.

Partal P, Martinez-Boza F, Conde B, Gallegos C. Rheological characterization of synthetic binders and unmodified bitumens. *Fuel*, 1999, 78, 1-10.

Polacco G, Stastna J, Biondi D, Antonelli F, Vlachovicova Z, Zanzotto L. Rheology of asphalts modified with glycidymethacrylate functionalized polymers. *J. Colloid. Interf. Sci.*, 2004, 280, 366-373.

Read J, Whiteoak D. The Shell Bitumen Handbook. 5th Edition London (UK), Thomas Telford Publishing 2003.

Stastna J, Zanzotto L. Linear response of regular asphalt to external harmonic fields. *J. Rheol.*, 1999, 43, 719-734.

Wang S, Gao Q, Wang J. Thermodynamic analysis of decomposition of thiourea and thiourea oxides. *J. Phys. Chem.*, 2005, 109, 17281-17289.

Yildirim Y. Polymer modified asphalt binders. *Constr. Build. Mater.*, 2007, 21, 66-72.

BITUMEN MODIFICATION BY -NCO FUNCTIONALIZED CASTOR OIL PREPOLYMERS

Chapter VI

*Physico-chemical modificacion of asphalt
bitumens by reactive agents*

6.1. INTRODUCTION

The modification of bitumen by two reactive agents, thiourea dioxide and thiourea, has been evaluated in the previous sections IV and V, respectively. These results showed that both additives can be seen as promising modifying agents, which can extend the in-service temperatures range at which bitumens present a satisfactory performance.

On the other hand, it is well-known that “active” polymer are able to form chemical bonds with some bitumen fractions, which prevent the resulting blend from phase separation during its storage at high temperature (between 160-200 °C) in absence of stirring (Pérez-Lepe et al., 2006). In this category, the MDI-derived prepolymers, which consists of a “soft or flexible segment” represented by polyols (PEG, PPG, etc.) and a “hard or stiff segment” constituted by diisocyanates (MDI, HDI, etc.), are the most widely used in the paving industry. Its modification route is expected to take place by reaction of this isocyanate (-NCO) terminated prepolymer with polar groups (-OH; -NH) in asphaltenes, resins and even aromatics molecules. However, previous studies pointed out that this bitumen modification is a complex process (Martín-Alfonso et al., 2008), involving chemical reactions with air moisture, when the material is stored under ambient conditions.

Recently, the utilization of renewable resources in the formulation of isocyanate-terminated prepolymers becomes of increasing interest due to their great potential as substitute for petro-chemical derivatives (Swamy et al., 2003). Among them, vegetable oils present advantages (Karak et al., 2009) such as: 1) renewability, 2) easy availability in a large quantity, 3) environmental friendliness, 4) biodegradability, and 5) overall low cost. In this sense, castor oil is the only commercially available natural oil polyol

produced directly by nature. Due to its high content in ricinoleic acid (around 80 wt. %), it has widely been used in a range of industrial applications (coatings, sealants and adhesives to flexible foams, thermoplastics elastomers, etc.). However, it is worth noting that castor oil derivatives have not been proposed elsewhere as reactive bitumen modifiers.

On these grounds, this chapter deals with the synthesis of NCO-functionalized prepolymers derived from castor oil aiming to achieve asphaltic bitumen with optimal thermal and rheological properties.

Therefore, the main goals of this chapter are:

- To study the effects that -NCO/-OH molar ratios (i.e. the molar relation between isocyanate and hydroxyl groups) exert on the properties of prepolymers, as well as on the thermo-rheological performance of bituminous binders.
- To explore the influence that different procedures (e.g. long or short processing times, curing process at ambient conditions or in an oven at high temperatures or final addition of water) provokes on the rheological response of modified binders.
- To improve the prepolymer behaviour as modifying agent by transesterification of castor oil with pentaerythritol.

Different tests were conducted on these prepolymers (TG/DTA, GPC, dynamic shear and modulated DSC) and their resulting bituminous modified binders (viscous flow, dynamic shear, modulated DSC and AFM).

6.2. TESTING PROCEDURES

Different rheology tests were conducted in a controlled-stress rheometer Physica MCR-301 (Anton Paar, Austria): a) viscous flow measurements, at 60 °C; and b) temperature sweep tests in oscillatory shear, from -20 to 200 °C (for isocyanate-prepolymers) and from 30 to 80 °C (for their modified binders), at a heating rate of 1 °C/min, a frequency of 10 rad/s and 1 % strain (within LVR interval). Plate-and-plate geometry (25 or 50 mm diameter, depending on the sample, and 1 mm gap) was always used.

Simultaneous thermo gravimetric/differential thermal analyses (TG/DTA) were conducted using a Seiko TG/DTA 6200 (Japan). Temperature ramps at 10 °C/min, from 40 to 600 °C, under N₂ atmosphere, and isothermal time sweeps at 180 °C, for 120 min, with air, were carried out on 5-10 mg of sample (polymeric MDI, PEG, castor oil and the resulting prepolymers).

Modulated Differential Scanning Calorimetry (MDSC) was performed with a TA Q-100 (TA Instruments, USA). Samples of 5-10 mg were always subjected to the following testing procedure: temperature range from -60 to 190 °C for prepolymers and from -40 to 85 °C for modified binders; heating rate of 5 °C/min; amplitude of modulation of ±0.5 °C; a period of 60 s; and N₂ as purge gas, with a flow rate of 50 mL/min. In order to provide the same recent thermal history, all the samples were placed into hermetic aluminium pans for 24 h before measurement.

The average molecular weight (M_w) of the polymeric MDI, castor oil and the resulting prepolymers were determined by means of GPC, by using a Waters apparatus, equipped with a Styragel® HR 4E column and using THF as solvent. Polypropylene glycol (PPG) standards covering a wide range of molecular weights were used for the calibration.

The microstructural characterization of the bituminous binders was carried out by means of Atomic Force Microscopy (AFM), with a MultiMode AFM connected to a Nanoscope IV scanning probe microscope controller (Digital Instruments, Veeco Metrology Group Inc., USA). All the images were acquired in tapping mode at 30 °C. The samples were prepared by heat-casting, a method that causes a negligible effect on the material morphology if compared to solvent-casting (Masson et al., 2006).

The bitumen SARAs fractions were determined by thin layer chromatography coupled with a flame ionization detector (TLC/FID), using an Iatroscan MK-6 analyzer (Iatron Corporation Inc., Japan). The elutions were performed in hexane, toluene and dichloromethane/methanol (95/5), following the procedure outlined elsewhere (Ecker, 2001).

6.3. PREPOLYMERS CHARACTERIZATION

6.3.1. Synthesis

Castor oil (designated CO and with hydroxyl index of 125 mg KOH/g) was functionalized with isocyanate groups, by its reaction with polymeric 4,4'-diphenylmethane diisocyanate (with -NCO index of 31 wt.%).

Table 6.1. Average molecular weight (M_w) relative to polypropylene glycol (PPG), -NCO content (% wt.) and glass transition temperature ($T_{g,DSC}$) for MDI-CO prepolymers, polymeric MDI and castor oil.

Samples	M_w (g/mol)	-NCO content (% wt.) ^a	$T_{g,DSC}$ (°C)
MDI-CO(8:1)	2640.3	19.4	-36.4
MDI-CO(4:1)	3375.8	12.6	-19.0
MDI-CO(2:1)	---	5.9	-15.5
Polymeric MDI	363.5	31.1	-49.5
Castor oil	1087.5	---	-63.2

^aAccording to ASTM D2572

As previously reported, these MDI-CO prepolymers are expected to bring out “chemical” modification of bitumen, via free -NCO groups. In addition, and with the aim of establishing a comparative analysis on the thermal stability of the castor oil-based prepolymer, another prepolymer was prepared with the same polymeric MDI and polyethylene glycol (designated PEG, donated by Repsol YPF, with a molecular weight of 350 g·mol⁻¹ and a hydroxyl index of 180 mg KOH/g). This new prepolymer will be referred to as MDI-PEG.

6.3.2. Effects of -NCO/-OH ratio on thermo-rheological prepolymer response

The morphology and thermorheological properties of these prepolymers depend on the structure and relative amount of soft and hard phases and their ordering. The thermal behaviour of polymeric MDI, castor oil (CO) and the resulting MDI-CO prepolymers was studied by means of MDSC and TG/DTA tests (Figures 6.2 and 6.3). This study may give an insight into the effect that different -NCO/-OH molar ratios exert on the prepolymers

thermal properties and on their potential applicability as bitumen modifiers.

In that sense, Figure 6.2, which presents reversing heat flow thermograms from -80 to 190 °C, reveals glass transition temperatures at -49 and -63 °C for the polymeric MDI and castor oil, respectively.

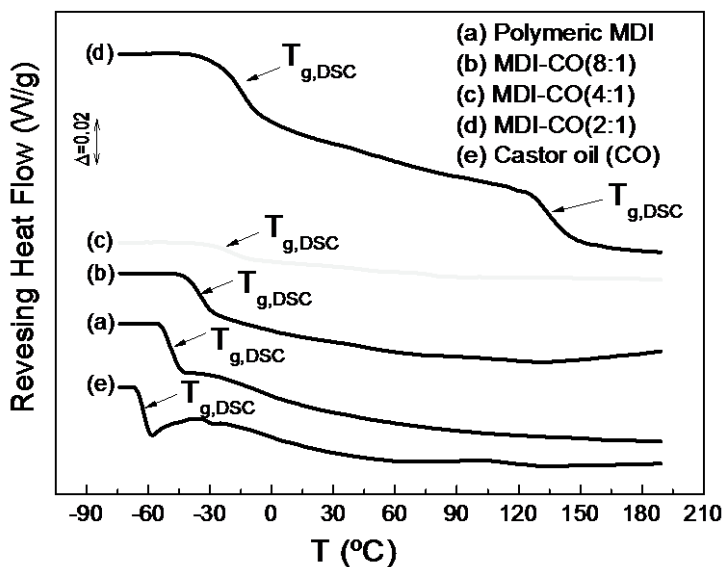


Figure 6.2. Reversing heat flow thermograms for polymeric MDI, castor oil, and MDI-CO prepolymers.

On the other hand, MDI-CO(2:1) presents two well-defined glass transitions. The first one, located at -37 °C, may be assigned to non-reacted polymeric MDI. The shortest chains in the polymeric MDI, with higher mobility, are assumed to react with the castor oil. Consequently, the longest chains, which would remain unbound, are the responsible for the higher value of T_g observed. The second peak, found at 135 °C, is attributed to the products formed by the functionalization of the castor oil with isocyanate groups, following the reaction scheme illustrated above. Instead, MDI-CO(8:1) and MDI-CO(4:1) prepolymers only display one glass

transition temperature each, located at -36 and -19 °C, respectively. The reaction products would be homogeneously dispersed in a continuous phase of polymeric MDI in excess, giving rise to an overall single thermal event.

Therefore, the resulting MDI-CO prepolymers with molar ratios of 8:1 and 4:1 are light brownish liquids. On the contrary, a yellowish infusible solid (decomposes without melting), not suitable for bitumen reactive modification, is obtained by decreasing the excess of isocyanate down to a molar ratio of 2:1. In fact, this prepolymer cannot be dissolved in THF and was not characterized by GPC. However, the study of its properties may provide valuable information on the wide range of polyurethane products which can be obtained by a simple change in their formulation and may help to establish the adequate application limits. In that sense, this study has also been included in the present investigation.

As reported by Corcuera et al. (2011), MDI-prepolymers thermal decomposition is known to occur as a result of multitude of physical and chemical phenomena and is not dominated by a single process. Thus, Figures 6.3A and 6.3B reveal the existence of three different degradation stages. The first one, from 160 to 340 °C (with a DTG peak at 280 °C) is related to the urethane bond decomposition into its parent isocyanate and alcohol, the formation of primary amines and a terminal olefinic group on the polyester chain and the formation of secondary amines and CO₂ (Hablott et al., 2008). The second stage, extending over a temperature range between 340 and 430 °C, corresponds to the degradation of the soft segments (castor oil, in this case). Finally, it is possible to observe a third weight loss between 430 and 530 °C (with a DTG peak at 470 °C) which relates to the degradation of the polyurethanes networks formed or some

other remaining structures (Corcuera et al., 2010). TG/DTG curves for castor oil and polymeric MDI are also included for the sake of comparison.

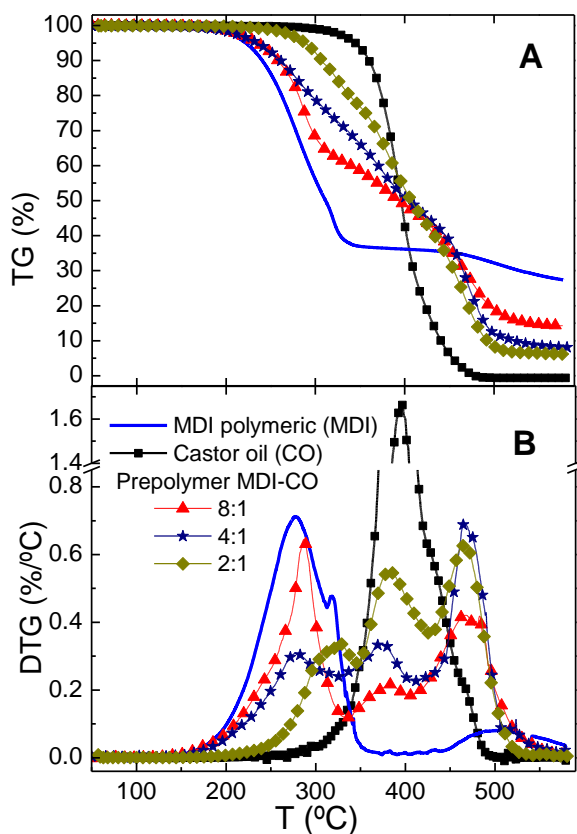


Figure 6.3. TG/DTG curves, between 40 and 600 $^{\circ}\text{C}$ and under N_2 atmosphere, for polymeric MDI, castor oil, and MDI-CO prepolymers.

Interestingly, the thermal decomposition of these MDI-CO prepolymers was strongly influenced by the $-\text{NCO}/-\text{OH}$ molar ratio. In this sense, a higher content in MDI (i.e., a larger $-\text{NCO}/-\text{OH}$ ratio) had two clear effects. On the one hand, the DTG peak corresponding to the thermal decomposition of castor oil, at around 400 $^{\circ}\text{C}$, becomes significantly narrower. On the other hand, a notable decrease in the rate corresponding to the first degradation process is observed with decreasing the $-\text{NCO}/-\text{OH}$

ratio. Furthermore, if compared to the polymeric MDI, which presents its first decomposition peak at 276 °C, the MDI-CO(2:1) prepolymer peak is clearly seen to increase up to 324 °C. These two last results may be attributed to the longest chains of polymeric MDI which remain unreacted after the polymerisation. In fact, they present lower mobility than the shortest chains and, as previously revealed by curves in Figure 2, their presence become more significant for the MDI-CO(2:1) prepolymer. For higher -NCO/-OH ratios, prepolymer molecules are diluted in a large excess of polymeric MDI.

On the other hand, isothermal TG experiments (at 180 °C, for 2 h) were conducted on the different MDI-CO prepolymers and one selected MDI-PEG prepolymer, in order to establish a comparative analysis on their thermal stability. This study also allowed the influence of the selected -NCO/-OH molar ratio to be determined. Castor oil, polyethylene glycol and polymeric MDI curves are also included. As shown in Figure 6.4, PEG displays a very significant weight loss during a prolonged period of time, with mass going down to 10 wt.% of its initial value after 60 min of testing. In contrast, no weight loss was observed for the castor oil at 180 °C. Moreover, the polymeric MDI also undergoes a very important weight loss of about 50 wt.% after 60 min. With regards to the resulting prepolymers, the combined effect of MDI/CO or MDI/PEG, influenced by their relative proportion, should be expected. Thus, the petroleum-based prepolymer (MDI-PEG), with a very high excess of polymeric MDI, presents a response very similar to this (Martín-Alfonso et al., 2009). However, results obtained for the vegetable oil-based prepolymer (MDI-CO) point out the strong influence that a small proportion of this type polyol can exert on their NCO-functionalized prepolymers. In fact, even for the MDI-CO prepolymer with the highest excess of -NCO (-NCO/-OH molar ratio of 8:1), a very high thermal stability, quite close to the pure castor oil's, can be observed

(weight loss less than 15 wt.% after 2 h). This weight loss goes down to 9 wt.% or even become negligible for MDI-CO(4:1) and MDI-CO(2:1), respectively.

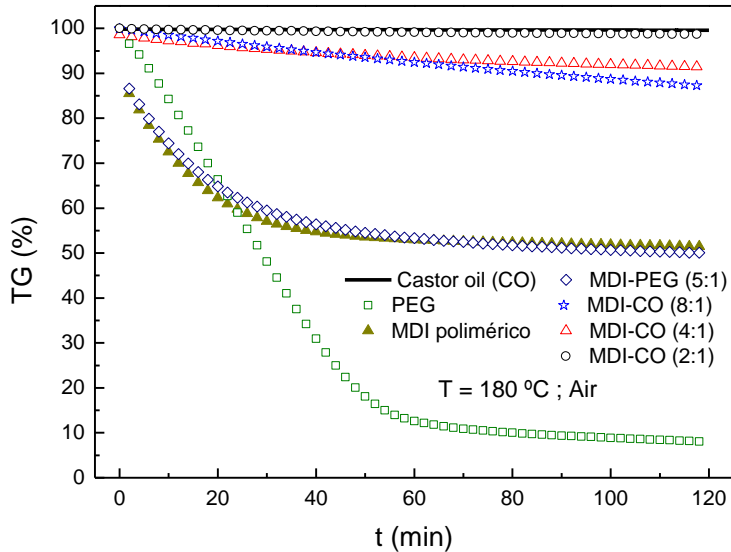


Figure 6.4. Isothermal weight loss at 180 °C for polymeric MDI, castor oil, polyethylene glycol (PEG), MDI-PEG and MDI-CO prepolymers, under air atmosphere.

A practical consequence, in relation with the bitumen-prepolymer mixing stage during the bitumen modification, derives from the result above. Hence, MDI-CO has shown its adequacy at the high processing temperatures required for those bitumens with low values of penetration. However, the weight loss observed for MDI-PEG may represent a handicap in that range of temperature.

Finally, the rheological behaviour of the three MDI-CO prepolymers was studied by means of temperature sweep tests in oscillatory shear mode (at a selected temperature interval for each of them). In this sense, Figure 6.5

shows the evolution with temperature of the dynamic viscous (G'') and elastic (G') moduli.

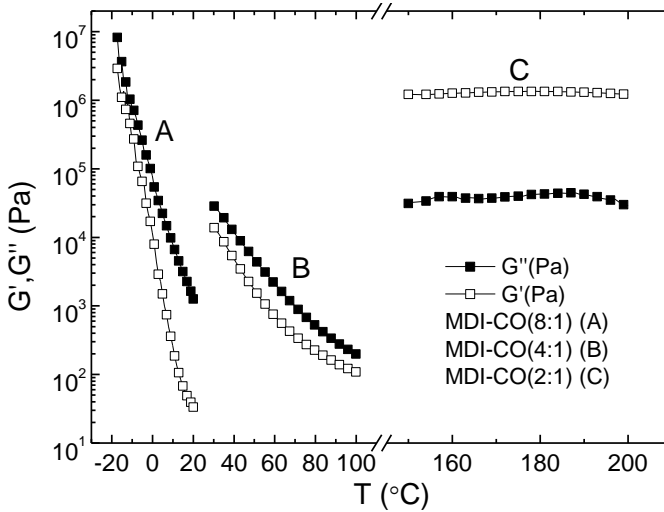


Figure 6.5. Sweep temperature tests, in shear mode, between -20 and 200 °C, for MDI-CO prepolymers.

It can be seen that, for the MDI-CO(8:1) and MDI-CO(4:1) prepolymers, both moduli monotonously decrease with increasing temperature, from -20 to 20 °C and from 30 to 100 °C, respectively. Moreover, the viscous modulus clearly prevails over the elastic one in the entire temperature interval tested, which points out a predominantly viscous behaviour (liquid-like behaviour). In fact, the MDI-CO(8:1) prepolymer shows the typical behaviour corresponding to the so-called viscous flow region. However, MDI-CO(2:1) presents, in a temperature range between the second glass transition (135 °C) and thermal degradation (about 200 °C), constant values of the dynamic moduli, with a significantly higher contribution of G' (solid-like behaviour), which typically corresponds to cross-linked networks above T_g (Ross-Murphy, 1995).

6.4. BITUMEN MODIFICATION BY MDI-CO PREPOLYMERS

6.4.1. Materials and modified binders preparation

Bitumen with a penetration grade of 100/150 has been used as base material for the modification. Details of technological properties (penetration grade and R&B softening temperature, according to EN 1426:2007 and EN 1427:2007, respectively) and chemical composition, in terms of SARAs fractions, are shown in Table 6.2.

Table 6.2. Penetration value, ring & ball softening temperatures, SARA's fraction and colloidal index values for the neat bitumens studied.

	Bitumen 100/150
Penetration (dmm)	114
R&B softening point (°C)	40.0
Saturates (wt.%)	6.9
Aromatics (wt.%)	60.6
Resins (wt.%)	19.8
Asphaltenes (wt.%)	12.7
Colloidal Index (C.I.) ^a	0.24

$$^a\text{Colloidal Index} = (\text{asphaltenes} + \text{saturates}) / (\text{resins} + \text{aromatics})$$

Blends of bitumen with 2 wt.% MDI-CO(8:1) or MDI-CO(4:1) were processed in a batch mixer (a cylindrical vessel of 60 mm diameter and 140 mm height), using an IKA RW-20 stirring device (Germany) equipped with a four-bladed 45°-pitched turbine. MDI-CO binders were performed following two different procedures:

- 1) Firstly, bitumen and MDI-CO were mixed for 1 h, at 90 °C and 1200 rpm, and the resulting modified bitumen was then divided into three parts: a) one was used as such (“non-cured” binder); b) another one was mixed with 2 wt.% water for 45 min at 90 °C (“water-fast” binder); and c) the third part was poured onto aluminium foil, forming a thin layer which was exposed for 6 months to the ambient (“water-slow” binder).
- 2) In the second procedure, prepolymer and bitumen were mixed for 1 h and stored in an oven for 24 h at 90 °C; afterwards, again, the resulting binder was divided into the same three parts above commented in the procedure 1).

For the sake of the clarity, samples prepared according to procedure 1) will, henceforth, be referred to as “1 h processing” and those corresponding to procedure 2) as “24 h processing”.

In addition, a reference sample containing bitumen and 3 wt.% of SBS (binder formulation commonly used by the paving industry) was prepared for 1.5 h, at 180 °C, under high shear conditions.

6.4.2. Influence of prepolymer formulation

The effect that prepolymer formulation, more precisely, the molar relation between isocyanate and hydroxyl groups (-NCO/-OH), provokes on bitumen modification, was evaluated. With this aim, binders of bitumen with the different MDI-CO prepolymers have been manufactured following the procedure 2) (“24 h processing”) and their thermo-rheological responses have also been studied.

Figure 6.6 displays viscous flow curves, at 60 °C, of 2 wt.% MDI-CO(8:1) binders as a function of curing time (“water-slow” binders). Neat bitumen, the reference 3 wt.% SBS binder and the “water-fast” binder have been

included for the sake of comparison. A nearly Newtonian behaviour in the whole range of shear rates tested is shown by neat bitumen. On the contrary, modified binders with 2 wt.% MDI-CO(8:1) leads to a different viscous flow behaviour, with a constant viscosity at low shear rate, η_0 , followed by shear-thinning region above a “critical” shear rate value, $\dot{\gamma}_c$. This behaviour can be described by the Carreau’s model fairly well:

$$\frac{\eta}{\eta_0} = \frac{1}{\left[1 + (\lambda \cdot \dot{\gamma})^2\right]^s} \quad (6.1)$$

where η_0 (Pa·s) is the zero-shear-rate-limiting viscosity, λ (s) is a time constant whose inverse approximately matches the threshold shear rate, $\dot{\gamma}_c$, above, and ‘s’ is a parameter related to the slope in the shear-thinning region.

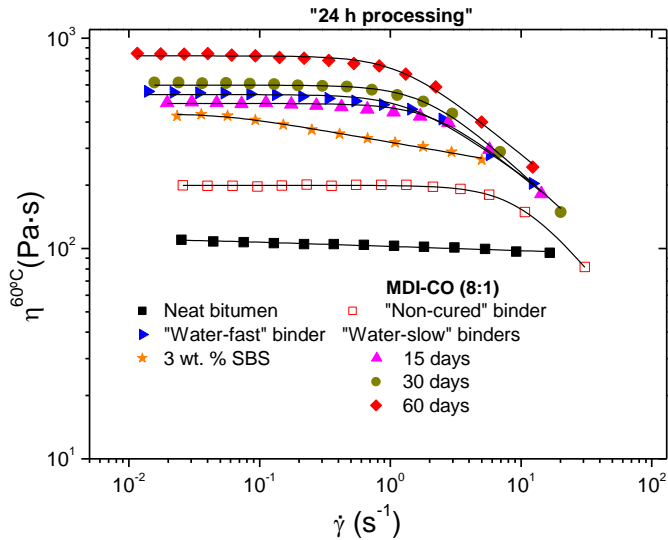
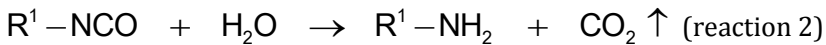


Figure 6.6. Viscous flow curves, at 60 °C, for a selected 2 wt.% MDI-CO(8:1) modified binder, as a function of curing time (“water-slow” binders). Neat bitumen, 3 wt.% SBS and “water-fast” binder are also included.

As can be observed in Figure 6.6, the “non-cured” 2 wt.% MDI-CO(8:1) binder presents a clearly higher value of viscosity if compared to the neat bitumen (viscosity goes from 100 up to 200 Pa·s, approximately). Thus, during the bitumen-prepolymer blending and further storage at 90 °C for 24 hours (“short-term” modification), a part of the free -NCO groups in the prepolymer are known to react with certain groups, mainly hydroxyl, present in the asphaltene molecules. This provokes a notable increase in the binder viscosity, due to the formation of urethane linkages according the following reaction (Singh et al., 2003):



However, a much higher degree of modification was observed when the binder was subjected to a further curing stage of up to 60 days at room temperature (“long-term” modification). With this regard, some water from the ambient is expected to slowly diffuse into the modified bitumen, promoting the two following series reactions (Carrera et al., 2010):



A significant increase in the binder viscosity derived from the development of a complex microstructure is achieved (Martín-Alfonso et al., 2008; Segura et al., 2005). This viscosity enhancement, which becomes larger with as curing time is longer, may be of up to one order of magnitude after 60 days of curing. On the other hand, water in a concentration of 2 wt.%, was added to the binder during its preparation, in an attempt to spare the time required for maturing. As a result, a binder with similar viscosity to

that resulting from 15 days of curing, and higher than the reference rubber-modified binder is attained.

The results of Carreau's model parameters, presented in Table 6.3, reveal the development of a more complex microstructure for the largest -NCO content (i.e., MDI-CO(8:1) prepolymer) and the longest curing time, as demonstrated by a higher value of viscosity along with a lower value of $\dot{\gamma}_c$ (Martín-Alfonso et al., 2008).

Table 6.3. Evolution with curing time of Carreau's model parameters for "water-slow" modified binders. Neat bitumen, reference SBS binder and "water-fast" are included.

	Binders	η_0 (Pa·s)	λ (s)	s
	Neat bitumen	110	---	0.01
	3 wt.% SBS	438	16.6	0.05
MDI-CO (4:1)	Non-cured	199	0.10	0.38
	15 days	305	0.22	0.31
	30 days	321	0.29	0.28
	60 days	375	0.35	0.26
	2 wt. % H ₂ O	266	0.25	0.25
MDI-CO (8:1)	Non-cured	202	0.10	0.39
	15 days	489	0.53	0.29
	30 days	598	0.84	0.25
	60 days	824	1.44	0.24
	2 wt. % H ₂ O	539	0.72	0.22

A modification index, $(M.I.)_A^{60^\circ C}$, written in terms of the zero-shear viscosity values at 60 °C, results a very adequate parameter to quantify the bitumen modification at high in-service temperatures. This index is defined as follows:

$$(M.I.)_A^{60^\circ C} = \frac{\eta_{0,mod} - \eta_{0,neat}}{\eta_{0,neat}} \quad (6.2)$$

where $\eta_{0,mod}$ and $\eta_{0,neat}$ are the zero-shear viscosity values, at 60 °C, for MDI-CO modified binders and neat bitumen, respectively. So, $(M.I.)_A^{60^\circ C}$ is a measure of the viscosity increase produced by the modifier, relative to the original viscosity of the non-modified bitumen. Figure 6.7 presents the evolution of the modification index with curing time for the 2 wt.% MDI-CO bituminous binders (“water-slow” binders). As references, modification indexes for 3 wt.% SBS and “water-fast” binders were also included. If no curing is conducted (only Reaction 1 takes place) the degree of bitumen modification attained is just slightly affected by the type of MDI-CO used. In other words, “short-term” modification does not seem to greatly depend on the prepolymer -NCO/-OH molar ratio.

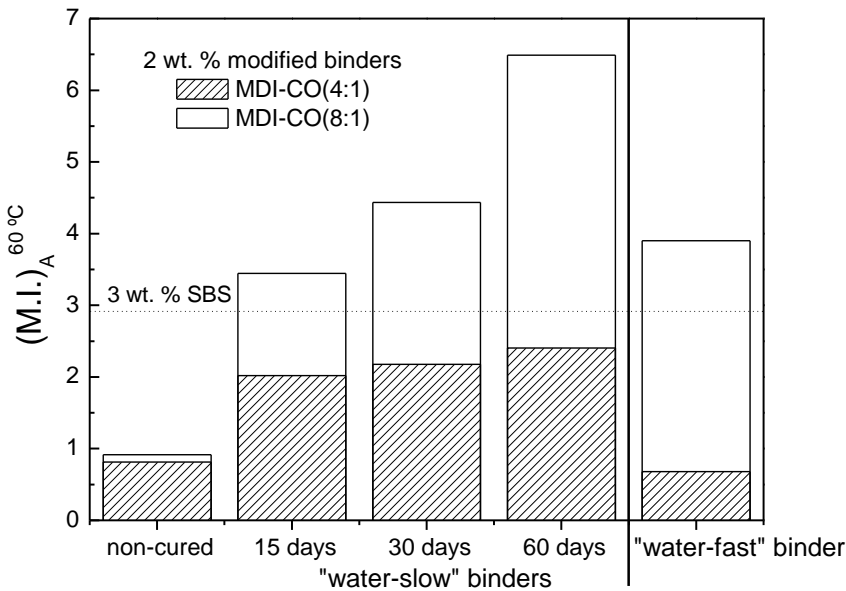


Figure 6.7. Evolution of the modification index with curing time for 2 wt.% MDI-CO modified binders (“water-slow” binders). “Water-fast” binders and 3 wt.% SBS are included as reference.

However, when a thin sheet of the resulting modified bitumen (“water-slow” binders) is exposed to the environment for a prolonged period of time, the prepolymer with the highest -NCO/-OH ratio produces a much more significant increase in the modification index values. In this case, a larger content of free -NCO groups are yet available to react through the scheme detailed in Reactions 2 and 3. For example, the binder with 2 wt.% MDI-CO(8:1) exhibits, just after 15 days of curing, a higher value of M.I.^{60°C} (about 3.45) than the 3 wt.% SBS binder (2.80). On the other hand, as previously commented, water addition on “non-cured” binders may lead to a material with improved resistance to permanent deformation (higher viscosity) without the need for curing. However, it was not possible to obtain a material equivalent to the 60 days-cured binder by mere addition of water.

These observations confirm two ideas of paramount importance: a) on the one hand, water (either added or absorbed from air) promotes reactions with free -NCO groups which significantly improve the binders rheological response at 60 °C; b) on the other hand, the slow diffusion for a prolonged period of time (of up to 60 days in this case) of water into previously MDI-CO modified binder results in a more efficient method of bitumen chemical modification, if compared to the direct water addition. Thus, Reactions 1, 2 and 3 would be occurring simultaneously during the curing stage. In terms of product application, it means that modification would be able to continue under environmental conditions even after asphalt laydown operations have concluded. On the contrary, direct addition of water would compete with bitumen for the free -NCO sites available and Reaction 1 would be hampered, which limits the resulting degree of modification.

The viscoelastic performance of the MDI-CO modified binders has been evaluated by means of temperature sweep tests, in oscillatory shear mode from 30 to 80 °C. Figure 6.8A displays the evolution of the “rutting parameter”, $|G^*|/\sin \delta$, with temperature for neat bitumen, 3 wt.% SBS and two selected MDI-CO(8:1) (“non cured” and 60-days-cured) modified binders. As commented in the previous Chapter V, the “rutting parameter” derived from simple dynamic temperature sweep tests may be considered an easier and more hands-on way to compare the degree of improvement attained after modification. On these grounds, the values of temperatures at which $|G^*|/\sin \delta$ (under certain testing conditions outlined by AASHTO MP1 (1993) equals 1 kPa have been calculated and are shown in Figure 6.8B, for 2 wt.% MDI-CO modified binders, as a function of curing time. These temperatures represent the in-service limits at which the binder would offer a satisfactory response. As may be seen, the addition of 2 wt.% of MDI-CO(8:1) leads to a first increase in the $T_{|G^*|/\sin \delta}$ value just after processing, from 62 °C for neat bitumen up to 65 °C. Further, this value goes up to 73 °C after 60 days of curing, which represents 11 °C of increase if compared to the straight-run bitumen. Once more, the effect of the -NCO/-OH molar ratio is almost negligible for the “non-cured” binders, but results very noticeable as the curing time increases (same as shown for viscosity). In conclusion, bitumen modification by MDI-CO prepolymers would reduce the progressive accumulation of permanent deformations produced by the traffic at high temperatures, with rutting resistance being favoured by a larger -NCO/-OH ratio and longer curing times.

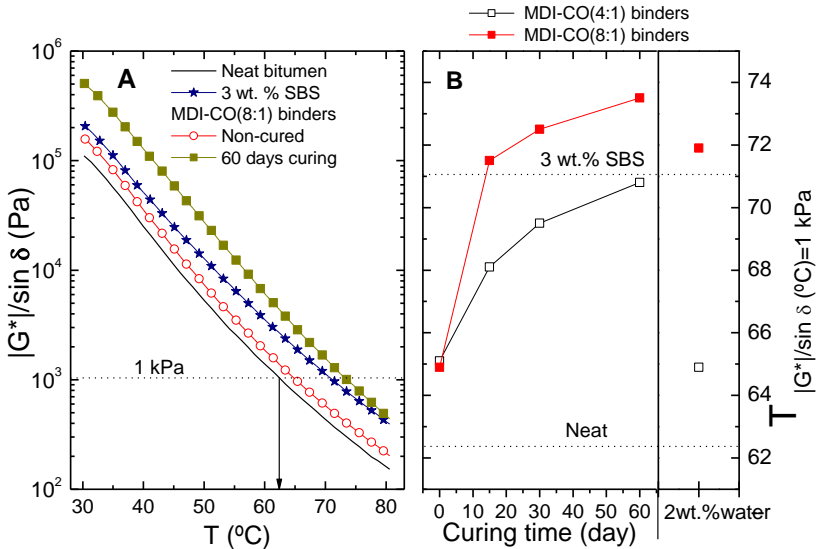


Figure 6.8. (A) Evolution of the “rutting parameter”, $|G^*|/\sin \delta$, for neat bitumen, 3 wt. % SBS and two selected binders: “non-cured” 2wt.% MDI-CO(8:1) and 60-days-cured; (B) “Rutting” temperatures with curing time for “water-slow” modified binders. Neat bitumen, 3 wt.% SBS and “water-fast” binders are also included.

The above-mentioned enhancements in the binders rheological behaviour suggest significant changes in their microstructure, which can be detected by means of the non-reversing component of the heat flow curve obtained by modulated DSC. Bitumen is well known to be a multiphase system mainly composed of two fractions: maltenes (which include three different families of compounds: saturates, aromatics and resins) and asphaltenes. According to Masson and Polomark (Masson and Polomark, 2001; Masson et al., 2002), they order in four stages upon cooling from melt, yielding four specific thermal events in the non-reversing heat flow curve.

Figure 6.9 shows the non-reversing thermograms for neat bitumen and the 2 wt.% MDI-CO(8:1) modified binders, as a function of curing time. If attention is paid to the modified binder after 60 days of curing, those four

thermal events can be appreciated: a) a broad endothermic background from -40 to 80 °C (first event); b) two exotherms, located at about -20 °C and 35 °C (second and third events, respectively); c) an endothermic at around 50 °C (fourth event). Interestingly, the third and fourth events are not clearly defined in the neat bitumen curve. The analysis of the fourth thermal event may provide an approximate idea on changes occurred at a microstructural level. In fact, that endotherm at 50 °C relates to the diffusion of relatively large structures with high molecular weight, as those found in resins and asphaltenes, to form independent domains. Thus, the extent of that endotherm is clearly seen to increase after modification and further curing, and corroborates the rearrangement of domains composed by large molecular weight structures, with melting temperatures between 40 and 80 °C, which form by the addition of the modifier. In order to provide a comparative analysis, enthalpy values associated to this event are listed in Table 6.4, with the largest value corresponding to the 60 days-cured modified bitumen.

Table 6.4. Fourth event enthalpies (ΔH_{4th}) for neat bitumen and 2 wt.% MDI-CO(8:1) modified binders, as a function of curing time.

	Binders	ΔH_{4th} (J/g)
		Neat bitumen
MDI-CO (8:1)	Non-cured	0.49
	15 days	1.72
	30 days	2.07
	60 days	4.41

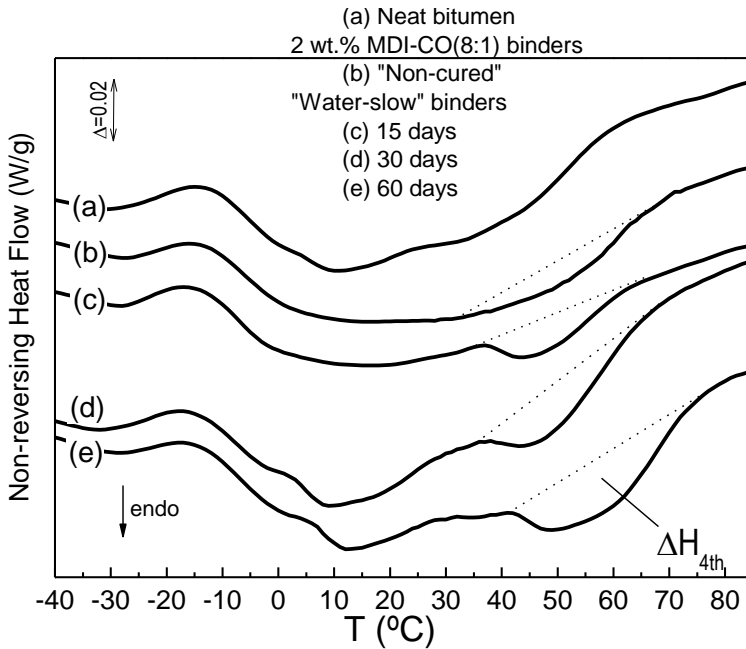


Figure 6.9. Non-reversing heat flow thermograms for neat bitumen and 2 wt.% MDI-CO(8:1) “water-slow” binders at different curing time.

Finally, additional support to previous results is provided by the AFM pictures, taken at 30 °C, shown in Figure 6.10 for neat bitumen, 2 wt.% MDI-CO(8:1) “water-fast” and “water-slow”, after 60 days of curing, modified binders. Bitumen microstructure, pictured as solid particles of asphaltenes (black and white streaks) covered by a shell of resins (light areas) and surrounded by the molten maltenic matrix (darkest areas) (Masson et al., 2006), matches pretty well the traditional bitumen colloidal model (Lesueur et al., 1996; Lesueur, 2009). If compared to neat bitumen, the MDI-CO modified binders present much larger asphaltenic regions, particularly for the modified binder exposed at room curing for 60 days (see previous explanations on that issue). Consequently, AFM observations seem to be in accordance with previous viscous flow, viscoelasticity and calorimetry tests results. Also it constitutes a valuable tool for providing

evidence on the existence of a more compact microstructure originated by the formation of covalent bonds between the MDI-CO prepolymers and certain bitumen groups (Carrera et al., 2010). This microstructure leads to observed enhancement in bitumen performance.

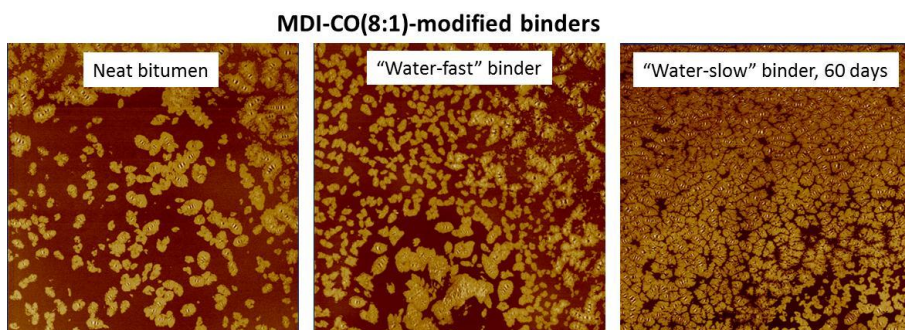


Figure 6.10. AFM micrographs ($50 \times 50 \mu\text{m}^2$), at $30 \text{ }^\circ\text{C}$, for neat bitumen, 2 wt.% MDI-CO(8:1) binders “water-fast” and “water-slow”, after 60 days of curing, binders.

6.4.3. Effects of processing/curing conditions

Previous results have showed a significant degree of bitumen modification after addition of 2 wt. of MDI-CO prepolymer, which was further enhanced by a room curing stage, particularly for the polyurethane prepolymer with the highest -NCO/-OH molar ratio (this is, for the MDI-CO(8:1) prepolymer). According to this, once the material is in use, water from the air would be able to diffuse into bitumen and react with the remaining isocyanate groups (referred to as “*water-slow*” modification). In this way, as an attempt to spare the curing period detailed above, water could be added to fresh, or “non-cured”, MDI-CO/bitumen samples (giving rise to the so-called “*water-fast*” modification). The goal of the present section was explore the effect that processing/curing conditions exert on the thermo-rheological behaviour of the resulting modified binders, as well as to

understand how “water-slow” and “water-fast” modification processes occur. With this objective, binders of bitumen with the MDI-CO(8:1) prepolymer have been manufactured following the procedure 1) (“1 h processing”) and 2) (“24 h processing”), described the section 6.4.1.

The viscous behaviour of these MDI-CO modified samples, at 60 °C, can be described by the Carreau’s model fairly well (equation 6.1), and their fitting parameters are gathered in Table 6.5.

Table 6.5. Evolution with curing time of Carreau’s model parameters and SHRP maximum temperatures for “water-slow” binders. Neat bitumen, reference SBS binder and “water-fast” binders are included as references.

		Carreau’s model parameters			$T_{ G^* /\sin \delta=1}$ kPa (°C)
Binders	η_0 (Pa·s)	λ (s)	s		
	Neat	110	---	0.01	62.4
	3 wt.% SBS	438	16.67	0.05	71.1
“1 h processing”	Non-cured	170	0.22	0.20	64.5
	1 month	751	0.78	0.24	72.4
	2 months	1123	1.47	0.23	76.3
	6 months	1683	2.51	0.22	77.7
	Water-fast binder	322	0.33	0.26	69.6
“24 h processing”	Non-cured	203	0.10	0.39	65.1
	1 month	600	0.53	0.28	72.2
	2 months	824	0.84	0.25	73.5
	6 months	1174	1.44	0.25	75.8
	Water-fast binder	540	0.72	0.22	71.9

In order to compare the degree of bitumen modification achieved at high in-service temperatures, a new modification index, $(M.I.)_B^{60^\circ C}$, in terms of the Newtonian viscosities at 60 °C, listed on Table 6.5, has been defined as follows:

$$(\text{M.I.})_{\text{B}}^{60^{\circ}\text{C}} = \frac{\eta_{0,\text{mod}} - \eta_{0,\text{non-cured}}}{\eta_{0,\text{non-cured}}} \quad (6.3)$$

On the contrary to $(\text{M.I.})_{\text{A}}^{60^{\circ}\text{C}}$, this index expresses the relative viscosity increase due to water (either added or absorbed from air) with reference to the “non-cured” binder. Hence, it will allow us to study the effect that processing/curing procedure provokes on “water-slow” and “water-fast” modification processes.

On these grounds, Figure 6.11 shows the values of the modification index for MDI-CO modified binders, as a function of curing time, as well as “water-modified” binders prepared following the two processing conditions.

On the other hand, “water-modified” binder presents a higher modification degree when MDI-CO prepolymer and bitumen react for 24 h at 90 °C, prior to the water reaction, probably because longer processing times yield a larger concentration of new reactive molecules by Reaction 1, making the water addition process (Reaction 2 and 3) more effective. Thus, this result suggests that bitumen-prepolymer reactions should be promoted in a large extent before water is added (“water-fast” modification) (Izquierdo et al., 2011). On the contrary, when a thin sheet of the resulting modified binder processed for 1 h is exposed to the environment at room temperature for a long period of time (“water-slow” modification) a higher value of $(\text{M.I.})_{\text{B}}^{60^{\circ}\text{C}}$ than those prepared for 24 h is observed. Therefore, during the processing at 90 °C, while -NCO is progressively consumed by reaction 1, there is a worsening in the modifying efficiency of “water-slow” modification. This discrepancy between both water types of modification is probably related to different modification pathways. In this sense, “water-fast” modification happens quickly at 90 °C via Reaction 2 and 3. By contrast, “slow-water”

modification occurs during longer times at room temperature where Reactions 2 and 3, but also Reaction 1, are still taking place.

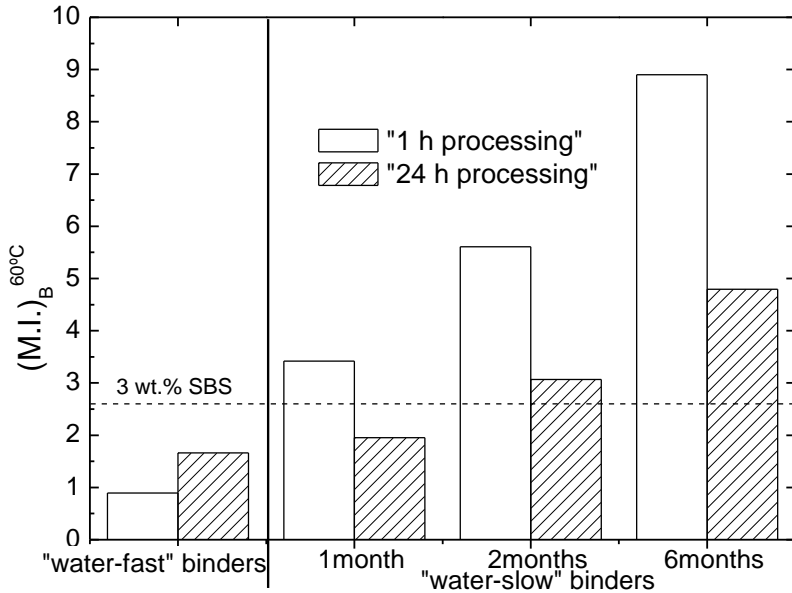


Figure 6.11. Modification index values, $(M.I.)_B^{60^\circ C}$, for “water-slow” MDI-CO binders as a function of curing time, manufactured following the two procedures. “Water-fast” binders and SBS reference binders are included as references.

Taking into account that clearly higher $(M.I.)_B^{60^\circ C}$ values are obtained from ambient curing process, slow diffusion of water into modified binders, after a curing time (i.e. 6 months), brings about higher viscosity enhancements than the modification resulting from the addition 2 wt.% water. Interestingly, MDI-CO modified binders could undergo a “water-slow” modification under environmental conditions even after asphalt laydown has finished.

Temperature sweep tests in oscillatory shear, from 30 to 100 °C, were carried out on the neat bitumen, “non-cured”, “water-slow”, after 6 months of curing and “water-fast” MDI-CO modified binders, manufactured

following procedures 1) (1 h processing) and 2) (24 h processing). Figure 6.12 displays the evolution with temperature of the storage modulus, G' , and loss tangent, $\tan \delta$, for different samples.

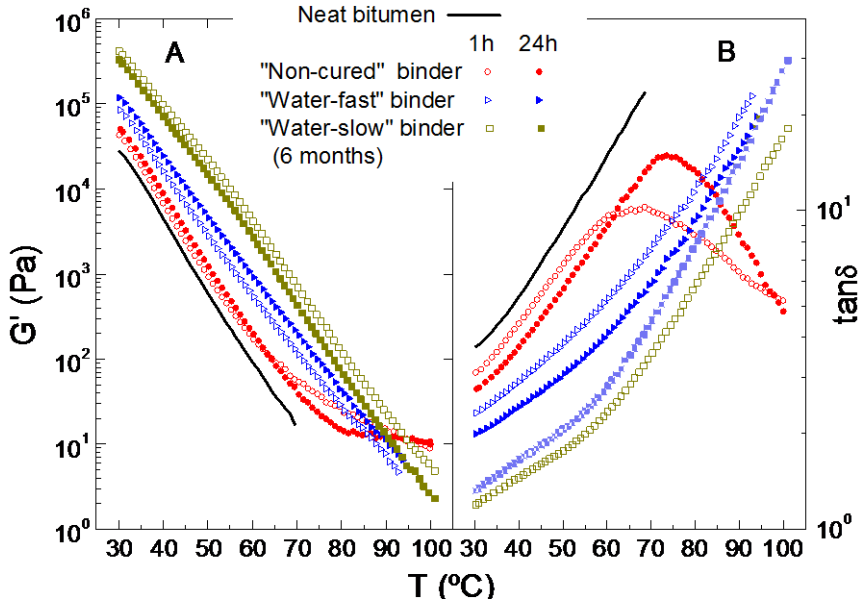


Figure 6.12. Evolution with the temperature of (A) storage modulus, G' , and (B) loss tangent, $\tan \delta$, for neat bitumen, “non-cured”, “water-slow”, after 6 months of curing and “water-fast” MDI-CO modified binders, manufactured following the two procedures.

It can be observed a prevailing viscous behaviour, with $\tan \delta > 1$ over the entire temperature interval tested. Moreover, whilst neat bitumen, “water-slow” MDI-CO modified samples (after 6 months of curing time) and “water-fast” binders display a direct transition from the glassy to the flow region, “non-cured” MDI-CO modified binder shows a different linear viscoelastic behaviour. Thus, G' versus temperature curves for “non-cured” samples show a shoulder, which gives rise to a maximum in the loss tangent, at high temperature. This new transition is related to the deformation-relaxation process of the new and enlarged dispersed phase,

originated by local reactions between prepolymer and asphaltenes cluster occur during processing (Reaction 1). Thus, when the continuous phase is soft enough at high temperature, the presence of this phase is revealed. However, after water addition or slow diffusion of moisture from air, this transition is masked by the stiffening chemical process previously mentioned (Carrera et al., 2009; Izquierdo et al., 2012).

Furthermore, MDI-CO addition produces a decrease in $\tan \delta$ values (enhancing binder elastic properties), mainly for those samples processed for 1 h and after a long period of curing time. On the other hand, the average slope of the curve of the loss tangent vs. temperature, within the interval 30-55 °C, can be related to binder thermal susceptibility at medium/high in-service temperatures. Thus, this average slope decreases from $2 \cdot 10^{-2}$ for neat bitumen down to $8 \cdot 10^{-3}$ for its corresponding 2 wt. % MDI-CO modified binder, processed for 1 h or after 6 months of curing time at room temperature. This result would suggest a lower thermal susceptibility, in the temperature range considered, and, consequently, an improved thermal resistance would be expected for these modified binders (Fuentes et al., 2008).

In that sense, it is well-know that the Strategic Highway Research Program (SHRP) proposed the parameter $|G^*|/\sin \delta$ as a manner to efficiently determine the maximum temperature below which bitumen will show a satisfactory performance. Figure 6.13 shows the evolution of the “rutting” parameter with temperature for the different samples considered, and the Table 6.5 gathers the temperature at which $|G^*|/\sin \delta$ equals 1 kPa.

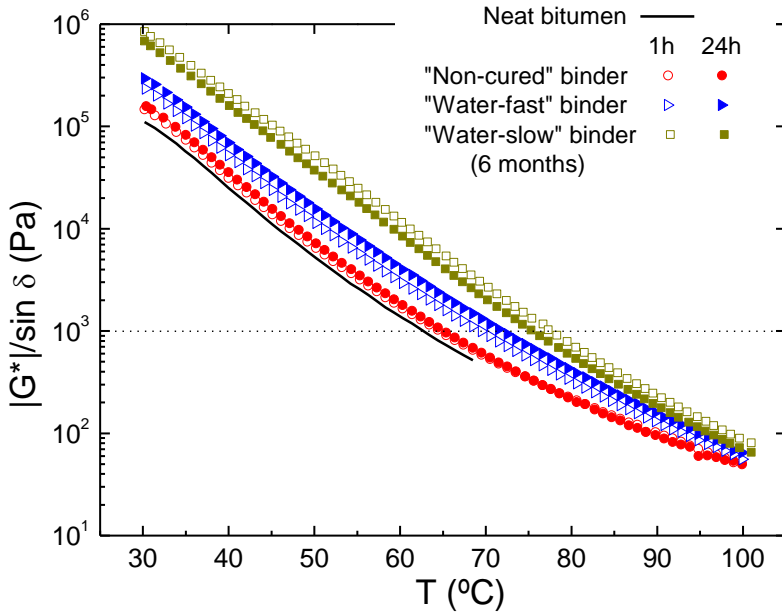


Figure 6.13. Temperature dependence of the “rutting parameter”, $|G^*|/\sin \delta$, for neat bitumen, “non-cured”, “water-slow”, after 6 months of curing, and “water-fast” MDI-CO modified binders, manufactured following the two procedures.

As can be observed, SHRP maximum temperature (and therefore, rutting resistance) is notably increased after modification and curing, mainly for those samples processed for 1 h. If compared with neat bitumen, an increase of nearly 14 °C is observed after addition of 2 wt. % MDI-CO, 1 h of blending, and curing for 6 months, clearly higher than the reference SBS modification.

Previous rheological tests point out that the modification degree achieved depends on the processing/curing procedure carried out. Aiming to obtain further insight into this issue, additional techniques were used. Firstly, the thermal behaviour of neat bitumen and MDI-CO modified binders has been evaluated by means of modulated differential scanning calorimetry (MDSC). Figure 6.14 displays non-reversing heat flow thermograms for neat bitumen, “water-slow”, after 6 months of curing, and “water-fast”

MDI-CO binders, manufactured following “1 h processing” and “24 h processing” procedures.

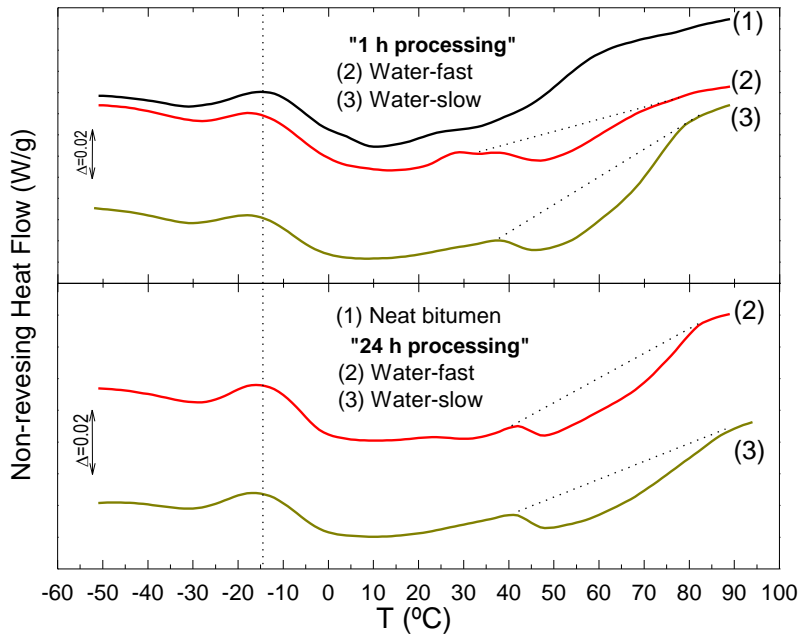


Figure 6.14. Non-reversing heat flow curves for neat bitumen, “water-slow”, after 6 months of curing, and “water-fast” MDI-CO binders, manufactured following “1 h processing” and “24 h processing” procedures.

Table 6.6 displays the temperatures at which the second event (T_{2nd}) appears. It can be noticed a decrease in T_{2nd} for MDI-CO modified binders after water addition or prolonged curing times. The decrease in T_g values hints that, after chemical reactions, low temperature chain mobility increases, reducing temperature at which cold crystallization begins. Consequently, low temperature properties would be enhanced.

On the other hand, the endotherm at 50 °C is related to the diffusion of relatively large and high molecular weight structures, as those found in resins and asphaltenes, to form independent domains. As can be seen, the

area of that endothermic peak and thus, its associated energy, undergoes a higher increase for the “water-modified” binder processed for 24 h (Figure 6.14 and Table 6.6). However, the highest value for this event is found when samples are prepared for 1 h and after 6 months of curing time.

Table 6.6. Temperatures of the second thermal event (T_{2nd}) and energy associated with the endothermic fourth event (ΔH_{4th}) for neat bitumen, “water-slow”, after 6 months of curing, and “water-fast” MDI-CO binders, manufactured following “1 h processing” and “24 h processing” procedures.

	Binders	T_{2nd} (°C)	ΔH_{4th} (J/g)
	Neat bitumen	-14.3	---
“1 h processing”	“Water-slow”	-18.3	6.82
	“Water-fast”	-17.3	2.55
“24 h processing”	“Water-slow”	-17.7	3.86
	“Water-fast”	-16.0	3.39

Therefore, these results are in good agreement with the observed rheological behaviour and corroborate the rearrangement of the largest molecular weight structures due to chemical reaction in the “water-fast” and “water-slow” modification processes, between 40 °C and 80 °C.

In order to better understand changes in the chemical composition occurring after the prepolymer modification, Figure 6.15 presents the evolution of the SARAs fractions, as a function of curing time, for the different bituminous binders studied. As can be observed, the bitumen asphaltene fraction increases after any type of modification partially attributed to the reaction of MDI-CO molecules with maltenic compounds occurred during processing, and also to derived products as a consequence of the reactions involving water. Thus, these new compounds (NCO/polars)

cannot be eluted by any of the three different solvents used in the chromatographic method to separate saturates, aromatics and resins and consequently, they appear together with the asphaltene fraction in the TLC/FID tests.

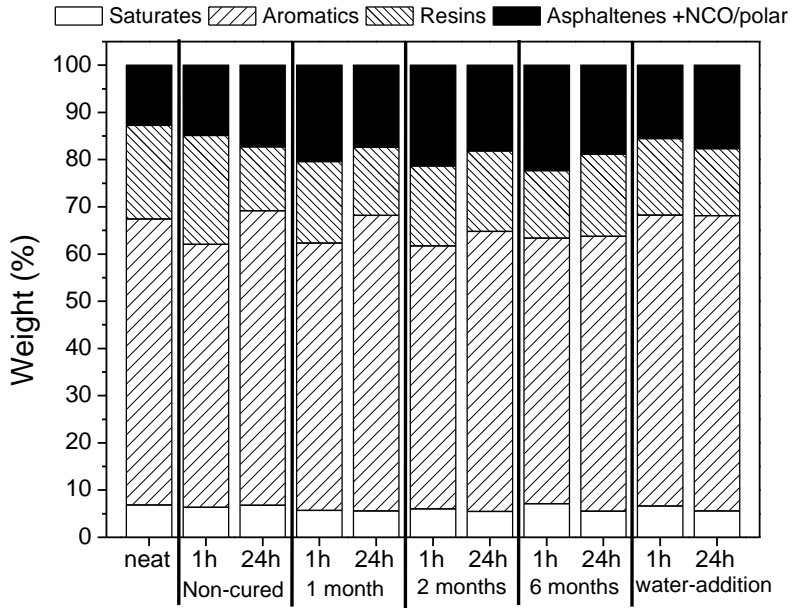


Figure 6.15. Evolution of bitumen SARAs fractions for “water-slow” MDI-CO binders, manufacture following the two procedures, as a function of curing time. Neat bitumen, “non-cured” and “water-fast” MDI-CO binders are also included as references.

Aiming a further insight into the effect of processing, a “reactive” Gaestel colloidal index, $C.I._{reactive}$, which accounts for the changes in chemical composition, due to bitumen reactive modification by MDI-CO, has been defined as follows:

$$C.I._{reactive} = \frac{\text{saturates} + \text{asphaltenes} + \text{NCO/polars}}{\text{aromatics} + \text{resins}} \quad (6.4)$$

where NCO/polars refers to the resulting species formed by chemical reactions between polymer and the polar bitumen compounds, as well as the species originated by the reaction between non-reacted polymer and water, detailed below. Figure 6.16 displays the evolution of the “modified” colloidal index for “water-slow” MDI-CO binders, as a function of curing time, and “water-fast” binders.

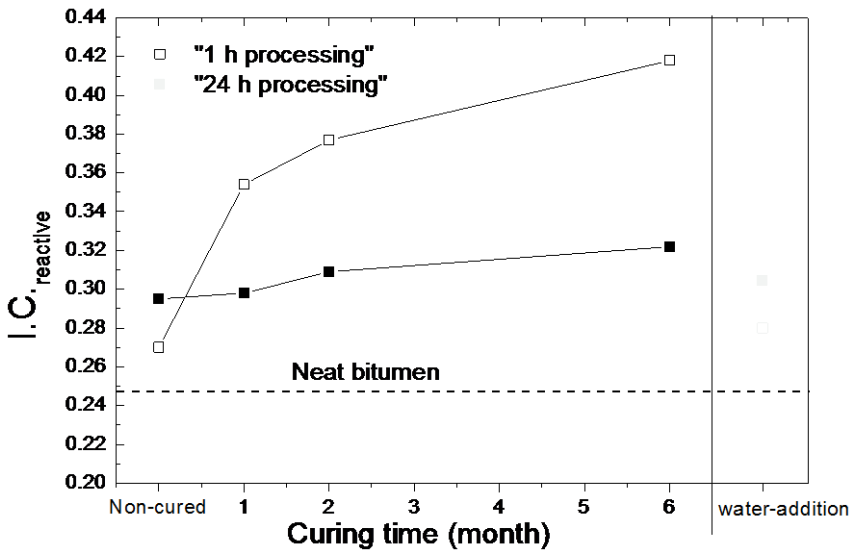


Figure 6.16. Evolution of the “reactive” colloidal index for “water-slow” MDI-CO binders, manufacture following the two procedures, as a function of curing time. Neat bitumen, “non-cured” and “water-fast” MDI-CO binders are also included as references.

According to the above-defined $I.C._{reactive}$, a higher modified colloidal index would mean larger asphaltenes clusters, leading to materials with more significant gel-like behaviours (i.e., higher elasticity) (Carrera et al. 2009 and 2010; Izquierdo et al. 2011 and 2012). As can be observed, longer curing times gives rise to binders with the highest colloidal indexes, being more apparent for modified bitumen processed for 1 h. By contrast, only a slight increase is noticed for the “water-fast” addition process.

Consequently, the evolution of $C.I_{\text{reactive}}$ is in good agreement with the observed rheological behaviour (Figures 6.11 to 6.13).

Finally, the different thermo-rheological and chemical composition observed for MDI-CO binders, as a consequence of its processing procedure, can be supported by AFM pictures. Figure 6.17 displays the micrographs taken at 30 °C for the neat bitumen, “water-slow”, after 6 months of curing, and “water-modified” MDI-CO binders, processed following the above-described two processing procedures.

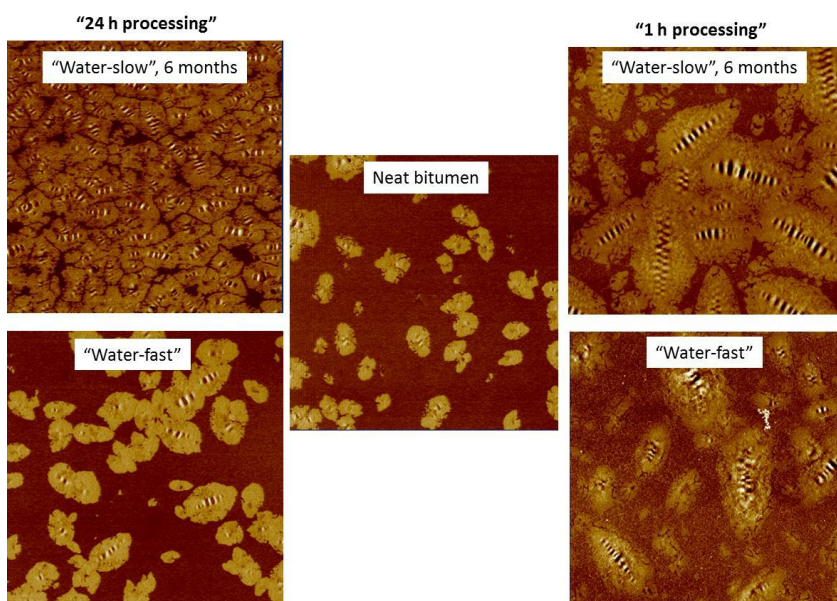


Figure 6.17. AFM micrographs ($20 \times 20 \mu\text{m}^2$), at 30 °C, for the neat bitumen, “water-slow”, after 6 months of curing, and “water-modified” MDI-CO binders, processed following the two processing procedures.

As can be observed, processing/curing conditions carried out strongly affect bitumen microstructure. Thus, the MDI-CO bituminous binders cured after 6 months at room temperature present much larger asphaltenic regions, particularly for those systems processed for 1 h. Therefore, the

high level of interactions among asphaltenic micelles, at 30 °C, in these MDI-CO modified samples would explain the remarkable modification degree attained (see Figure 6.11). Consequently, the previous observed increases in the viscosity, viscoelastic moduli and endothermic peak (appeared around 50 °C in modulated DSC tests) seem to be in accordance with the AFM observations.

6.4.4. Enhancement of MDI-CO modifier

With the aim to explore new modification routes based on MDI-CO prepolymers, the modification of castor oil by transesterification with pentaerythritol was performed. Thus, this subsection studies the effect that the transesterification degree achieved and processing conditions have on the rheological properties and microstructure of the modified bitumen when this isocyanate-based polymer is used as modifying agent. To that end, the isocyanate-based reactive modification of bitumen was performed under different processing procedures and formulations. Binder characteristics were assessed through rheological, microstructural and thermal tests such as: viscous flow tests, viscoelastic characterization, atomic force microscopy (AFM) and thermo-gravimetric (TG) analysis.

6.4.4.1. Materials and modified binders preparation

The new MDI-CO prepolymers were synthesized through two steps:

Step 1: Modification of castor oil by transesterification with pentaerythritol

The transesterification of castor oil (CO) using pentaerythritol was carried out in a 500 mL four-necked flask equipped with a magnetic stirred, thermometer, inert atmosphere and a reflux condenser. The reaction was carried out at 210 °C for 2 h, using lead oxide (PbO) as catalyser (at 0.0005 PbO/CO weight ratio) and different concentrations of pentaerythritol,

between 4 and 12 wt.% (Valero et al., 2008). According to the actual transesterification achieved in each case, modified castor oils were denoted as CO^{n%} (where “n” is the reacted pentaerythritol concentration that will be discussed later).

Step 2: Synthesis of prepolymers from modified castor oil and polymeric MDI

Modified castor oils were functionalized with isocyanate groups, -NCO, by their reaction with polymeric MDI (4,4'-diphenylmethane diisocyanate, having -NCO content of 31 wt.%) in N₂ atmosphere, at 60 °C, for 48 h and under agitation. A constant -NCO/-OH molar ratio of 8:1 was selected for the synthesis of all systems. The resulting prepolymers, with different transesterification degree, n%, are referred to as MDI-CO^{n%}, hereinafter.

Regarding the bituminous binders preparation, modification was carried out by mixing a 70/100 neat bitumen and 2 wt.% MDI-CO^{n%} prepolymers, at 90 °C for 1h, with a four-blade turbine rotating at 1200 rpm, and subsequently settling the blend in an oven at 90 °C for 24h (that is, “24 h processing” procedure). The resulting modified bitumen was subjected to different treatments: (a) a sample was used as such (MDI-CO^{n%} modified bitumen, hereinafter); (b) another one was mixed with 2 wt. % water for 45 min at 90 °C (called as MDI-CO^{n%}/water modified bitumen); (c) a third sample was obtained by the addition of 2 wt.% castor oil transesterified with 4 wt.% of pentaerythritol CO^{4%} (labeled as MDI-CO^{n%}/CO^{4%} modified bitumen); and (d) the sample “c” was subsequently cured in closed vessels for 7 days in an oven at 90 °C (giving the MDI-CO^{n%}/CO^{4%}-90°C modified binders).

In addition, bitumen was also mixed for 2 h at 180 °C with 2 wt.% MDI-CO^{n%} and, after 1 h processing, with 2 wt.% CO^{4%}, leading to the MDI-CO^{n%}/CO^{4%}-180°C modified bitumens.

6.4.4.2. Prepolymer synthesis and characteristics

Figure 6.18 shows the reaction scheme and their products derived from castor oil transesterification, COⁿ%. After the reaction with 8 and 12 wt. % pentaerythritol, a white precipitate due to unreacted pentaerythritol was observed (Valero et al., 2008) and separated by centrifugation. Then, the resulting modified castor oils, COⁿ%, were titrated according to ASTM D1957.

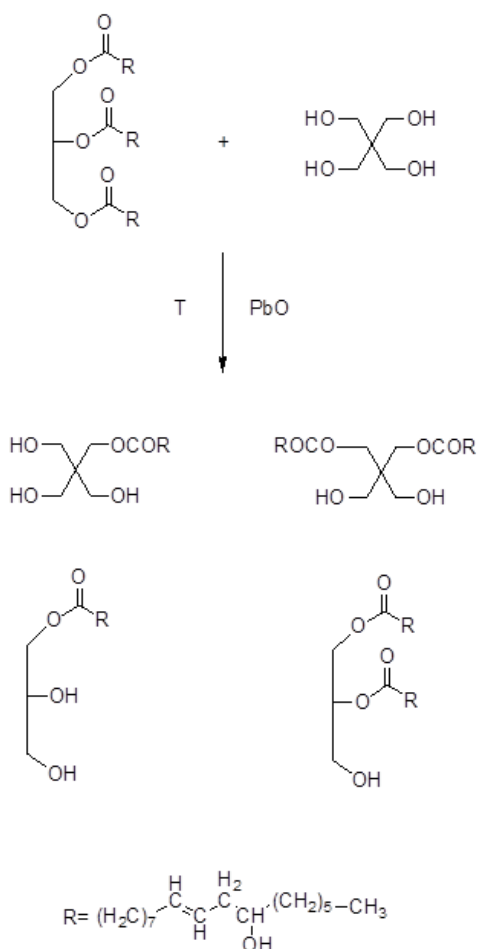


Figure 6.18. Reaction scheme for the transesterification reaction of castor oil with pentaerythritol.

The reacted concentration of pentaerythritol (n%) may be calculated by comparing the hydroxyl values of the different modified castor oils with the theoretical value for pure pentaerythritol (calculated as 1646 mg KOH/g). The hydroxyl values and the reacted concentrations for these systems are gathered in Table 6.7, showing that 8 % is the highest transesterification achieved.

Table 6.7. Hydroxyl values and nomenclature of the unmodified/modified castor oils.

	Added wt.% pentaerythritol	Reacted wt.% pentaerythritol	Hydroxyl value, mg KOH/g ^a	CO ^{n%}
Unmodified castor oil	0	0	125	CO ^{0%}
Modified castor oil 1	4	4	190	CO ^{4%}
Modified castor oil 2	8	7	230	CO ^{7%}
Modified castor oil 3	12	8	246	CO ^{8%}

^aAccording to ASTM D1957

According to such hydroxyl values, prepolymers were synthesized by selecting the same -NCO/-OH molar ratio of 8:1, which was found optimal in the previous subsections. Figure 6.19 illustrates the reaction scheme for the synthesis of MDI-CO^{n%} prepolymers. Thus, similar values of free -NCO groups, according to ASTM D2572, were obtained for the MDI-CO^{n%} polymers as shown in Table 6.8. Therefore, bitumen “chemical” modification will take place with prepolymers having the same concentration of free -NCO groups available for reaction.

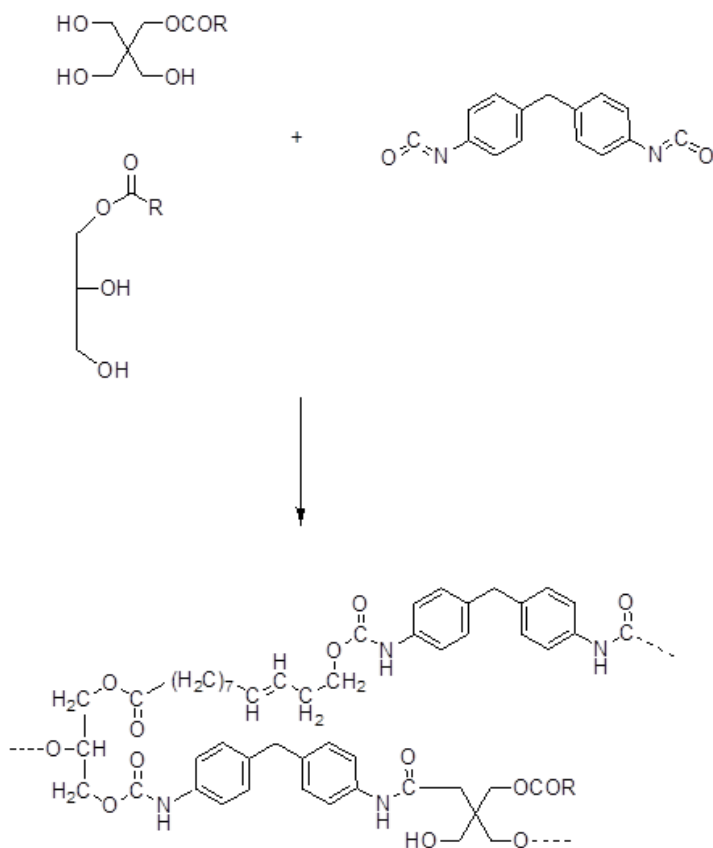


Figure 6.19. Reaction scheme for the synthesis of MDI-CO^{n%} prepolymers.

Table 6.8. Free -NCO content (wt.%) for MDI-CO^{n%} prepolymers.

	-NCO content (wt.%)
Unmodified castor oil	19.4
Modified castor oil 1	21.6
Modified castor oil 2	22.4
Modified castor oil 3	22.5

^aAccording to ASTM D1957

Viscous flow measurements carried out on native and transesterified castor oils, CO^{n%}, and on MDI-CO^{n%} prepolymers showed a Newtonian

behaviour for all samples at 30 °C. As seen in Figure 6.20, castor oil transesterification leads to more viscous polyols, CO^{n%}, as pentaerythritol concentration rises. This increase can be attributed to the presence of new polar groups (i.e. a higher number hydroxyl groups, as seen in Table 6.7), which increase the interactions between molecules (Valero et al., 2008, Mutlu, 2010). Similarly, the resulting prepolymers, MDI-CO^{n%}, are more viscous than the transesterified polyols, CO^{n%}. Furthermore, as a result of the reactions, MDI-CO^{7%} and MDI-CO^{8%} show higher values of viscosity than that observed for MDI-CO^{0%}. However, compared to the latter, a significant viscosity decrease is found for MDI-CO^{4%} (see figure 6.20).

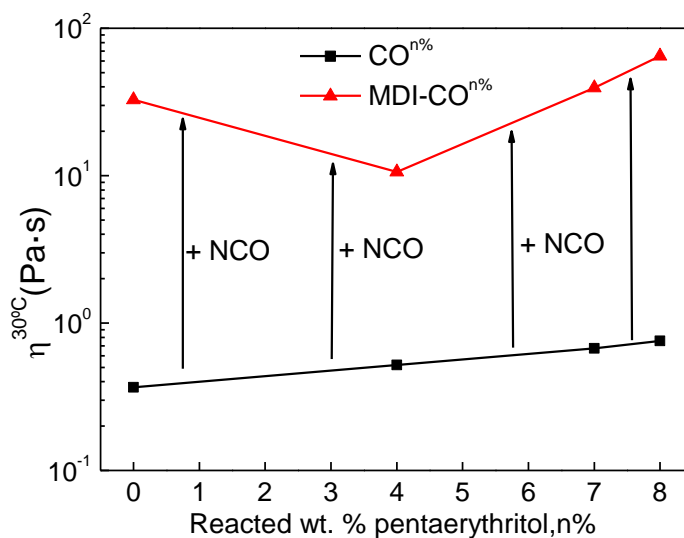


Figure 6.20. Newtonian viscosity, at 30 °C, for native/transesterified castor oils (CO^{n%}) and MDI-CO^{n%} prepolymers.

Thermal stability is key a factor to establish the feasible use of these polymers as bitumen modifiers. To that end, isothermal TG experiments, at 180 °C for 2 h under air atmosphere, were conducted on MDI-CO^{n%} prepolymers and compared to MDI-PEG, a widely studied petroleum-based bitumen modifier derived from petroleum (Martín-Alfonso et al, 2009)

(Figure 6.21). As may be seen, MDI-PEG and polymeric MDI present similar weight loss curves, losing about 50 % weight after 60 min (Figure 6.21). Such a fast degradation rate arises from the poor stability of PEG and from MDI degradation into aromatic nitriles and hydrogen cyanide (Han et al., 1995). Conversely, a higher thermal stability can be observed for vegetable oil-based polymers (MDI-COⁿ%), pointing out the strong influence that this type of polyol provokes on isocyanate-based polymers. As seen in Figure 6.21, no weight loss was observed for unmodified castor oil (CO⁰%) and the same reading were recorder for the different modified castor oil, COⁿ% (results not shown in this figure for sake of clarity).

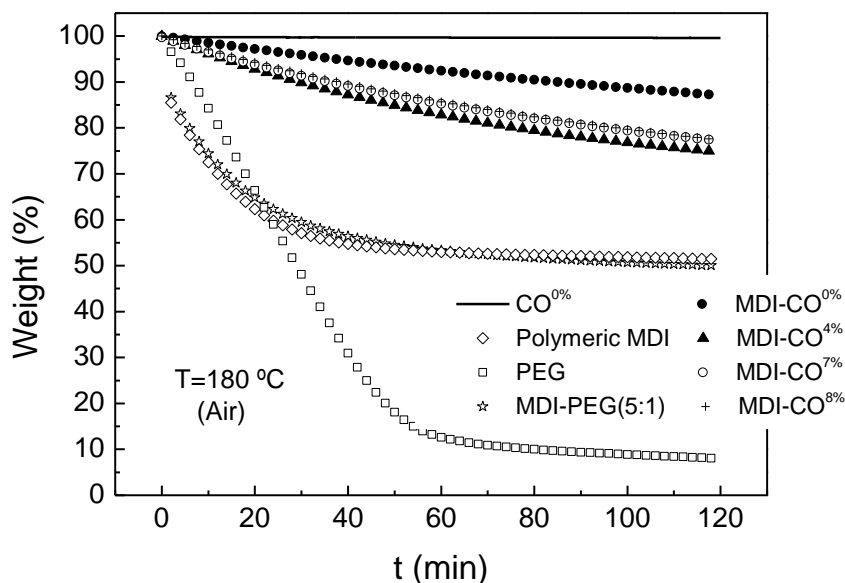


Figure 6.21. Isothermal weight loss at 180 °C for polymeric MDI, polyethylene (PEG), castor oils (COⁿ%), MDI-COⁿ% and MDI-PEG prepolymers.

Modified castor oil with pentaerythritol produces prepolymers with lower thermal stability than those prepared with virgin castor oil, undergoing a weight loss of 10 wt. % for MDI-CO⁰% and 20 wt. % for MDI-CO⁴% (mostly

due to the added excess of polymeric MDI). In any case, MDI-COⁿ% synthesis leads to prepolymers with higher stability than MDI-PEG.

6.4.4.3. Bitumen reactive modification through urethane/urea chemical bonds

Figure 6.22 shows the viscous flow behaviour, at 60 °C, of selected binders modified by 2 wt. % MDI-CO⁸%. As reference systems, the viscosities at 60 °C of the neat bitumen and the 3 wt. % SBS modified bitumen have also been included. It can be observed that neat bitumen shows an almost constant value of viscosity in the entire range of the shear rates studied. Instead, the addition of 2 wt.% MDI-CO⁸% leads to a non Newtonian behaviour, with a constant value of viscosity at low shear rate, η_0 , followed by a shear-thinning region once a “critical” value of shear rate, $\dot{\gamma}_c$, is reached. Interestingly, the addition of 2 wt.% water to the MDI-CO⁸% modified binder (giving the MDI-CO⁸%/water modified bitumen) leads to a much more viscous product than that obtained by adding 3 wt.% SBS.

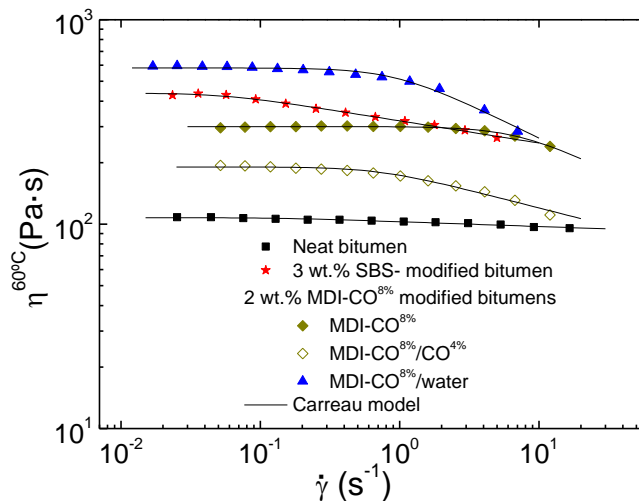


Figure 6.22. Viscous flow curves, at 60 °C, for selected binders modified by 2 wt. % MDI-CO⁸%. Neat and 3 wt.% SBS-modified bitumens are also included.

The results obtained can be explained by means of the isocyanate-bitumen chemistry described in the previous Subsection 6.4.2. (through the Reactions 1 to 3). Thus, during the blending of bitumen and prepolymer, -NCO groups are known to partially react with hydroxyl groups in the asphalts. This provokes an increase in viscosity due to formation of urethane linkages according the Reaction 1.

On the other hand, water addition provokes a higher degree of modification. Water reacts with the remaining isocyanate groups, leading the formation of an amine and carbon dioxide (Reaction 2). Further reactions occur between the highly reactive amine and the isocyanate groups left in the cluster previously formed, with the development of an extended three-dimensional polymer network throughout the bituminous matrix (Reaction 3) (Segura 2005; Martin-Alfonso et al., 2008).

Table 6.9. Carreau’s model parameters for all the modified samples studied.

		η_0 (Pa·s)	λ (s)	s
	Neat bitumen	110	---	---
	3 wt. SBS	438	16.66	0.05
	Cured neat	223	---	---
MDI-CO ^{0%}	MDI-CO	199	0.08	0.38
	MDI-CO/water	541	0.75	0.22
	MDI-CO/CO ^{4%}	156	1.30	0.06
	MDI-CO/CO ^{4%} -90°C	407	1.73	0.11
MDI-CO ^{4%}	MDI-CO	343	0.16	0.44
	MDI-CO/water	697	1.78	0.16
	MDI-CO/CO ^{4%}	313	1.23	0.14
	MDI-CO/CO ^{4%} -90°C	6288	26.70	0.16
MDI-CO ^{7%}	MDI-CO	305	0.19	0.26
	MDI-CO/water	561	1.01	0.17
	MDI-CO/CO ^{4%}	261	2.04	0.09
	MDI-CO/CO ^{4%} -90°C	1294	13.79	0.10
MDI-CO ^{8%}	MDI-CO	300	0.19	0.23
	MDI-CO/water	578	0.71	0.33
	MDI-CO/CO ^{4%}	187	0.50	0.17
	MDI-CO/CO ^{4%} -90°C	465	0.56	0.19

For a quantitative analysis of the different degrees of modification achieved, the Carreau model (Equation 6.1) model was fitted to the viscous flow results and the Carreau's model parameters for the MDI-CO^{n%} modified bitumens are shown in Table 6.9.

Carreau model parameters confirm that addition of 2 wt. % water after reactive modification of bitumen promotes more apparent shear-thinning behaviours (with longer times, λ and lower "s" values), which suggests the development of a binder with higher level of microstructural complexity than the unmodified neat bitumen (Martín-Alfonso et al., 2008).

The modification index, $(M.I.)_A^{60^\circ C}$, defined in equation 6.2, written in terms of the binder zero-shear-limiting viscosity at 60 °C, are shown in the Figure 6.23.

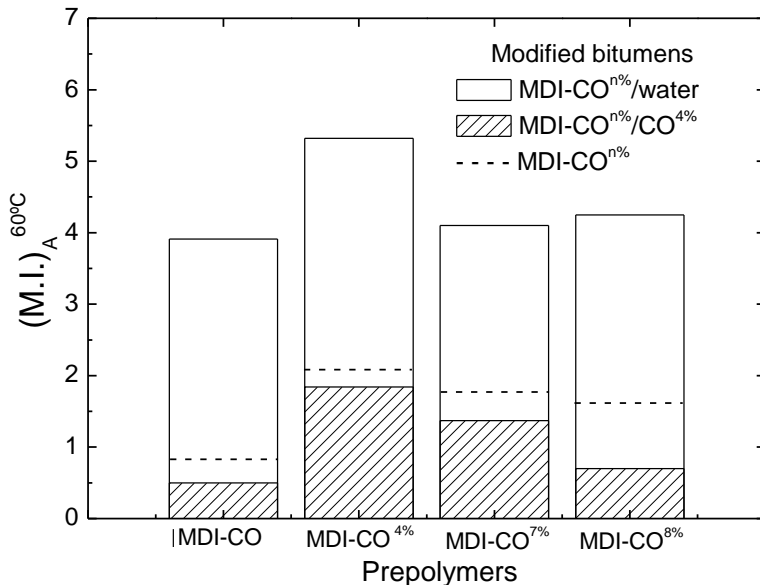


Figure 6.23. Modified index, $(M.I.)_A^{60^\circ C}$, for MDI-CO^{n%} modified bitumens.

Even though viscosity increases after the addition of MDI-CO^{n%} (due to Reaction 1), the subsequent addition of 2 wt. % water leads to the highest

degree of modification. Thus, sample modified by MDI-CO^{4%}/water is 5 times more viscous than the neat bitumen. This fact confirms the relevant role in the bitumen modification of Reactions 2 and 3 (between water and still non-reacted, or free, –NCO groups available in the bituminous matrix), which significantly alters the binder microstructure (Martín-Alfonso, 2008).

6.4.4.4. Urethane-based bitumen modification

With the aim of processing at higher temperatures, avoiding possible bitumen foaming derived from the CO₂ produced in reaction 2 and obtaining a polymer network composed of flexible molecular chains, instead of water, 2 wt.% CO^{4%} was added to consume the remaining -NCO groups still present after the initial addition of 2 wt.% MDI-CO^{n%}. Accordingly, this modification procedure is expected to take place exclusively through the Reaction 1 (i.e. through urethane linkages), giving rise the MDI-CO^{n%}/CO^{4%} modified bitumens. However, as can be observed in Figures 6.22 and 6.23, the addition of 2 wt. % CO^{4%} has a plasticizing effect on non-cured samples. Thus, the MDI-CO^{n%}/CO^{4%} modified binders present lower values of viscosities than those of their original MDI-CO^{n%} modified bitumens (Figure 6.23). Such a result is more pronounced as the reacted concentration of pentaerythritol, n%, rises.

This fact seems to be related to the slow reaction rate at this temperature. In this regard, Figure 6.24A shows the viscous flow curves, at 60 °C, of neat and MDI-CO^{n%}/CO^{4%} modified bitumens after being stored at 90 °C for 7 days (the so-called high temperature curing, which leads to the MDI-CO^{n%}/CO^{4%}-90°C modified binders). As expected, this curing process causes an increase in the neat bitumen viscosity (giving rise to the “cured-neat”), which results from the oxidation of the maltene fraction (Navarro et al, 2009). Both samples, neat and cured-neat bitumens, present a

Newtonian behaviour. Nevertheless, MDI-CO^{n%}/CO^{4%}-90°C modified samples show a constant viscosity at low shear rates followed by a shear-thinning region. Again, this non-Newtonian behaviour can be described by the Carreau's model (Equation 6.1) fairly well, and their fitting parameters are displayed in Table 6.9. As may be seen, the MDI-CO^{4%}/CO^{4%}-90°C modified sample yields a very significant increase in viscosity, almost two orders of magnitude higher than that measured for the cured neat (Figure 6.24A).

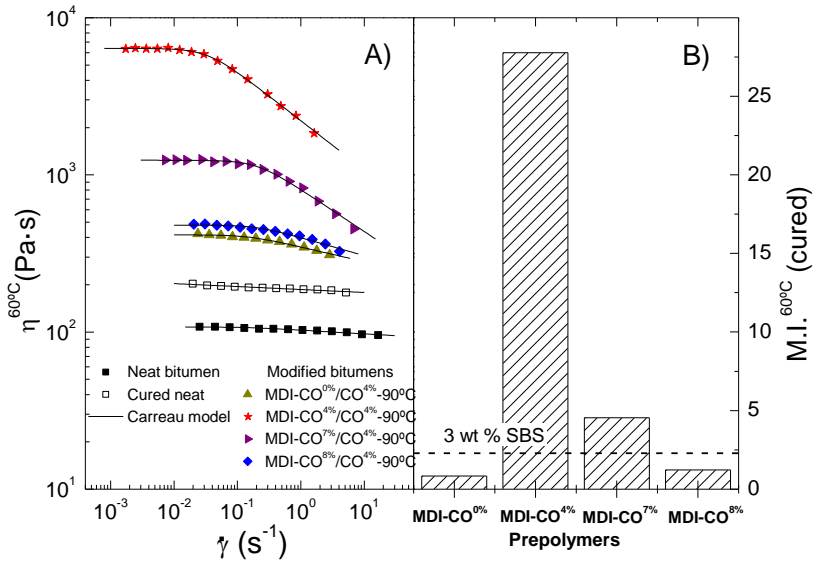


Figure 6.24. (A) Viscous flow curves, at 60 °C, and (B) “adapted” modification indexes, M.I.^{60°C}(cured), for MDI-CO^{n%}/CO^{4%}-90 modified bitumens. Neat, “cured neat” and 3 wt.% SBS-modified bitumens are also included.

Likewise, the neat viscosity change undergone by modified samples, mainly due to Reaction 1, can be quantified by means of an “adapted” modification index, M.I.^{60°C}(cured), written as:

$$\text{M.I.}^{60^\circ\text{C}}(\text{cured}) = \frac{\eta_{0,\text{mod}} - \eta_{0,\text{cured neat}}}{\eta_{0,\text{cured neat}}} \quad (6.5)$$

where $\eta_{0,\text{mod}}$ and $\eta_{0,\text{cured neat}}$ refer to the modified and cured-neat bitumen viscosities, respectively. Figure 6.24B shows the values of M.I.^{60°C}(cured) for the different samples studied. The binder modified by MDI-CO^{4%} presents, by far, the highest degree of modification after curing at high temperature for 7 days. Likewise, the MDI-CO^{7%}/CO^{4%}-90°C modified bitumen exhibits a lower value of modification after curing, but higher than that obtained for the 3 wt.% SBS modified bitumen.

In addition to viscous flow curves, temperature sweep tests in oscillatory shear (10 rad/s and 1 °C/min heating rate), from 30 to 100 °C, have also been carried out on 90°C-cured samples. Figure 6.25A shows the evolution with temperature of the loss tangent ($\tan \delta = G''/G'$), making clear the prevailing viscous behaviour of the samples, $\tan \delta > 1$, over the entire temperature interval tested.

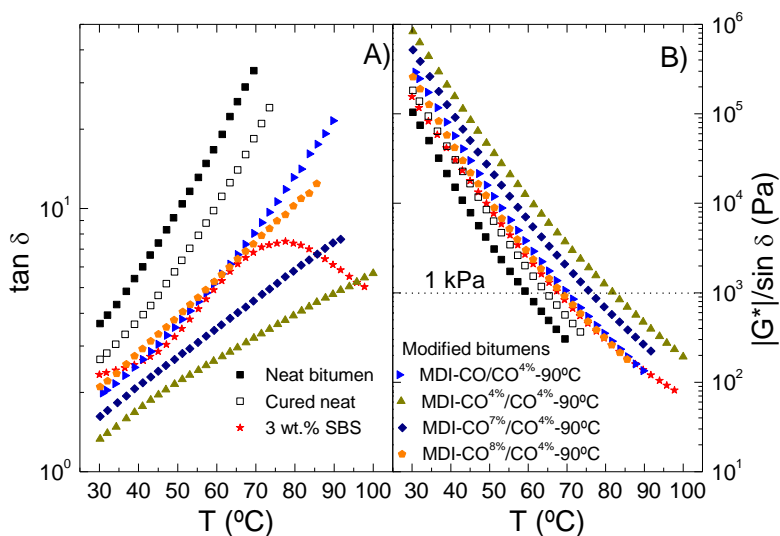


Figure 6.25. (A) Evolution with the temperature of loss tangent, $\tan \delta$, and (B) temperature dependence of the “rutting parameter”, $|G^*|/\sin \delta$, for MDI-CO^{n%}/CO^{4%}-90°C modified bitumens. Neat, “cured neat” and 3 wt.% SBS-modified bitumens are also included.

The high temperature curing process produces a decrease in $\tan \delta$ values (enhancing binder elastic properties), which is more significant for the binder modified with MDI-CO^{4%}/CO^{4%}. In addition, these bituminous binders show a notable decrease in the average slope of $\tan \delta$ curves between 30 and 70 °C, which would result in lower thermal susceptibility in this temperature range. As a consequence, the observed increase in elasticity (and the lower thermal susceptibility) is expected to reduce the progressive accumulation of permanent deformation (the so-called “rutting”) produced by traffic at high in-service temperatures (Carrera et al., 2010).

Table 6.10. SHRP maximum temperatures for MDI-CO^{n%}/CO^{4%}-90°C binders.

	T _{G* /sen $\delta=1$ kPa} (°C)
Neat bitumen	59.4
3 wt. SBS	67.8
Cured neat	64.9
MDI-CO ^{0%} /CO ^{4%} -90°C	70.0
MDI-CO ^{4%} /CO ^{4%} -90°C	82.3
MDI-CO ^{7%} /CO ^{4%} -90°C	76.5
MDI-CO ^{8%} /CO ^{4%} -90°C	68.7

As shown in Table 6.10, SHRP maximum temperature and so, rutting resistance, is notably increased after curing process. If compared to the cured neat bitumen, an increase of nearly 18 °C is observed for MDI-CO^{4%}/CO^{4%}-90°C modified sample after curing, which is clearly higher than the value reached after SBS modification.

The previous enhancements in viscous and viscoelastic behaviours, after the curing process, hint significant changes in binder microstructure (Figure 6.26). AFM micrographs were taken at 30 °C from neat bitumen (Figure 6.26A), MDI-CO^{4%}/water modified binder (Figure 6.26B) and a MDI-CO^{4%}/CO^{4%}-90°C modified bitumen (Figure 6.26C). Neat bitumen, at 30 °C, clearly presents the so-called “bee-like” dispersion. By comparison,

MDI-CO^{4%} modified samples (particularly, the sample modified by MDI-CO^{4%}/CO^{4%}-90°C) are composed of larger “bee” structures or asphaltene domains. Such structures result from the association of round asphaltene particles (with a diameter of about 100-200 nm) which are surrounded by maltene fractions (Loeber et al. 1996; Loeber et al., 1998). Therefore, the previously observed increases in the viscosity and viscoelastic moduli might be attributed to the development of a more compact microstructure originated by the formation of covalent bonds between the MDI-CO prepolymer and certain bitumen groups, as a consequence of the reaction described above (Reactions 1 to 3) (Carrera et al., 2010).

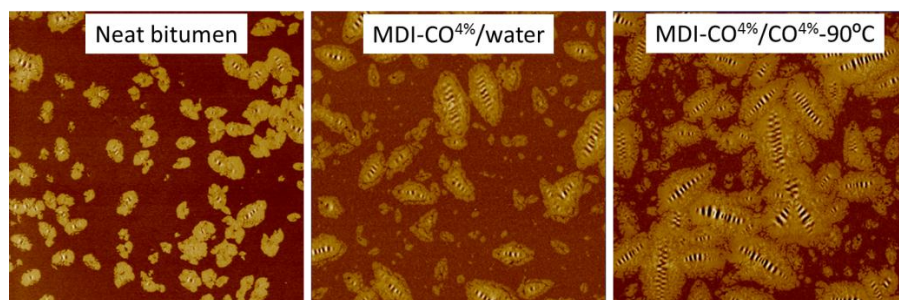


Figure 6.26. AFM micrographs ($30 \times 30 \mu\text{m}^2$), at $30 \text{ }^\circ\text{C}$, for neat bitumen, MDI-CO^{4%}/water and MDI-CO^{4%}/CO^{4%}-90°C.

In summary, the modification of bitumen by MDI-CO^{4%} seems to yield the most remarkable improvement in bitumen behaviour at high in-service temperatures, since it increases binder viscosity (at $60 \text{ }^\circ\text{C}$) and enhances both its elastic properties and thermal resistance. This result is particularly evident for the bitumen modified by MDI-CO^{4%}/CO^{4%}-90°C. Even though, MDI-CO^{4%} has similar concentration of free –NCO groups to the other transesterified prepolymers (Table 6.8) and, therefore, it should exhibit similar reactivity with bitumen compounds (and modification degree). The improved modification ability shown by MDI-CO^{4%} seems to be related to its lower viscosity (Figure 6.20), which would favour the transport of the

polymer chains, and therefore, the reactions during the curing process. Consequently, a higher bitumen modification is expected for MDI-CO^{4%} cured samples at 90 °C.

Aiming to confirm such assumptions, bitumen modification was carried out with MDI-CO^{4%} and MDI-CO^{7%} at a higher mixing temperature of 180 °C for 2 h processing (with the addition of 2 wt.% CO^{4%} after the first hour of processing), obtaining the MDI-CO^{n%}/CO^{4%}-180°C modified bitumens. It is worth noting this is the typical processing temperature used in the asphalt industry for the SBS/bitumen blending and these MDI-CO based prepolymers were found stable enough under such conditions (Figure 6.21).

As expected, Figure 6.27 shows both prepolymers lead to the same modification degree when processed at 180 °C (i.e. when their viscosities become similar, in addition to their free-NCO content). What is more, these processing conditions lead to similar viscosities obtained by MD-CO^{n%}/water modifier at 90 °C, but significantly lower than those obtained after curing for 7 days at 90 °C. This result would suggest that, in addition to Reaction 1, other water-involved reactions (i.e. Reaction 2 and 3 due to the air moisture diffusion during curing) would further increase binder viscosity.

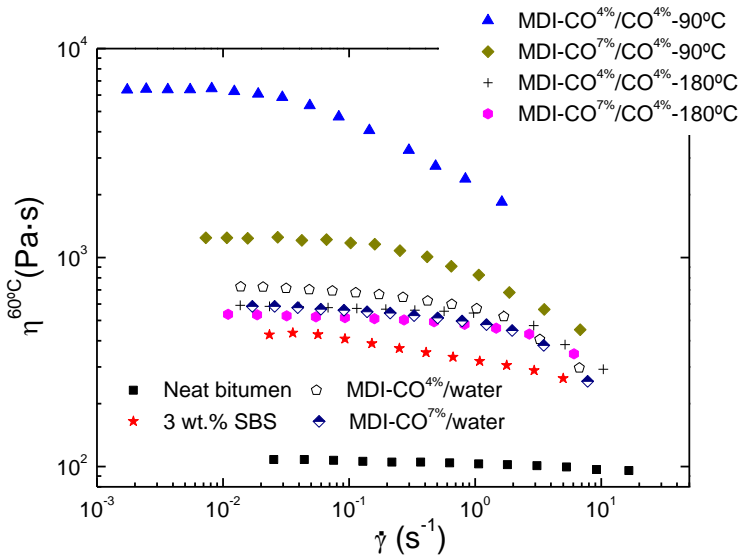


Figure 6.27. Viscous flow curves, at 60 °C, for selected MDI-CO^{n%} modified binders. Neat and 3 wt.% SBS-binder are also included as references.

6.5. REFERENCES

American Society for Testing and Materials. Standard test method for hydroxyl value of fatty oils and acids. ASTM D1957.

EN 1426:2007: Bitumen and bituminous binders. Determination of needle penetration.

EN 1427:2007: Bitumen and bituminous binders. Determination of the softening point. Ring and ball method.

American Association of State Highway and Transportation Officials, Standard specification for performance graded binder, AASHTO Designation MP1, Gaithersburg, 1993.

Carrera V, Partal P, García-Morales M, Gallegos C, Pérez-Lepe A. Effect of processing on the rheological properties of poly-urethane/urea bituminous products. *Fuel Process. Technol.*, 2010, 91, 1139-1145.

Corcuera MA, Rueda L, Saralegui A, Martín MD, Fernández-d'Arlas B, Mondragon I, Eceiza A. Effect of diisocyanate structure on the properties and microstructure of polyurethanes based on polyols derived from renewable resources. *J. Appl. Polym. Sci.*, 2011, 122, 3677-3685.

Corcuera MA, Rueda L, Fernández-d'Arlas B, Arbelaiz A, Marieta C, Mondragon I, Eceiza A. Microstructure and properties of polyurethanes derived from castor oil. *Polym. Degrad. Stabil.*, 2010, 95, 2175-2184.

Lesueur D, Gerard JF, Claudy P, Letoffe JF, Planche JP, Martin D. A structure-related model to describe asphalt linear viscoelasticity. *J. Rheol.*, 1996, 40, 813-836.

Lesueur, D. The colloidal structure of bitumen: Consequences on the rheology and on the mechanisms of bitumen modification. *Adv. Colloid. Interfac.*, 2009, 145,42-82.

Hablott E, Zheng D, Bouquey M, Avérous L. Polyurethanes based on castor oil: kinetics, chemical, mechanical and thermal properties. *Macromol. Mater. Eng.*, 2008, 293, 922-929.

Martín-Alfonso MJ, Partal P, Navarro Navarro FJ, García-Morales M, Gallegos C. Use of a MDI-functionalized reactive polymer for the manufacture of modified bitumen with enhanced properties for roofing applications. *Eur. Polym. J.*, 2008, 44, 1451-1461.

Karak N, Sravendra R, Jae Whan C. Synthesis and characterization of castor-oil-modified hyperbranched polyurethanes. *J. Appl. Polym. Sci.*, 2009, 112(2), 736-743.

Perez-Lepe A, Martinez-Boza FJ, Attané P, Gallegos C. Destabilization mechanism of polyethylene-modified bitumen. *J. Apply. Polym. Sci.*, 2006, 100, 260-267.

Masson FJ, Polomark GM. Bitumen microstructure by modulated diferencial scanning calorimetry. *Thermochim. Acta*, 2001, 374, 105-114.

Masson FJ, Leblond V, Margeson J. Bitumen morphologies by phase-detection atomic force microscopy. *J. Microsc.*, 2006, 221, 17-29.

Masson JF, Polomark GM, Collins P. Time-dependent microstructure of bitumen and its fractions by modulated Differential Scanning Calorimetry. *Energ. Fuel*, **2002**, 16, 470.

Mutlu H, Meier MAR. Castor oil a renewable resource for the chemical industry. *Eur. J. Lipid Sci. Technol.*, 2010, 112, 10-30.

Segura DM, Nurse AD, McCourt A, Phelps R, Segura A. Chemistry of polyurethane adhesives and sealants, in: P. Cognard (Ed.), Handbook of adhesives and sealants, Elsevier Ltd., Oxford, 2005, 101-162.

Ross-Murphy, SB. Structure-property relationships in food biopolymer gels and solutions. *J. Rheol.*, 1995, 39(6), 1451-1463.

Martín-Alfonso MJ, Partal P, Navarro FJ, García-Morales M, Gallegos C. Use of a MDI-functionalized reactive polymer for the manufacture of modified bitumen with enhanced properties for roofing applications. *Eur. Polym. J.*, 2008, 44, 1451-1461.

Martín-Alfonso MJ, Partal P, Navarro FJ, García-Morales M, Gallegos C. Use of a MDI-functionalized reactive polymer for the manufacture of modified bitumen with enhanced properties for roofing applications. *Eur. Polym. J.* 2008, 44, 1451-1461.

Swamy BKK, Siddaramaiah, Somashekar R. Structure-property relationship of castor oil based diol chain extended polyurethanes (PUs). *J. Mater. Sci.*, 2003, 38, 451-460.

Singh B, Tarannum H, Gupta M. Use of isocyanate production waste in the preparation of improved waterproofing bitumen. *J. Appl. Polym. Sci.*, 2003, 90(5), 1365-1377.

Xu Y, Petrovic Z, Das S, Wilkes LG. Morphology and properties of the thermoplastic polyurethanes with dangling chains in ricinoleate-based soft segments. *Polymer*, 49, 2008, 4248-4258.

Loeber L, Sutton O, Morel J, Valleton JM, Muller G. New direct observations of asphalts and asphalt binders by scanning electron microscopy and atomic force microscopy. *J. Microsc.*, 1996, 182, 32-39.

Loeber L, Muller G, Morel J, Sutton O. Bitumen in colloid science: a chemical, structural and rheological approach. *Fuel*, 1998, 73(13), 1443-1450.

Han S, Kim C, Kwon D. Thermal degradation of poly(ethyleneglycol). *Polym. Degrad. Stab.*, 1995, 47, 203-208.

Carrera V, Partal P, García-Morales M, Gallegos C, Páez A. Influence of bitumen colloidal nature on the design of isocyanate-based bituminous products with enhanced rheological properties. *Ind. Eng. Chem. Res.*, 2009, 48, 8464-8470.

Izquierdo MA, Navarro FJ, Martínez-Boza FJ, Gallegos C. Bituminous polyurethane foams for building applications: Influence of bitumen hardness. *Constr. Build. Mater.*, 2012, 30, 706-713.

Izquierdo MA, Navarro FJ, Martínez-Boza FJ, Gallegos C. Novel stable MDI isocyanate-based bituminous foams. *Fuel*, 2011, 90, 681-688.

Fuentes-Audén C, Sandoval JA, Jerez A, Navarro FJ, Martínez-Boza FJ, Partal P, Gallegos C. Evaluation of thermal and mechanical properties of recycled polyethylene modified bitumen. *Polym. Test.*, 2008, 27, 1005-1012.

Valero MF, Pulido JE, Ramírez A. Polyurethanes synthesized of polyols obtained from castor oil modified by transesterification with pentaerythritol. *Quim. Nova*, 2008, 31, 2076-2082.

Navarro FJ, Partal P, García-Morales M, Martín-Alfonso MJ, Martínez-Boza F, Gallegos C, Bordado JCM, Diogo AC. Bitumen modification with reactive and non-reactive (virgin and recycled) polymers: A comparative analysis. *J. Ind. Eng. Chem.*, 2009, 15, 458-464.

Ecker A. The application of Iatroscan-technique for analysis of bitumen. *Petrol. Coal*, 2001, 43, 51-53.

CONCLUSIONS

Chapter VII

*Physico-chemical modificacion of asphalt
bitumens by reactive agents*

7.1. CONCLUSIONS

This manuscript has described the results found during the development of bituminous binders by new modification routes. The use of three novel reactive agents have been assessed: two non-polymeric additives (thiourea dioxide and thiourea) and a castor oil functionalized with isocyanate groups prepolymer.

From this work, the following conclusions have been highlighted:

- 1) The results obtained seem to support the use of thiourea dioxide (“ThD”) and thiourea (“Th”) as promising reactive modifiers in the manufacture of bituminous binders with enhanced thermo-rheological properties in a wide range of temperatures.
- 2) Non-polymeric derivatives from ThD and Th, containing N-H bonds, have succeeded forming adducts, which contribute to enhance the colloidal structure of bitumen by means of hydrogen-bond network. These adducts (derived from the interaction of urea or ammonium thiocyanate with asphaltenes) seem to be responsible for the rheological enhancement, and their contribution becomes more important as curing time increases.
- 3) This research proposes the use of master curves, obtained by application of the TTSP to isothermal frequency sweeps at different temperatures, and further frequency-temperature conversion, in order to attain a suitable viscoelastic characterisation of bituminous binders at low temperatures.
- 4) Castor oil appears to be a promising alternative to the use of petroleum-based polyols in the manufacture of polyurethane prepolymers for bitumen modification.

- 5) The bitumen modification route experienced by the MDI/castor oil binder is a complex process involving reactions between isocyanate groups/bitumen/water, controlled by two defined pathways:
- a) “Short-term” modification, during binder manufacture at processing temperature.
 - b) “Long-term” modification, during binder exposure to ambient conditions.
- 6) The degree of modification achieved by the MDI/castor oil binders is influenced by two key factors:
- a) Prepolymer formulation: ratio of isocyanate to hydroxyl groups (i.e.-NCO/-OH molar ratio).
 - b) Processing/curing conditions, that is, the influence that different procedures exert on modified samples (long or short processing conditions, curing processing at room temperature, final addition of water, etc.).
- 7) Previous procedures (processing/curing conditions) led to MDI/castor oil binders with a rheological response largely improved in the high in-service temperature window.

**RESUMEN Y
CONCLUSIONES EN
ESPAÑOL**

Chapter VIII

*Physico-chemical modificacion of asphalt
bitumens by reactive agents*

8.1. VISIÓN GENERAL

El betún es un subproducto procedente de los procesos de destilación del crudo del petróleo, obtenido a partir de la eliminación de la mayor parte de los componentes volátiles del mismo. Este material ha sido ampliamente usado en numerosas aplicaciones ingenieriles, que van desde su uso en la industria de la pavimentación hasta membranas impermeables para la cubierta de techos.

Debido a sus propiedades (impermeabilidad, elasticidad, ductilidad, adhesividad, etc.), el betún es el material más adecuado para ser usado como aglutinante de los áridos que conforman el pavimento de las carreteras. Aunque sólo representa aproximadamente el 5 % en peso de la mezcla asfáltica final, el betún es el único componente deformable, y constituye la fase continua de esa mezcla. En consecuencia, al ser el responsable del comportamiento viscoelástico de la mezcla asfáltica, el betún juega un papel clave a la hora de predecir el comportamiento final del asfalto. Por ello, uno de los objetivos mayores de la industria de la pavimentación consiste en mejorar las propiedades reológicas y mecánicas del betún y, de esta forma, mejorar la durabilidad del producto final.

Es conocido que, después de un limitado tiempo de vida, la acción combinada de las temperaturas extremas, junto con un aumento continuo de las cargas generadas por el tráfico y la densidad del mismo pueden producir diferentes defectos en el pavimento. Los fallos más importantes a considerar son las deformaciones permanentes (a altas temperaturas de servicio), la fractura térmica o “cracking” térmico (a bajas temperaturas), el daño por la humedad o la formación de grietas debido a la fatiga del material (Newman, 1998; Yousefi, 2003).

En este sentido, tres requisitos han de cumplirse en las mezclas bituminosas:

- Deben ser lo suficientemente fluidas, a altas temperaturas (160 °C), como para ser bombeadas en las distintas operaciones requeridas para el recubrimiento de los áridos.
- A altas temperaturas, deben tener la suficiente dureza como para evitar el fenómeno de “rutting” (bandas de rodaduras).
- Finalmente, este material debe mantener su flexibilidad a baja temperatura (en torno a -20 °C, dependiendo del clima local) con objeto de evitar el “cracking” térmico.

Todos estos requerimientos a conseguir por los betunes modificados son bastantes opuestos en su finalidad y, en consecuencia, numerosos esfuerzos están destinados a conseguir materiales válidos en todos los climas posibles. Por ello, la industria de la pavimentación ha mejorado las propiedades mecánicas del betún mediante la adición de distintos polímeros (Singh y col., 2003; Akmal y col., 1999; Bellio y col., 1995; Navarro y col., 2002).

En general, los polímeros más comúnmente usados pueden ser clasificados en: (1) sistemas “dispersos” o (2) “reactivos”. Los sistemas betún-polímero “dispersos” son obtenidos mediante la adición de polímeros de tipo SBS, SBR, EVA, SEBS, PE, etc., y creando interacciones físicas entre el polímero y el betún. Sin embargo, a altas temperaturas de almacenamiento (160-220 °C) estos sistemas son termodinámicamente inestables, pudiendo separarse en dos fases. En oposición a los anteriores, los sistemas “reactivos” son capaces de crear uniones polímero-betún mediante reacciones químicas, evitándose la separación de fases.

Hoy en día, la industria de la pavimentación está desarrollando nuevas rutas de modificación mediante agentes reactivos. Estos aditivos interactúan químicamente con ciertos componentes del betún, resolviendo el problema de almacenamiento a alta temperatura. Con objeto de obtener nuevos ligantes bituminosos con propiedades reológicas mejoradas, en un amplio intervalo de temperaturas de servicio, se proponen el uso de nuevos agentes reactivos para la industria de la pavimentación: dos aditivos no-poliméricos (tiourea y dióxido de tiourea, abreviados como “ThD” y “Th”) y un aceite de ricino funcionalizado con grupos isocianatos.

De los resultados obtenidos, se puede concluir que estos dos aditivos pueden considerarse como agentes modificadores del betún, extendiendo el rango de temperatura en el cual el betún se comporta de forma satisfactoria. Así mismo, la modificación propuesta tras la adición de tiourea y dióxido de tiourea (sustancias ampliamente usadas en otras aplicaciones industriales) representan una alternativa a otros reactivos usados en la modificación de betunes, como el PPA (ácido polifosfórico). Así pues, las propiedades anticorrosivas de los modificantes aquí propuestos evitarían la corrosión en los tanques de almacenamiento.

Por otro lado, el uso de poliuretanos como agentes modificadores para la obtención de mezclas bituminosas han sido ampliamente estudiados en la industria de la pavimentación (Martín-Alfonso y col., 2008; Carrera y col.,2010; Izquierdo y col., 2011; Singh y col., 2003). Estos agentes son el producto de la reacción entre los grupos isocianatos e hidroxilos, a temperatura ambiente y sin catalizador. En este trabajo, un polioli de origen natural (aceite de ricino) funcionalizado con MDI (4,4', difenilmetano diisocianato) polimérico puede ser considerado un prepolímero alternativo a aquellos obtenidos de polioles derivados del petróleo (PPG ó PEG).

8.2. PLANTEAMIENTO DE LA PROBLEMÁTICA

Hoy en día, el 95 % del betún que se produce anualmente en todo el mundo se utiliza como ligante en la industria de la pavimentación (Lesueur, 2009). Existen muchos factores que influyen en el rendimiento de las carreteras: la naturaleza de los áridos, la interacción entre el betún y los agregados, la permeabilidad de la mezcla, el clima, etc...

Existen dos problemas principales asociados a las cargas en los pavimentos: i) Fractura (grietas por fatiga o térmicas) y ii) la deformación permanente.

El fenómeno de fractura se asocia a la tensión inducida en las capas asfálticas por las cargas de los vehículos, a los esfuerzos de tensión debido a las contracciones térmicas, o a una combinación de ambos. El agrietamiento se produce cuando la tensión de tracción y la tensión inducida por el tráfico y/o los cambios de temperatura exceden la resistencia a la rotura de la mezcla (Brown y Brunton, 1986).

Por su parte, la deformación permanente o la fatiga, a altas temperaturas de servicio, consiste en la formación de depresiones longitudinales (o surcos) en la trayectoria de las ruedas de los vehículos. Esto puede ocurrir con el tráfico en movimiento como estacionado y, en particular, bajo la elevada cizalla que se produce al frenar, acelerar o en los giros (Whiteoak y Read, 2003). Las principales causas que inducen las deformaciones permanentes en los asfaltos son: la mala calidad de los materiales, un diseño defectuoso de la mezcla, la mala construcción y/o la selección incorrecta del tipo de asfalto más apropiado para esa zona.

8.3. OBJETIVOS DE LA INVESTIGACIÓN

El objetivo principal de este trabajo, realizado a través de la concesión de una beca de investigación del programa de “Formación del Profesorado Universitario” (Código de Ref.: AP2008-01419) y también financiado por el proyecto de investigación (Código de Ref.: TEP6689)”de la “Junta de Andalucía”, es la obtención de ligantes bituminosos con mejores propiedades reológicas mediante nuevas rutas de modificación que incluyan agentes reactivos. Esto permitirá la obtención de materiales estables en condiciones de almacenamiento a altas temperaturas (operación requerida en numerosas aplicaciones de la industria de la pavimentación). Con objeto de alcanzar con éxito este objetivo, a) dióxido de tiourea, b) tiourea y c) un prepolímero basado en isocianatos y formulado con un poliol de origen vegetal (aceite de ricino) son propuestos como agentes modificadores.

Los principales objetivos se pueden resumir en:

1. Encontrar nuevas rutas de modificación del betún mediante agentes reactivos que mejoren las propiedades ingenieriles de las mezclas bituminosas.
2. Entender cómo se produce la modificación mediante la adición de aditivos no-poliméricos (dióxido de tiourea y tiourea).
3. Desarrollar prepolímeros basados en isocianatos obtenidos mediante polioles vegetales, como un procedimiento de modificación más sostenible y respetuoso con el medioambiente.
4. Estudiar los efectos que la formulación del prepolímero y las condiciones de procesado provocan sobre las propiedades reológicas del producto final.

8.4. MATERIALES DE PARTIDA

8.4.1. Betún

Tres betunes, con distinta dureza y composición química, fueron usado como material base en la modificación:

- Betún 40/50
- Betún 100/150
- Betún 150/200

Los valores de penetración y temperatura de anillo-bola, así como la fracción SARAs, de cada uno de ellos están recogidos en la Tabla 3.1.

8.4.2. Agentes modificadores

Diferentes tipos de agentes modificadores del betún, que varían desde los catalogados como “activos” y “pasivos”, fueron estudiados en el presente trabajo de investigación. Respecto a la primera categoría, dos no-poliméricos aditivos (dióxido de tiourea y tiourea) y un prepolímero basado en isocianatos han sido considerados:

- A. Por un lado, dióxido de tiourea y tiourea (abreviados como “ThD” y “Th”, respectivamente) son dos aditivos ampliamente utilizados como agentes reductores en muchas aplicaciones industriales. Sus estructuras, temperaturas de fusión y pesos moleculares se muestran en la Figura 3.1 y la Tabla 3.2.
- B. Por otro lado, un prepolímero basado en isocianatos fue preparado mediante la reacción de grupos isocianatos e hidroxilos. Con este prepolímero se espera que se lleven a cabo reacciones químicas entre los grupos $-NCO$ del prepolímero y

ciertas fracciones del betún. Para la síntesis de estos prepolímeros se usaron:

Diisocianato de metilendifenilo polimérico

Se ha utilizado un diisocianato de metilendifenilo polimérico (pol-MDI), proporcionado por la empresa T.H. Tecnic, S.L. (Sevilla), con un contenido en grupos isocianatos del 31.1 % en peso. Los grupos isocianatos reaccionan con una infinidad de compuestos, entre ellos incluimos las fracciones más polares del betún, las cuales poseen hidrógenos activos (-OH, -NH) (Ver figura 3.2).

Poliol (aceite de ricino)

Los polioles son cadenas hidrocarbonadas con grupos -OH terminales, capaces de reaccionar con los grupos isocianatos para formar polímeros de poliuretano. En esta investigación se ha utilizado un poliol de origen vegetal, aceite de ricino (abreviado como "CO"; ver Figura 3.3), en la formulación de dichos prepolímeros.

Con objeto de aumentar el número de grupos -OH reactivos, se llevó a cabo una transesterificación del aceite de ricino mediante pentaeritritol (ver Figura 3.4). Este proceso fue descrito en el capítulo VI.

Junto al aceite de ricino, polietilenglicol (PEG) (ver Figura 3.5), otro poliol derivado del petróleo y ampliamente utilizado en la formulación de prepolímeros basados en isocianatos, ha sido considerado en esta investigación. Así pues, estos dos polioles permitieron comparar la estabilidad térmica de los distintos prepolímeros, MDI-CO y MDI-PEG, formulados con ellos.

8.5. ESTRUCTURA DE LA TESIS

Este trabajo de investigación se estructura en los nueve siguientes capítulos:

CAPÍTULO I: incluye una breve introducción y una visión general del betún, presentándose los objetivos y el alcance de esta investigación.

CAPÍTULO II: se detallan los conceptos generales acerca de los ligantes bituminosos y se proporciona información sobre los polímeros utilizados para la modificación del betún, con especial énfasis en la descripción de los distintos agentes modificadores estudiados y su interacción con el betún. Además se incluyen conceptos básicos de reología, que pueden facilitar la comprensión de los resultados obtenidos.

CAPÍTULO III: describe las diferentes materias primas utilizadas, los procedimientos seguidos en la preparación de las mezclas bituminosas y los métodos de ensayo para obtener sus propiedades físico-químicas, termo-mecánica y la caracterización reológica.

CAPÍTULO IV: evalúa los efectos que tiene la adición de dióxido de tiourea y tiourea en las propiedades termo-reológicas, en un amplio rango de temperaturas, de dos betunes base con distintos valores de penetración. También se describen las distintas rutas de modificación obtenidas al cambiar la temperatura de procesado.

CAPÍTULO V: estudia la mejora en las propiedades viscoelásticas lineales de ligantes bituminosos mediante la adición de tiourea, explorando los procesos de modificación que dicha modificación produce. Además, se enfatiza en el uso de barridos de frecuencia a distintas temperaturas, y su posterior conversión frecuencia-temperatura, a la hora de caracterizar el comportamiento a baja temperatura.

CAPÍTULO VI: propone el uso de prepolímeros basados en isocianatos y un polioli vegetal (aceite de ricino), como alternativa a aquellos que se formulan con polioles derivados del petróleo, como agente modificador en la manufactura de nuevos ligantes bituminosos con mejores propiedades reológicas. Además, el efecto que produce cambios en la formulación del prepolímero y condiciones de procesado betún-polímero sobre dichas propiedades fueron evaluadas.

CAPÍTULO VII: resume las conclusiones más relevantes derivadas de esta investigación.

CAPÍTULO VIII: contiene un resumen y las conclusiones de la memoria en español.

CAPÍTULO IX: incluye un recopilatorio de las publicaciones y varios documentos surgidos como resultado de la investigación.

8.6. RESULTADOS MÁS RELEVANTES

En este apartado se reúnen los datos más relevantes de los capítulos de resultados y discusión.

8.6.1. Capítulo IV: Modificación del betún mediante dióxido de tiourea

8.6.1.1. Efecto sobre la formulación de las mezclas bituminosas

El principal objetivo de esta sección fue estudiar el grado de modificación alcanzado por la mezcla bituminosa mediante la adición de dióxido de tiourea (ThD), a 130 °C, sobre dos betunes vírgenes con distintos valores de penetración, así como explorar el efecto que provoca un aumento en la concentración de ThD en las propiedades reológicas a media/alta temperatura de servicio también fue considerado.

Además, la respuesta reológica a baja temperatura de servicio, dentro del rango viscoelástico lineal (LVR) de una muestra seleccionada (mezcla bituminosa con un 9 %, en masa, de ThD tras 60 días de curado ambiental) fue también considerada.

Comportamiento reológico a media/alta temperatura de servicio

La figura 4.1 muestra las curvas de flujo, a 60 °C, de distintas mezclas bituminosas preparadas usando dos betunes vírgenes distintos y modificados con diferentes porcentajes de ThD. Como puede observarse, el betún virgen 150/200 y sus modificados con un 3 y 9 % (resultados no mostrados en la Figure 4.1) presentan un comportamiento Newtoniano en todo el rango de velocidades de cizalla aplicado. Sin embargo, el betún virgen 40/50 y sus mezclas bituminosas con un 9 % muestran un comportamiento Newtoniano a bajas-intermedias velocidades de cizalla, seguidas por un comportamiento pseudoplástico cuando la velocidad de cizalla es incrementada por encima de un determinado valor.

Así, la adición de ThD sobre los betunes vírgenes produce un ligero incremento en los valores de viscosidad después de una hora de procesado. Sin embargo, la evolución de los valores de viscosidad de las mezclas bituminosas con el tiempo de curado es distinta dependiendo del betún virgen de partida. De esta forma, los betunes modificados partiendo del betún 150/200 sufren un importante incremento en su viscosidad entre los días 20 y 60, mucho más aparente que el observado para aquellos que parten del betún virgen 40/50.

El índice de modificación, $M.I.^{60^{\circ}C}$, definido en la ecuación 4.1, permite cuantificar los cambios en viscosidad debido exclusivamente a la adición de agente modificador (ThD), sin tener en cuenta el aumento de viscosidad que se produce en el betún virgen como consecuencia de la “oxidación

primaria”. De esta forma, la Figura 4.2 muestra claramente dos procesos de modificación: a) por un lado, una “modificación a corto plazo”, ocurrida durante la mezcla del betún/ThD a 130 °C; b) y por otro lado, una “modificación a largo plazo”, como consecuencia del curado ambiental de las muestras.

El comportamiento viscoelástico lineal de estas mezclas bituminosas fue estudiado mediante barridos de temperatura, en cizalla oscilatoria, entre 30 y 75 °C. La evolución de $\tan \delta$ en función del tiempo de curado (ver Figura 4.3) mostró un comportamiento predominantemente viscoso, el cual se hizo más aparente conforme la temperatura aumentaba. Además, un descenso en los valores de $\tan \delta$ (y por lo tanto, una mejora en el comportamiento elástico) es observado a medida que el tiempo de curado aumenta, especialmente para aquellas mezclas bituminosas con la mayor concentración de ThD. De la misma forma, los valores medios de la pendiente de estas curvas son reducidos, implicando una menor susceptibilidad térmica de las mezclas bituminosas a la temperatura.

Comportamiento reológico a baja temperatura de servicio

Barridos de frecuencia a distintas temperaturas, en modo “bending”, han sido utilizados para estudiar la respuesta, en el rango viscoelástico lineal, del betún virgen 40/50 y una mezcla bituminosa con un 9 % de ThD (procesada a 130 °C) curada al ambiente durante 60 días. Los resultados experimentales mostraron un comportamiento predominantemente elástico ($E' > E''$) a bajas temperaturas (por debajo de 0 °C). Igualmente, estos barridos de frecuencia, en el rango de temperaturas estudiado, pueden ser superpuestos mediante el uso de un “shift factor”, a_T (ver Figura 4.4).

Con la intención de obtener información en un rango de temperatura más amplio, los barridos de frecuencia fueron combinados en un diagrama de "Black" (Figura 4.5), representándose el ángulo de fase (δ) frente al módulo complejo ($|E^*|$). Como puede observarse, en la zona de baja temperatura (o altos valores de $|E^*|$) el betún modificado presenta un valor de ángulo de fase (δ) mayor que el betún virgen. Por otro lado, en la zona de altas temperaturas (o bajos valores de $|E^*|$) la tendencia es opuesta, mostrándose menores valores de δ que el betún virgen. Por lo tanto, una mejora en el comportamiento reológico, en un amplio rango de temperaturas, es observada tras la adición de ThD y su curado ambiental, mejorándose la elasticidad y la flexibilidad, a altas y bajas temperaturas de servicio, respectivamente.

En el mismo sentido, la Figura 4.6 muestra los barridos de temperatura, a 1 Hz, entre -30 y 35 °C, para el betún virgen 40/50 y su correspondiente blanco procesado una hora a 130 °C, así como una mezcla bituminosa con un 9 % de ThD curada durante 60 días. De estos ensayos, se puede determinar una "temperatura de transición mecánica" ($T_{g(1Hz)}$) como la temperatura a la cual E' alcanza su máximo. Así, esta temperatura característica representaría la temperatura a la que se produciría la salida del material de su zona vítrea, produciéndose la fractura a baja temperatura. Por tanto, nuestros esfuerzos deben ir dirigidos a disminuir esta temperatura y, como puede observarse en la Figura 4.6, una reducción de 8 °C es conseguido en la muestra modificada con ThD.

8.6.1.2. Efecto de la temperatura de procesado

En la sección anterior se estudió la modificación del betún mediante la adición de ThD a 130 °C, así como las mejoras obtenidas en las propiedades termo-reológicas en un amplio rango de temperaturas. Intentando profundizar en este agente modificador, el interés ahora está centrado en

el efecto que un cambio en la temperatura de procesado provoca en las mismas propiedades reológicas. Con este objetivo, el betún virgen 40/50 fue modificado con un 9 % de ThD a tres temperaturas de procesado distintas: 90, 130 y 180 °C.

Influencia en el comportamiento de flujo viscoso

La Figura 4.7 recoge las curvas de flujo, a 60 °C, para las mezclas bituminosas procesadas a 90 y 180 °C, en función del tiempo de curado. De la misma forma, los valores de " η_0 " y " $\dot{\gamma}$ " para todas las muestras son mostradas en la Tabla 4.3. Los resultados mostraron que, para cualquier temperatura de procesado, la adición de ThD produce un aumento de viscosidad, el cual es más pronunciado cuando las muestras son almacenadas a temperaturas ambiente. Así, después de 12 meses de curado, temperaturas de procesado de 90 y 180 °C producen mezclas bituminosas con valores de viscosidad superiores a los obtenidos para la muestra de referencia (3 wt.% SBS).

Los valores de I.M. obtenidos para las muestras preparadas a las tres temperaturas de procesado parecen sugerir una ruta de modificación distinta en función de la temperatura de procesado.

Influencia en el comportamiento viscoelástico lineal

La influencia que la temperatura de procesado exhibe en el comportamiento viscoelástico lineal de las mezclas bituminosas fue estudiada mediante barridos de temperaturas en modo cizalla (media/alta temperatura de servicio) y en modo "bending" (baja temperatura de servicio).

La Figura 4.9 muestra la evolución de las funciones viscoelásticas lineales, G' y G'' , con la temperatura de procesado para las muestras "no curadas".

Un incremento en estos módulos es observado cuando se aumenta la temperatura de procesado, de 90 a 180 °C (resultados similares a aquellos obtenidos para el comportamiento viscoso). La evolución de G' y G'' fue también estudiado en función del curado ambiental para las muestras procesadas a 90 °C. Así, la Figura 4.9B muestra, claramente, que $\tan \delta$ es siempre mayor que 1. Sin embargo, se produjo una mejora en el comportamiento elástico conforme aumenta el tiempo de curado, como puede ser deducido por la bajada en los valores de $\tan \delta$ después de 2 y 12 meses.

En cuanto a la respuesta a baja temperatura de servicio, se observa un descenso en la “temperatura de transición mecánica” de 8 °C, pasando de -2 °C para la muestra “blank” a 130 °C, hasta -10 °C, para su correspondiente mezcla bituminosa procesada a 130 °C. Por otro lado, para la temperatura de procesado de 90 °C, para la cual la “oxidación primaria” es despreciable, se produce un descenso de 3 °C entre el betún virgen 40/50 y la muestra modificada a 90 °C. Finalmente, para un temperatura de procesado de 180 °C, el valor de esta $T_{g(1Hz)}$ es similar al obtenido para las otras temperaturas de procesado.

8.6.1.3. Rutas de modificación del betún y microestructura.

Las mejores observadas en el flujo viscoso así como en su respuesta viscoelástica lineal, a media/alta y baja temperaturas de servicio, son consecuencia de reacciones químicas ocurridas entre ThD y las fracciones del betún. Además, estos resultados parecen indicar una ruta de modificación distinta en función de la temperatura de procesado. En este sentido, el análisis térmico (mediante medidas de DTG/DTA y MDSC) y la cromatografía de capa fina (TLC-FID) son dos herramientas que pueden ayudar a estudiar las distintas rutas de modificación.

La Figura 4.11 muestra significativas diferencias en las curvas DTG/DTA obtenidas cuando se produce un incremento en la temperatura de procesado. El betún virgen presenta un largo proceso de descomposición (desde 300 a 500 °C, con un máximo en DTG a 455 °C) debido a la descomposición/volatilización de compuestos químicos con muy distinto peso molecular. Sin embargo, las muestras “no curadas” modificadas con ThD presentaron varios picos. En primer lugar, puede observarse que la altura del pico a 455 °C decrece conforme aumenta la temperatura de procesado, como consecuencia a la aparición de otros dos nuevos picos: el primero de ellos aparece a 220 °C, y el segundo a 300 y 310 °C, respectivamente. Interesantemente, estos picos no aparecen cuando la temperatura de procesado fue de 180 °C. Con objeto de comprender la aparición de estos picos, la descomposición térmica del ThD fue estudiado mediante las reacciones (R1) y (R2).

Por otro lado, la Figura 4.12 muestra la evolución de la fracción SARAs, con el tiempo de curado, para las mezclas bituminosas procesadas a 90 y 130 °C. Como puede observarse, la fracción de asfaltenos incrementa con el tiempo de curado para la temperatura de procesado de 130 °C. En oposición, una reducción mucho menos importante fue observada para aquellas muestras procesadas a 90 °C.

A partir de los resultados obtenidos por cromatografía, ensayos de filtración y distintos análisis térmicos, se puede concluir que para las muestras procesadas a 90 °C, el dióxido de tiourea “virgen” y la urea son las responsables de la modificación, ya que no se observó la descomposición de la ThD a esa temperatura de procesado. Por otro lado, la importante reducción observada en la fracción de los asfaltenos con el tiempo de curado, para las muestras modificadas a 130 °C, sugiera que la modificación es el resultado de nuevos productos de reacción originados

por los asfaltenos y la urea derivada de la descomposición del ThD (reacción (R1)). Finalmente, para las mezclas bituminosas procesadas a 180 °C, no se obtuvo residuo después de la filtración con tolueno y tampoco se obtuvieron picos en las curvas DTG de sus correspondientes betunes modificados. En base a estos hechos, una ruta de modificación mediante el ácido cianico derivado de la descomposición de la urea (reacción (R2)) y los componentes polares del betún es propuesto.

8.6.2. Capítulo V: Modificación del betún mediante tiourea

8.6.2.1. Respuesta a alta temperatura de servicio

La figura 5.1 muestra las curvas de flujo, a 60 °C, para mezclas bituminosas modificadas con un 3 y 9 % de tiourea (Th), en función del tiempo de curado ambiental. Así, la adición de Th produce significativos incrementos en la viscosidad, principalmente para los sistemas con la mayor concentración de Th y después de un tiempo de curado ambiental prolongado. Además todas las muestras modificadas mostraron una zona de comportamiento Newtoniano, a bajas velocidades de cizalla, seguido por una zona pseudoplástica. Este comportamiento puede ser descrito por el modelo de Carreau (ecuación 5.1), y sus parámetros de ajustes son recogidos en la Tabla 5.2.

La evolución de los I.M. con el tiempo de curado para las diferentes mezclas bituminosas formuladas con Th mostraron la existencia de dos procesos de modificación, uno de ellos a “corto” y otro a “largo” plazo de modificación (al igual que ocurría con el ThD). Así mismo, un exceso de Th sin reaccionar después de una hora de procesado produce un efecto “plastificante”, disminuyendo los valores de viscosidad. La Figura 5.2 mostró que después de dos años de curado ambiental los valores de viscosidad tienden a

estabilizarse, superándose en ocho veces el valor de viscosidad del betún virgen 40/50.

En adición, los parámetros de ajuste del modelo de Carreau indican una mayor estructuración del sistema, como puede observarse por el mayor valor de “ λ ” con el tiempo de curado, especialmente para los sistemas con mayor concentración de Th.

Por otro lado, los barridos de temperaturas (Figura 5.3) mostraron un comportamiento claramente viscoso, con valores de $\tan \delta$ menores (y por lo tanto con mejor comportamiento elástico) para altos tiempos de curado ambiental. De la misma forma, se produce un notable descenso de la pendiente media de la curva $\tan \delta$ frente a temperatura, un hecho que indica una mejora en la susceptibilidad térmica del material.

Finalmente, se propone el parámetro de “Rutting”, $|G^*|/\sin \delta$, como una manera eficiente de determinar la máxima temperatura a la cual el material se comportaría de forma satisfactoria, a alta temperatura de servicio. De acuerdo con este criterio, esta temperatura se puede determinar como aquella a la cual $|G^*|/\sin \delta$ es igual a 1 kPa. Si comparamos los valores de estas temperaturas, se observa un incremento de 7 °C, con respecto al betún virgen, para la mezcla bituminosa con un 9 % después de 12 meses de curado ambiental.

8.6.2.2. Respuesta a baja temperatura de servicio

La respuesta reológica a baja temperatura de servicio del betún virgen 40/50, muestra de referencia (3 % SBS) y una mezcla bituminosa con un 9 % de Th después de 60 días de curado ambiental ha sido considerada. La Figura 5.4 muestra los barridos de frecuencia, entre -30 y 15 °C, para el betún virgen 40/50. Éstos fueron superpuestos en una curva maestra mediante el uso de “shift factor”, a_T .

Con objeto de poder conocer la evolución de las propiedades reológicas con la temperatura, los valores de frecuencia de las curvas maestras fueron convertidos en temperatura usando la relación de Arrhenius (ecuación 5.4). Así, la Figura 5.5B para el betún virgen 40/50 muestra una clara transición desde la zona vítrea a la zona Newtoniana, con un cruce en los valores de E' y E'' , al aumentar la temperatura. Además, no se encontró una zona “plateau” a temperaturas intermedias, lo que pone de manifiesto la no existencia de entrecruzamientos (típicamente observado en polímeros fundidos). Finalmente, un máximo en E'' puede también observarse (representando la $T_{g(1Hz)}$, anteriormente comentada).

Los valores de $T_{g(1Hz)}$ obtenidas de las curvas convertidas para las distintas muestras bituminosas están recogidas en la Tabla 5.3 (aparecen como $T_{g,DMTA}$), mostrándose una mejora en la respuesta a baja temperatura de la muestra modificada con Th respecto a las muestras de betún virgen y modificada con SBS.

Con este procedimiento de conversión frecuencia-temperatura (obtenido mediante la aplicación del principio de superposición tiempo-temperatura) se obtienen valores de temperaturas de transiciones vítreas no afectados por la velocidad de calentamiento seleccionada en el barrido de temperatura (referidas en el capítulo como $T_{g,DMTA}$). Con objeto de validar esta suposición, barridos de temperatura a distintas velocidades de calentamiento (4,2 y 0.2 °C/min), y a una frecuencia fijada de 1 Hz, fueron comparadas con la obtenida tras la conversión frecuencia-temperatura, para la muestra modificada con Th (ver Figura 5.7).

Como era esperado por la baja conductividad térmica del betún, una velocidad de calentamiento elevada provoca grandes diferencias entre la temperatura programada y la temperatura real de la muestra. En consecuencia, sólo barridos de temperatura realizados a muy bajas

velocidades de calentamiento (0.2 °C/min) llevaría a una correcta caracterización de estos materiales a baja temperatura.

8.6.2.3. Cambios químicos del betún debido a la modificación

Los resultados anteriores sugieren interacciones entre Th y los componentes del betún, las cuales producen nuevos productos de reacción responsables de las mejoras observadas en el amplio intervalo de temperaturas de servicio estudiado. Con objeto de profundizar en esta materia, diferentes análisis químicos y térmicos pueden proporcionar resultados concluyentes.

La descomposición de los componentes puros (betún virgen y Th) fueron estudiados mediante medidas simultáneas de DTA y TG. La tiourea presenta un único pico de descomposición (a 210 °C); sin embargo, la curva de DTA presenta dos procesos endotérmicos solapados (ver Figura 5.9). El primero de ellos es debido a la fusión del Th (no produciéndose pérdida de masa). La reacción de isomerización (R1), que provoca la producción de tiocianato amónico (NH_4SCN), tiene lugar durante este primer proceso endotérmico. Por otro lado, el segundo pico (entre 190 y 270 °C) se debe a la descomposición térmica del NH_4SCN en CS_2 , HNCS and NH_3 , observándose una significativa pérdida de masa (con un máximo en la curva de DTG a 228 °C). Además, para confirmar la formación de NH_4SCN a partir de Th, la descomposición de esta sustancia también fue incluida en la Figura 5.9.

De estos resultados, se puede asumir que la modificación del betún mediante la adición de tiourea, y sus mejores respuestas reológicas, son el resultado de interacciones entre el NH_4SCN creado en la reacción (R1) y ciertos componentes del betún, formándose nuevos productos de reacción. Los análisis químicos, mediante cromatografía de capa fina (TLC/FID),

llevado a cabo en las distintas mezclas bituminosas confirmaron este hecho.

En este sentido, el betún virgen mostró los cuatro picos correspondiente a la fracción SARAs (saturados, aromáticos, resinas y asfaltenos). La tiourea presentó una única señal (cerca de la correspondiente a la resinas), mientras que el tiocianato amónico no mostró ninguna señal, debido a su insolubilización en los disolventes utilizados la para la cromatografía.

Al contrario de lo observado para el betún virgen, el pico correspondiente a los asfaltenos para la muestra modificada con Th muestra un desdoblamiento en otros dos picos (referidos como asfaltenos de alta y baja polaridad, HPAs y LPAs, respectivamente). Así, el mayor de ellos (LPAs), el cual es parcialmente eludido por la mezcla diclorometano/metanol, es el resultado de las interacciones entre el NH_4SCN y el betún, siendo los nuevos productos de reacciones responsables de la modificación. Además, dos disoluciones de betún virgen en tolueno con Th ó NH_4SCN fueron preparadas y agitadas durante 5 horas a 25 °C. Los resultados mostraron que el desdoblamiento de los asfaltenos solo se produce cuando NH_4SCN es adicionado. Este hecho parece indicar que el NH_4SCN formado por la reacción (R1), en lugar de la Th adicionada, es la sustancia realmente encargada de la formación de la fracción LPAs. Además, la fotografía tomada durante la elución en diclorometano/metanol para dos muestras (betún virgen y betún modificada con Th) confirmaron esta suposición. De esta forma, la fracción LPAs puede ser eludida por este disolvente usado para separar la fracción de resinas cuando la muestra a medir esta modificada con Th. Sin embargo, la fracción LPAs no aparece cuando la elución es realizada con el betún virgen.

Finalmente, las medidas de DSC dieron más información acerca de los cambios microestructurales ocurridos y justificaron las mejoras obtenidas

a altas y bajas temperaturas de servicio. La Figura 5.13 representa el flujo de calor no-reversible y la derivada del poder calorífico (dC_p/dT) para el betún virgen y para una mezcla bituminosa con un 9 % de Th, en función del tiempo de curado.

Así, el evento endotérmico observado a 50 °C está relacionado con la difusión de estructuras relativamente grandes y estructuradas, como son aquellas típicamente encontradas en las micelas asfálticas. Los valores obtenidos para este evento endotérmico (ver Tabla 5.4) incrementaron conforme lo hace el tiempo de curado ambiental, lo cual supone la formación de nuevas estructuras que requieren mayor cantidad de energía para su fusión. Este hecho estaría relacionado con la mejora obtenida a alta temperatura de servicio.

Por otro lado, las temperaturas obtenidas a partir de dC_p/dT (T_{g1} y T_{g2}) son transiciones vítreas correspondientes a las fracciones de saturados y aromáticos. De forma que estas temperaturas son reducidas tras la adición de Th, y después de una exposición prolongada al ambiente, corroborando la mejora del comportamiento a baja temperatura observado en los resultados de DMTA.

Finalmente, el origen del nuevo pico endotérmico obtenido a -30 °C en las mezclas bituminosas con Th puede ser atribuido a un proceso reversible de cambio de estructura del NH_4SCN , similar al que ocurre para esta misma sustancia a 90 °C.

8.6.3. Capítulo VI: Modificación del betún mediante prepolímeros basados aceite de ricino funcionalizados con grupos -NCO.

8.6.3.1. Caracterización de los prepolímeros

Aceite de ricino (abreviado como CO y con un índice de hidroxilo de 125 mg KOH/g) fue funcionalizado con grupos isocianatos mediante su reacción 4,4'-difenilmetano diisocianato (con un índice de isocianato de 31.1 %, en peso). La Figura 6.1 ilustra el esquema de reacción para la síntesis de los prepolímeros estudiados en este capítulo (referidos como MDI-CO) y, como puede observarse, enlaces uretanos son formados entre los grupos hidroxilos e isocianatos. La Tabla 6.1 recoge los peso moleculares medios (M_w), contenidos de -NCO libre y temperaturas de transición vítrea (determinada por MDSC) para los prepolímeros MDI-CO, MDI polimérico y el aceite de ricino.

Las propiedades termo-reológicas y la morfología de estos prepolímeros dependen de la estructura y la cantidad relativa de los segmentos duros y blandos que lo conforman. El comportamiento térmico del MDI polimérico, aceite de ricino y los resultante MDI-CO y MDI-PEG prepolímeros fue estudiado mediante medidas de MDSC y TG/DTA.

La Figure 6.2 presenta la componente reversible del flujo de calor, entre -80 y 190 °C, mostrando una transición vítrea a -49 y 63 °C para el MDI polimérico y el aceite de ricino, respectivamente. Por otro lado, MDI-CO(2:1) muestra dos picos bien definidos. El primero de ellos, localizado a -37 °C, puede ser atribuido al MDI polimérico no reaccionado. Así, las cadenas cortas de MDI polimérico, con mayor movilidad, son las que reaccionan con el aceite de ricino. Consecuentemente, las cadenas más

largas, las cuales permanecen sin reaccionar, son las responsables de los mayores valores de T_g observados.

El segundo pico, encontrado en 135 °C, corresponde a los productos formados por la funcionalización del aceite de ricino con los grupos isocianatos. Sin embargo, los prepolímeros MDI-CO(8:1) y MDI-CO(4:1) solo mostraron una transición vítrea cada uno de ellos, localizados a -36 y 19 °C, respectivamente. De esta forma, los productos de reacción serían homogéneamente dispersados en la fase continua de MDI polimérico que se encuentra en exceso, dando lugar a un único evento térmico. Esto provoca que los prepolímeros MDI-CO(8:1) y MDI-CO(4:1) sean líquidos de color marrón y el MDI-CO(2:1) un sólido amarillo que descompone sin fundir. Por lo tanto, este último prepolímero no puede ser usado como agente modificador del betún.

La Figura 6.3 muestra los efectos que la relación -NCO/-OH produce en la descomposición térmica de los prepolímeros. En este sentido, un mayor contenido de grupos -NCO provoca dos efectos: a) El pico de descomposición correspondiente al aceite de ricino, a 400 °C, es claramente reducido y b) un notable incremento en la velocidad de degradación del primer evento (relacionado con la descomposición del MDI) es también observado. Además, si comparamos con el MDI polimérico, el cual presenta su primer pico de descomposición a 276 °C, el prepolímero MDI-CO(2:1) lo tiene a 324 °C. Este incremento es debido a las largas cadenas de MDI polimérico que permanecen no reaccionadas después de la polimerización. Así, estas cadenas presentan mejor movilidad que las largas y, como previamente se demostró en la Figura 6.2, su presencia llega a ser más importante para el prepolímero MDI-CO(2:1). Para los otros prepolímeros, las moléculas productos de la polimerización son diluidas en el considerable exceso de MDI polimérico existente.

Por otro lado, la estabilidad térmica es un factor clave para usar los prepolímeros MDI-CO como agentes modificadores. En este sentido, a partir de la Figura 6.4, se puede observar la pérdida de masa, a 180 °C, durante dos horas. Estos resultados demuestran la influencia que el tipo de polioliol exhibe en la estabilidad térmica de los prepolímeros sintetizados con grupos isocianatos. Así, los prepolímeros formulados con un polioliol de origen vegetal (aceite de ricino) presentan mejores resultados que aquel sintetizado con un polioliol derivado del petróleo (como es el caso del PEG). De forma, que incluso el prepolímero MDI-CO con el mayor exceso de -NCO presenta una estabilidad térmica mucho mejor que el prepolímero MDI-PEG.

Finalmente, el comportamiento reológico de los prepolímeros MDI-CO fue estudiado mediante barridos de temperatura en modo oscilatorio. Así, la Figura 6.5 muestra la evolución de G' y G'' con la temperatura, en distintos rangos de temperatura, dependiendo del prepolímero considerado. Los prepolímeros MDI-CO(8:1) y MDI-CO(4:1) muestran un descenso monótono de las variables viscoelásticas lineales, con un comportamiento predominantemente viscoso. Sin embargo, el prepolímero MDI-CO(2:1) presenta, entre su segunda temperatura de transición vítrea y su temperatura de descomposición, valores constantes de G' y G'' , con una mayor contribución de G' .

8.6.3.2. Modificación del betón mediante MDI-CO prepolímeros

Influencia de la formulación del prepolímero

Los efectos que la formulación (es decir, la relación molar de -NCO/-OH) de los prepolímeros MDI-CO provoca en la modificación del betón fueron estudiadas mediante curvas de flujo y barridos de temperaturas, con

muestras modificadas con prepolímeros MDI-CO y siguiendo el procedimiento de “24 horas” (detallado en el Capítulo VI).

Así, después de la adición de un 2 % (en peso) del prepolímero MDI-CO(8:1), durante una hora de procesado, y su posterior almacenamiento a 90 °C durante 24 horas, se observó un considerable aumento en el valor viscosidad (ver Figura 6.6). Durante estos dos procesos consecutivos (el que ocurre durante la mezcla del prepolímero-betún y su posterior almacenamiento a 90 °C) una parte de los grupos -NCO del prepolímero son capaces de reaccionar con ciertos grupos (principalmente grupos hidroxilos) pertenecientes a la fracción asfáltica del betún. Esto provoca un notable aumento en la viscosidad de la mezcla bituminosa, debido a la formación de enlaces uretanos, de acuerdo a la reacción (1). Sin embargo, un mayor grado de modificación fue obtenido después de exponer las muestras a un curado ambiental de 60 días. En este sentido, agua procedente de la humedad del aire puede difundir lentamente en la mezcla bituminosa, promoviendo las reacciones (2) y (3). Una forma de acelerar este proceso consiste en adicionar un 2 % de agua, en peso, directamente a la mezcla bituminosa.

Los índices de modificación, definidos por la ecuación 6.2, obtenidos para distintas mezclas bituminosas modificadas con los prepolímeros MDI-CO(8:1) y MDI-CO(4:1), en función del tiempo de curado ambiental, son recogidos en la Figura 6.7. Los valores obtenidos tras la adición final de agua también son incluidos como valores de referencia. Como puede observarse, si las muestras no son curadas (ocurriendo solo la reacción 1) el grado de modificación alcanzado está ligeramente influenciado por el prepolímero usado. Sin embargo, cuando las muestras fueron expuestas al curado ambiental, el prepolímero con mayor contenido de grupos isocianatos disponibles para reaccionar proporciona mezclas bituminosas

con índices de modificaciones mayores. Finalmente, la Figura 6.7 muestra como no es posible obtener un material con un valor de viscosidad equivalente al obtenido después de 60 días de curado mediante la adición directa de agua.

Por otro lado, la respuesta viscoelástica de estas muestras fue estudiada mediante barridos de temperatura, en modo oscilatorio, entre 30 y 80 °C. Así, la adición de un 2 % de MDI-CO(8:1) aumentó 3 °C la temperatura de “rutting” característica ($T_{|G^*|/\sin\delta}$), pasando de 62 °C del betún virgen a 65 °C. Además, este valor aumenta hasta 73 °C después de 60 días de curado. Por lo tanto, la modificación del betún con prepolímeros MDI-CO aumentaría la temperatura a la cual se produce las deformaciones permanentes a alta temperatura.

Estas mejoras son corroboradas mediante las medidas calorimétricas de DSC y las fotos obtenidas por AFM. Así, la Tabla 6.4 recoge los valores de la entalpía del cuarto evento térmico (ΔH_{4th}) de muestras modificadas con un 2 % de MDI-CO(8:1) en función del tiempo de curado. Tras 60 días de curado se observó un significativo incremento de este evento, pasando de 0.49 J/g para la muestra no “curada” hasta 4.41 después de 60 días de curado ambiental. Finalmente las fotos de AFM mostraron una mucha mayor concentración de regiones asfálticas en la muestra modificada con MDI-CO(8:1), que para la muestra de betún virgen. Consecuentemente, las fotos de AFM están en concordancia con los resultados previos observado en las curvas de flujo, comportamiento viscoelástico y ensayos calorimétricos.

Efectos de las condiciones de procesado/curado

El objetivo de esta subsección fue estudiar el efecto que tiene las condiciones de procesado y/o curado en las propiedades termo-reológicas

de las muestras modificadas con MDI-CO. Para ello, el betún virgen fue modificado con un 2 % de MDI-CO(8:1) siguiendo las dos condiciones de procesado (detalladas en la sección 6.4.1), referidas como “1 hora” y “24 horas”.

El grado de modificación alcanzado en las distintas muestras modificadas, considerando solo el efecto que tiene el agua (bien directamente añadida o bien absorbida desde el aire), fue cuantificado mediante el uso del índice de modificación ($M.I.^{60^{\circ}C}$) definido en la ecuación 6.3. Así, la Figura 6.11 representa la evolución de las distintas mezclas bituminosas procesadas por el procedimiento de “1 hora” ó “24 hora” en función del tiempo de curado ambiental. Como puede observarse, las muestra terminadas por la adición directa de agua presentan un valor de $M.I.^{60^{\circ}C}$ mayores si son previamente almacenadas a 90 °C durante 24 h. De forma que, para alcanzar una buena modificación al adicionar agua, es necesario promover durante un tiempo razonable las reacciones betún-polímero. Sin embargo, cuando la mezcla bituminosa procesada durante 1 hora es expuesta al ambiente se obtienen valores de $M.I.^{60^{\circ}C}$ mayores. Así pues, la adición directa de agua ocurre rápidamente mediante las reacciones (2) y (3), sin embargo, durante la lenta difusión del agua del ambiente, se producen la reacciones (2) y (3), pero a la misma vez también tiene lugar la reacción (1).

Por otro lado, la evolución de G' y $\tan \delta$ con la temperatura (ver Figura 6.12) proporciona información interesante. Como puede observarse, la curva de G' para las muestras no curadas presenta una zona de allanamiento a temperaturas superiores a 60 °C, mostrando un máximo en la $\tan \delta$. Esta nueva transición está relacionada con los procesos de deformación-relajación de las nuevas fases dispersas creadas como consecuencia de las reacciones locales entre el prepolímero y las micelas

asfálticas (según la reacción (1)). Así, cuando la fase continua es lo suficientemente blanda al aumentar la temperatura, la presencia de esta fase dispersa aparece. Sin embargo, después de la adición de agua o tras su absorción lenta desde el ambiente, esta transición está marcada por el proceso químico de endurecimiento previamente mencionado.

Del mismo modo, los resultados obtenidos del parámetro "rutting" (recogidos en la Tabla 6.5) mostraron un incremento de 14 °C, respecto al betún virgen, de la temperatura a la cual se produce la deformación permanente, tras la modificación con un 2 % de MDI-CO(8:1) procesada durante una hora y expuesta 6 meses al ambiente.

8.6.3.3. Mejora de los prepolímeros MDI-CO como agentes modificadores

Con el objeto de explorar nuevas rutas de modificación usando prepolímeros basados en isocianatos y aceite de ricino (MDI-CO), la modificación del aceite de ricino mediante su transesterificación con pentaeritritol ha sido considerada. Por ello, esta subsección estudia el efecto que tiene el grado de transesterificación alcanzado y el proceso de manufactura de las mezclas bituminosas en sus propiedades termo-reológicas finales.

Síntesis de los nuevos prepolímeros MDI-CO(8:1) y sus características

La Figura 6.18 muestra el esquema de reacción y los productos derivados de la transesterificación del aceite de ricino (denominados como COⁿ%). Así, después de adicionar al aceite de ricino concentraciones superiores al 8 % de pentaeritritol, un precipitado blanco, debido al pentaeritritol no reaccionado, fue observado y, posteriormente, separado por centrifugación. La Tabla 6.7 recoge la nomenclatura y los valores

hidroxilos, en función de la concentración de pentaeritritol reaccionado (n%), para los distintos aceites modificados.

De acuerdo a cada uno de sus valores hidroxilos, los prepolímeros fueron sintetizados seleccionando una misma relación molar de -NCO/-OH igual a 8:1 (concentración óptima). La figura 6.19 muestra el esquema de reacción para la síntesis de los nuevos prepolímeros MDI-CO^{n%}.

Las curvas de flujo, a 30 °C, para el aceite de ricino “virgen”, los modificados con pentaeritritol (CO^{n%}) y los nuevos prepolímeros sintetizados (MDI-CO^{n%}) presentan un comportamiento Newtoniano, cuyos valores son recogidos en la Figura 6.20. Como puede ser observado, el aceite transesterificado presenta mayores valores de viscosidad conforme la concentración de pentaeritritol reaccionado (n%) aumenta. Esta tendencia en el comportamiento viscoso también es observada en los prepolímeros MDI-CO^{n%}, sin embargo, el prepolímero MDI-CO^{4%} (sintetizado con un aceite transesterificado con un 4 % de pentaeritritol) presenta un valor menor que aquel formulado con aceite no modificado.

Finalmente, en cuanto a las propiedades de los prepolímeros MDI-CO^{n%}, la estabilidad térmica es un factor clave a considerar. Los prepolímeros MDI-CO^{n%} presentan peor estabilidad que aquellos formulados con aceite de ricino virgen. Sin embargo, la estabilidad de los prepolímeros aquí propuestos sigue siendo superior a la obtenida para el prepolímero MDI-PEG (ampliamente utilizado en la industria de la pavimentación).

Modificación reactiva mediante enlaces uretano/urea

La Figura 6.22 muestra las curvas de flujo, a 60 °C, de seleccionadas muestras modificadas con el prepolímero MDI-CO^{8%}. Nuevamente, los resultados obtenidos pueden explicarse sobre la química de los isocianatos. Así, durante el procesado betún/prepolímero se produce un aumento de

viscosidad debido a la reacción (1). Por otro lado, después del procesado, la adición de agua lleva consigo un endurecimiento del material consecuencia de las reacciones (2) y (3), previamente detalladas.

Modificación reactiva mediante enlaces uretano

Con la intención de procesar a temperaturas más elevadas, evitando la posible formación de espumas debido a la liberación de CO₂ producido en la reacción (2), en lugar de añadir un 2 % de agua tras el procesado betún/prepolímero se hará adicionando un 2 % (en peso) de aceite transesterificado con un 4 % de pentaeritritol (CO^{4%}). Esta adición final de aceite modificado será el encargado de consumir los grupos isocianatos aun libres pertenecientes al prepolímero.

Sin embargo, como puede observarse en las Figuras 6.22 y 6.23, la adición de un 2 % de CO^{4%} tiene un efecto plastificante en las muestras no-curadas. Este resultado podría estar relacionado con la lenta velocidad de reacción a esta temperatura. En este sentido, la Figura 6.24A muestra las curvas de flujo, a 60 °C, de las muestras terminadas con CO^{4%} y sometidas a un proceso de curado a 90 °C durante 7 días. Después de este almacenamiento a esta temperatura, las muestras presentaron un significativo incremento en su viscosidad (de al menos 2 órdenes de magnitud). El índice de modificación, definido en la ecuación 6.5, M.I.^{60°C}, permite cuantificar la magnitud de la modificación teniendo en cuenta el propio incremento que sufre el betún virgen al almacenamiento a alta temperatura. La Figura 6.24B muestra un valor de M.I.^{60°C} mucho más elevado para la muestra que fue procesada con el prepolímero MDI-CO^{4%}. Los resultados obtenidos a partir de los barridos de temperaturas, los parámetros de ajuste al modelo de Carreau y las fotos obtenidas por AFM mostraron sistemas más complejos para las mezclas bituminosas modificadas con el prepolímero MDI-CO^{4%} y sometidas a un almacenamiento a alta temperatura.

De esta forma, la mejor capacidad de modificación exhibida por este prepolímero (MDI-CO^{4%}) parece estar relacionada con su baja viscosidad (ver Figura 6.20). De esta forma, una baja viscosidad del prepolímero podría favorecer el transporte de las cadenas poliméricas en el medio de reacción durante el proceso de curado a alta temperatura y, consecuentemente, obtener una mayor modificación para las muestras modificadas con MDI-CO^{4%} y curadas a 90 °C durante 7 días.

Para confirmar esta suposición, un nuevo proceso de modificación fue llevado a cabo con los prepolímeros MDI-CO^{4%} y MDI-CO^{7%} a una temperatura de procesamiento mayor, 180 °C. Durante las dos horas de procesamiento, en la primera de ellas se produce la reacción betún/prepolímero y, al inicio de la segunda, se adicionó el CO^{4%}. Estas son las condiciones de procesamiento típicamente usada en la industria de la pavimentación para las mezclas bituminosas con SBS, condiciones posibles a ser utilizadas en los prepolímeros MDI-CO^{n%}, según la estabilidad térmica mostrada en la Figura 6.21.

La Figura 6.27 muestra las curvas de flujo, a 60 °C, para estos dos nuevos procesados, además de aquellas correspondientes a las muestras almacenadas durante 7 días a 90 °C y terminadas con agua. Como era esperable, las mezclas bituminosas modificadas con MDI-CO^{4%} y MDI-CO^{7%} provocan valores de viscosidad muy similares cuando son procesadas a 180 °C. Es más, estas condiciones de procesamiento provocan modificaciones similares a aquellas obtenidas después de la adición de agua a 90 °C, pero significativamente menores tras el curado a alta temperatura (90 °C) durante 7 días. Estos resultados sugieren que, además de la reacción (1), otros procesos que involucran reacciones agua/mezcla bituminosa (debido a las reacciones (2) y (3)) ocurre durante dicho curado a alta temperatura.

8.7. CONCLUSIONES

Este trabajo de investigación ha descrito los resultados encontrados como consecuencia del desarrollo de mezclas bituminosas mediante nuevas rutas de modificación. El uso de tres novedosos agentes reactivos han sido propuestos: dos aditivos no-poliméricos (dióxido de tiourea y tiourea) y un prepolímero formulado a partir de aceite de ricino funcionalizado con grupos isocianatos.

A partir de este trabajo, las siguientes conclusiones han sido destacadas:

- 1) Los resultados obtenidos parecen soportar el uso de dióxido de tiourea (“ThD”) y tiourea (“Th”) como prometedores agentes modificadores en la manufactura de mezclas bituminosas con propiedades termo-reológicas mejoradas en un amplio intervalo de temperaturas de servicio.
- 2) Los derivados no-poliméricos provenientes del “ThD” y “Th”, conteniendo enlaces N-H, han demostrado la formación de aductos, los cuales contribuyen a mejorar la estructura coloidal del betún mediante enlaces de hidrógeno. Estos aductos (derivados de la interacción de urea o tiocianato amónico con los asfaltenos del betún) parecen ser los responsables de la mejora en las propiedades reológicas, y sus contribuciones llegan a ser más importantes conforme el tiempo de curado aumenta.
- 3) Esta investigación propone el uso de las curvas maestras, obtenidas mediante la aplicación del principio TTSP en los barridos isotérmicos de frecuencia a distintas temperaturas, y su posterior conversión frecuencia-temperatura, con objeto de obtener una caracterización viscoelástica a baja temperatura adecuada en las mezclas bituminosas.

- 4) El aceite de ricino aparece como una alternativa prometedora en lugar de los polioles basados procedentes del petróleo para la formulación de prepolímeros de poliuretanos para la modificación del betún.

- 5) La ruta de modificación experimentada por las mezclas bituminosas MDI/aceite de ricino es un complejo proceso que involucra reacciones entre los grupos isocianatos/betún/agua, controlada por dos etapas bien definidas:
 - a) Modificación “a corto plazo”, durante la manufactura de las mezclas bituminosas a la temperatura de procesado.
 - b) Modificación “a largo plazo”, durante la exposición en condiciones ambientales de las mezclas bituminosas.

- 6) El grado de modificación alcanzado por las mezclas bituminosas MDI/aceite de ricino está influenciada por dos factores claves:
 - a) Formulación del prepolímero: radio entre los grupos isocianatos e hidroxilos (relación molar -NCO/-OH).
 - b) Condiciones de procesado/curado, esto es, la influencia que los distintos procedimientos exhiben en las mezclas bituminosas (largos o cortos tiempos de procesado, proceso de curado a temperatura ambiente, adición final de agua, etc.).

- 7) Los procedimientos anteriores (condiciones de procesado/curado) producen mezclas bituminosas MDI/aceite de ricino con una respuesta reológica largamente mejorada a alta temperatura de servicio.

ANNEXES

Chapter IX

***Physico-chemical modificacion of asphalt
bitumens by reactive agents***

9.1. ANNEXE I: LIST OF FIGURES

Figure 1.1. Some examples of the different types of distresses: a) fatigue cracking; b) rutting; c) thermal cracking.	9
Figure 2.1. Schematic representation of the molecular structures of different components of bitumen. Data from Shell bitumen Handbook (2003).	27
Figure 2.2. Schematic representation of bitumen. Data from Shell bitumen Handbook (2003).	30
Figure 2.3. Reactions of the isocyanate group.	42
Figure 2.4. Reaction of a diol chain extender to create hard and soft segment in a polyurethane.	43
Figure 2.5. Rheology - its place among other sciences considering applied problems.	47
Figure 2.6. Particle motion in shear and extensional flows.	49
Figure 2.7. Stress components on a cubical material element.	50
Figure 2.8. Simple shear between two parallel plates.	51
Figure 2.9. Flow curves (a) and viscosity curves (b) for fluids: [1] Newtonian, [2] shear-thinning, [3] shear-thickening and [4] viscoplastic.	54
Figure 2.10. Schematic shear stress-shear rate behaviour for time-dependent fluid behaviour.	57
Figure 2.11. Input and response functions differing in phase by the angle δ .	58
Figure 2.12. Response from stress relaxation test.	59
Figure 2.13. Response from creep test.	60
Figure 2.14. Components of complex modulus and compliance in sinusoidal shear deformation.	63

Figure 2.15. Time-temperature superposition scheme. (a) Segments obtained at each temperature in the time experimental window; (b) Master curve developed.	69
Figure 2.16. Topographic AFM image of bitumen.	72
Figure 2.17. Principal scheme of the heat flux DSC.	74
Figure 2.18. Schematics of DSC curve as a function of temperature	75
Figure 3.1. Structure of thiourea dioxide (A) and thiourea (B).	89
Figure 3.2. Structure of Pol-MDI.	90
Figure 3.3. Structure of castor oil.	90
Figure 3.4. Structure of pentaerythritol.	91
Figure 3.5. Structure of polyethylene glycol.	91
Figure 3.6. Structure of tri-block SBS.	92
Figure 3.7. Penetration test device.	94
Figure 3.8. Softening point test apparatus.	95
Figure 3.9. A) TLC-FID analyzer Iatroscan MK-6. B) Chromatogram obtained.	97
Figure 3.10. Waters model 500 GPC.	98
Figure 3.11. Calibration curve performed with the different polypropylene-glycol standards.	99
Figure 3.12. A) Principle of AFM. B) MultiMode TM AFM (Digital Instruments, Veeco Metrology Group Inc., Santa Barbara, U.S.A.).	100
Figure 3.13. CR Rheometer ARES (U.S.A).	102
Figure 3.14. CS Rheometer PHYSICA MCR-301 (Anton Paar, Austria).	102
Figure 3.15. Seiko DMS 6100, Seiko Instruments Inc.	104

Figure 3.16. DSC Q100 TA instruments.	106
Figure 3.17. TG/DTA 6200, Seiko Instruments Inc.	107
Figure 4.1. Viscous flow curves, at 60 °C, for (A) 9 wt.% ThD modified bitumen 40/50 and (B) 3 wt.% ThD modified bitumen 150/200, as a function of curing time.	117
Figure 4.2. Evolution of the modification index with curing time, for three selected ThD modified bitumen samples.	118
Figure 4.3. Evolution of the loss tangent with temperature, for modified bitumen 150/200 samples, as a function of curing time.	120
Figure 4.4. Master curves of the linear viscoelastic moduli in dynamic bending, E' and E'' , for (A) neat bitumen 40/50 and (B) 9 wt.% ThD binder, after 60 days of curing time.(Inset: Temperature dependence of the shift factor, and WLF fitting, for both binders.)	122
Figure 4.5. “Black” diagram for neat bitumen 40/50 and its corresponding 9 wt.% ThD binder, after 60 days of curing.	123
Figure 4.6. Evolution of E' and E'' with temperature (temperature sweep tests) for 9 wt.% ThD modified bitumen 40/50, after 60 days of curing, and its corresponding “blank” sample.	125
Figure 4.7. Viscous flow curves, at 60 °C, for 9 wt.% ThD modified binders, processed at 90 °C (A) and 180 °C (B), as a function of curing time.	126
Figure 4.8. Evolution of the modification index with curing time for 9 wt.% ThD binders at the three selected processing temperatures.	128
Figure 4.9. Evolution with temperature of the (A) linear viscoelastic moduli, in oscillatory shear (G' and G''), for “non-cured” 9 wt.% ThD binders processed at different temperatures and (B) loss tangent for 9 wt.% ThD binders, processed at 90 °C, as a function of curing time.	130
Figure 4.10. Evolution with temperature of the linear viscoelastic moduli, in dynamic bending (E' and E''), for 9 wt.% ThD binders cured for 60 days and processed at 130 °C (A) and 90 °C(B). Neat bitumen and “blank”, processed at 130 °C, are included.	131

- Figure 4.11.** TG/DTG and DTA curves between 40 and 600 °C and under N₂ atmosphere for thiourea dioxide, neat bitumen, and “non-cured” 9 wt.% ThD binders processed at the three selected processing temperatures. 133
- Figure 4.12.** Evolution of SARAs fractions with curing time for 9 wt.% ThD binders processed at 90 (A) and 130 °C (B). 136
- Figure 4.13.** DTG curve between 40 and 600 °C and under N₂ atmosphere for thiourea dioxide, neat bitumen, and filtration residues of 9 wt. ThD binders cured for 60 days and processed at 90 and 130 °C. Inset: photographs of residues described in the text. 138
- Figure 4.14.** Non-reversing heat flow thermograms for 9 wt.% ThD binders cured for 60 days and processed at 90 °C and 130 °C. Neat bitumen and “blank” samples included as references. 141
- Figure 5.1.** Viscous flow curves, at 60 °C, for a 3 wt.% Th binders (A) and a 9 wt.% Th binders (B), as a function of curing time. 154
- Figure 5.2.** Evolution of the modification index with curing time for all Th-modified binders studied. 157
- Figure 5.3.** Evolution with temperature of loss tangent (A) and “rutting parameter”, $|G^*|/\sin \delta$ (B), for selected Th binders, as a function of curing time. 159
- Figure 5.4.** Evolution with frequency of the elastic (E') and viscous (E'') moduli in dynamic bending, as a function of temperature, for neat bitumen. 160
- Figure 5.5.** (A) Empirical master curves of storage (E') and loss (E'') moduli vs. reduced frequency, $f \cdot a_T$, for neat bitumen (Inset: Temperature dependence of the shift factor and Arrhenius fitting). (B) Evolution of the linear viscoelastic functions vs. temperature obtained by frequency/temperature-conversion. 161
- Figure 5.6.** (A) Evolution of the linear viscoelastic functions (E', E'') with temperature, obtained from frequency/temperature-conversions, for for neat bitumen, reference SBS binder and 9 wt.% Th binder after 60 days of curing time. 164
- Figure 5.7.** Effect of heating rate on temperature sweep tests

- performed at 1 Hz for a 9 wt.% Th binder after 60 days of curing. Results compared with viscoelastic functions (E, E'') obtained from the frequency/temperature conversion (master curve). 165
- Figure 5.8.** “Black” diagram for neat bitumen and 9 wt.% Th binder (60 days-cured). 166
- Figure 5.9.** (A) DTA and (B) DTG curves for neat bitumen, pure thiourea and pure ammonium thiocyanate. 168
- Figure 5.10.** TLC/FID chromatograms for neat bitumen, pure thiourea and 9 wt.% Th-modified binder (60 days-cured). 169
- Figure 5.11.** (A) SARAs fractions contents and (B) “modified” colloidal index values for neat bitumen, “blank” sample and 3 and 9 wt.% Th-modified binders at different curing times. 171
- Figure 5.12.** Picture taken during the elution of the resins fraction with a blend of dichloromethane/methanol (95/5). 172
- Figure 5.13.** (A) Non-reversing heat flow and (B) C_p -derivate curves obtained by MDSC for neat bitumen and 9 wt.% Th binders at different curing times. 174
- Figure 5.14.** Non-reserving heat flow for curves for pure ammonium thiocyanate and 9 wt.% Th-modified binder (60 days-cured). 177
- Figure 6.1.** Reaction scheme for the synthesis of MDI-CO prepolymers. 187
- Figure 6.2.** Reversing heat flow thermograms for polymeric MDI, castor oil and MDI-CO prepolymers. 189
- Figure 6.3.** TG/DTG curves, between 40 and 600 °C and under N_2 atmosphere, for polymeric MDI, castor oil, and MDI-CO prepolymers. 191
- Figure 6.4.** Isothermal weight loss at 180 °C for polymeric MDI, castor oil, polyethylene glycol (PEG), MDI-PEG and MDI-CO prepolymers, under air atmosphere. 193
- Figure 6.5.** Sweep temperature tests, in shear mode, between -20 and 200 °C, for MDI-CO prepolymers. 194

- Figure 6.6.** Viscous flow curves, at 60 °C, for a selected 2 wt.% MDI-CO(8:1) modified binder, as a function of curing time (“water-slow” binders). Neat bitumen, 3 wt.% SBS and “water-fast” binder are also included. 197
- Figure 6.7.** Evolution of the modification index with curing time for 2 wt.% MDI-CO modified binders (“water-slow” binders). “Water-fast” binders and 3 wt.% SBS are included as reference. 200
- Figure 6.8.** (A) Evolution of the “rutting parameter”, $|G^*|/\sin \delta$, for neat bitumen, 3 wt. % SBS and two selected binders: “non-cured” 2wt.% MDI-CO(8:1) and 60 days cured; (B) “Rutting” temperatures with curing time for “water-slow” modified binders. Neat bitumen, 3 wt.% SBS and “water-fast” binders are also included. 203
- Figure 6.9.** Non-reversing heat flow thermograms for neat bitumen and 2 wt.% MDI-CO(8:1) “water-slow” binders at different curing time. 205
- Figure 6.10.** AFM micrographs ($50 \times 50 \mu\text{m}^2$), at 30 °C, for neat bitumen, 2 wt.% MDI-CO(8:1) binders “water-fast” and “water-slow”, after 60 days of curing, binders. 206
- Figure 6.11.** Modification index values, $(M.I.)_B^{60^\circ\text{C}}$, for “water-slow” MDI-CO binders as a function of curing time, manufactured following the two procedures. “Water-fast” binders and SBS reference binders are included as references. 209
- Figure 6.12.** Evolution with the temperature of (A) storage modulus, G' , and (B) loss tangent, $\tan \delta$, for neat bitumen, “non-cured”, “water-slow”, after 6 months of curing and “water-fast” MDI-CO modified binders, manufactured following the two procedures. 210
- Figure 6.13.** Temperature dependence of the “rutting parameter”, $|G^*|/\sin \delta$, for neat bitumen, “non-cured”, “water-slow”, after 6 months of curing, and “water-fast” MDI-CO modified binders, manufactured following the two procedures. 212
- Figure 6.14.** Non-reversing heat flow curves for neat bitumen, “water-slow”, after 6 months of curing, and “water-fast” MDI-CO binders, manufactured following “1 h processing” and “24 h 213

processing" procedures.

Figure 6.15. Evolution of bitumen SARAs fractions for "water-slow" MDI-CO binders, manufacture following the two procedures, as a function of curing time. Neat bitumen, "non-cured" and "water-fast" MDI-CO binders are also included as references. 215

Figure 6.16. Evolution of the "reactive" colloidal index for "water-slow" MDI-CO binders, manufacture following the two procedures, as a function of curing time. Neat bitumen, "non-cured" and "water-fast" MDI-CO binders are also included as references. 216

Figure 6.17. AFM micrographs ($20 \times 20 \mu\text{m}^2$), at 30°C , for the neat bitumen, "water-slow", after 6 months of curing, and "water-modified" MDI-CO binders, processed following the two processing procedures. 217

Figure 6.18. Reaction scheme for the transesterification reaction of castor oil with pentaerythritol. 220

Figure 6.19. Reaction scheme for the synthesis of MDI-CO^{n%} prepolymers. 222

Figure 6.20. Newtonian viscosity, at 30°C , for native/transesterified castor oils (CO^{n%}) and MDI-CO^{n%} prepolymers. 223

Figure 6.21. Isothermal weight loss at 180°C for polymeric MDI, polyethylene (PEG), castor oils (CO^{n%}), MDI-CO^{n%} and MDI-PEG prepolymers. 224

Figure 6.22. Viscous flow curves, at 60°C , for selected binders modified by 2 wt. % MDI-CO^{8%}. Neat and 3 wt.% SBS-modified bitumens are also included. 225

Figure 6.23. Modified index, $(\text{M.I.})_A^{60^\circ\text{C}}$, for MDI-CO^{n%} modified bitumens. 227

Figure 6.24. (A) Viscous flow curves, at 60°C , and (B) "adapted" modification indexes, $\text{M.I.}^{60^\circ\text{C}}(\text{cured})$, for MDI-CO^{n%}/CO^{4%-90} modified bitumens. Neat, "cured neat" and 3 wt.% SBS-modified bitumens are also included. 229

Figure 6.25. (A) Evolution with the temperature of loss tangent, $\tan \delta$, and (B) temperature dependence of the “rutting parameter”, $|G^*|/\sin \delta$, for MDI-CO^{n%}/CO^{4%}-90°C modified bitumens. Neat, “cured neat” and 3 wt.% SBS-modified bitumens are also included. 230

Figure 6.26. AFM micrographs (30 x 30 μm^2), at 30 °C, for neat bitumen, MDI-CO^{4%}/water and MDI-CO^{4%}/CO^{4%}-90°C binders. 232

Figure 6.27. Viscous flow curves, at 60 °C, for selected MDI-CO^{n%} modified binders. Neat and 3 wt.% SBS-binder are also included as references. 234

9.2. ANNEXE II: LIST OF TABLES

Table 2.1. Chemical composition of bitumen. Data from Lesueur (2009). 26

Table 2.2. Bitumens modifiers. Extracted from Bahía et al., 1998. 36

Table 3.1. Penetration values, ring & ball softening temperatures, SARA’s fraction and colloidal index values for the neat bitumens studied. 88

Table 3.2. Melting point and molecular weight of thiourea dioxide and thiourea. 89

Table 3.3. SBS Kraton D-1101 properties. 92

Table 4.1. Penetration values, ring & ball softening temperatures, SARAs fraction and colloidal index values for the two neat bitumens studied. 112

Table 4.2. Parameters C_1 and C_2 of WLF equation for the neat bitumen and 9 wt.% ThD binder after 60 days of curing. 121

Table 4.3. Evolution with curing time of zero-shear limiting viscosity, η_0 , and critical shear rate, $\dot{\gamma}_c$, for 9 wt.% ThD modified binders prepared. 127

Table 4.4. DMTA glass transition temperatures ($T_{g(1\text{Hz})}$) for 9 wt.% ThD binder processed at different temperatures, after 60 days of curing. 132

Table 4.5 Evolution with curing time of the colloidal index (C.I.) for 9 wt.% ThD binders processed at the three selected processing temperatures.	137
Table 4.6. Second event temperatures (T_{2nd}) and fourth event enthalpies (ΔH_{4th}) for 9 wt.% ThD binder processed at different temperatures, after 60 days of curing.	142
Table 5.1 Penetration value, ring & ball softening temperatures, SARAs fraction and colloidal index values for the neat bitumen studied.	150
Table 5.2. Evolution with curing time of Carreau's model parameters and SHRP maximum temperatures for neat bitumen, "blank" sample, reference SBS binder and Th-modified binders.	155
Table 5.3. Activation energy values (E_a) and DMTA glass transition temperatures ($T_{g,DMTA}$) for neat bitumen, reference SBS binder and 9 wt.% Th binder after 60 days of curing time.	162
Table 5.4. Glass transition temperatures obtained by MDSC (T_{g1} and T_{g2}); second event temperatures (T_{2nd}); and energy associated with the endothermic fourth even (ΔH_{4th}), for selected binders studied.	175
Table 6.1. Average molecular weight (M_w) relative to polypropylene glycol (PPG), -NCO content (% wt.) and glass transition temperature ($T_{g,DSC}$) for MDI-CO prepolymers, polymeric MDI and castor oil.	188
Table 6.2. Penetration value, ring & ball softening temperatures, SARA's fraction and colloidal index values for the neat bitumens studied.	195
Table 6.3. Evolution with curing time of Carreau's model parameters for "water-slow" modified binders. Neat bitumen, reference SBS binder and "water-fast" are included.	199
Table 6.4. Fourth event enthalpies (ΔH_{4th}) for neat bitumen and 2 wt.% MDI-CO(8:1) modified binders, as a function of curing time.	204
Table 6.5. Evolution with curing time of Carreau's model parameters and SHRP maximum temperatures for "water-slow" binders. Neat bitumen, reference SBS binder and "water-fast"	207

binders are included as references.

Table 6.6. Temperatures of the second thermal event (T_{2nd}) and energy associated with the endothermic fourth event (ΔH_{4th}) for neat bitumen, “water-slow”, after 6 months of curing, and “water-fast” MDI-CO binders, manufactured following “1 h processing” and “24 h processing” procedures.	214
Table 6.7. Hydroxyl values and nomenclature of the unmodified/modified castor oils.	221
Table 6.8. Free -NCO content (wt.%) for MDI-CO ^{n%} prepolymers.	222
Table 6.9. Carreau’s model parameters for all the modified samples studied.	226
Table 6.10. SHRP maximum temperatures for MDI-CO ^{n%} /CO ^{4%} -90°C binders.	231

9.3. ANNEXE III: LIST OF ACRONYMS AND SYMBOLS

This index includes the nomenclature used to prepare this thesis:

AFM	Atomic force microscopy
ASTM	American society for testing and material
DMTA	Dynamic mechanical thermal analysis
DPF	Dispersed polar fluid
DSC	Differential scanning calorimetry
EN	European normalization
FID	Flame ionization detector
FTIR	Fourier transform infrared
GPC	Gel permeation chromatographic
ISO	International standardization organization
LVR	Linear viscoelasticity region
MDI	Diphenylmethane diisocyanate
NCO	Isocyanate
PPG	Polypropylene glycol
R&B	Ring and ball test
SARA	Saturates-aromatics-resins-asphaltenes
SBS	Styrene butadiene styrene

TGA	Thermogravimetric analysis
THF	Tetrahydrofuran
TLC	Thin layer chromatographic
PMB	Polymer modified bitumen
SBR	Styrene butadiene rubber
SEBS	Styrene ethylene butylene styrene
EVA	ethylene vinyl acetate
PE	Polyethylene
PPA	Polyphosphoric acid
ThD	Thiourea dioxide
Th	Thiourea
PEG	Polyethylene glycol
LDPE	Low density polyethylene
EVA	Ethylene vinyl acetate
TDI	Toluene diisocyanate
WLF	Williams-Landel-Ferry equation
TTSP	Time-Temperature-Superposition principle
DTA	Differential thermal analysis

SYMBOLS

μ	Dynamic viscosity
a_T	Horizontal shift factor
C_p	Heat capacity
$ G' $	Storage modulus (oscillatory shear mode)
$ G'' $	Loss modulus (oscillatory shear mode)
$ G^* $	Complex modulus (oscillatory shear mode)
$ E' $	Storage modulus (bending mode)
$ E'' $	Loss modulus (bending mode)
$ E^* $	Complex modulus (bending mode)
$ J $	Compliance
$ J' $	Storage compliance
$ J'' $	Loss compliance
m	Mass
$^{\circ}\text{C}$	Degree Celsius
Q	Heat flow
R	Universal gas constant
T	Temperature
δ	Phase angle

η	Apparent viscosity
η_0	Zero shear rate limiting viscosity
η_∞	High shear rate limiting viscosity
ν	Kinematic viscosity
ν_T	Heating rate
ρ	Density
τ	Shear stress
f	Frequency
$\dot{\gamma}$	Shear rate
γ	Shear strain
M.I.	Modification index
C_1, C_2	Parameters of WLF equation
T_g	Glass transition temperature
E_a	Activation energy
ω_{exp}	Reduced frequency
ω_R	Reference frequency
C.I.	Gaestel colloidal index

9.4. ANNEXE IV: PAPERS PUBLISHED AND CONFERENCES CONTRIBUTIONS

9.4.1. Conferences contributions

- Modificación de la estructura coloidal del betún mediante aditivos químicos. A.A. Cuadri, P. Partal, F.J. Navarro, M. García-Morales, C. Gallegos. V Congreso de Jóvenes Investigadores en Polímeros, Girona (España), 2-6 Mayo 2010.
- Rheology and microstructure of bitumen modified by chemical agents. A.A. Cuadri, P. Partal, F.J. Navarro, M. García-Morales, C. Gallegos. Annual European Rheology Conference 2010, April 7-9, Göterborg, Sweden.
- Rheological behaviour and microstructure of bitumens modified by thiourea-based compounds. A.A. Cuadri, P. Partal, F.J. Navarro, M. García-Morales, C. Gallegos. Alpine Rheology Meeting, January 9-12, Les Gets, France.
- Thiourea derived compounds for bitumen modification: Rheology and microstructure. A.A. Cuadri, P. Partal, F.J. Navarro, M. García-Morales, C. Gallegos. Rheology Trends: from nano to macro systems (IBERHEO), 7-9 September 2011, Caparica, Portugal.
- Thermorheological properties of bitumens modified by thiourea-based compounds. A.A. Cuadri, P. Partal, F.J. Navarro, M. García-Morales, C. Gallegos. Annual European Rheology Conference 2011, May 10-14, Suzdal, Russia.
- Bitumen chemical modification by thiourea: rheological behaviour at low in-service temperatures and microstructure. A.A. Cuadri, P. Partal,

F.J. Navarro, M. García-Morales, C. Gallegos, A. Pérez-Lepe, A. Páez.
Eurasphalt & Eurobitume Congress 2012, June 13-15, Istanbul.

- Betunes modificados con polímeros reactivos formulados con MDI (4,4'-diphenylthane diisocyanate) y aceite de ricino. A.A. Cuadri, P. Partal, F.J. Navarro, M. García-Morales. VI Congreso de Jóvenes Investigadores en Polímeros, Huelva (España), 22-26 Abril 2012.

9.4.2. Patents

- Título: Ligante bituminoso para el reciclado de pavimentos.
Inventores: P. Partal, F.J. Navarro, M. García-Morales, F.J. Martínez-Boza, I. Martínez, C. Gallegos, V. Carrera, A.A. Cuadri.
Nº de publicación: ES-2375125-B2.
Fecha de concesión: 10/12/2012.

9.4.3. Papers published

- Title: Bitumen chemical modification by thiourea dioxide.
Authors: A.A. Cuadri, P. Partal, F.J. Navarro, M. García-Morales, C. Gallegos.
Journal: Fuel (2011, 90, 2294-2300).
- Title: Influence of processing temperature on the modification route and rheological properties of thiourea dioxide-modified bitumen.
Authors: A.A. Cuadri, P. Partal, F.J. Navarro, M. García-Morales, C. Gallegos.
Journal: Energy & Fuels (2011, 25, 4055-4062).
- Title: Enhancing the viscoelastic properties of bituminous binders via thiourea-modification.
Authors: A.A. Cuadri, M. García-Morales, F.J. Navarro, P. Partal.

Journal: Fuel (2012, 97, 862-868).

- Title: End-performance evaluation of thiourea-modified bituminous binders through viscous flow and linear viscoelasticity testing.

Authors: A.A. Cuadri, M. García-Morales, F.J. Navarro, G.D. Airey, P. Partal.

Journal: Rheologica Acta (2013, 52, 145-154).

- Title: Isocyanate-functionalized castor oil as a novel bitumen modifier.

Authors: A.A. Cuadri, M. García-Morales, F.J. Navarro, P. Partal.

Journal: Chemical Engineering Science (2013, 97, 320-327).

PAPERS PUBLISHED

Los artículos que forman parte del anexo “**Papers Published**” han sido retirados de la tesis debido a restricciones relativas a los derechos de autor. Dichos artículos han sido sustituidos por la referencia bibliográfica, enlace al texto completo (solo miembros de la UHU) y/o enlace Arias Montano, Repositorio Institucional de la Universidad de Huelva, así como resumen.

- Cuadri Vega, A.A., Partal López, P., Navarro Domínguez, F.J., García Morales. M., Gallegos Montes, C.: "Bitumen chemical modification by thiourea dioxide". Fuel. 2011, vol. 90, n. 6, págs. 2294–2300, (2011). DOI: 10.1016/j.fuel.2011.02.035

Enlace al texto completo del artículo (solo para miembros de la UHU)

<http://dx.doi.org/10.1016/j.fuel.2011.02.035>

Acceso Abierto a la versión post-print del artículo en Arias Montano, Repositorio Institucional de la Universidad de Huelva:

<http://hdl.handle.net/10272/12098>

RESUMEN:

This work evaluates a novel bitumen modification through the use of a chemical agent, thiourea dioxide, substance which has been traditionally used as a reducing agent. Thermogravimetric analysis demonstrated the formation of new chemical compounds, most probably originated through reactions between products from thiourea dioxide thermal decomposition and some highly polar bitumen molecules. As a result of these reactions, which continues even after 60 days, bitumen permanent deformation resistance at high temperature is enhanced, as indicated by a significant increase in its viscosity and elastic features. On the other hand, thiourea dioxide addition produces changes in the bitumen colloidal nature, which improve its flexibility at low in-service temperatures, and consequently its resistance to thermal cracking under loading. In fact, dynamic bending tests indicated a remarkable decrease in the value of binder glass transition temperature, which was further corroborated by differential scanning calorimetry. As a conclusion, thiourea dioxide can be seen as a promising modifying agent, which can extend the in-service temperature range at which bitumen would present a satisfactory performance.

- Cuadri Vega, A.A., Partal López, P., Navarro Domínguez, F.J., García Morales, M., Gallegos Montes, C.: "Influence of processing temperature on the modification route and rheological properties of thiourea dioxide-modified bitumen". *Energy & Fuels*. Vol 25 (9), págs. 4055-4062, (2011). DOI: 10.1021/ef200801h

Enlace al texto completo del artículo:

<http://dx.doi.org/10.1021/ef200801h>

RESUMEN:

This work deals with the effect that processing temperature exerts on the modification of bitumen by thiourea dioxide (ThD). In that sense, shear and bending rheological tests, (thermal analysis thermogravimetric analysis/derivative thermogravimetric analysis/differential thermal analysis (TG/DTG/DTA) and modulated differential scanning calorimetry (MDSC)), and chemical characterization by thin layer chromatography coupled with a flame ionization detector (TLC-FID) were carried out on neat bitumen with a penetration grade (pen.) of 40/50 and corresponding 9 wt % ThD modified samples, prepared at 90, 130, and 180 °C. Tests carried out on those binders revealed the existence of a different modification mechanism at every temperature. In any case, viscosity was always seen to increase after ThD addition. Also, modification enhanced elastic properties and thermal susceptibility at high in-service temperatures and yielded improved binder resistance to thermal cracking by a decrease in its glass transition temperature. These results suggest that the use of thiourea dioxide may become a promising alternative to the use of other chemical modifiers for the paving industry.

- Cuadri Vega, A.A., García Morales, M., Navarro Domínguez, F.J., Partal López, P.: "Enhancing the viscoelastic properties of bituminous binders via thiourea-modification". *Fuel*. Vol. 97, págs. 862-868, (2012). DOI: 10.1016/j.fuel.2012.03.012

Enlace al texto completo del artículo (solo para miembros de la UHU):

<http://dx.doi.org/10.1016/j.fuel.2012.03.012>

Acceso Abierto a la versión post-print del artículo en Arias Montano, Repositorio Institucional de la Universidad de Huelva:

<http://hdl.handle.net/10272/12114>

RESUMEN:

Although added in a very low concentration, bitumen controls the final properties and performance of the resulting asphalt mixture. As an alternative to classic bitumen modification with polymers, we herein propose the use of thiourea, which has proved to efficiently enhance the binder thermo-rheological properties in a broad

temperature interval. As revealed by thermogravimetric and chemical analysis, benefits above may derive from new structures, probably formed by the interaction between ammonium thiocyanate and bitumen most polar fraction. Thus, flexural DMTA and dynamic shear tests demonstrated an improvement in the binder flexibility and an increase in its elasticity, at low and medium/high in-service temperatures, respectively. In addition, this research emphasizes the use of isothermal frequency sweep tests (and frequency/temperature-dependence conversion) as a means of achieving glass transition temperature values which, in contrast to isochronal temperature sweep tests, do not depend on the selected heating rate.

- Cuadri Vega, A.A., García Morales, M., Navarro Domínguez, F.J., Airey, G., Partal López, P.: "End-performance evaluation of thiourea-modified bituminous binders through viscous flow and linear viscoelasticity testing. *Rheologica Acta*. Vol. 52, n. 2, págs. 145-154. DOI: 10.1007/s00397-012-0671-5

Enlace al texto completo del artículo (solo para miembros de la UHU):

<http://dx.doi.org/10.1007/s00397-012-0671-5>

Acceso Abierto a la versión post-print del artículo en Arias Montano, Repositorio Institucional de la Universidad de Huelva:

<http://hdl.handle.net/10272/12113>

RESUMEN:

Straight-run bitumens are no longer suitable in new asphalt mixtures. Consequently, the use of modified bitumens has become more important. In order to both improve binders' mechanical properties and prevent it from phase separation whilst stored at high temperature, the paving industry is currently developing new modification routes based on reactive agents. This work studies the use of thiourea, which has proven to efficiently broaden the temperature interval over which the binder demonstrates an adequate performance. On the one hand, viscous flow and dynamic shear tests indicate an enhancement in the high in-service temperature strength, along with a reduced thermal susceptibility. On the other hand, results of dynamic flexural tests reveal a significant decrease in the binder glass transition temperature. Finally, the use of master curves and a further frequency/temperature conversion are proposed, in order to attain a suitable viscoelastic characterisation of bituminous binders at low temperatures.

- Cuadri Vega, A.A., García Morales, M., Navarro Domínguez, F.J., Partal López, P.: "Isocyanate-functionalized castor oil as a novel bitumen modifier". Vol. 97, págs.. 320-327, (2013). DOI: 10.1016/j.ces.2013.04.045

Enlace al texto completo del artículo (solo para miembros de la UHU):

<http://dx.doi.org/10.1016/j.ces.2013.04.045>

Acceso Abierto a la versión post-print del artículo en Arias Montano, Repositorio Institucional de la Universidad de Huelva:

<http://hdl.handle.net/10272/12112>

RESUMEN:

The use of raw materials from renewable sources in the synthesis of polyurethane-derived polymers is lately receiving great attention from social, environmental and economic standpoints. In this work, prepolymers having different –NCO/–OH ratios were synthesised, by reaction of 4,4'-diphenylmethane diisocyanate (MDI) with castor oil (CO), to be used as the modifying agent of asphaltic bitumen. Reactions between MDI and CO, performed with –NCO/–OH molar ratios of 8:1 and 4:1, have led to suitable bitumen modifiers. Modification has been related to chemical reactions between –NCO groups, some bitumen compounds and air moisture (or added water), which gave rise to binders with enhanced resistance to permanent deformation. The results showed that a 2 wt% of MDI–CO prepolymer leads to binders with higher viscosity than that corresponding to a 3 wt% Styrene–Butadiene–Styrene (SBS) block copolymer, a polymer and concentration widely used in the paving industry. Furthermore, the resulting prepolymers are liquids that can be easily mixed with bitumen at 90 °C, which significantly lowers the typical temperature used for commercial SBS-modified bitumen (about 180 °C). This fact may represent energy savings, reduce bitumen oxidation and result in improvements of health and safety conditions during the product manufacture. However, if high processing temperatures are required, MDI–CO based modifiers have demonstrated much higher thermal stability than prepolymers derived from crude oil (e.g. based on polyethylene glycol). As a result, NCO-terminated prepolymers obtained from biomass-derived polyols (castor oil in this article) may become a promising alternative to the use of other petrochemicals in the paving industry.

